



Particle Collider Interaction Regions

Nikolai Mokhov, Mauro Pivi, Andrei Seryi

International Linear Collider



Linear Collider – two main challenges

- **Energy** – need to reach at least 500 GeV CM as a start

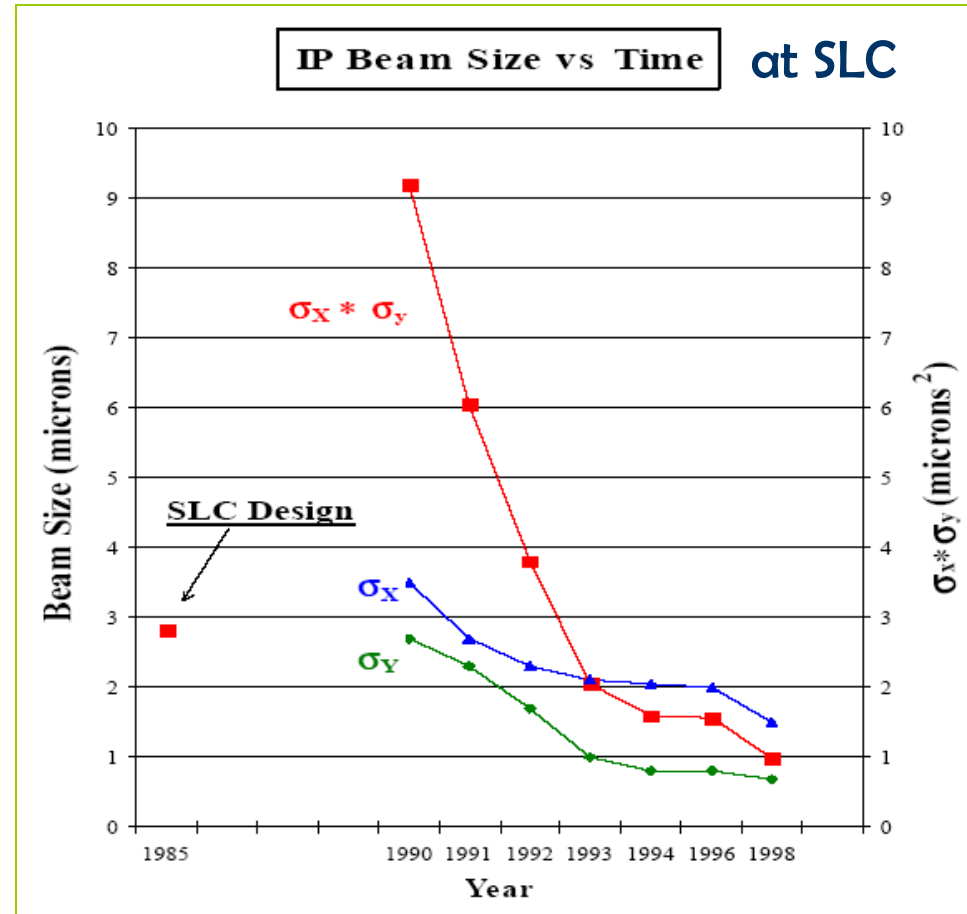


- **Luminosity** – need to reach 10^{34} level



The Luminosity Challenge

- Must jump by a Factor of 10000 in Luminosity !!!
(from what is achieved in the only so far linear collider SLC)
- Many improvements, to ensure this : generation of smaller emittances, their better preservation, ...
- Including better focusing, dealing with beam-beam, safely removing beams after collision and better stability

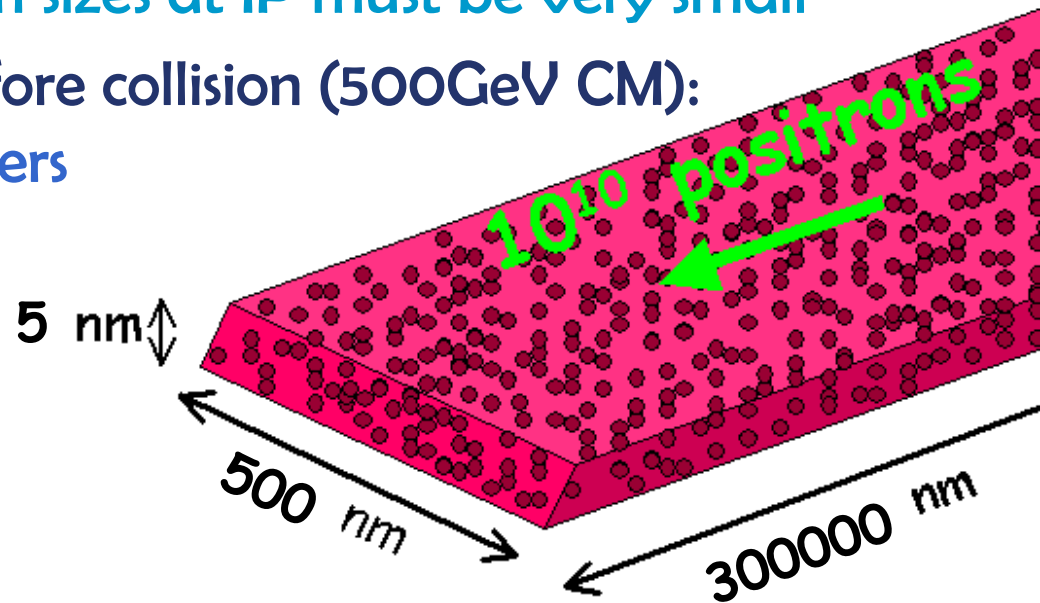
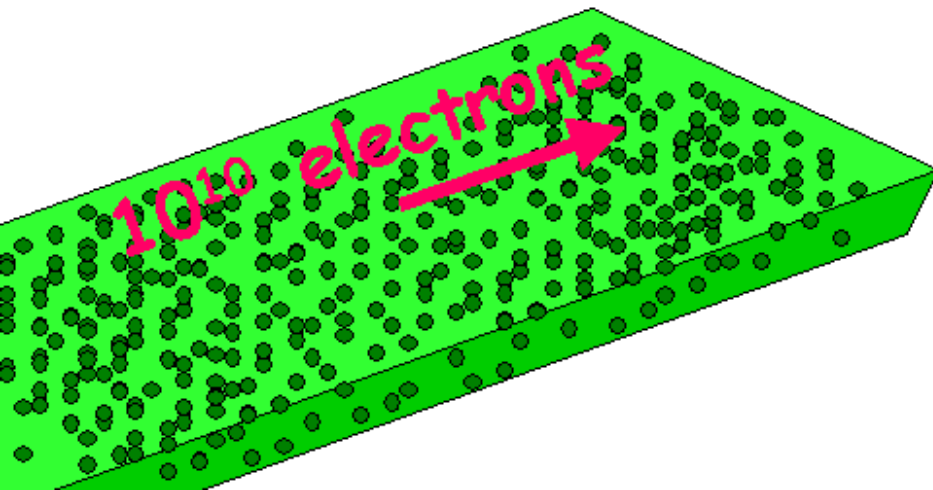


How to get Luminosity

- To increase probability of direct e^+e^- collisions (luminosity) and birth of new particles, beam sizes at IP must be very small
- E.g., ILC beam sizes just before collision (500GeV CM):
500 * 5 * 300000 nanometers

(x y z)

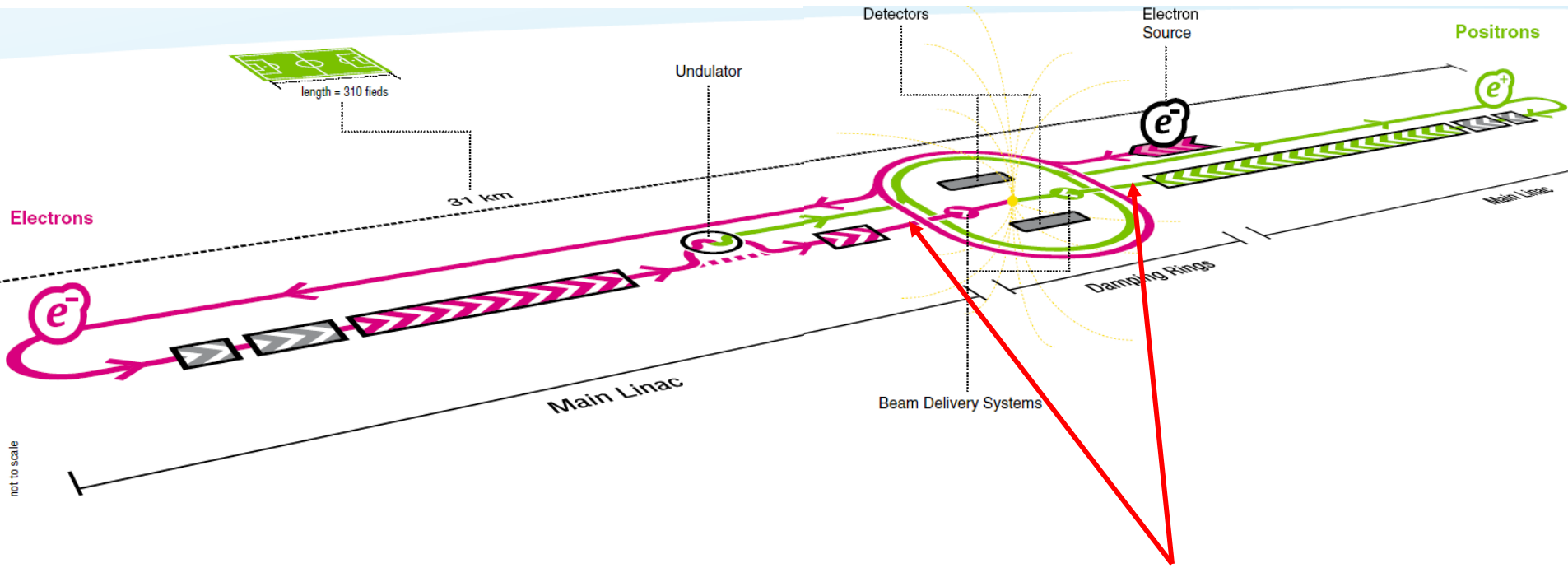
↑
Vertical size
is smallest



$$L = \frac{f_{rep}}{4\pi} \frac{n_b N^2}{\sigma_x \sigma_y} H_D$$



BDS: from end of linac to IP, to dumps

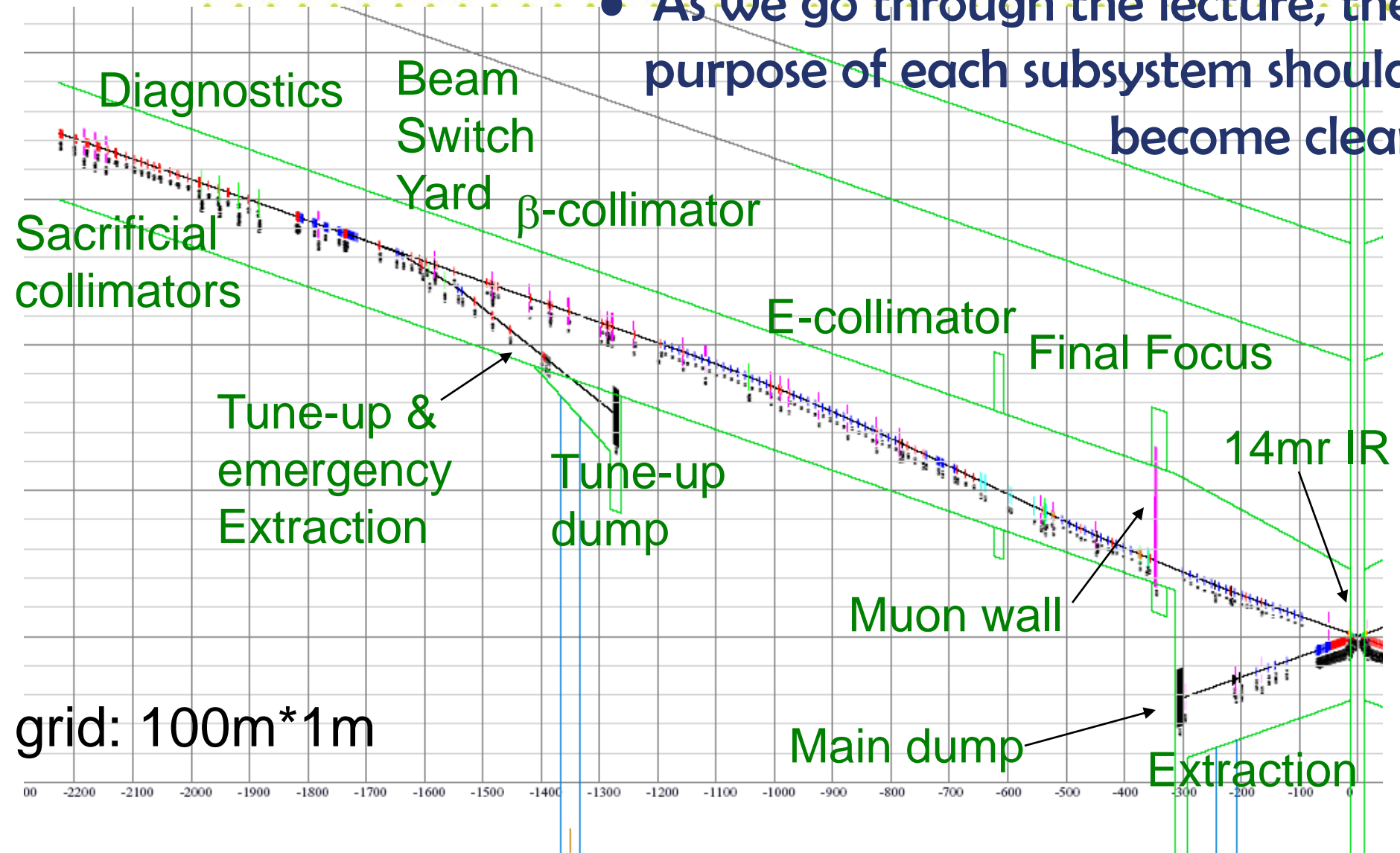


Beam Delivery System (BDS)



Beam Delivery subsystems

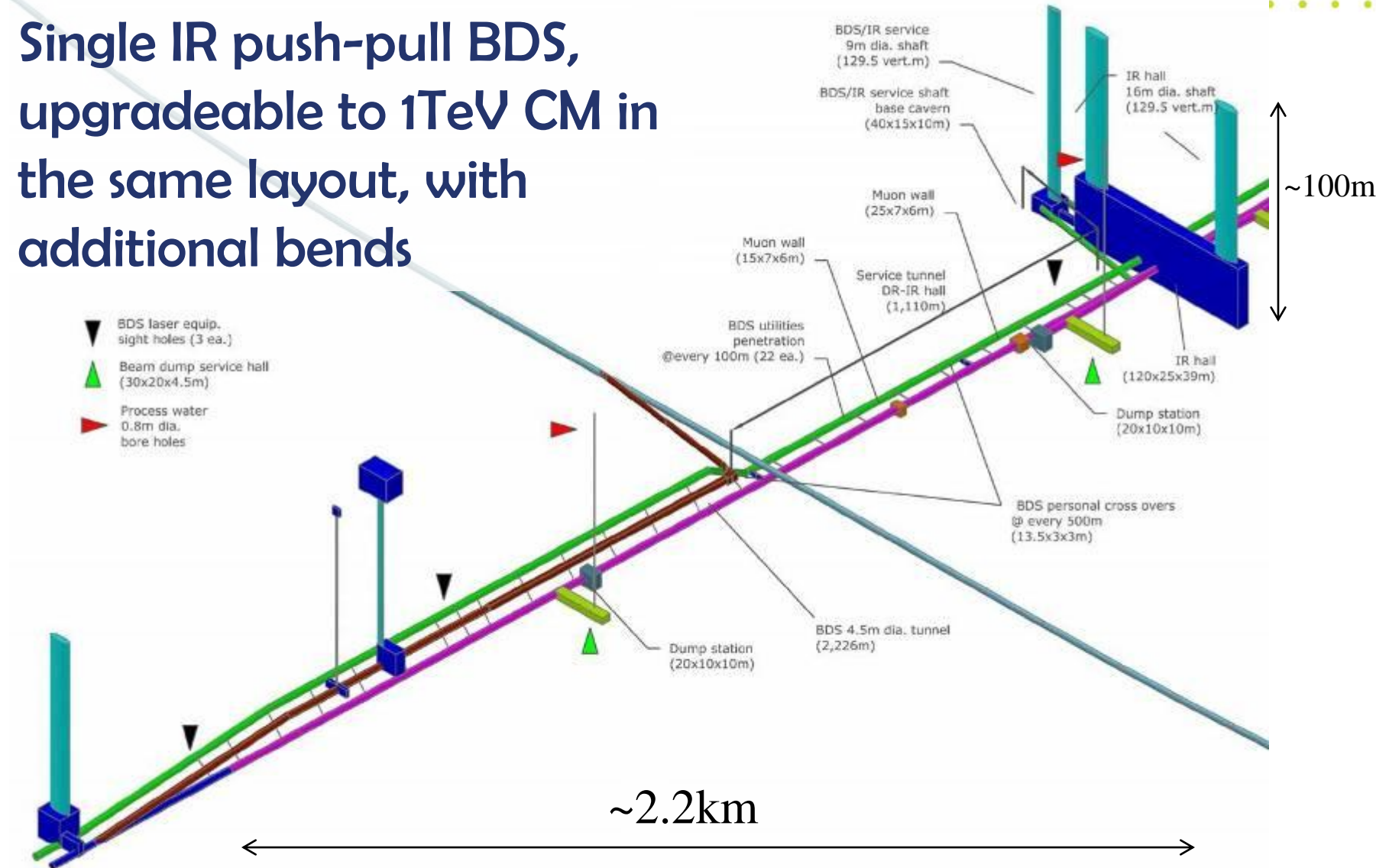
- As we go through the lecture, the purpose of each subsystem should become clear





Layout of Beam Delivery tunnels

- Single IR push-pull BDS, upgradeable to 1TeV CM in the same layout, with additional bends





Beam Delivery System challenges

- measure the linac beam and match it into the final focus
- remove any large amplitude particles (beam-halo) from the linac to minimize background in the detectors
- measure and monitor the key physics parameters such as energy and polarization before and after the collisions
- ensure that the extremely small beams collide optimally at the IP
- protect the beamline and detector against mis-steered beams from the main linacs and safely extract them to beam dump
- provide possibility for two detectors to utilize single IP with efficient and rapid switch-over

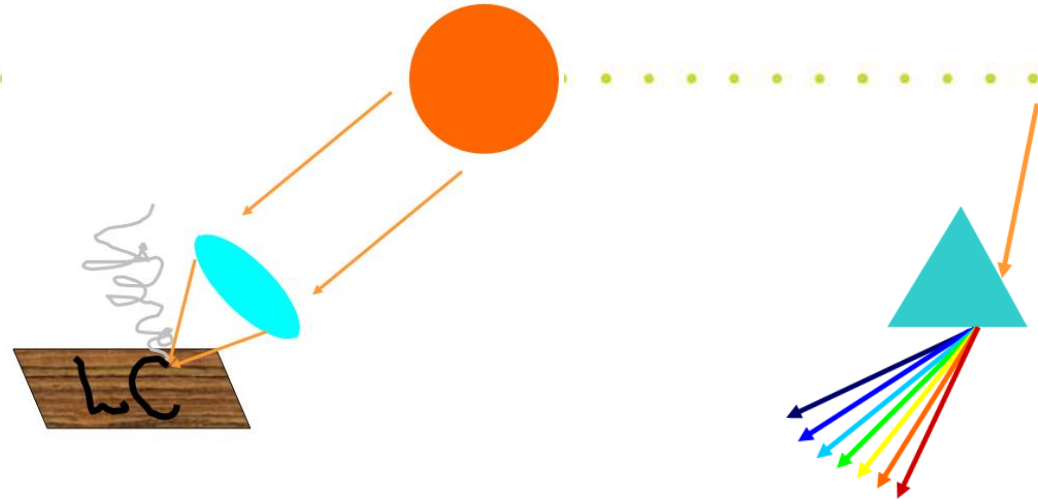




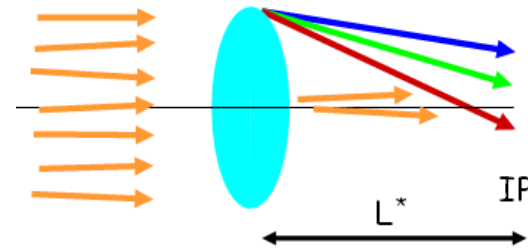
Parameters of ILC BDS

Length (linac exit to IP distance)/side	m	2226
Length of main (tune-up) extraction line	m	300 (467)
Max Energy/beam (with more magnets)	GeV	250 (500)
Distance from IP to first quad, L^*	m	3.5-(4.5)
Crossing angle at the IP	mrad	14
Nominal beam size at IP, σ^* , x/y	nm	655/5.7
Nominal beam divergence at IP, θ^* , x/y	μrad	31/14
Nominal beta-function at IP, β^* , x/y	mm	21/0.4
Nominal bunch length, σ_z	μm	300
Nominal disruption parameters, x/y		0.162/18.5
Nominal bunch population, N		2×10^{10}
Max beam power at main and tune-up dumps	MW	18
Preferred entrance train to train jitter	σ	< 0.5
Preferred entrance bunch to bunch jitter	σ	< 0.1
Typical nominal collimation depth, x/y		8–10/60
Vacuum pressure level, near/far from IP	nTorr	1/50

- Strong focusing



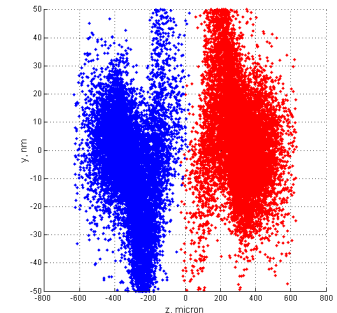
- Chromaticity



- Beam-beam effects

- Synchrotron radiation

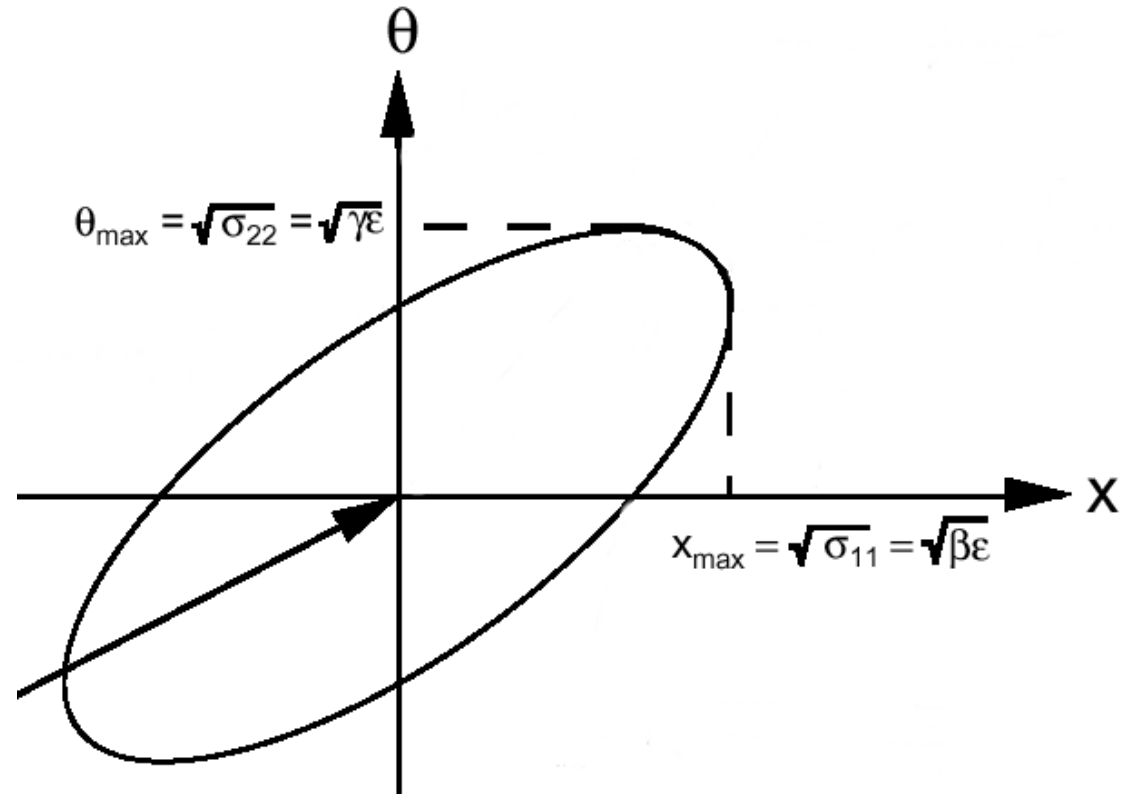
– let's consider some of this in more details





Recall couple of definitions

- Beta function β characterize optics
- Emittance ε is phase space volume of the beam
- Beam size: $(\varepsilon \beta)^{1/2}$
- Divergence: $(\varepsilon/\beta)^{1/2}$



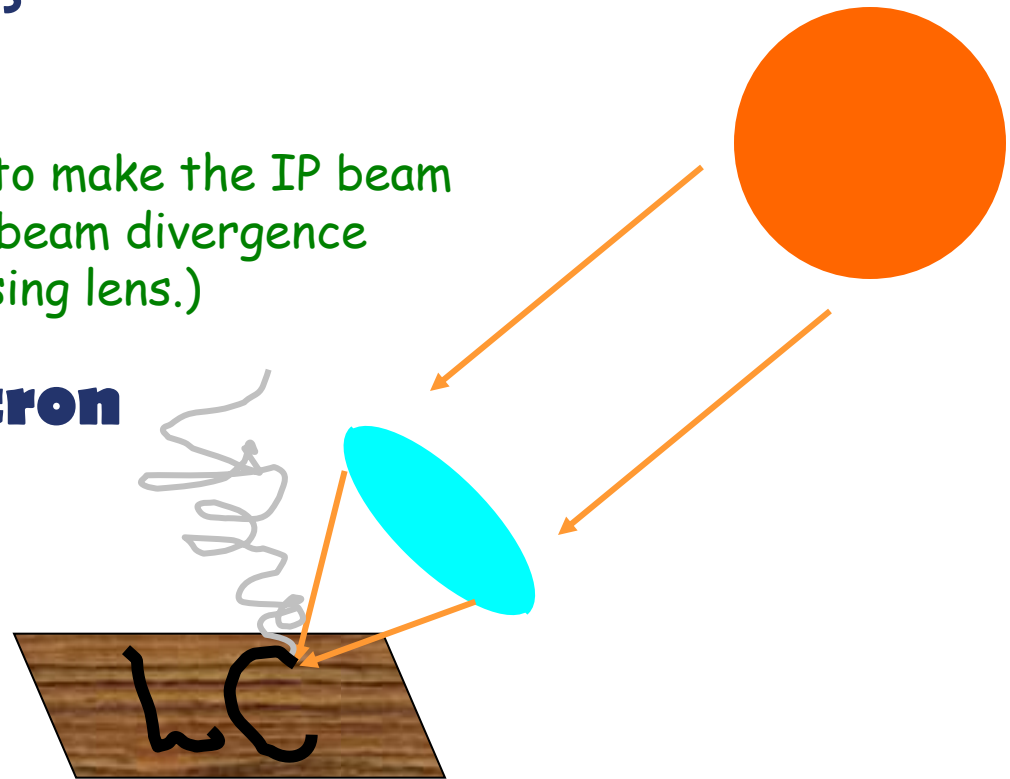
- Focusing makes the beam ellipse rotate with “betatron frequency”
- Phase of ellipse is called “betatron phase”

How to focus the beam to a smallest spot?

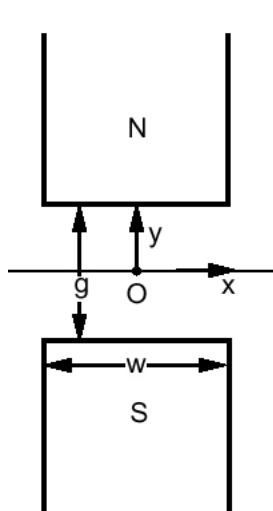
- If you ever played with a lens trying to burn a picture on a wood under bright sun, then you know that one needs a strong and big lens

(The emittance ε is constant, so, to make the IP beam size $(\varepsilon \beta)^{1/2}$ small, you need large beam divergence at the IP $(\varepsilon / \beta)^{1/2}$ i.e. short-focusing lens.)

- It is very similar for **electron** or **positron** beams
- But one have to use **magnets**

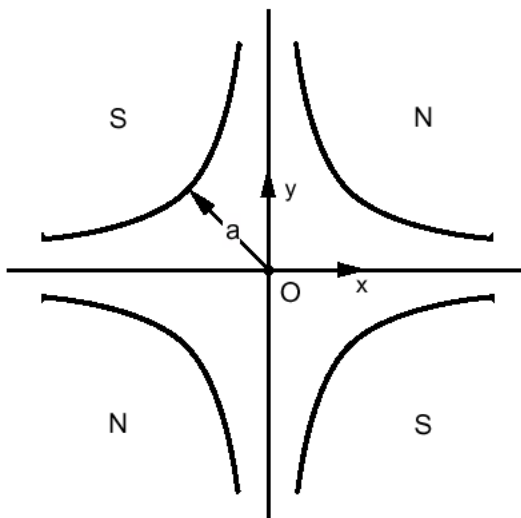
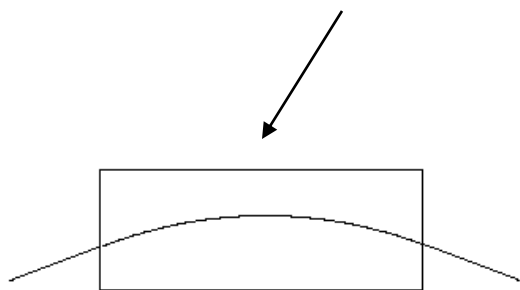


What we use to handle the beam



DIPOLE

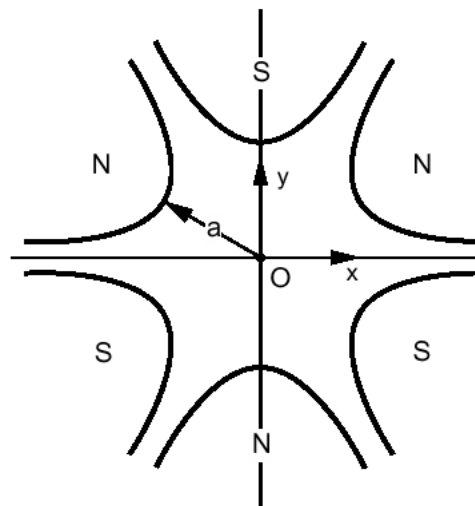
Just bend the trajectory



QUADRUPOLE

Focus in one plane,
defocus in another:

$$\begin{aligned} x' &= x' + G x \\ y' &= y' - G y \end{aligned}$$



SEXTUPOLE

Second order
effect:

$$\begin{aligned} x' &= x' + S (x^2 - y^2) \\ y' &= y' - S 2xy \end{aligned}$$

Etc...

Here x is transverse coordinate, x' is angle



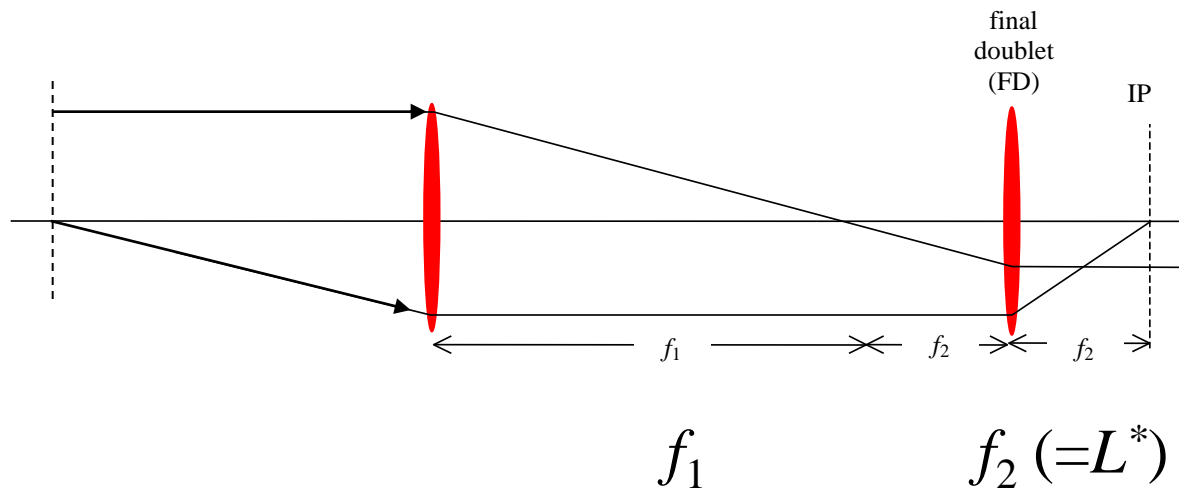
Optics building block: telescope

Essential part of final focus is final telescope. It “demagnify” the incoming beam ellipse to a smaller size. Matrix transformation of such telescope is diagonal:

$$R_{x,y} = \begin{pmatrix} -1/M_{x,y} & 0 \\ 0 & -M_{x,y} \end{pmatrix}$$

A minimal number of quadrupoles, to construct a telescope with arbitrary demagnification factors, is four.

If there would be no energy spread in the beam, a telescope could serve as your final focus (or two telescopes chained together).



Use telescope optics to demagnify beam by factor $m = f1/f2 = f1/L^*$

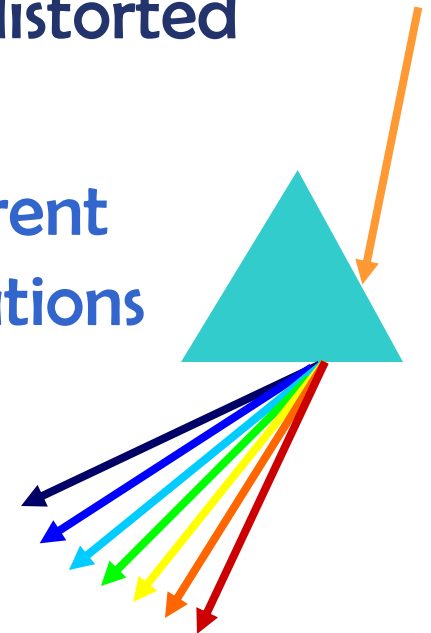
Matrix formalism for beam transport:

$$x_i^{out} = R_{ij} x_j^{in}$$

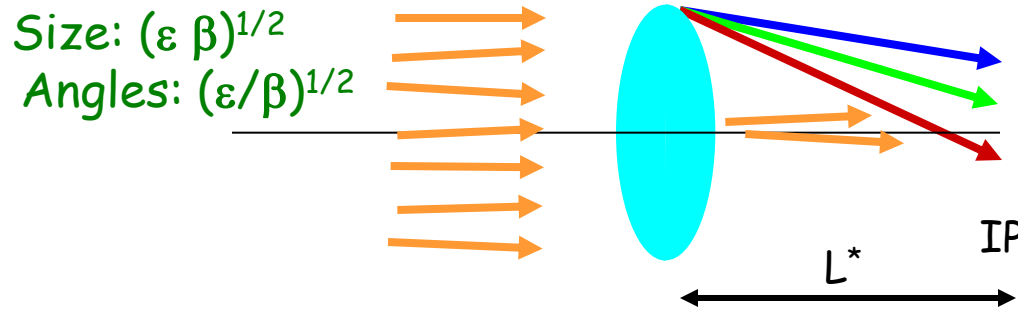
$$x_i = \begin{pmatrix} x \\ x' \\ y \\ y' \\ \Delta l \\ \delta \end{pmatrix}$$

Why nonlinear elements

- As sun **light** contains different colors, **electron beam** has energy spread and get dispersed and distorted => **chromatic aberrations**
- For **light**, one uses lenses made from different materials to compensate chromatic aberrations
- Chromatic compensation for particle beams is done with **nonlinear** magnets
 - Problem: Nonlinear elements create **geometric** aberrations
- The **task of Final Focus system (FF)** is to focus the beam to required size and compensate aberrations



How to focus to a smallest size and how big is chromaticity in FF?



Size at IP:
 $L^* (\epsilon/\beta)^{1/2}$
 $+ (\epsilon \beta)^{1/2} \sigma_E$

Beta at IP:
 $L^* (\epsilon/\beta)^{1/2} = (\epsilon \beta^*)^{1/2}$
 $\Rightarrow \beta^* = L^{*2}/\beta$

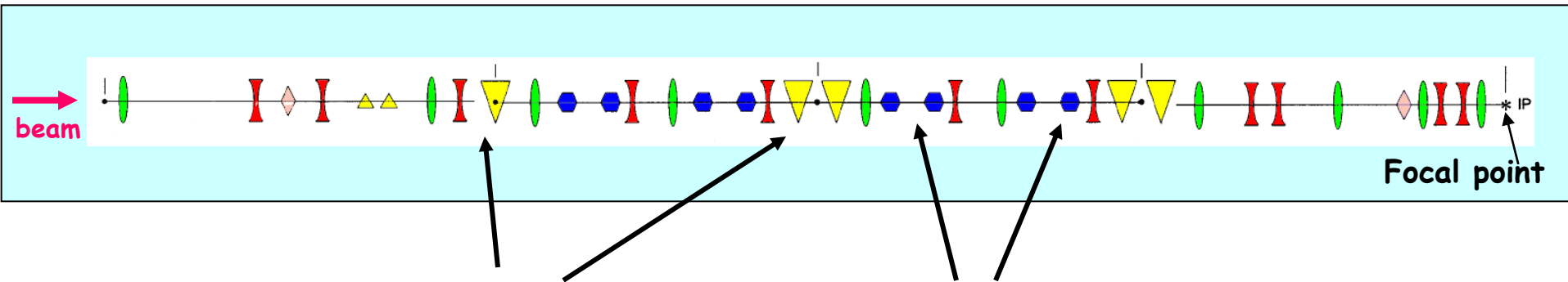
Chromatic dilution:
 $(\epsilon \beta)^{1/2} \sigma_E / (\epsilon \beta^*)^{1/2}$
 $= \sigma_E L^*/\beta^*$

- The final lens need to be the strongest
 - (two lenses for both x and y => “Final Doublet” or FD)
 - FD determines chromaticity of FF
 - Chromatic dilution of the beam
 size is $\Delta\sigma/\sigma \sim \sigma_E L^*/\beta^*$
- Typical: σ_E -- energy spread in the beam $\sim 0.002-0.01$
 L^* -- distance from FD to IP $\sim 3 - 5$ m
 β^* -- beta function in IP $\sim 0.4 - 0.1$ mm

- For typical parameters, $\Delta\sigma/\sigma \sim 15-500$ **too big !**
- => Chromaticity of FF need to be compensated

Example of traditional Final Focus

Sequence of elements in ~100m long Final Focus Test Beam



Dipoles. They bend trajectory, but also disperse the beam so that x depend on energy offset δ

Sextupoles. Their kick will contain energy dependent focusing

$$x' \Rightarrow S (x + \delta)^2 \Rightarrow 2S x \delta + ..$$

$$y' \Rightarrow -S 2(x + \delta)y \Rightarrow -2S y \delta + ..$$

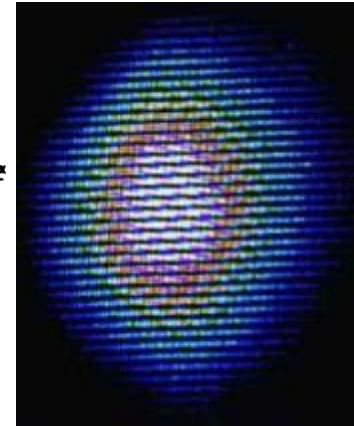
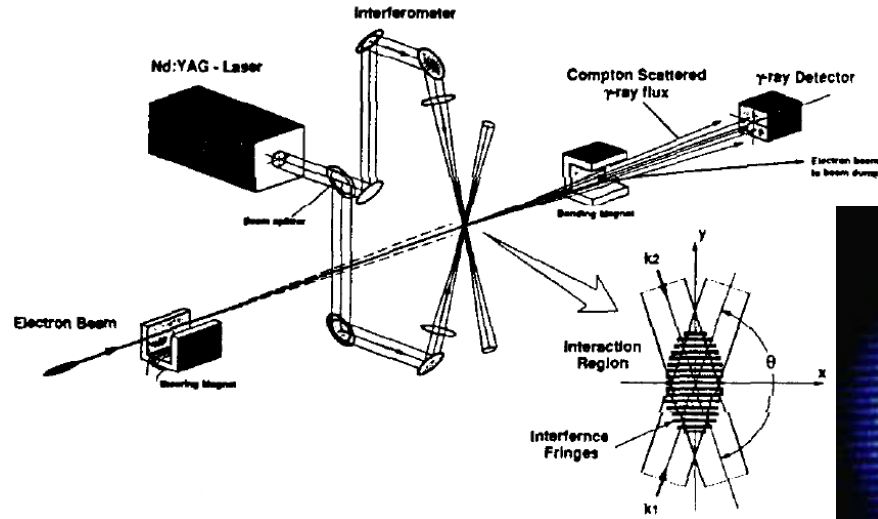
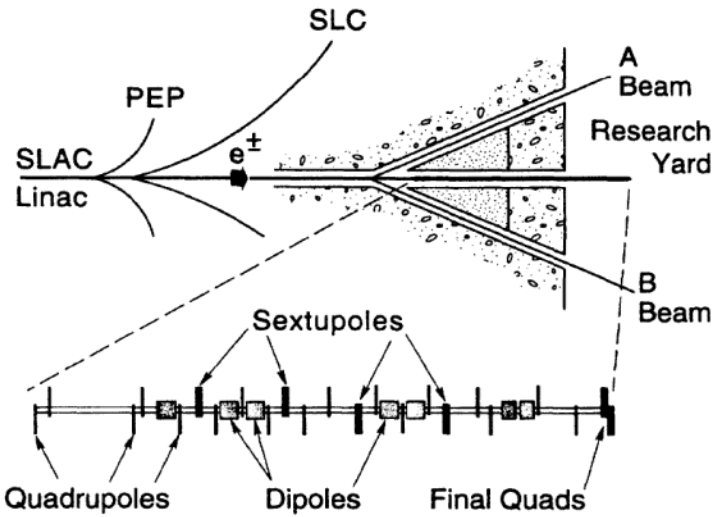
that can be used to arrange chromatic correction

Necessity to compensate chromaticity is a major driving factor of FF design

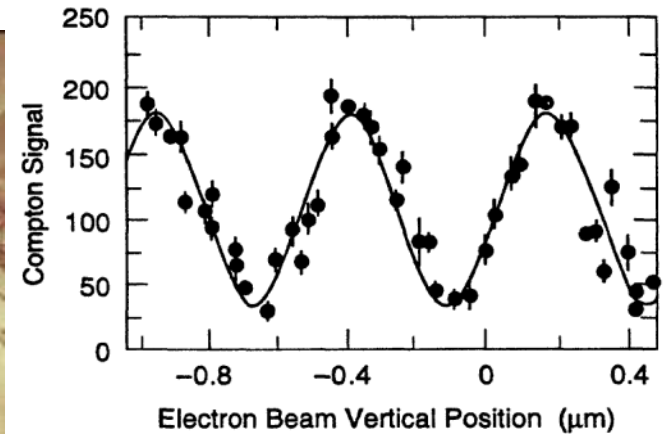
Terms x^2 are geometric aberrations and need to be compensated also



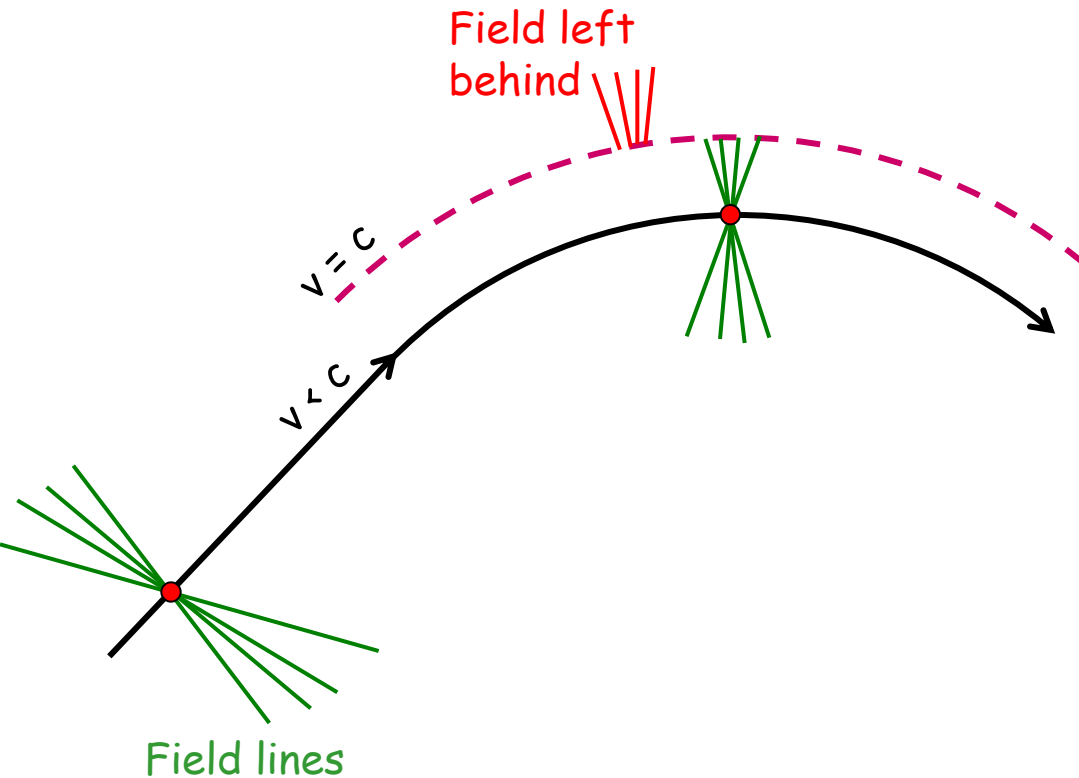
Final Focus Test Beam



Achieved ~70nm vertical beam size



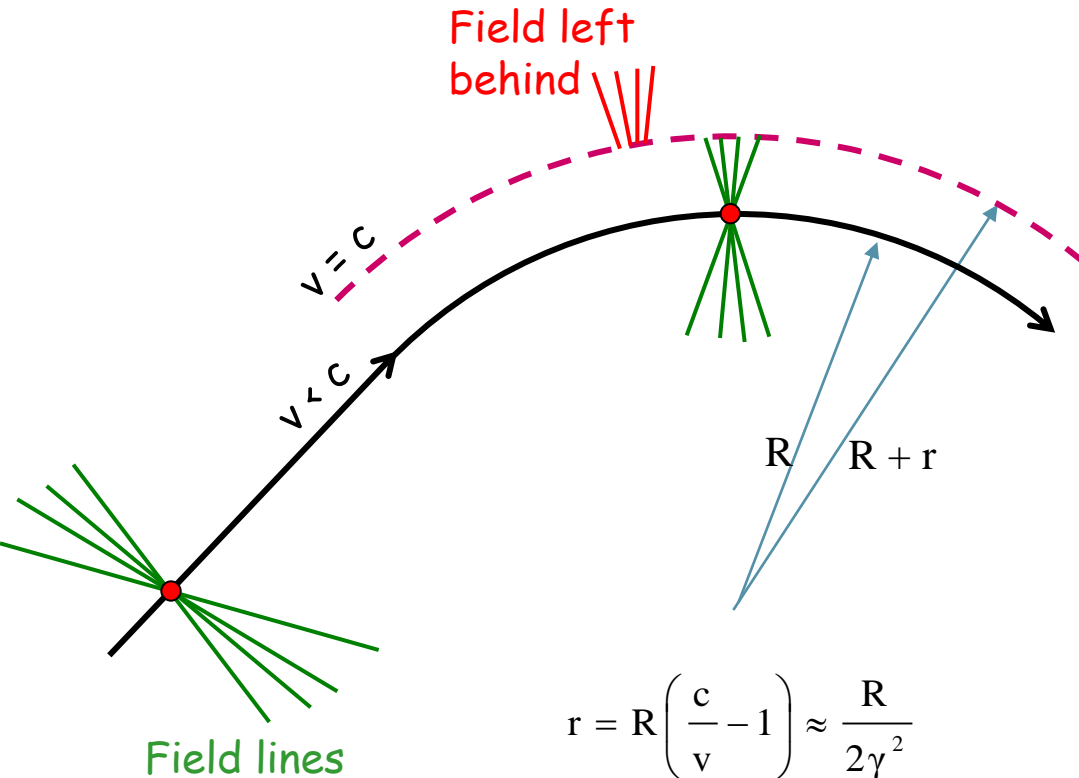
Synchrotron Radiation in FF magnets



Energy spread caused by SR in bends and quads is also a major driving factor of FF design

- Bends are needed for compensation of chromaticity
- SR causes increase of energy spread which may perturb compensation of chromaticity
- Bends need to be long and weak, especially at high energy
- SR in FD quads is also harmful (Oide effect) and may limit the achievable beam size

Let's estimate SR power



Energy in the field left behind (radiated !):

$$W \approx \int E^2 dV$$

The field $E \approx \frac{e}{r^2}$ the volume $V \approx r^2 dS$

Energy loss per unit length:

$$\frac{dW}{dS} \approx E^2 r^2 \approx \left(\frac{e}{r^2} \right)^2 r^2$$

Substitute $r \approx \frac{R}{2\gamma^2}$ and get an estimate:

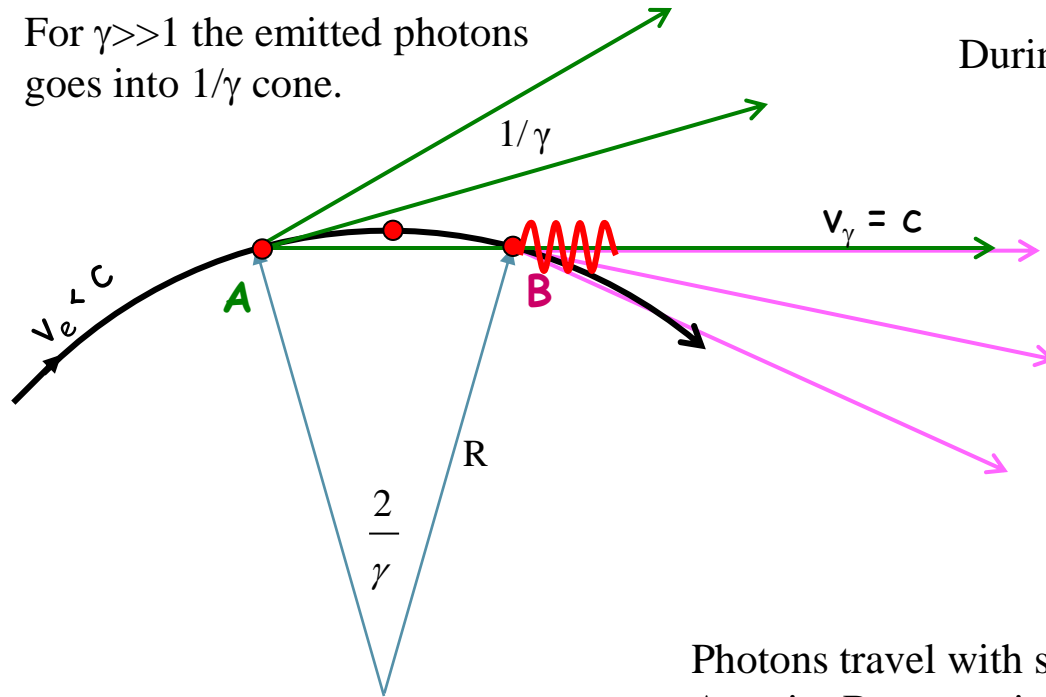
$$\frac{dW}{dS} \approx \frac{e^2 \gamma^4}{R^2}$$

Compare with exact formula: $\frac{dW}{dS} = \frac{2}{3} \frac{e^2 \gamma^4}{R^2}$



Let's estimate typical frequency of SR photons

For $\gamma \gg 1$ the emitted photons goes into $1/\gamma$ cone.



During what time Δt the observer will see the photons?



Photons emitted during travel along the $2R/\gamma$ arc will be observed.

Photons travel with speed c , while particles with v .

At point B, separation between photons and particles is

$$dS \approx \frac{2R}{\gamma} \left(1 - \frac{v}{c} \right)$$

Therefore, observer will see photons during $\Delta t \approx \frac{dS}{c} \approx \frac{2R}{c\gamma} (1 - \beta) \approx \frac{R}{c\gamma^3}$

Estimation of characteristic frequency

$$\omega_c \approx \frac{1}{\Delta t} \approx \frac{c\gamma^3}{R}$$

Compare with exact formula: $\omega_c = \frac{3}{2} \frac{c\gamma^3}{R}$



Let's estimate energy spread growth due to SR

We estimated the rate of energy loss : $\frac{dW}{dS} \approx \frac{e^2 \gamma^4}{R^2}$ And the characteristic frequency $\omega_c \approx \frac{c \gamma^3}{R}$

The photon energy $\varepsilon_c = \hbar \omega_c \approx \frac{\gamma^3 \hbar c}{R} = \frac{\gamma^3}{R} \lambda_e mc^2$ where $r_e = \frac{e^2}{mc^2}$ $\alpha = \frac{e^2}{\hbar c}$ $\lambda_e = \frac{r_e}{\alpha}$

Number of photons emitted per unit length $\frac{dN}{dS} \approx \frac{1}{\varepsilon_c} \frac{dW}{dS} \approx \frac{\alpha \gamma}{R}$ (per angle θ : $N \approx \alpha \gamma \theta$)

The energy spread $\Delta E/E$ will grow due to statistical fluctuations (\sqrt{N}) of the number of emitted photons :

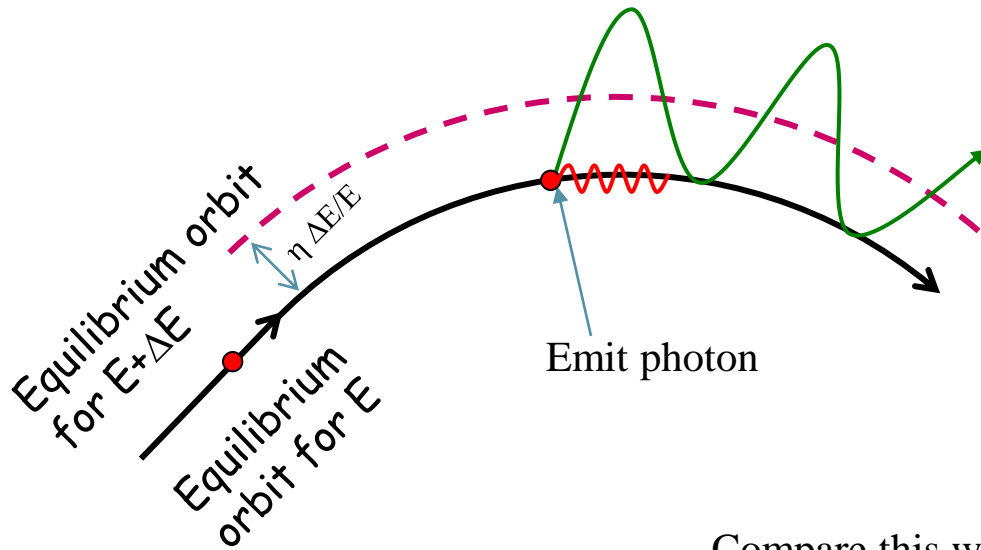
$$\frac{d((\Delta E/E)^2)}{dS} \approx \varepsilon_c^2 \frac{dN}{dS} \frac{1}{(\gamma mc^2)^2}$$

Which gives: $\frac{d((\Delta E/E)^2)}{dS} \approx \frac{r_e \lambda_e \gamma^5}{R^3}$

Compare with exact formula: $\frac{d((\Delta E/E)^2)}{dS} = \frac{55}{24\sqrt{3}} \frac{r_e \lambda_e \gamma^5}{R^3}$



Let's estimate emittance growth rate due to SR



Dispersion function η shows how equilibrium orbit shifts when energy changes

When a photon is emitted, the particle starts to oscillate around new equilibrium orbit

Amplitude of oscillation is $\Delta x \approx \eta \Delta E/E$

Compare this with betatron beam size: $\sigma_x = (\epsilon_x \beta_x)^{1/2}$

And write emittance growth: $\Delta \epsilon_x \approx \frac{\Delta x^2}{\beta}$

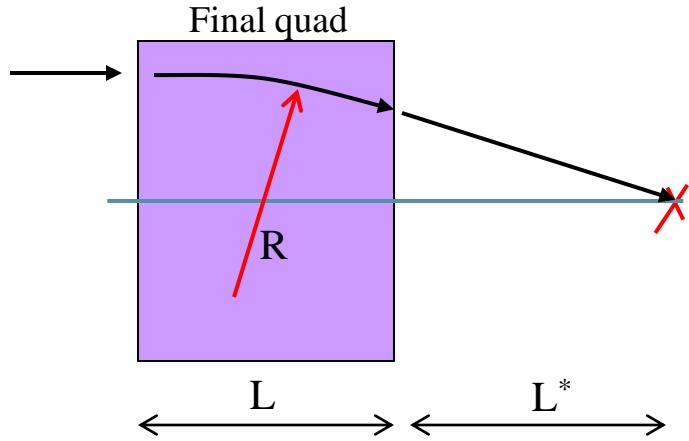
Resulting estimation for emittance growth:
$$\frac{d\epsilon_x}{dS} \approx \frac{\eta^2}{\beta_x} \frac{d((\Delta E/E)^2)}{dS} \approx \frac{\eta^2}{\beta_x} \frac{r_e \lambda_e \gamma^5}{R^3}$$

Compare with exact formula (which also takes into account the derivatives):
$$\frac{d\epsilon_x}{dS} = \frac{(\eta^2 + (\beta_x \eta' - \beta_x' \eta / 2)^2)}{\beta_x} \frac{55}{24 \sqrt{3}} \frac{r_e \lambda_e \gamma^5}{R^3}$$

$$= \mathcal{H}$$



Let's apply SR formulae to estimate Oide effect (SR in FD)



IP divergence:

$$\theta^* = \sqrt{\varepsilon/\beta^*}$$

IP size:

$$\sigma^* = \sqrt{\varepsilon \beta^*}$$

Energy spread obtained in the quad:

$$\left(\frac{\Delta E}{E}\right)^2 \approx \frac{r_e \lambda_e \gamma^5 L}{R^3}$$

Radius of curvature of the trajectory: $R = L / \theta^*$

Growth of the IP beam size: $\sigma^2 \approx \sigma_0^2 + (L^* \theta^*)^2 \left(\frac{\Delta E}{E}\right)^2$

Which gives $\sigma^2 \approx \varepsilon \beta^* + C_1 \left(\frac{L^*}{L}\right)^2 r_e \lambda_e \gamma^5 \left(\frac{\varepsilon}{\beta^*}\right)^{5/2}$ (where C_1 is ~ 7 (depend on FD params.))

This achieve minimum possible value:

$$\sigma_{\min} \approx 1.35 C_1^{1/7} \left(\frac{L^*}{L}\right)^{2/7} (r_e \lambda_e)^{1/7} (\gamma \varepsilon)^{5/7}$$

When beta* is:

$$\beta_{\text{optimal}} \approx 1.29 C_1^{2/7} \left(\frac{L^*}{L}\right)^{4/7} (r_e \lambda_e)^{2/7} \gamma (\gamma \varepsilon)^{3/7}$$

Note that beam distribution at IP will be non-Gaussian. Usually need to use tracking to estimate impact on luminosity. Note also that optimal β may be smaller than the σ_z (i.e cannot be used).



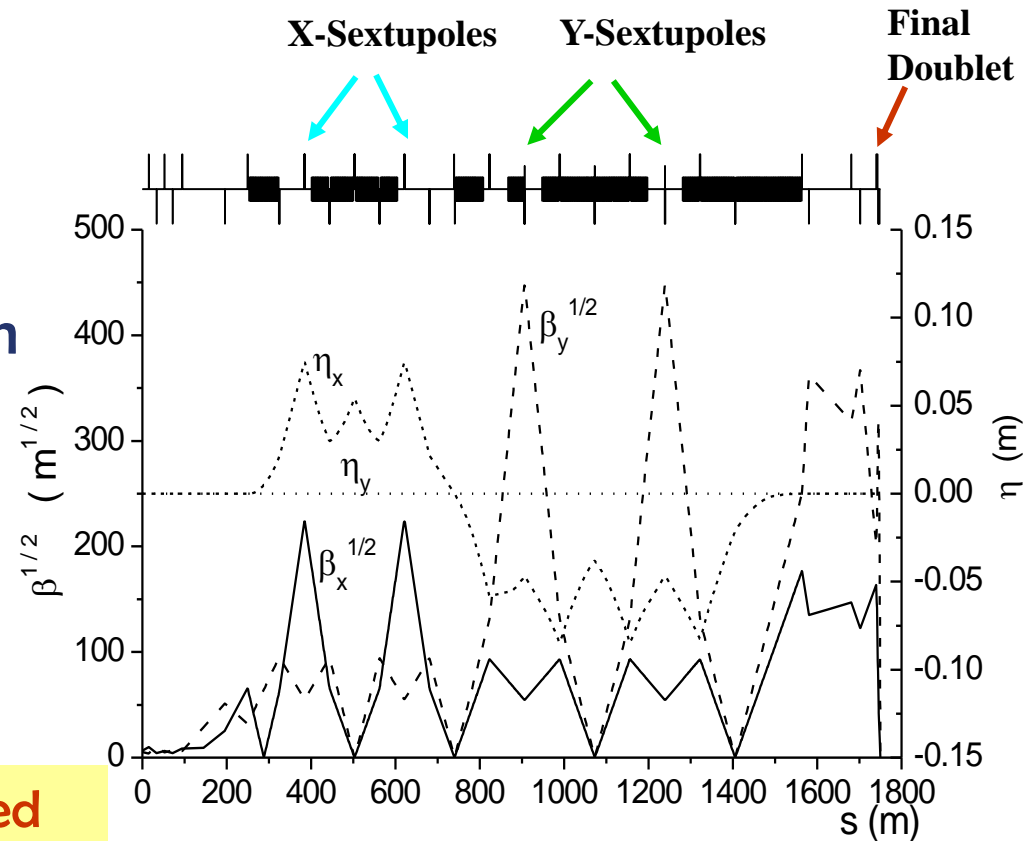
FF with non-local chromaticity compensation

- Chromaticity is compensated by sextupoles in dedicated sections
- Geometrical aberrations are canceled by using sextupoles in pairs with $M = -1$

Chromaticity arise at FD but pre-compensated 1000m upstream

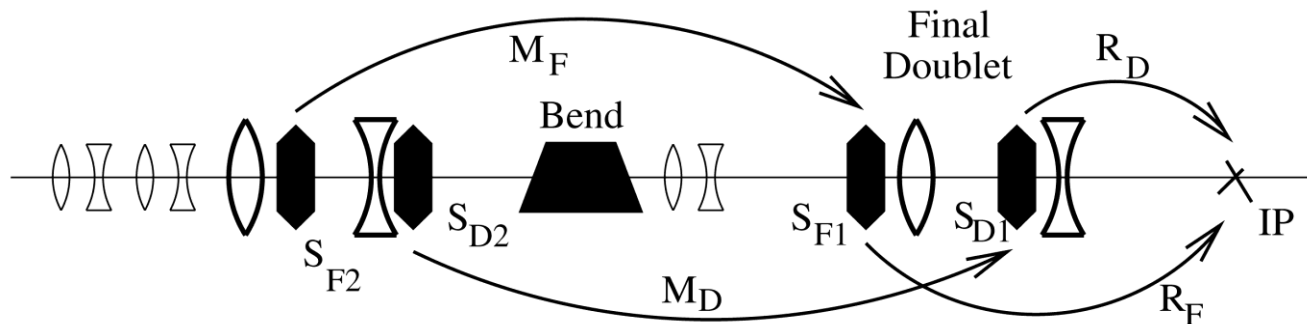
Problems:

- Chromaticity not locally compensated
 - Compensation of aberrations is not ideal since $M \neq -1$ for off energy particles
 - Large aberrations for beam tails
 - ...



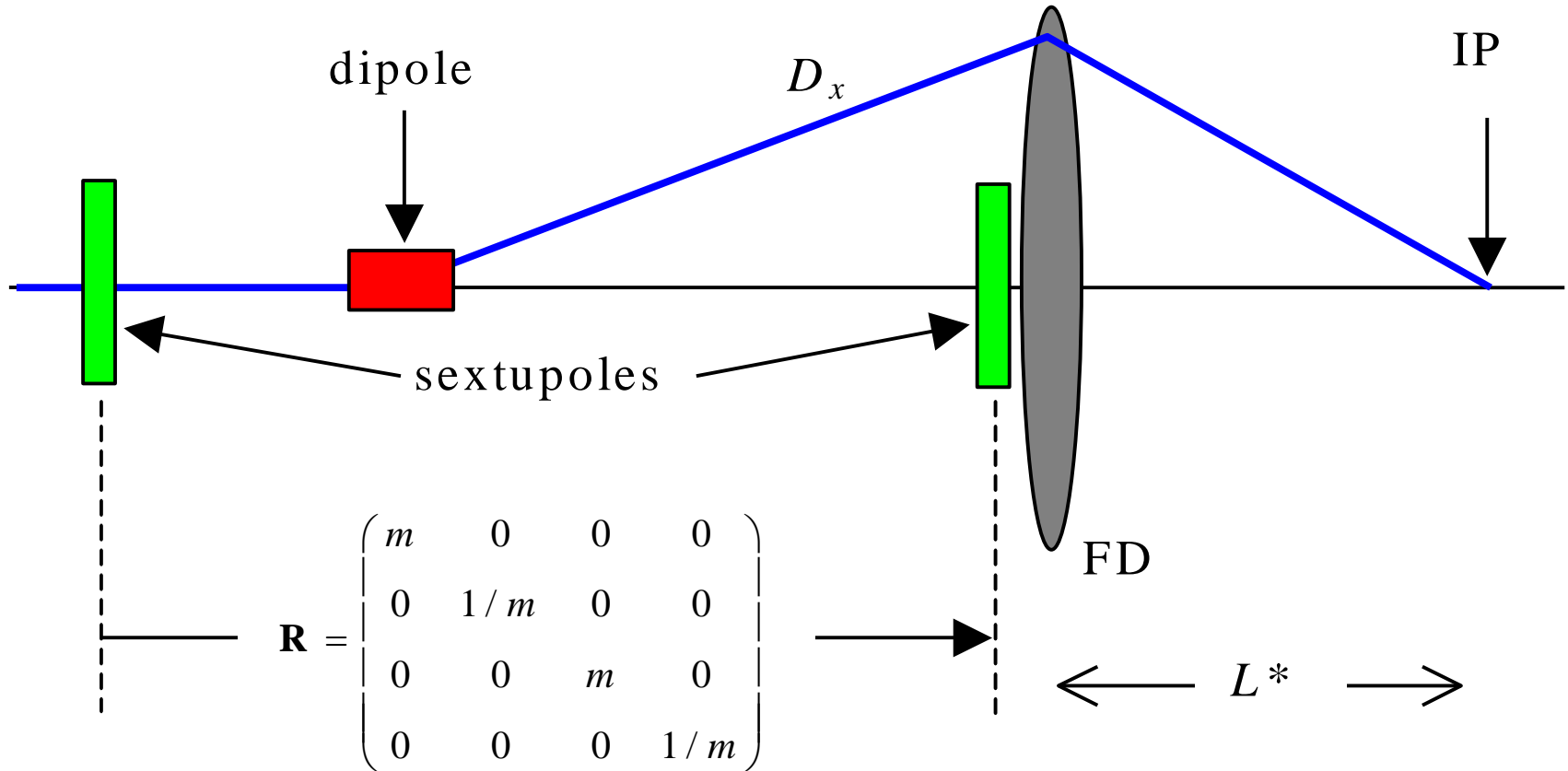
Traditional FF

FF with local chromatic correction



- **Chromaticity** is cancelled locally by two sextupoles interleaved with FD, a bend upstream generates dispersion across FD
- **Geometric aberrations** of the FD sextupoles are cancelled by two more sextupoles placed in phase with them and upstream of the bend

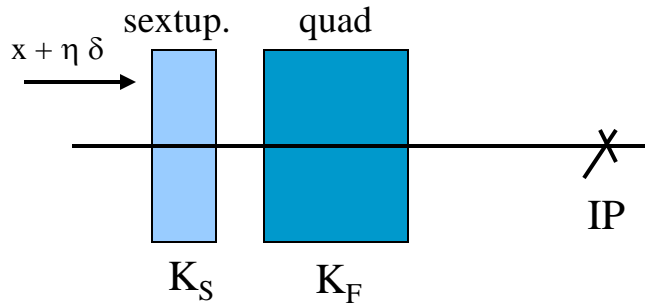
Local chromatic correction



- The value of dispersion in FD is usually chosen so that it does not increase the beam size in FD by more than 10-20% for typical beam energy spread



Chromatic correction in FD



- Straightforward in Y plane
- a bit tricky in X plane:

Quad: $\Delta x' = \frac{K_F}{(1 + \delta)}(x + \eta\delta) \Rightarrow K_F(-\delta x - \eta\delta^2)$

chromaticity

Second order dispersion

Sextupole: $\Delta x' = \frac{K_S}{2}(x + \eta\delta)^2 \Rightarrow K_S\eta\left(\delta x + \frac{\eta\delta^2}{2}\right)$

If we require $K_S\eta = K_F$ to cancel FD chromaticity, then half of the **second order dispersion** remains.

$\Delta x' = \frac{K_F}{(1 + \delta)}(x + \eta\delta) + \frac{K_{\beta\text{-match}}}{(1 + \delta)}x \Rightarrow 2K_F\left(-\delta x - \frac{\eta\delta^2}{2}\right)$

Solution:

The β -matching section produces as much X chromaticity as the FD, so the X sextupoles run twice stronger and cancel the **second order dispersion** as well.

$$K_{\beta\text{-match}} = K_F \quad K_S = \frac{2K_F}{\eta}$$



Definitions of chromaticity

1st : TRANSPORT

Storage Rings: chromaticity defined as a change of the betatron tunes versus energy.

In single path beamlines, it is more convenient to use other definitions.

$$\mathbf{x}_i = \begin{pmatrix} x \\ x' \\ y \\ y' \\ \Delta l \\ \delta \end{pmatrix} \quad \mathbf{x}_i^{\text{out}} = \mathbf{R}_{ij} \mathbf{x}_j^{\text{in}}$$

The second, third, and so on terms are included in a similar manner:

$$\mathbf{x}_i^{\text{out}} = \mathbf{R}_{ij} \mathbf{x}_j^{\text{in}} + \mathbf{T}_{ijk} \mathbf{x}_j^{\text{in}} \mathbf{x}_k^{\text{in}} + \mathbf{U}_{ijkn} \mathbf{x}_j^{\text{in}} \mathbf{x}_k^{\text{in}} \mathbf{x}_n^{\text{in}} + \dots$$

In FF design, we usually call ‘chromaticity’ the second order elements T_{126} and T_{346} . All other high order terms are just ‘aberrations’, purely chromatic (as T_{166} , which is second order dispersion), or chromo-geometric (as U_{32446}).



Definitions of chromaticity

2nd : W functions

Lets assume that betatron motion without energy offset is described by twiss functions α_1 and β_1 and with energy offset δ by functions α_2 and β_2

Let's define chromatic function \mathbf{W} (for each plane) as $W = (i A + B) / 2$ where $i = \sqrt{-1}$

And where:
$$B = \frac{\beta_2 - \beta_1}{\delta (\beta_2 \cdot \beta_1)^{1/2}} \approx \frac{\Delta\beta}{\delta \beta} \quad \text{and} \quad A = \frac{\alpha_2\beta_1 - \alpha_1\beta_2}{\delta (\beta_2 \cdot \beta_1)^{1/2}} \approx \frac{\Delta\alpha}{\delta} - \frac{\alpha}{\beta} \frac{\Delta\beta}{\delta}$$

Using familiar formulae
$$\frac{d\beta}{ds} = -2\alpha \quad \text{and} \quad \frac{d\alpha}{ds} = K \cdot \beta - \frac{(1 + \alpha^2)}{\beta} \quad \text{where} \quad K = \frac{e}{pc} \frac{dB_y}{dx}$$

And introducing
$$\Delta K = \frac{K(\delta - K(0))}{\delta} \approx -K$$
 we obtain the equation for \mathbf{W} evolution:

Can you show this?

$$\rightarrow \frac{dW}{ds} = \frac{2i}{\beta} W + \frac{i}{2} \beta \Delta K$$

knowing that the betatron phase is

$$\frac{d\Phi}{ds} = \frac{1}{\beta}$$

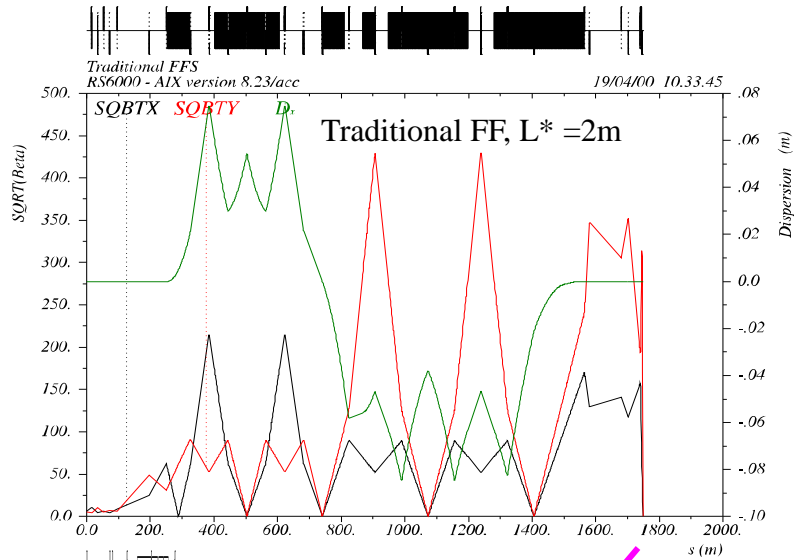
can see that if $\Delta K=0$, then \mathbf{W} rotates with double betatron frequency and stays constant in amplitude. In quadrupoles or sextupoles, only imaginary part changes.

Show that if in a final defocusing lens $\alpha=0$, then it gives $\Delta W=L^*/(2\beta^*)$

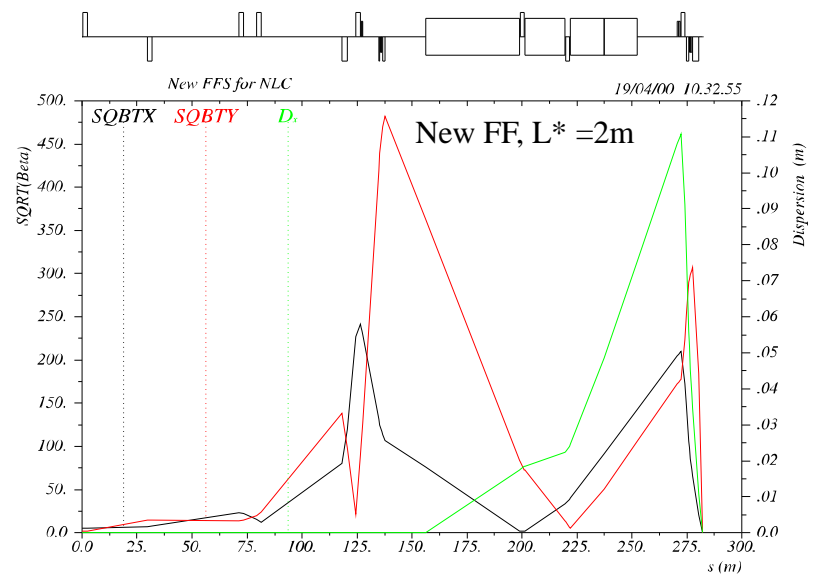
Show that if T_{346} is zeroed at the IP, the W_y is also zero. Use approximation $\Delta R_{34}=T_{346}^* \delta$, use $R_{34}=(\beta\beta_0)^{1/2} \sin(\Delta\Phi)$, and the twiss equation for $d\alpha/d\Phi$.



Compare FF designs

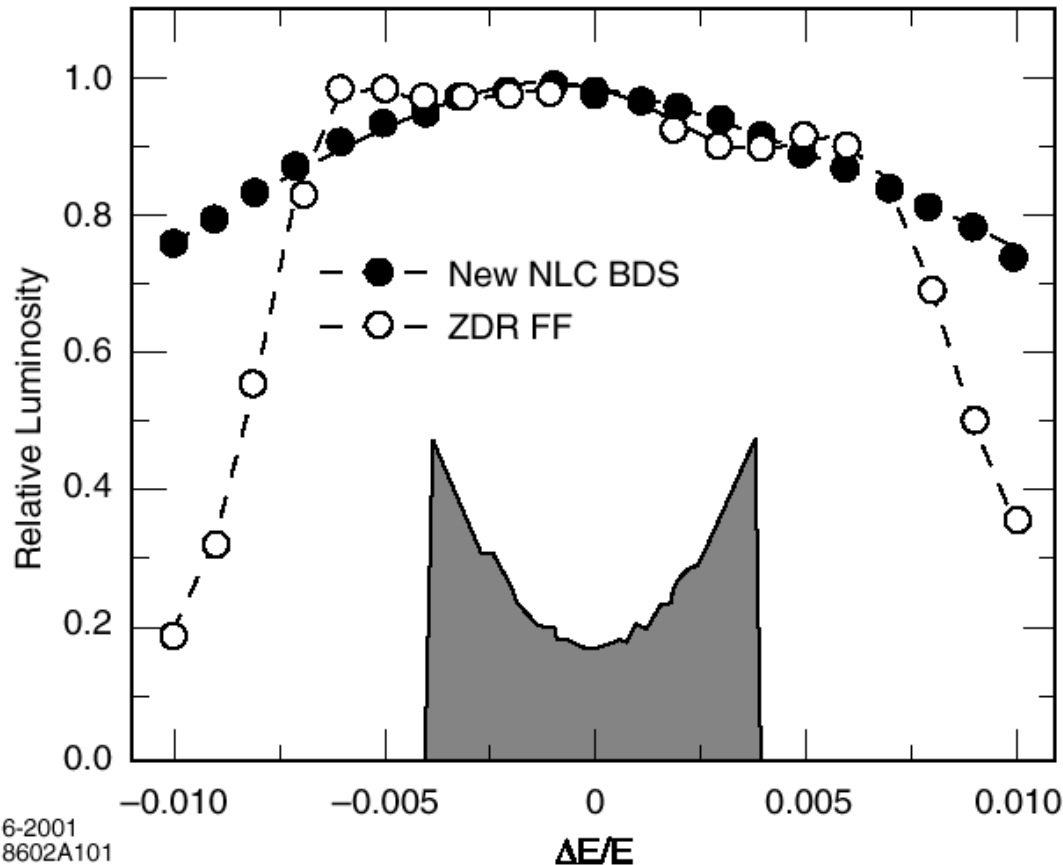


FF with local chromaticity compensation with the same performance can be ~300m long, i.e. 6 times shorter



new FF

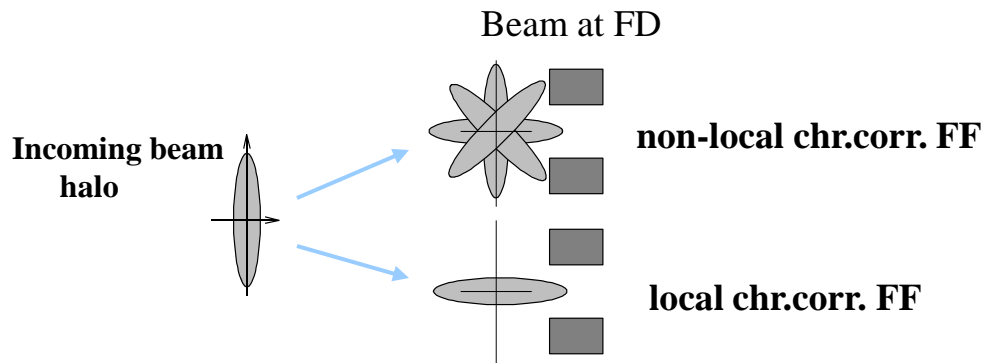
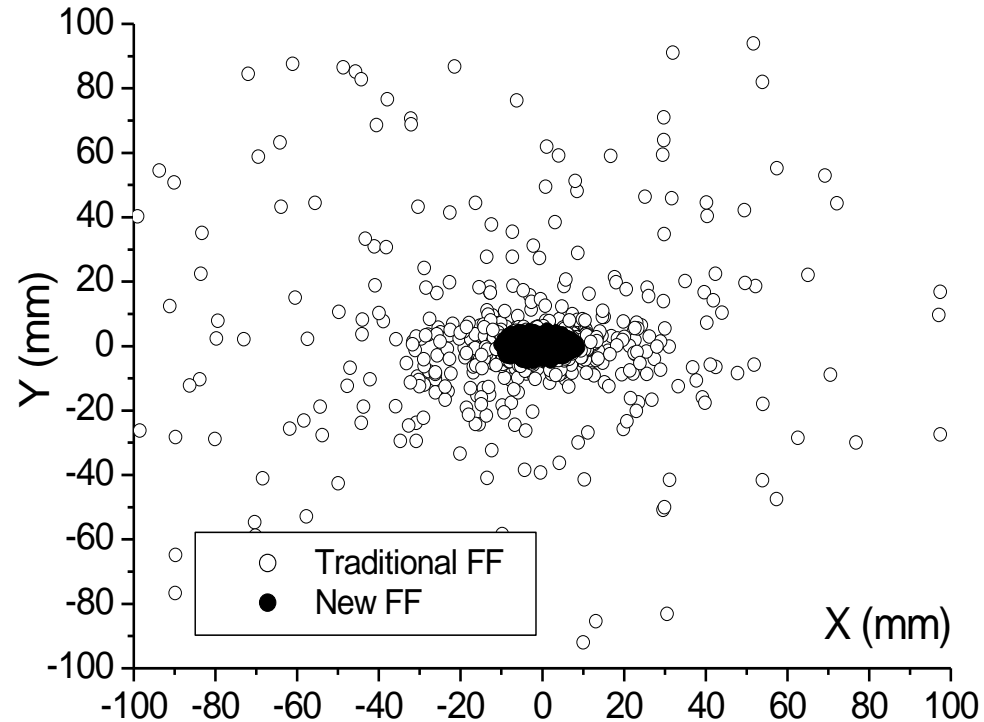
IP bandwidth



Bandwidth of FF with local chromaticity correction can be better than for system with non-local correction

Aberrations & halo generation in FF

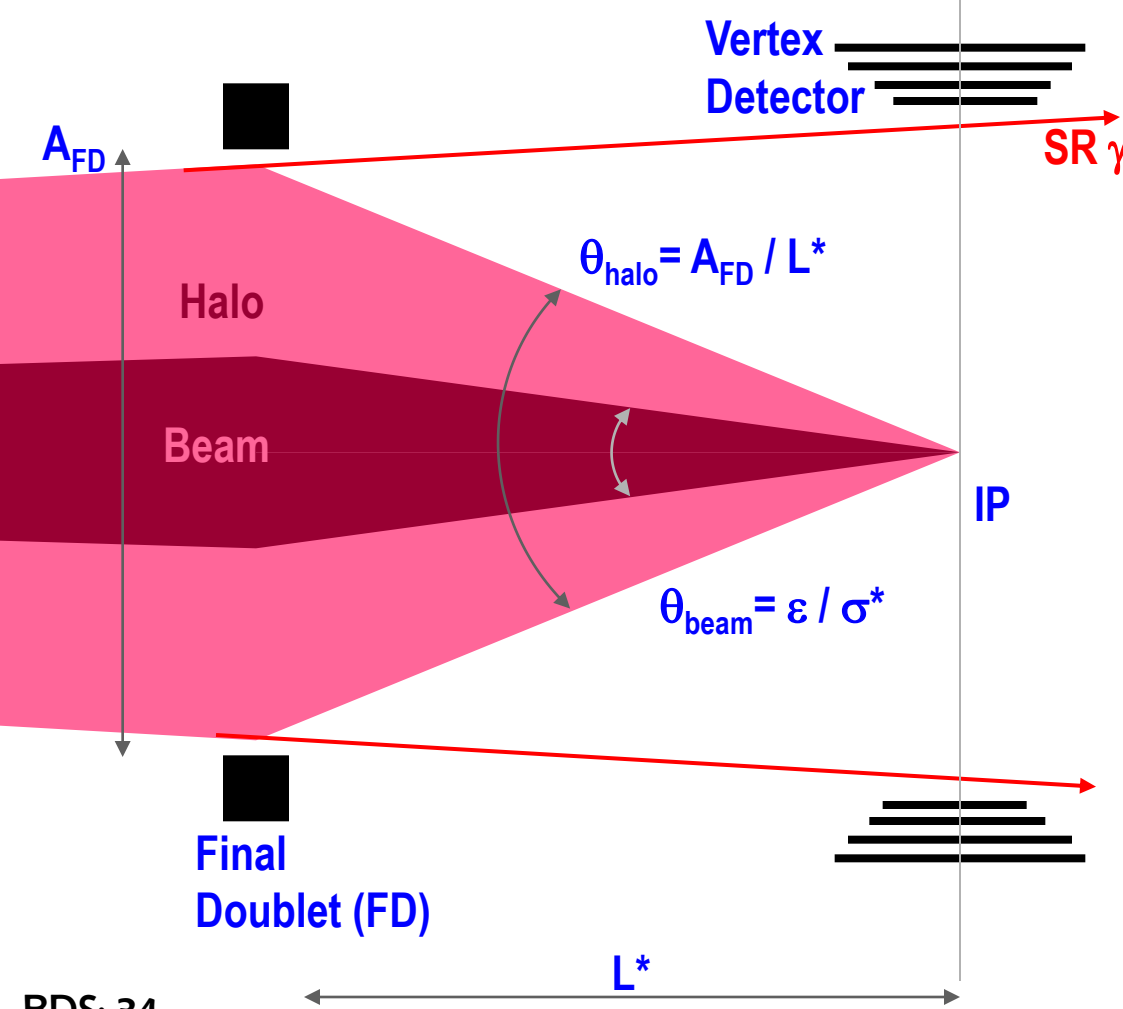
- FF with non-local chr. corr. generate beam tails due to aberrations and it does not preserve betatron phase of halo particles
- FF with local chr. corr. has much less aberrations and it does not mix phases particles



**Halo beam at the FD entrance.
Incoming beam is ~ 100 times larger than nominal beam**

Beam halo & collimation

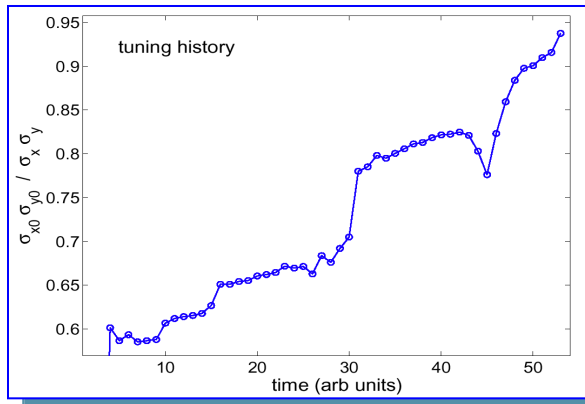
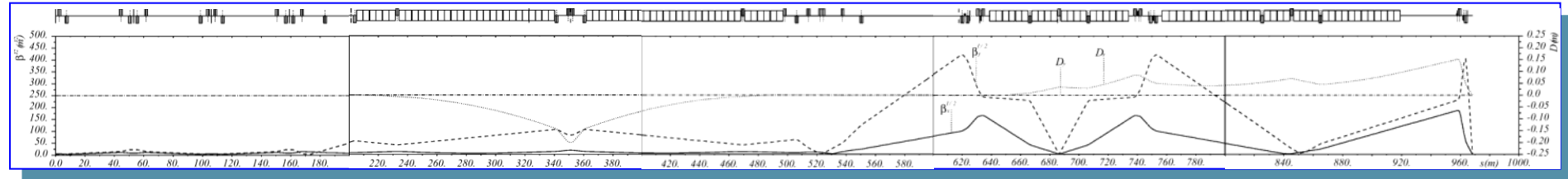
- Even if final focus does not generate beam halo itself, the halo may come from upstream and need to be collimated



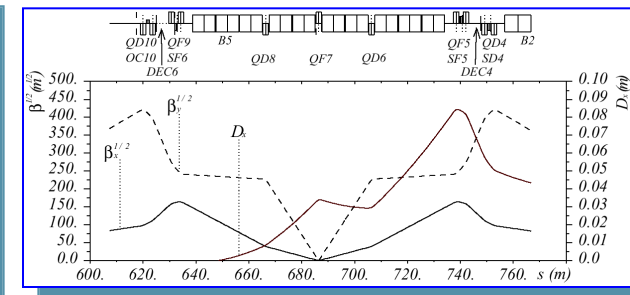
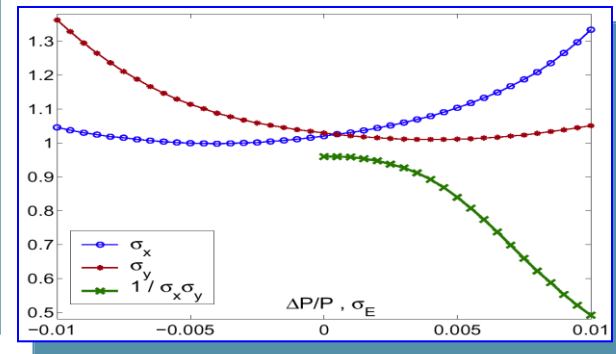
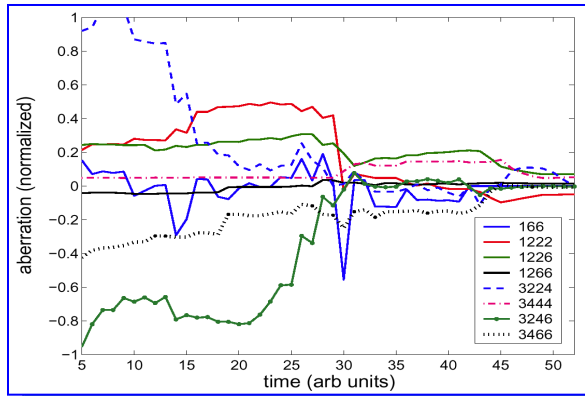
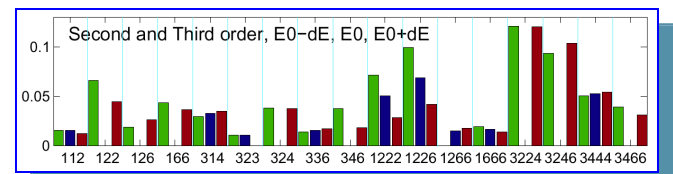
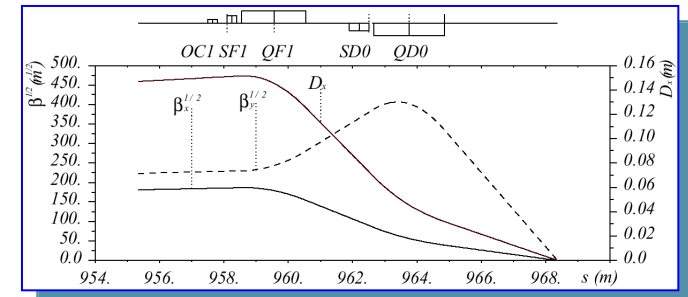
- Halo must be collimated upstream in such a way that SR γ & halo e^+ do not touch VX and FD
- \Rightarrow VX aperture needs to be somewhat larger than FD aperture
- Exit aperture is larger than FD or VX aperture
- Beam convergence depend on parameters, the halo convergence is fixed for given geometry
- $\Rightarrow \theta_{halo} / \theta_{beam}$ (collimation depth) becomes tighter with larger L^* or smaller IP beam size
- Tighter collimation \Rightarrow MPS issues, collimation wake-fields, higher muon flux from collimators, etc.



BDS design methods & examples



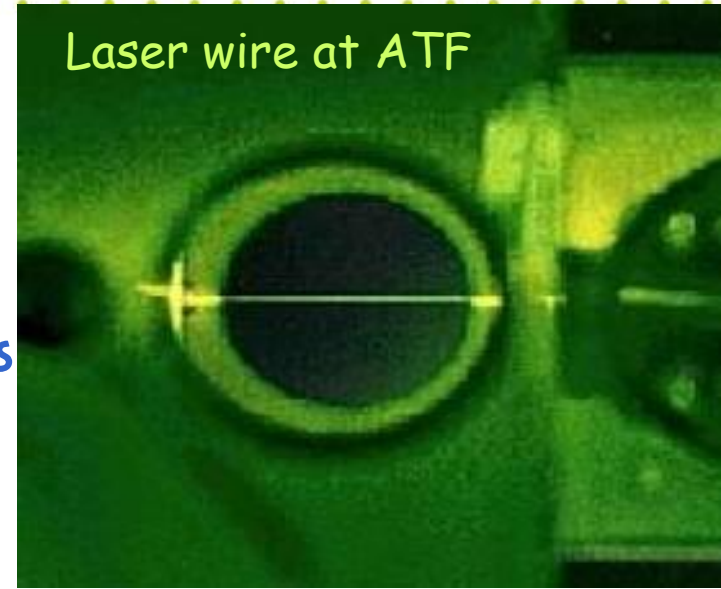
Example of a 2nd IR BDS optics for ILC; design history; location of design knobs



In a practical situation ...

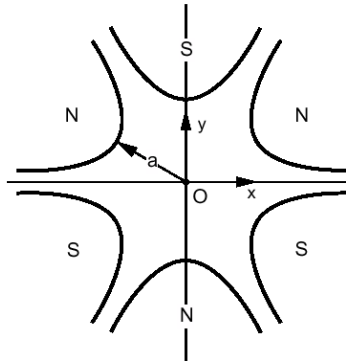
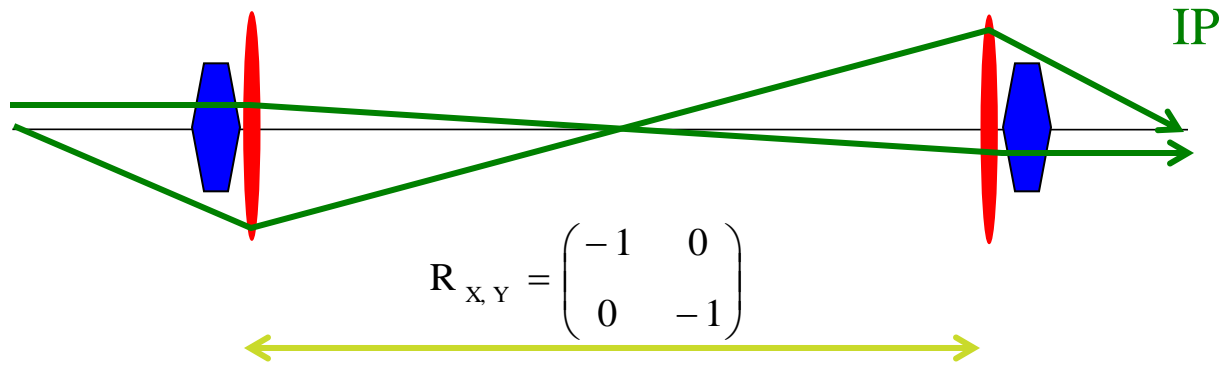
- While **designing** the FF, one has a **total control**
- When the system is built, one has just limited number of observable parameters (measured orbit position, beam size measured in several locations)
- The system, however, may initially have **errors** (errors of strength of the elements, transverse misalignments) and initial aberrations may be large
- **Tuning** of FF is done by optimization of “**knobs**” (strength, position of group of elements) chosen to affect some particular aberrations
- Experience in SLC FF and FFTB, and simulations with new FF give confidence that this is possible

Laser wire at ATF



Laser wire will be a tool for tuning and diagnostic of FF

Sextupole knobs for BDS tuning



SEXTUPOLE

Second order effect:

$$x' = x' + S (x^2 - y^2)$$

$$y' = y' - S 2xy$$

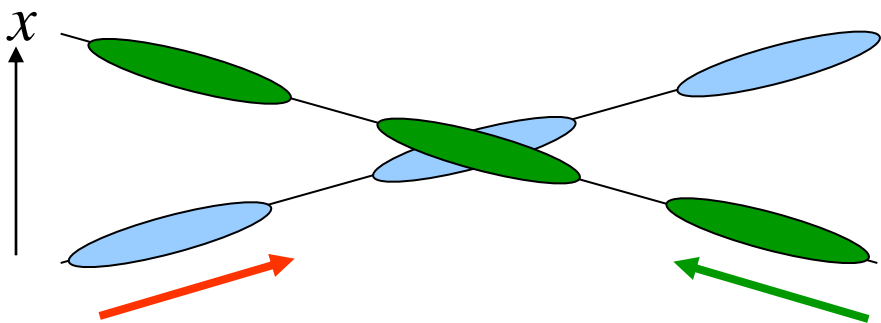
- Combining offsets of sextupoles (symmetrical or anti-symmetrical in X or Y), one can produce the following corrections at the IP

- waist shift
- coupling
- dispersion

To create these knobs, sextupole placed on movers



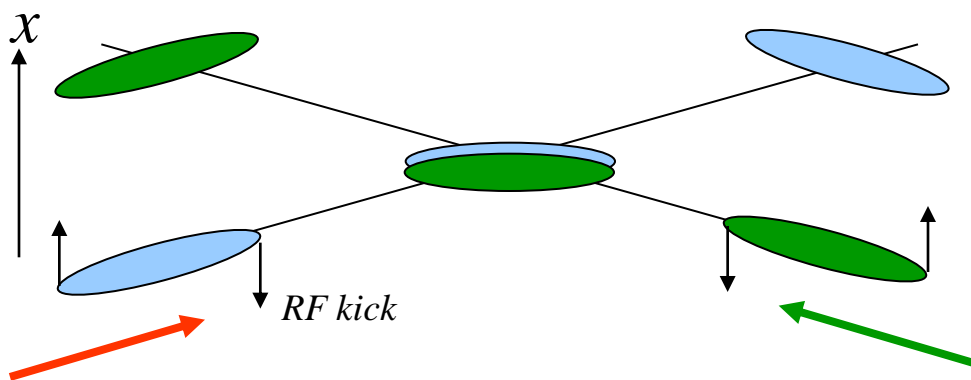
Crab crossing



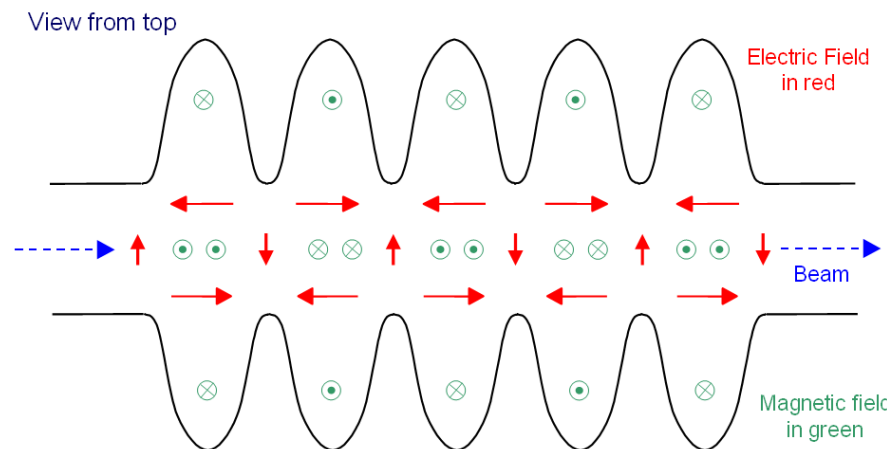
With crossing angle θ_c , the projected x-size is

$$(\sigma_x^2 + \theta_c^2 \sigma_z^2)^{0.5} \sim \theta_c \sigma_z \sim 4 \mu\text{m}$$

→ several time reduction in L without corrections



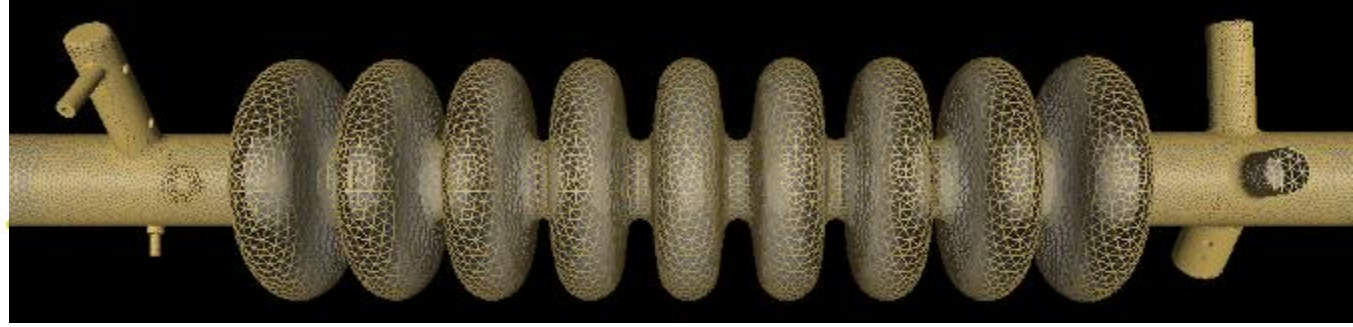
Use transverse (crab) RF cavity to ‘tilt’ the bunch at IP



For a crab cavity the bunch centre is at the cell centre when E is maximum and B is zero



Crab cavity design

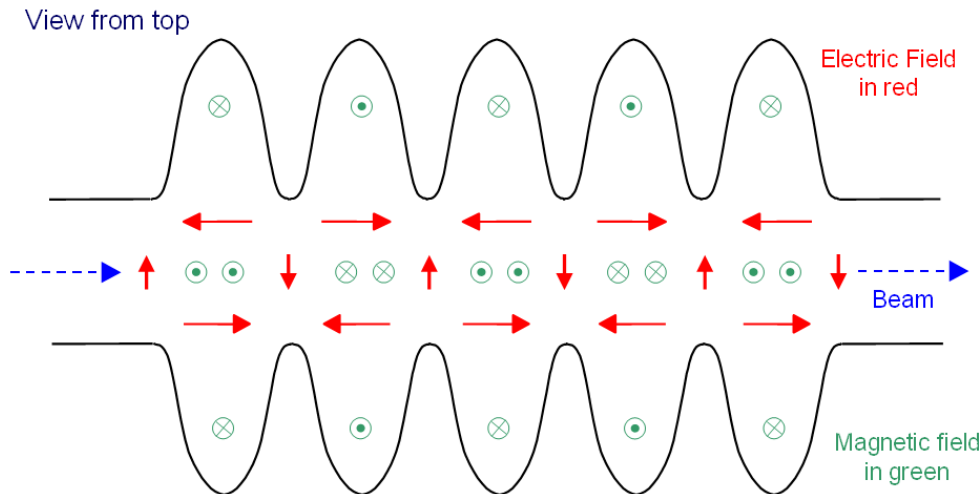


FNAL 3.9GHz 9-cell cavity in Opega3p. *K.Ko, et al*



3.9GHz cavity achieved 7.5 MV/m (FNAL)

- Prototypes of crab cavity built at FNAL and 3d RF models
- Design & prototypes been done by UK-FNAL-SLAC collaboration



For a crab cavity the bunch centre is at the cell centre when E is maximum and B is zero

TM110 Dipole mode cavity



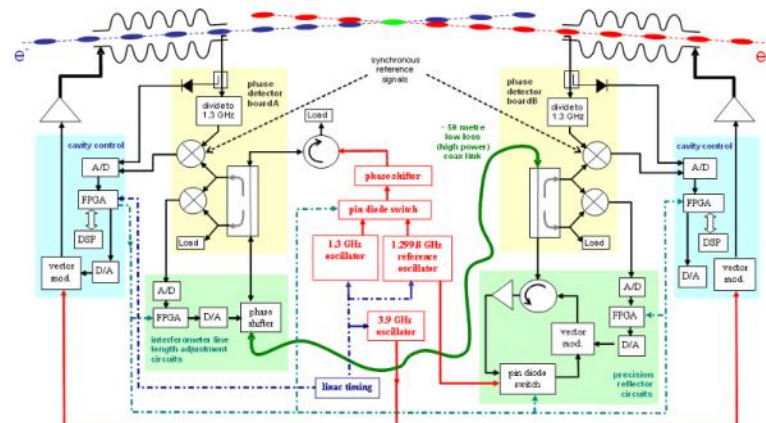
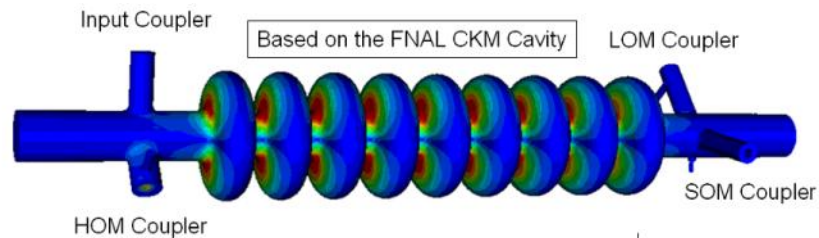
Crab cavity



Cavities limited in gradient to 1 MV/m (~40kV/cell) – shielding implications.

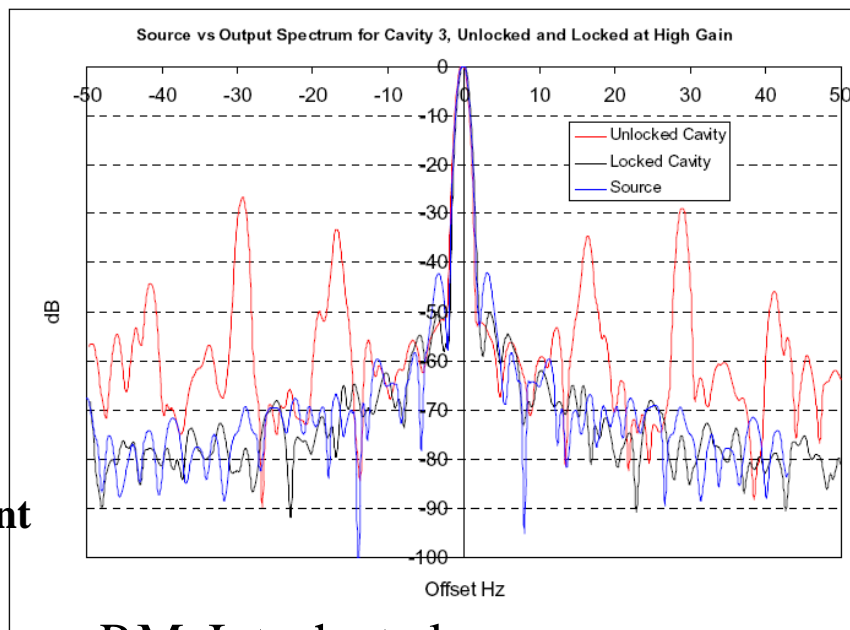


SLAC ACD



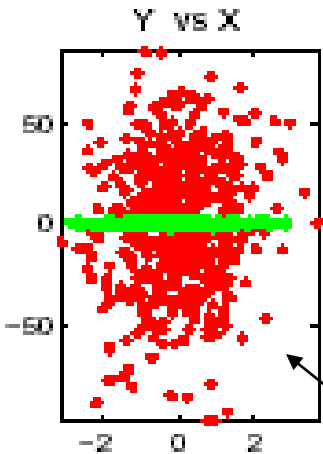
Independent phase lock achieved for both cavities:

- Unlocked => 10° r.m.s.
- Locked => 0.135° r.m.s.
- Performance limited by:
 - Source noise (dominant); ADC noise; Measurement noise;
 - Cavity frequency drift; Microphonics
- Improvements being made; new tests being prepared

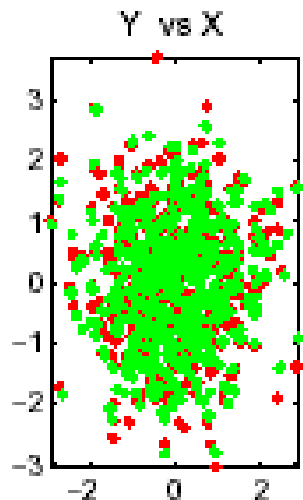


P.McIntosh at al

IR coupling compensation



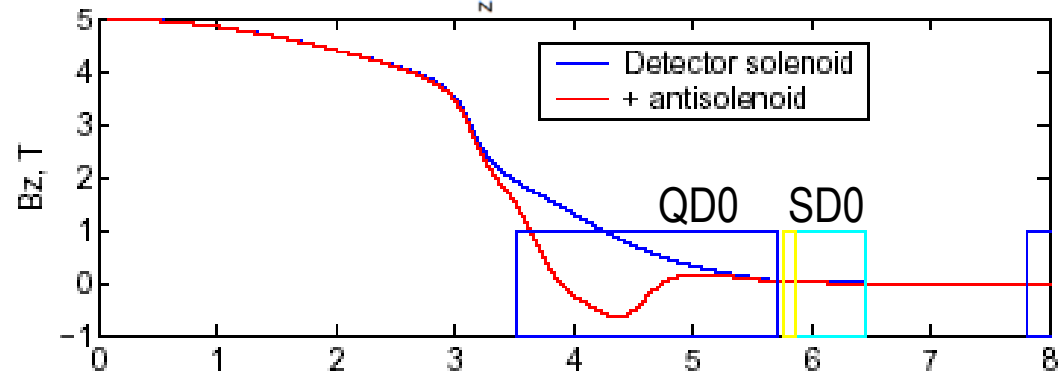
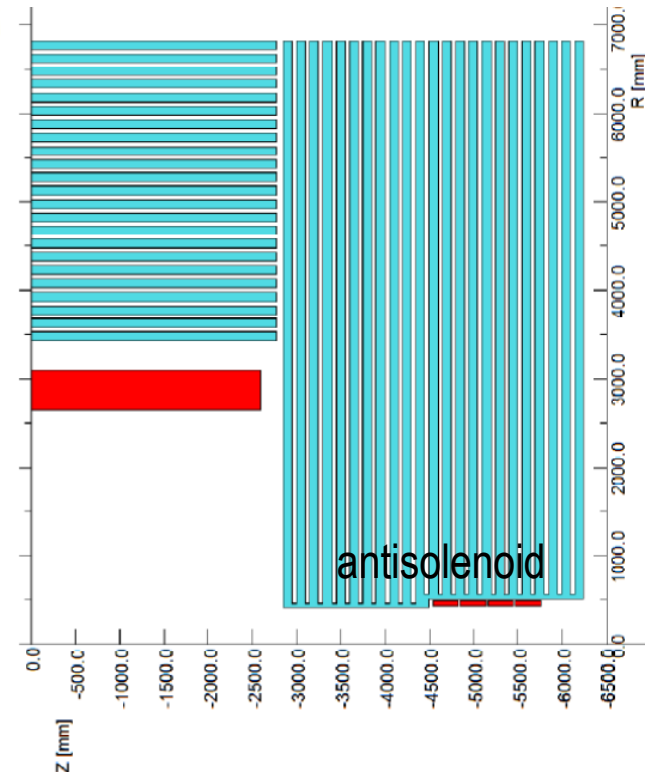
without compensation
 $\sigma_y / \sigma_y(0) = 32$



with compensation by antisolenoid
 $\sigma_y / \sigma_y(0) < 1.01$

When detector solenoid overlaps QD0, coupling between y & x' and y & E causes large (30 – 190 times) increase of IP size (green=detector solenoid OFF, red=ON)

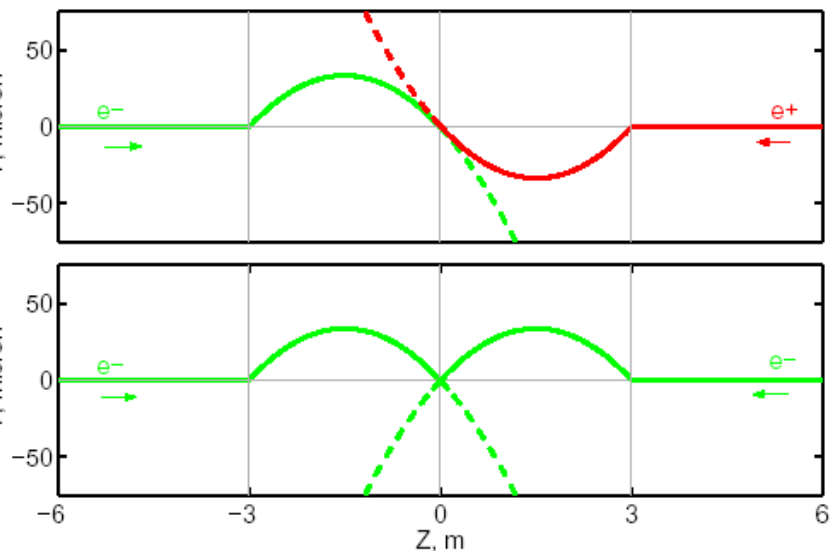
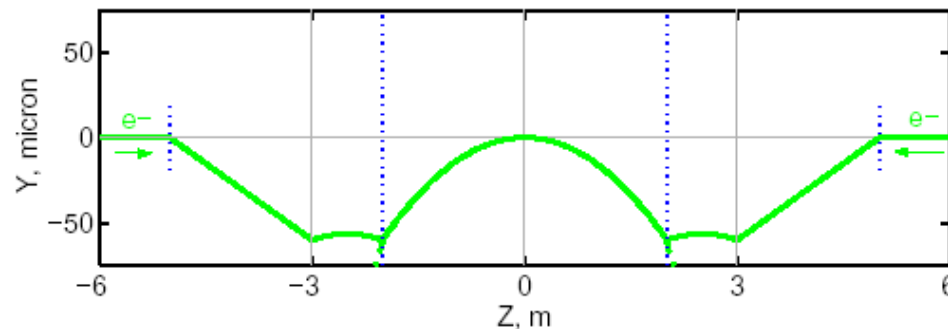
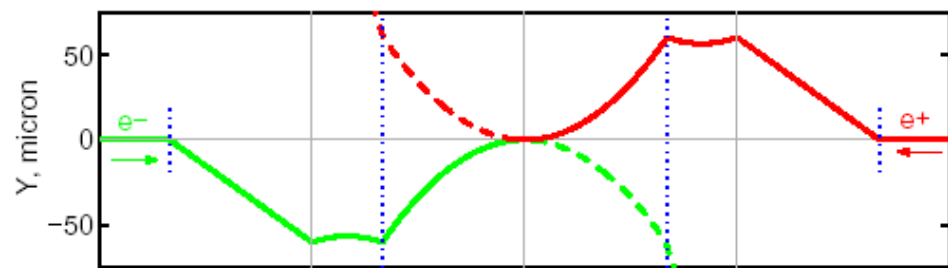
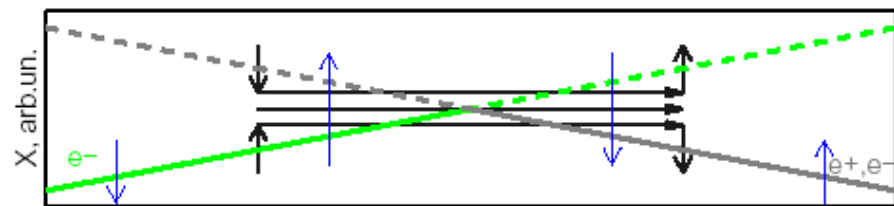
Even though traditional use of skew quads could reduce the effect, the local compensation of the fringe field (with a little skew tuning) is the most efficient way to ensure correction over wide range of beam energies



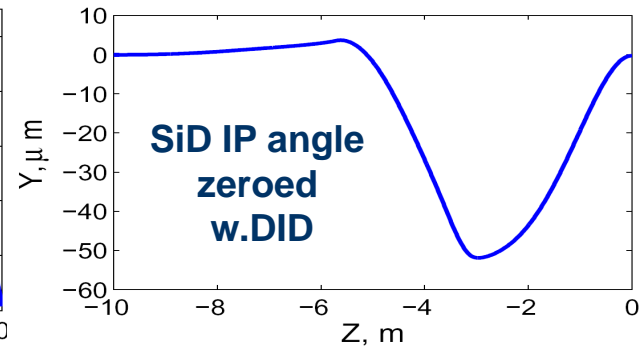
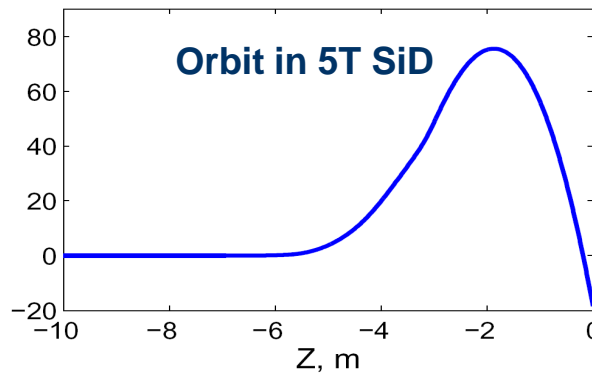


Detector Integrated Dipole

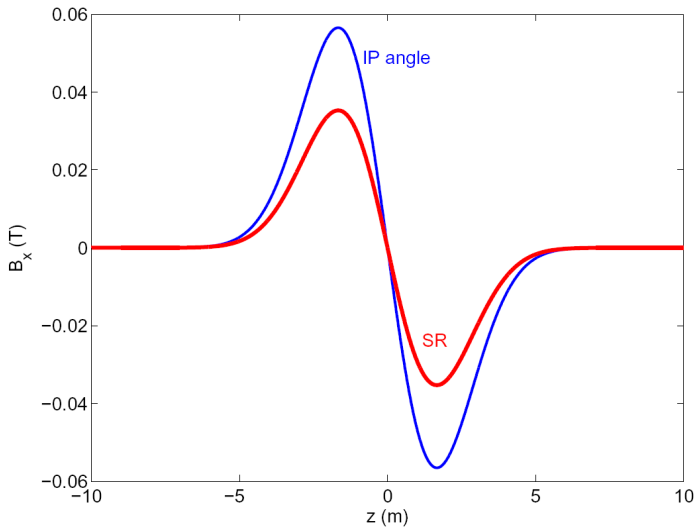
- With a crossing angle, when beams cross solenoid field, vertical orbit arise
- For e^+e^- the orbit is anti-symmetrical and beams still collide head-on
- If the vertical angle is undesirable (to preserve spin orientation or the e^-e^- luminosity), it can be compensated locally with DID
- Alternatively, negative polarity of DID may be useful to reduce angular spread of beam-beam pairs (anti-DID)



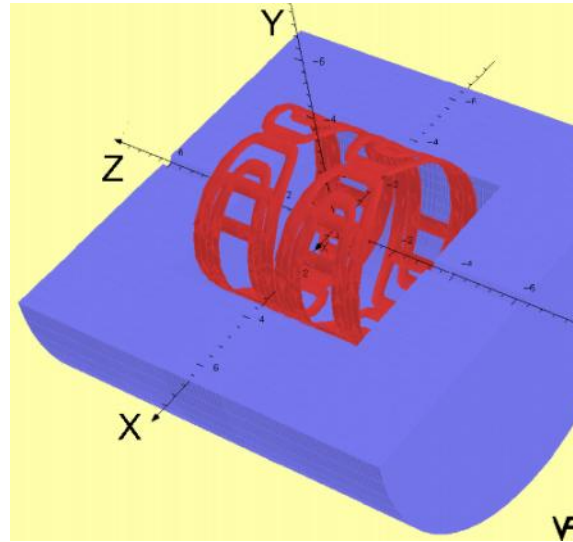
Use of DID or anti-DID



DID field shape and scheme



DID case

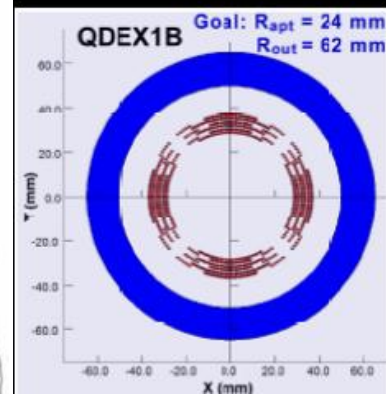
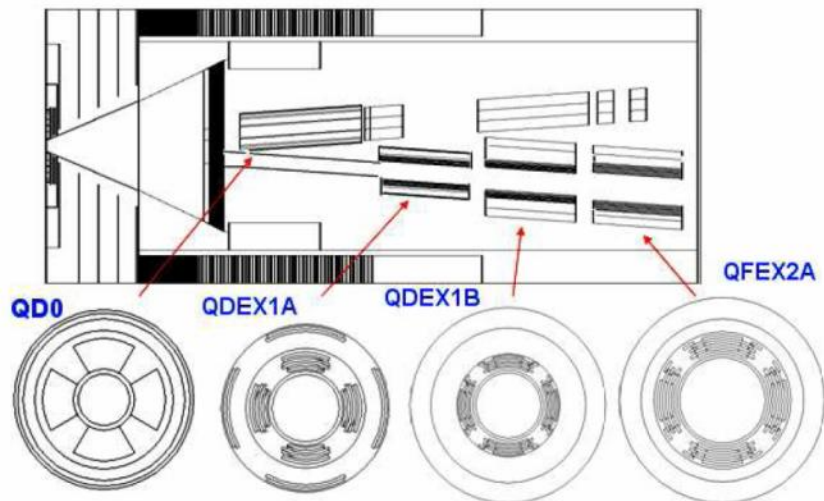
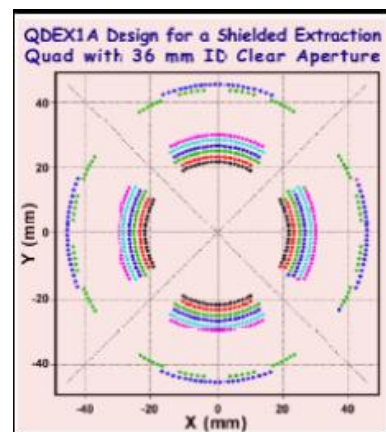
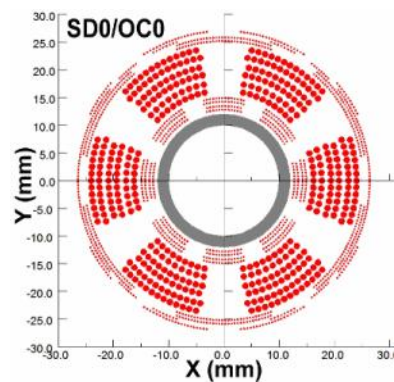
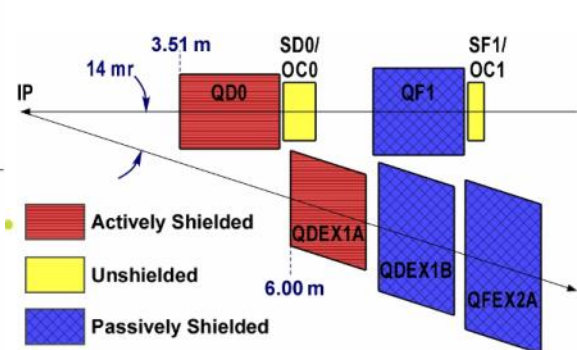
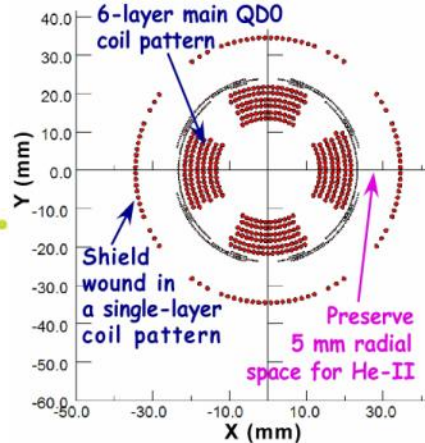
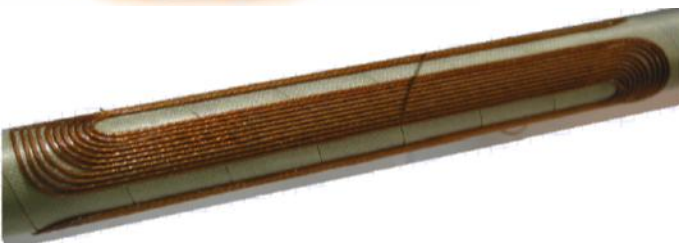
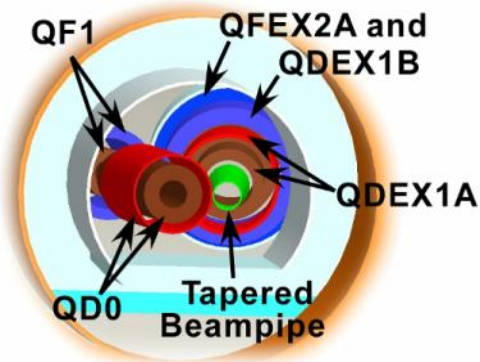
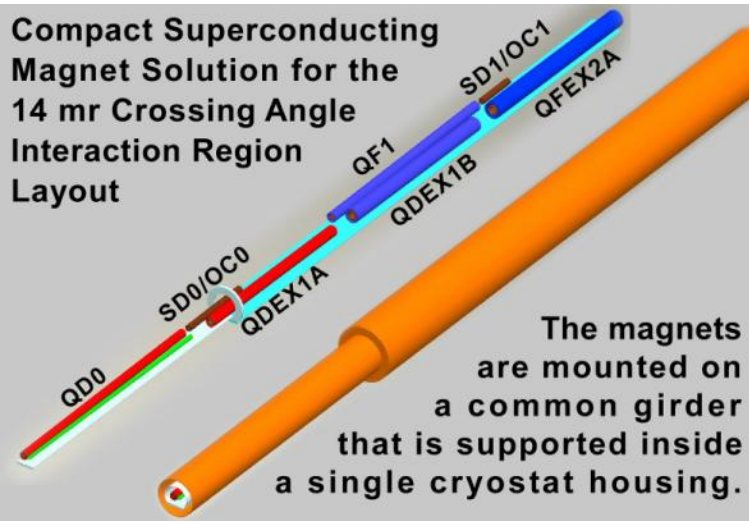


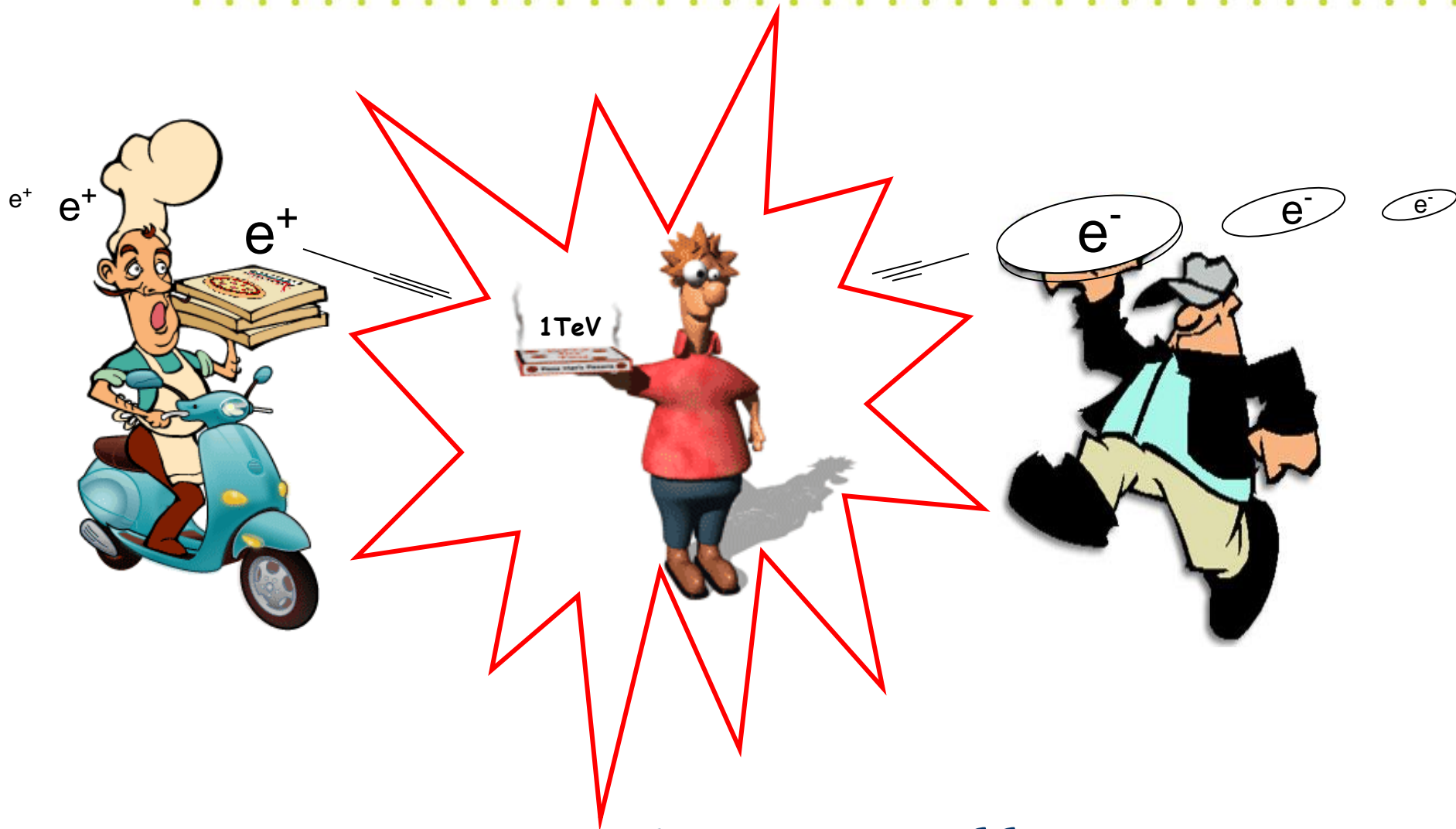
- The negative polarity of DID is also possible (called anti-DID)
- In this case the vertical angle at the IP is somewhat increased, but the background conditions due to low energy pairs (see below) and are improved



14 mrad IR

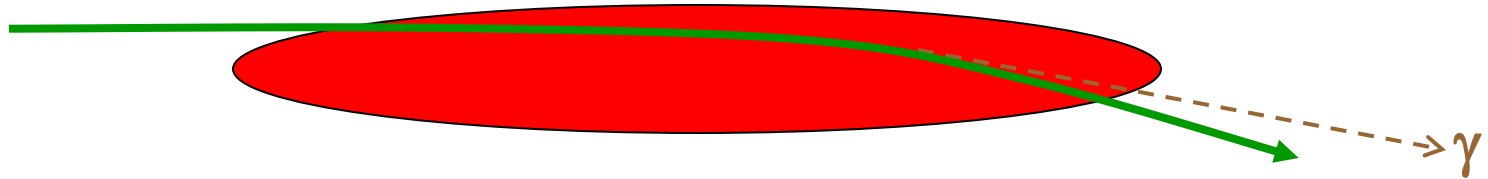
Compact Superconducting Magnet Solution for the 14 mr Crossing Angle Interaction Region Layout





Beam-beam effects

Beam-beam interactions



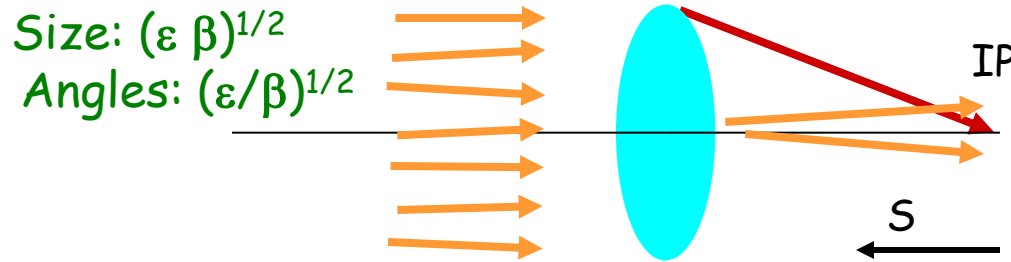
- Transverse fields of ultra-relativistic bunch
 - focus the incoming beam (electric and magnetic force add)
 - reduction of beam cross-section leads to more luminosity
 - H_D - the luminosity enhancement factor
 - bending of the trajectories leads to emission of beamstrahlung



Parameters of ILC BDS

Length (linac exit to IP distance)/side	m	2226
Length of main (tune-up) extraction line	m	300 (467)
Max Energy/beam (with more magnets)	GeV	250 (500)
Distance from IP to first quad, L^*	m	3.5-(4.5)
Crossing angle at the IP	mrad	14
Nominal beam size at IP, σ^* , x/y	nm	655/5.7
Nominal beam divergence at IP, θ^* , x/y	μrad	31/14
Nominal beta-function at IP, β^* , x/y	mm	21/0.4
<u>Nominal bunch length, σ_z</u>	<u>μm</u>	<u>300</u>
<u>Nominal disruption parameters, x/y</u>		<u>0.162/18.5</u>
Nominal bunch population, N		2×10^{10}
Max beam power at main and tune-up dumps	MW	18
Preferred entrance train to train jitter	σ	< 0.5
Preferred entrance bunch to bunch jitter	σ	< 0.1
Typical nominal collimation depth, x/y		8–10/60
Vacuum pressure level, near/far from IP	nTorr	1/50

Hour-glass effect



Size at IP: $L^* (\epsilon/\beta)^{1/2}$

Beta at IP:

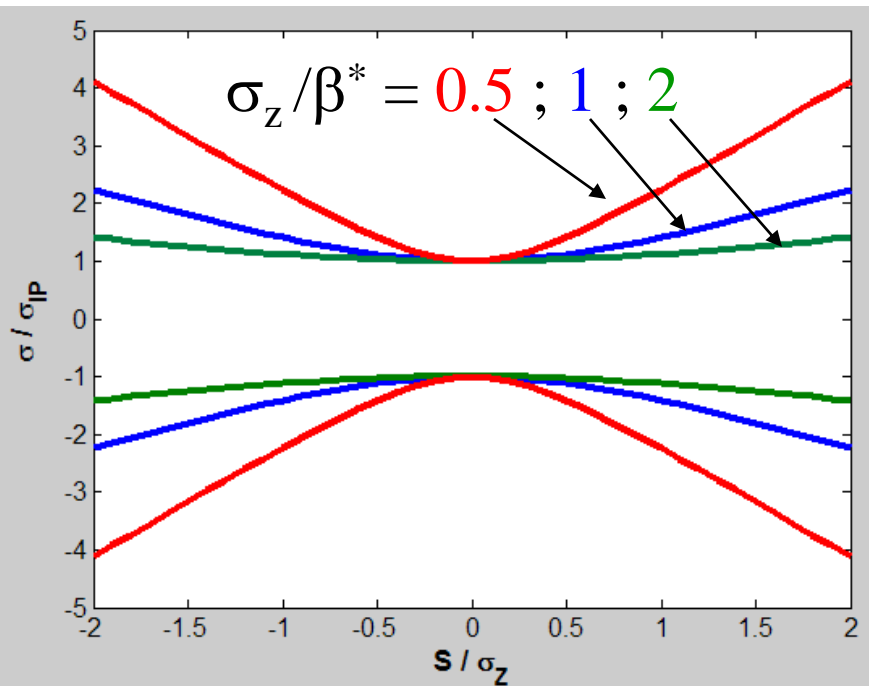
$$L^* (\epsilon/\beta)^{1/2} = (\epsilon \beta^*)^{1/2}$$

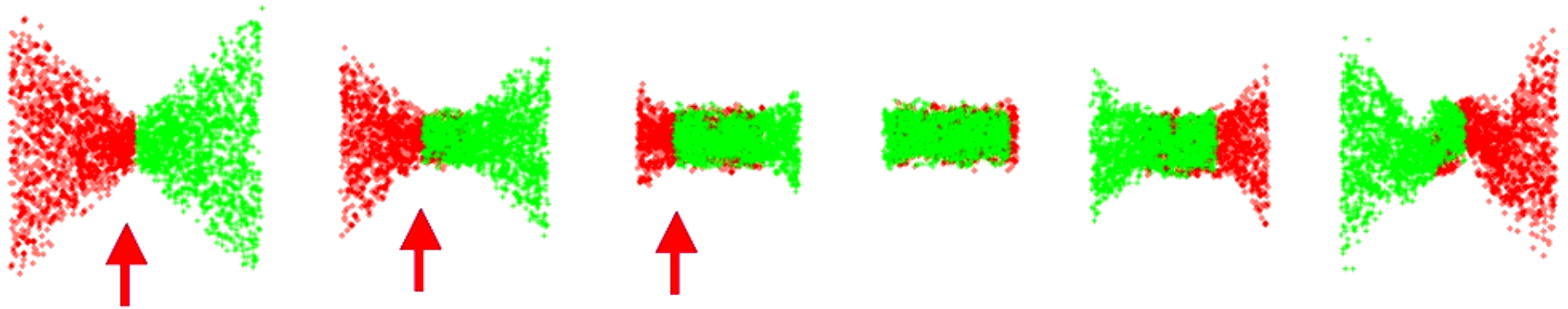
$$\Rightarrow \beta^* = L^{*2}/\beta$$

Behavior of beta-function along the final drift:

$$(\beta)^{1/2} = (\beta^* + S^2/\beta^*)^{1/2}$$

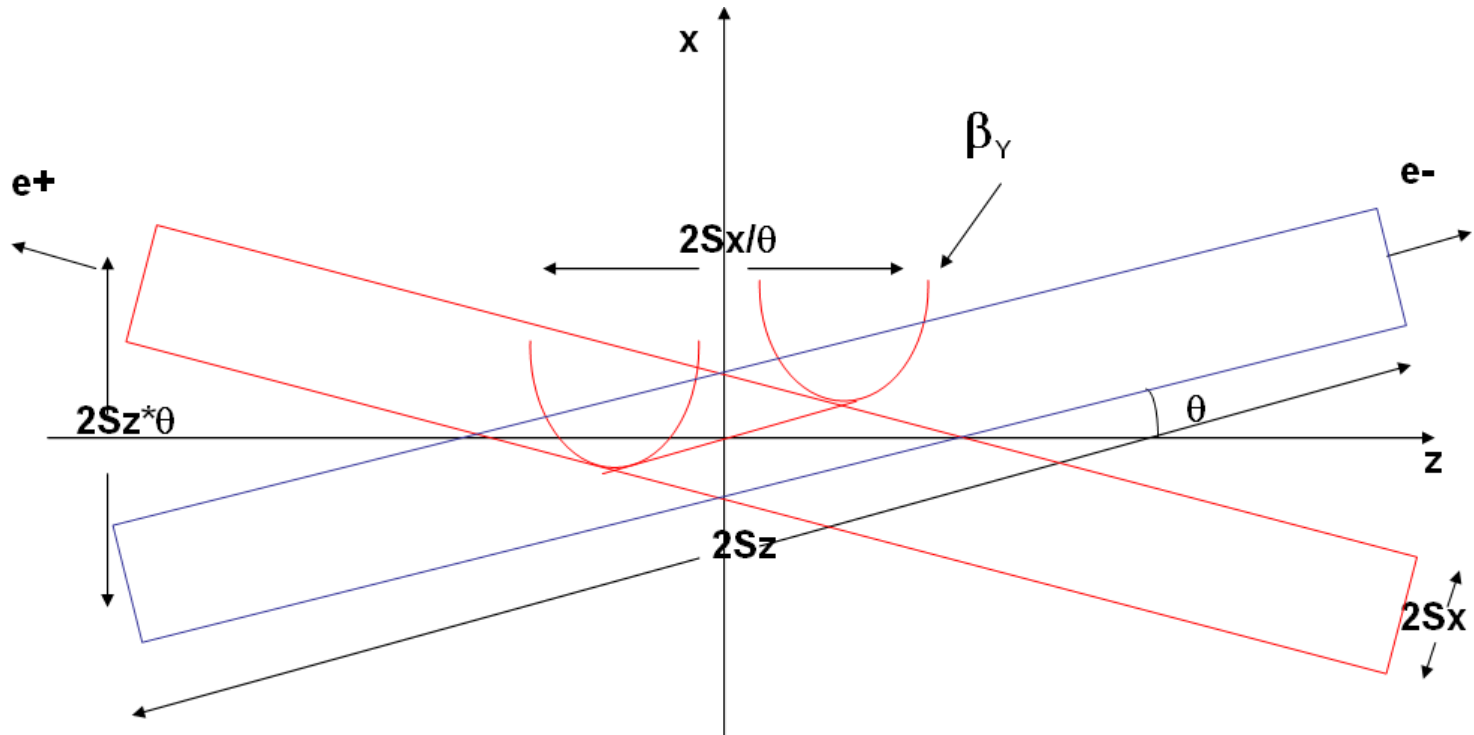
Reduction of β^* below σ_z does not give further decrease of effective beam size (usually)





- Suggested by V.Balakin – idea is to use beam-beam forces for additional focusing of the beam – allows some gain of luminosity or overcome somewhat the hour-glass effect
- Figure shows simulation of traveling focus. The arrows show the position of the focus point during collision
- So far not yet used experimentally

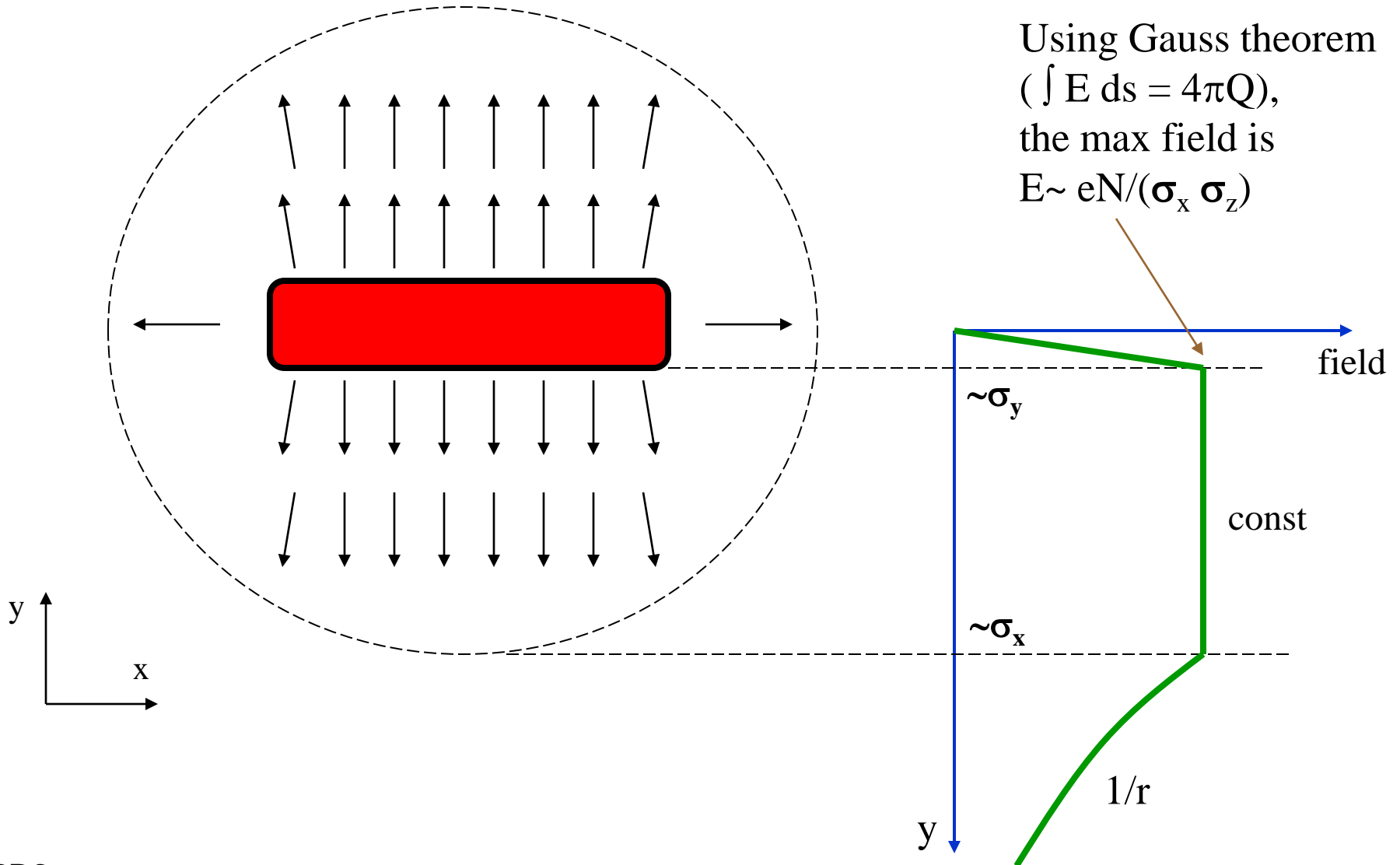
Beam-beam: Crabbed-waist



- Suggested by P.Raimondi for Super-B factory
- Vertical waist has to be a function of X. In this case coupling produced by beam-beam is eliminated
- Experimentally verified at DAFNE



Fields of flat bunch, qualitatively





Disruption parameter

- For Gaussian transverse beam distribution, and for particle near the axis, the beam kick results in the final particle angle:

$$\Delta x' = \frac{dx}{dz} = - \frac{2Nr_e}{\gamma\sigma_x(\sigma_x + \sigma_y)} \cdot x \qquad \Delta y' = \frac{dy}{dz} = - \frac{2Nr_e}{\gamma\sigma_y(\sigma_x + \sigma_y)} \cdot y$$

- “Disruption parameter” – characterize focusing strength of the field of the bunch ($D_y \sim \sigma_z/f_{\text{beam}}$)

$$D_x = \frac{2Nr_e\sigma_z}{\gamma\sigma_x(\sigma_x + \sigma_y)} \qquad D_y = \frac{2Nr_e\sigma_z}{\gamma\sigma_y(\sigma_x + \sigma_y)}$$

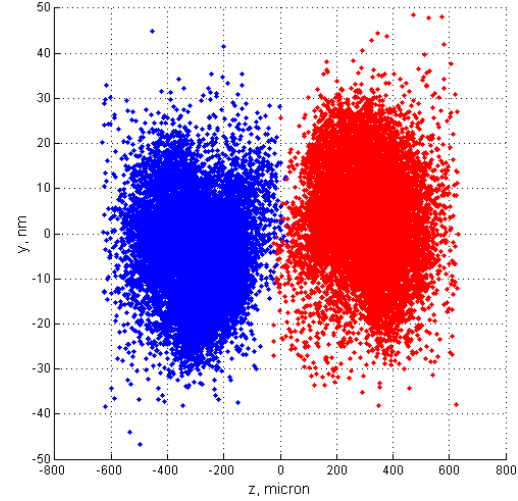
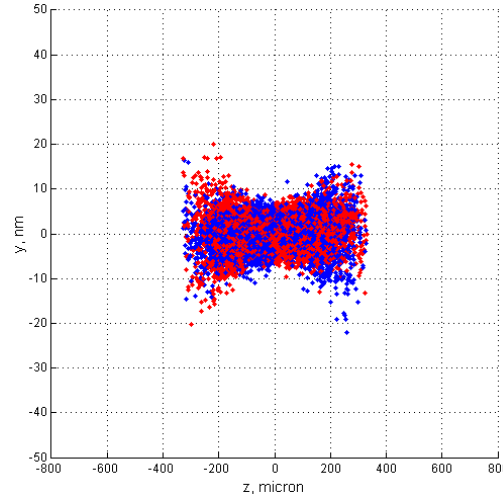
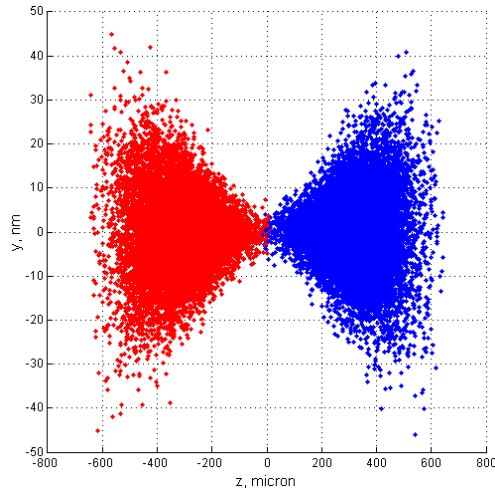
- $D \ll 1$ – bunch acts as a thin lens
- $D \gg 1$ – particle oscillate in the field of other bunch
 - If D is bigger than ~ 20 , instability may take place



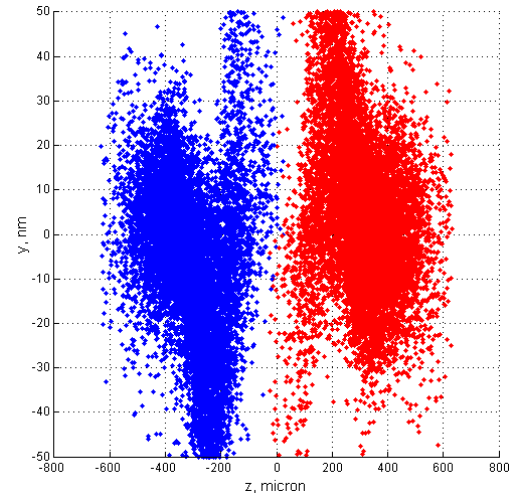
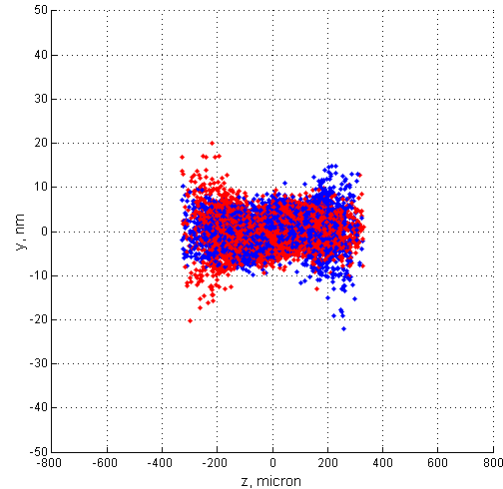
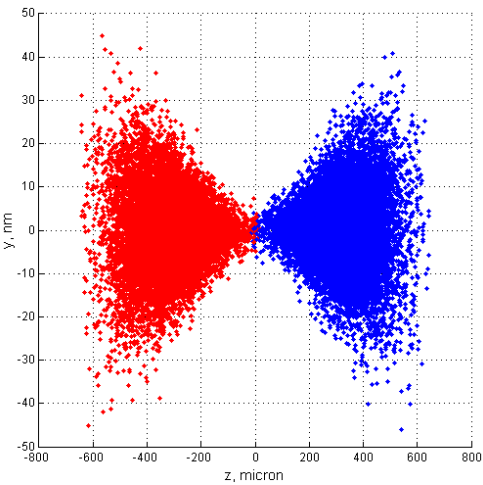
Beam-beam effects

H_D and instability

$$D_y = \frac{2r_e}{\gamma} \frac{N\sigma_z}{\sigma_x\sigma_y}$$



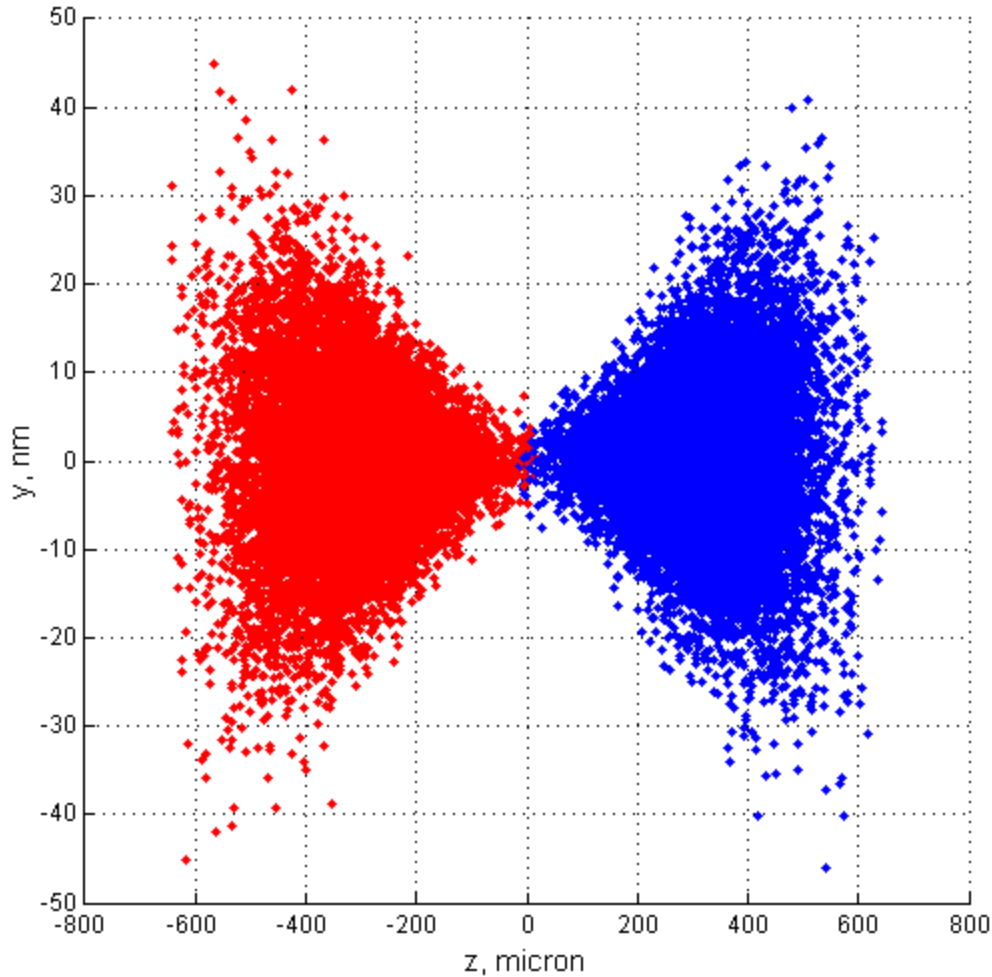
$D_y \sim 12$



$N \times 2$
 $D_y \sim 24$

Beam-beam effects

H_D and instability

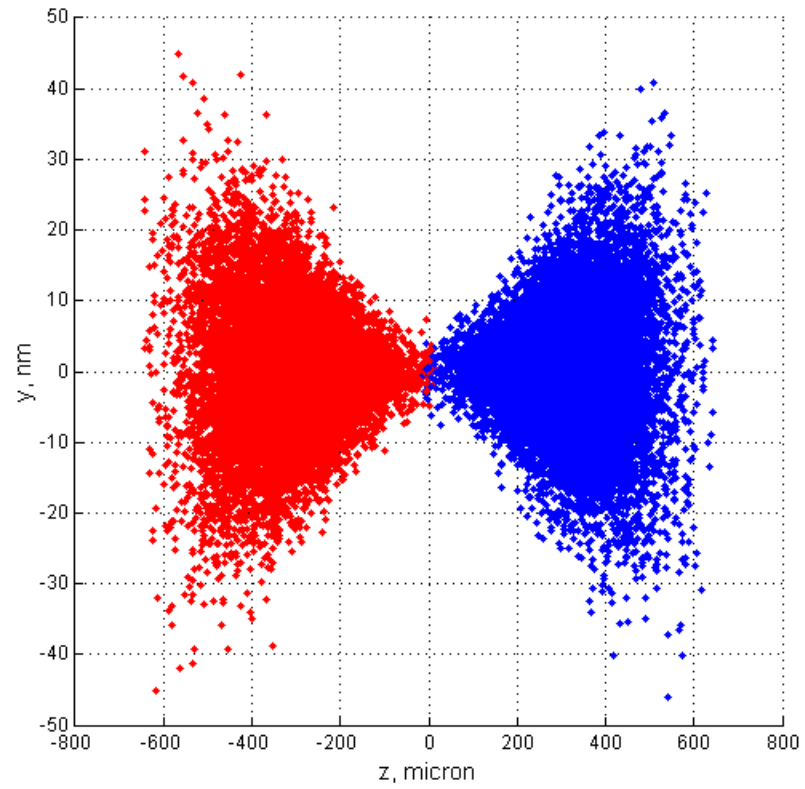


LC parameters
 $D_y \sim 12$

Luminosity
enhancement
 $H_D \sim 1.4$

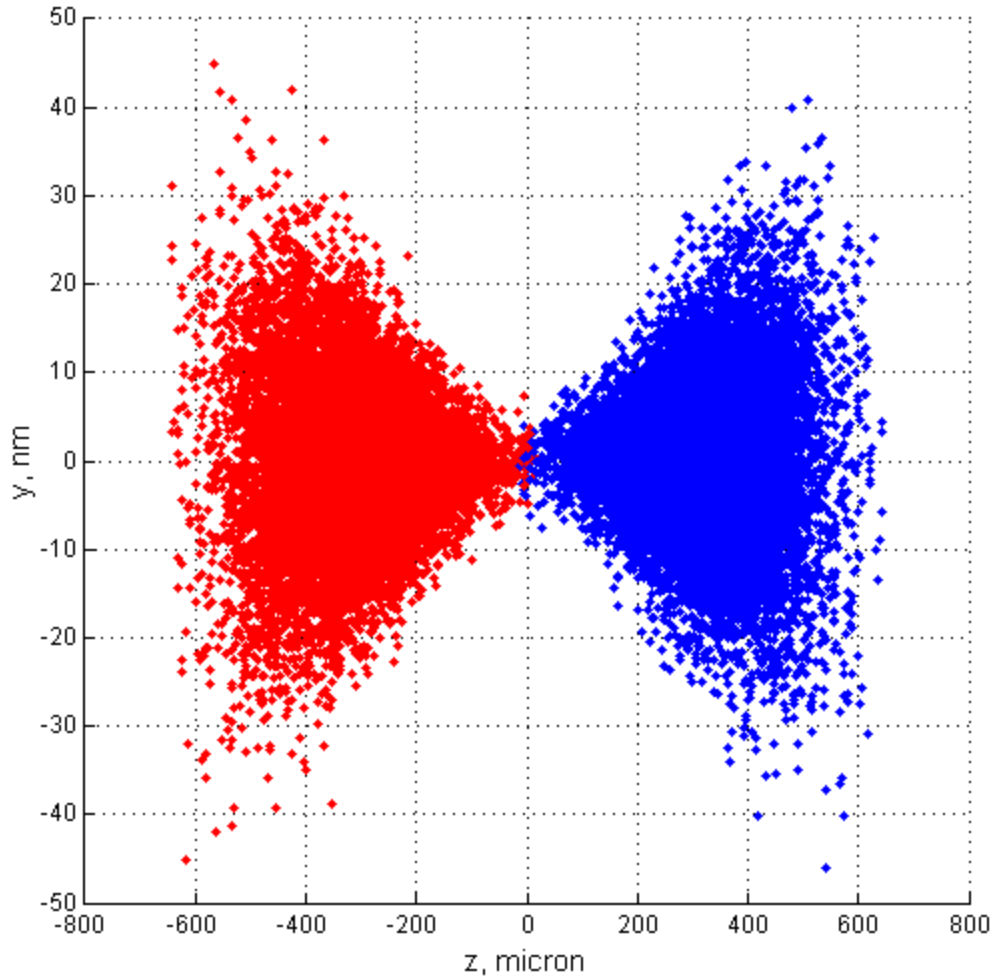
Not much of an
instability





Beam-beam effects

H_D and instability

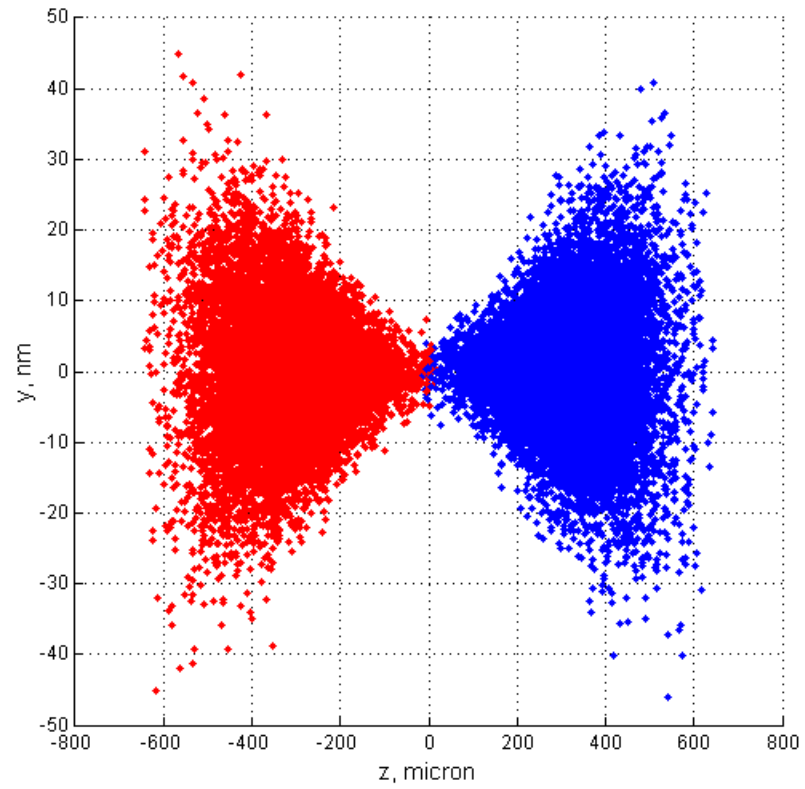


$N \times 2$
 $D_y \sim 24$

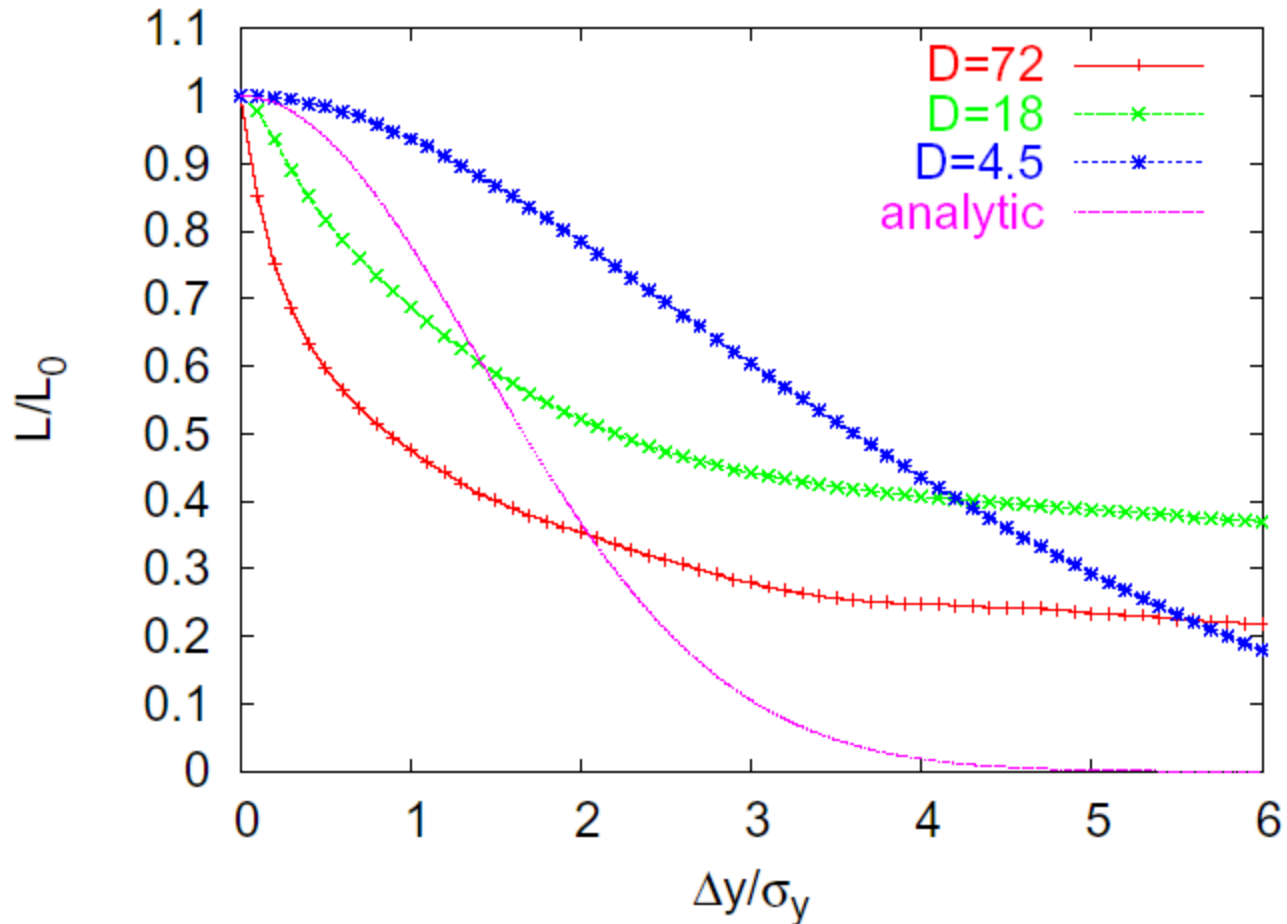
Beam-beam
instability is
clearly
pronounced

Luminosity
enhancement is
compromised by
higher
sensitivity to
initial offsets





Sensitivity to offset at IP



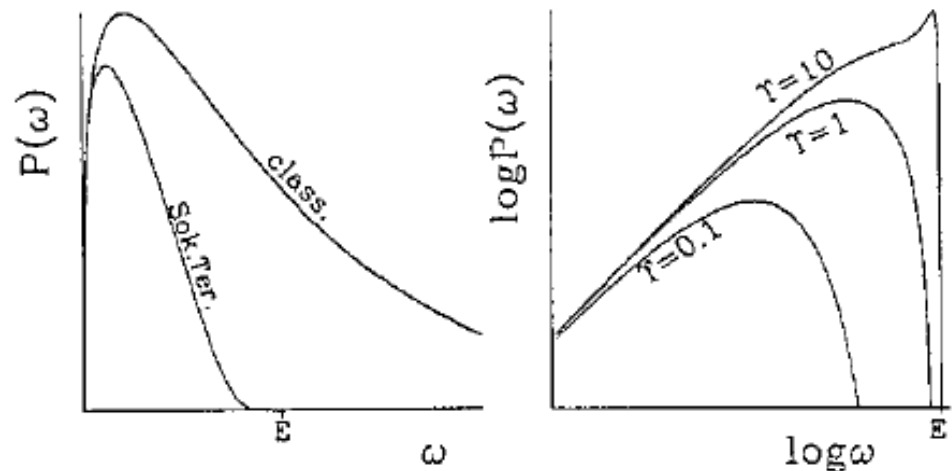
- Luminosity (normalized) versus offset at IP for different disruption parameters

- Synchrotron radiation in field of opposite bunch
- Estimate R of curvature as $R \sim \sigma_z^2 / (D_y \sigma_y)$
- Using formulas derived earlier, estimate ω_c and find that $h\omega_c/E \sim \gamma N r_e^2 / (\alpha \sigma_x \sigma_z)$ and call it “Upsilon”

More accurate formula:
$$\Upsilon_{avg} \approx \frac{5}{6} \frac{N r_e^2 \gamma}{\alpha \sigma_z (\sigma_x + \sigma_y)}$$

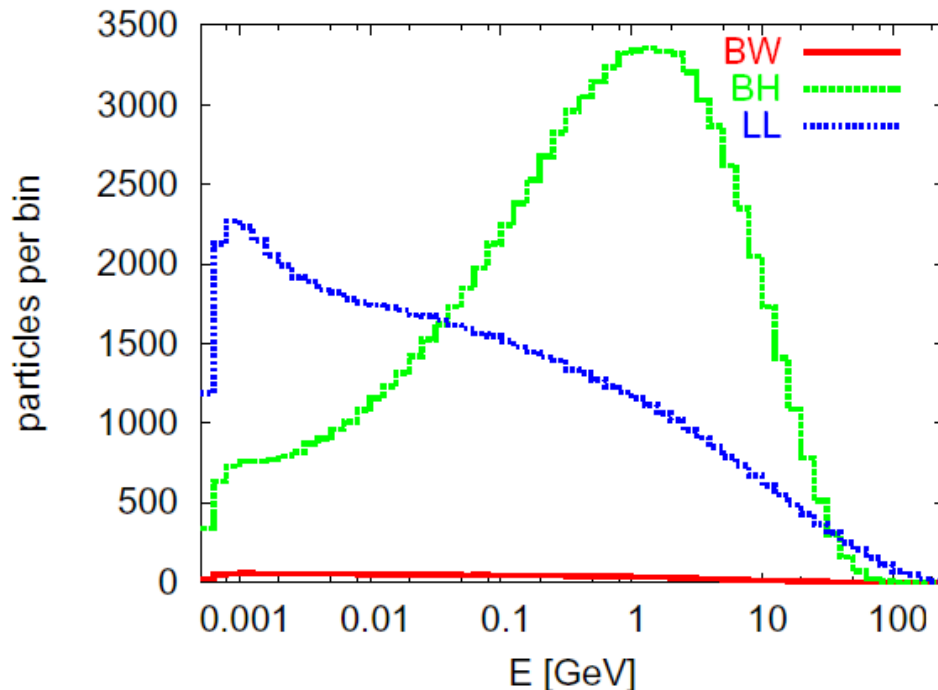
- The energy loss also can be estimated from earlier derived formulas: $dE/E \sim \gamma r_e^3 N^2 / (\sigma_z \sigma_x^2)$
 - This estimation is very close to exact one
- Number of γ per electron estimated $n_{\gamma/e} \sim \alpha r_e N / \sigma_x$
 - which is usually around one γ per e

- The “upsilon” parameter, when it is $\ll 1$, has meaning of ratio of photon energy to beam energy
- When Upsilon become ~ 1 and larger, the classical regime of synchrotron radiation is not applicable, and quantum SR formulas of Sokolov-Ternov should be used.
- Spectrum of SR change ...

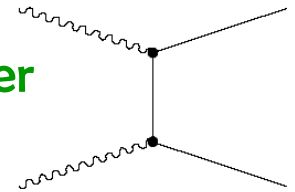


Incoherent* production of pairs

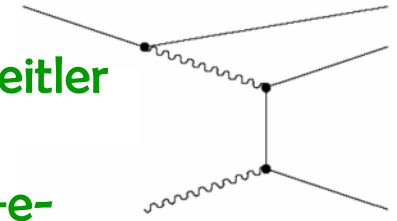
- Beamstrahlung photons, particles of beams or virtual photons interact, and create e^+e^- pairs



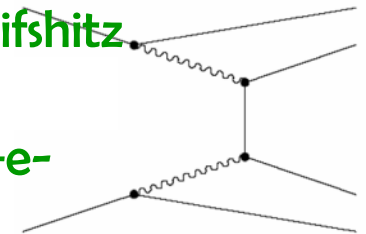
Breit-Wheeler
process
 $\gamma\gamma \rightarrow e^+e^-$



Bethe-Heitler
process
 $e\gamma \rightarrow ee^+e^-$



Landau-Lifshitz
process
 $ee \rightarrow eee^+e^-$



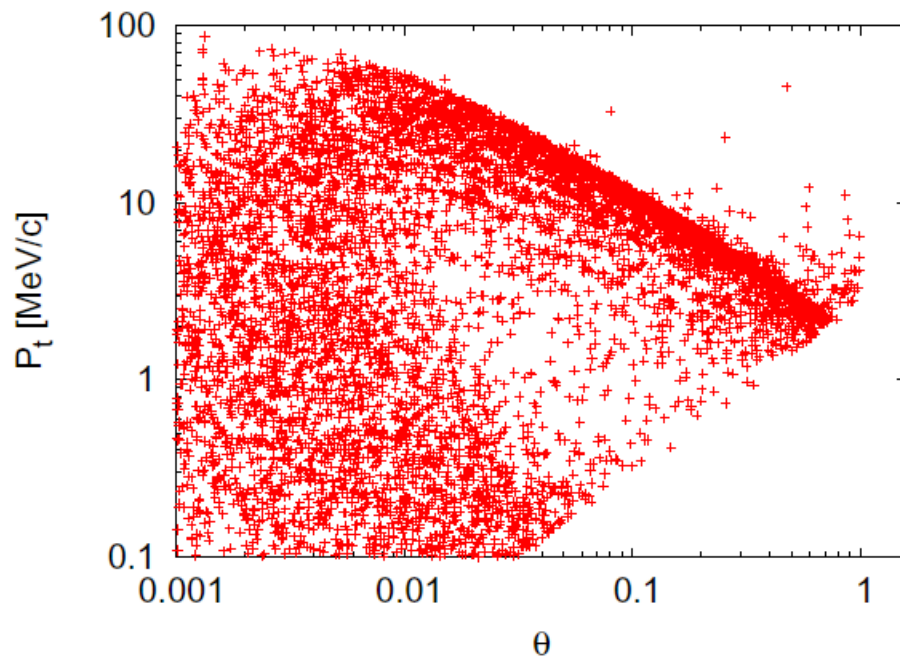
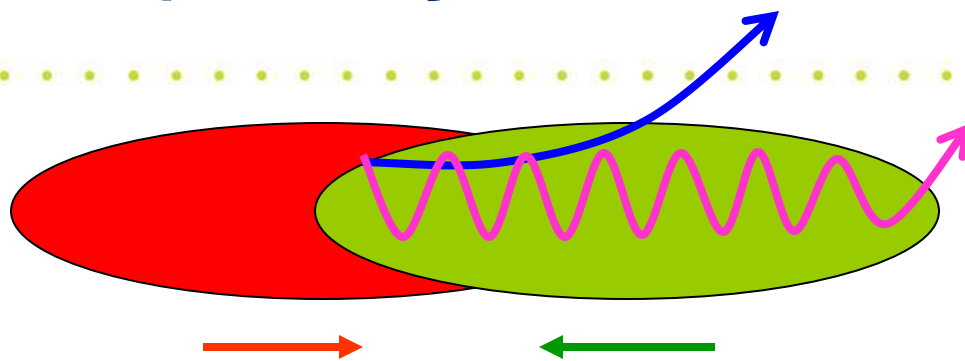
*) Coherent pairs are generated by photon in the field of opposite bunch. It is negligible for ILC parameters.

Deflection of pairs by beam

- Pairs are affected by the beam (focused or defocused)
- Deflection angle and P_t correlate
- Max angle estimated as (where ϵ is fractional energy):

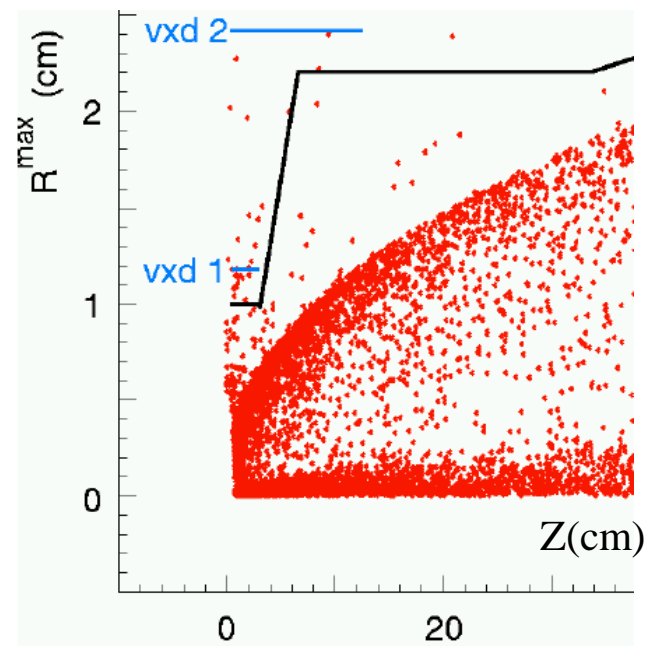
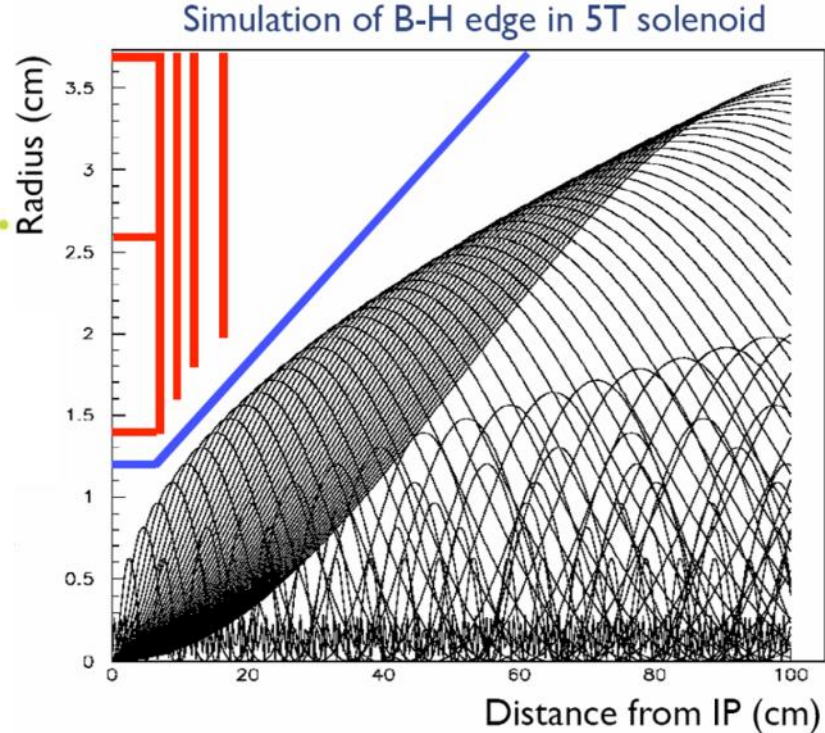
$$\theta_m = \sqrt{4 \frac{\ln\left(\frac{D}{\epsilon} + 1\right) D \sigma_x^2}{\sqrt{3} \epsilon \sigma_z^2}}$$

- Bethe-Heitler pairs have hard edge, Landau-Lifshitz pairs are outside



Deflection of pairs by detector solenoid

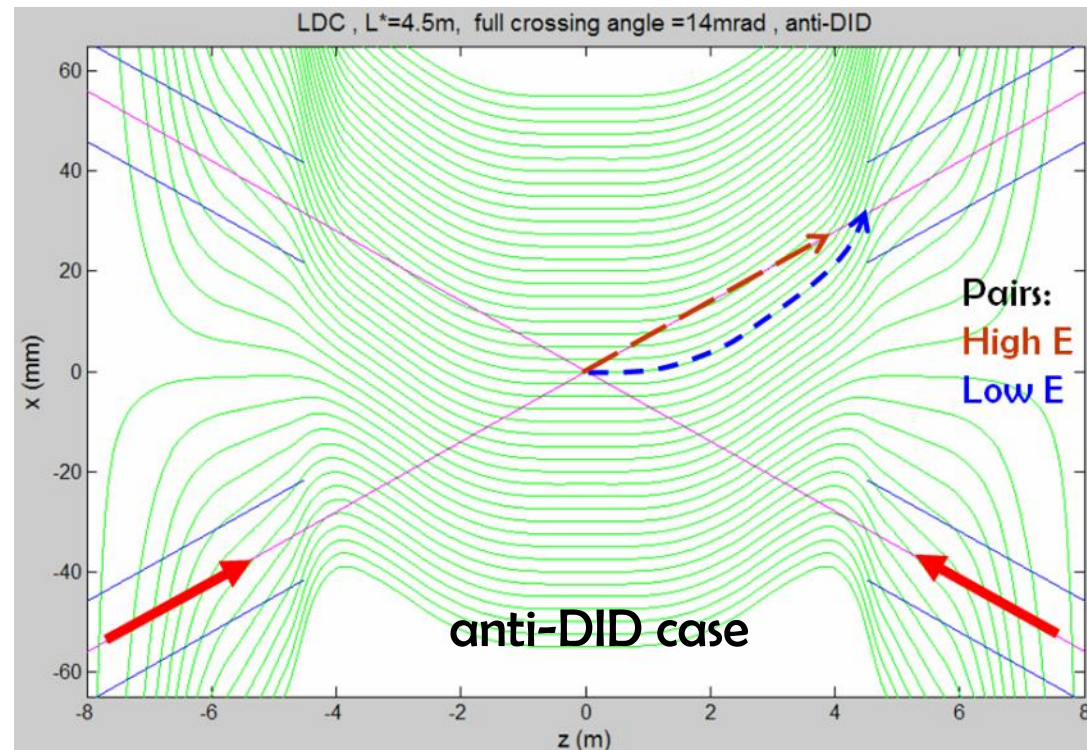
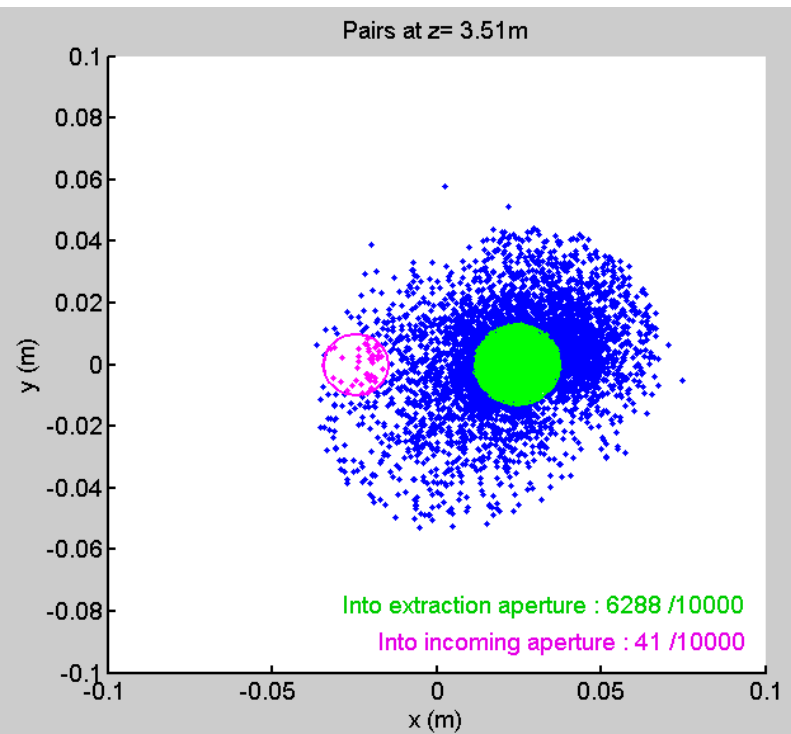
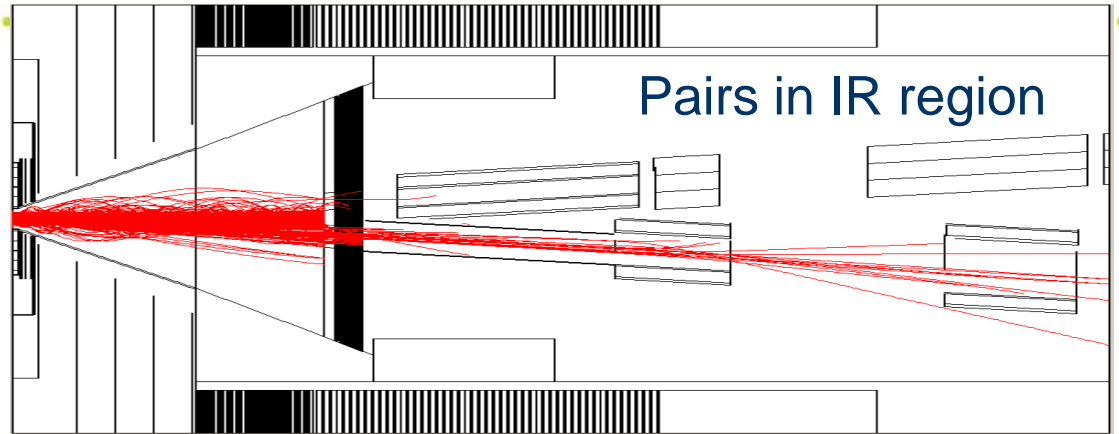
- Pairs are curled by the solenoid field of detector
- Geometry of vertex detector and vacuum chamber chosen in such a way that most of pairs (B-H) do not hit the apertures
- Only small number (L-L) of pairs would hit the VX apertures





Use of anti-DID to direct pairs

Anti-DID field can be used to direct most of pairs into extraction hole and thus improve somewhat the background conditions





Overview of beam-beam parameters (D_y , δ_E , Υ)

$$\text{Lumi} \sim H_D \frac{N^2}{\sigma_x \sigma_y}$$

- Luminosity per bunch crossing. H_D – luminosity enhancement

$$D_y \sim \frac{N \sigma_z}{\gamma \sigma_x \sigma_y}$$

- “Disruption” – characterize focusing strength of the field of the bunch
($D_y \sim \sigma_z / f_{\text{beam}}$)

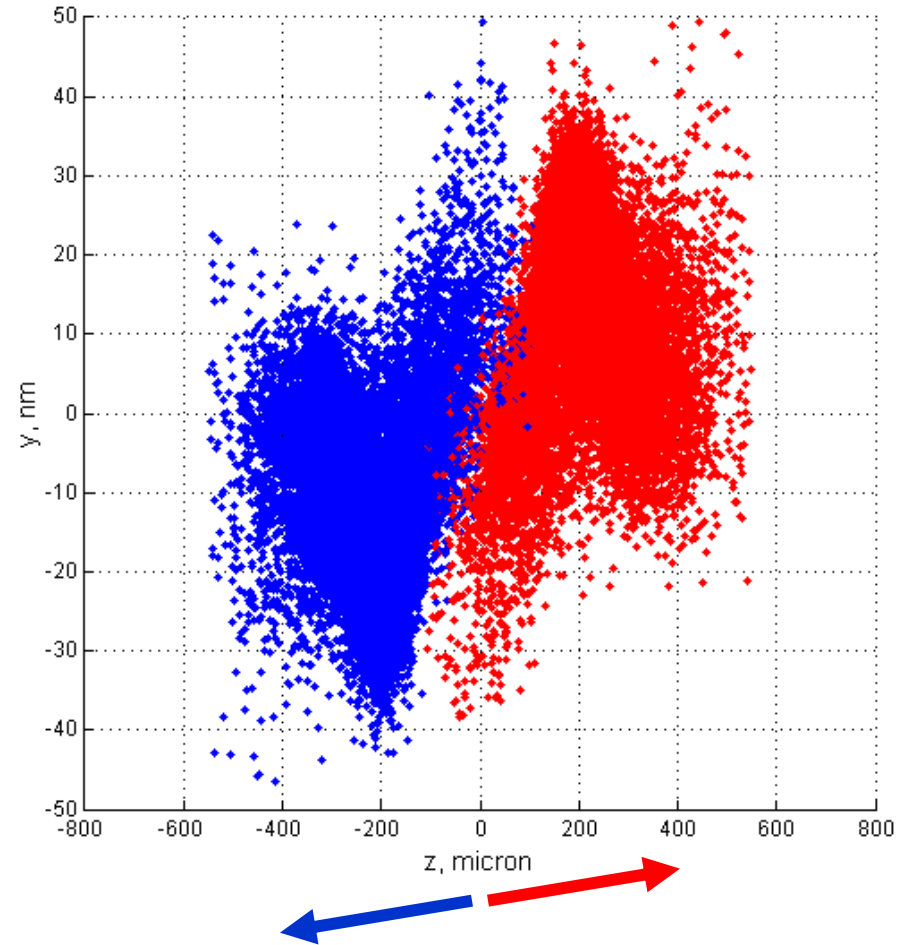
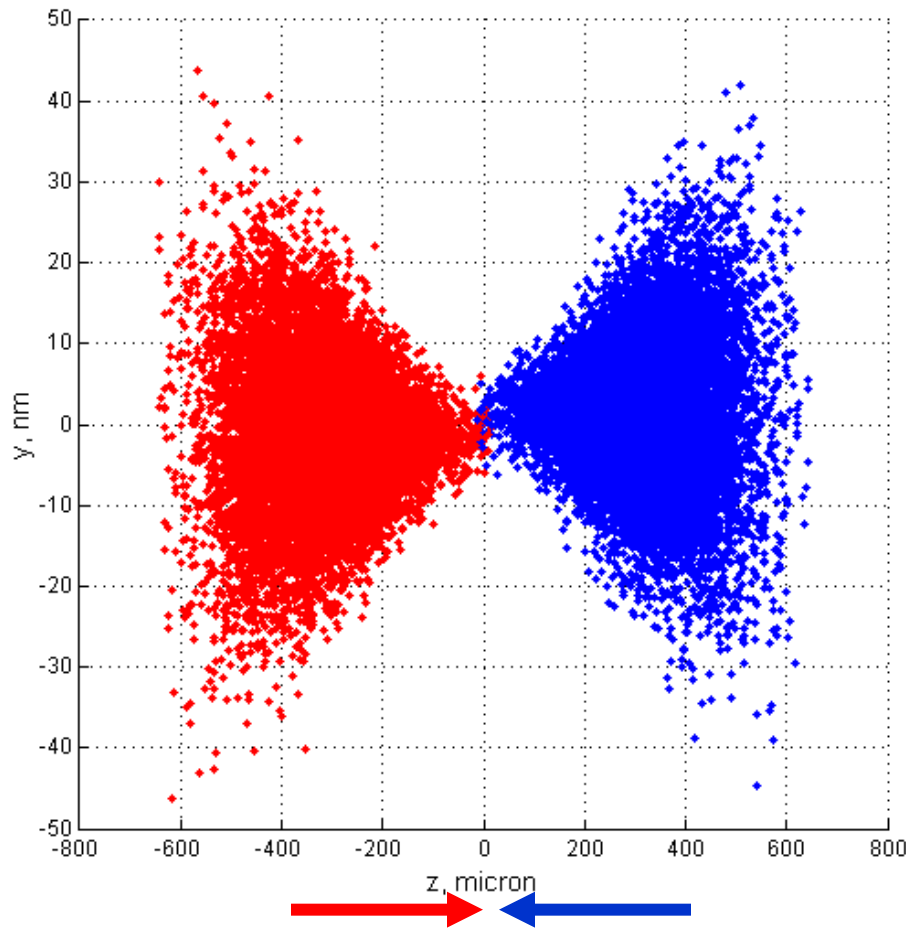
$$\delta_E \sim \frac{N^2 \gamma}{\sigma_x^2 \sigma_z}$$

- Energy loss during beam-beam collision due to synchrotron radiation

$$\Upsilon \sim \frac{N \gamma}{\sigma_x \sigma_z}$$

- Ratio of critical photon energy to beam energy (classic or quantum regime)

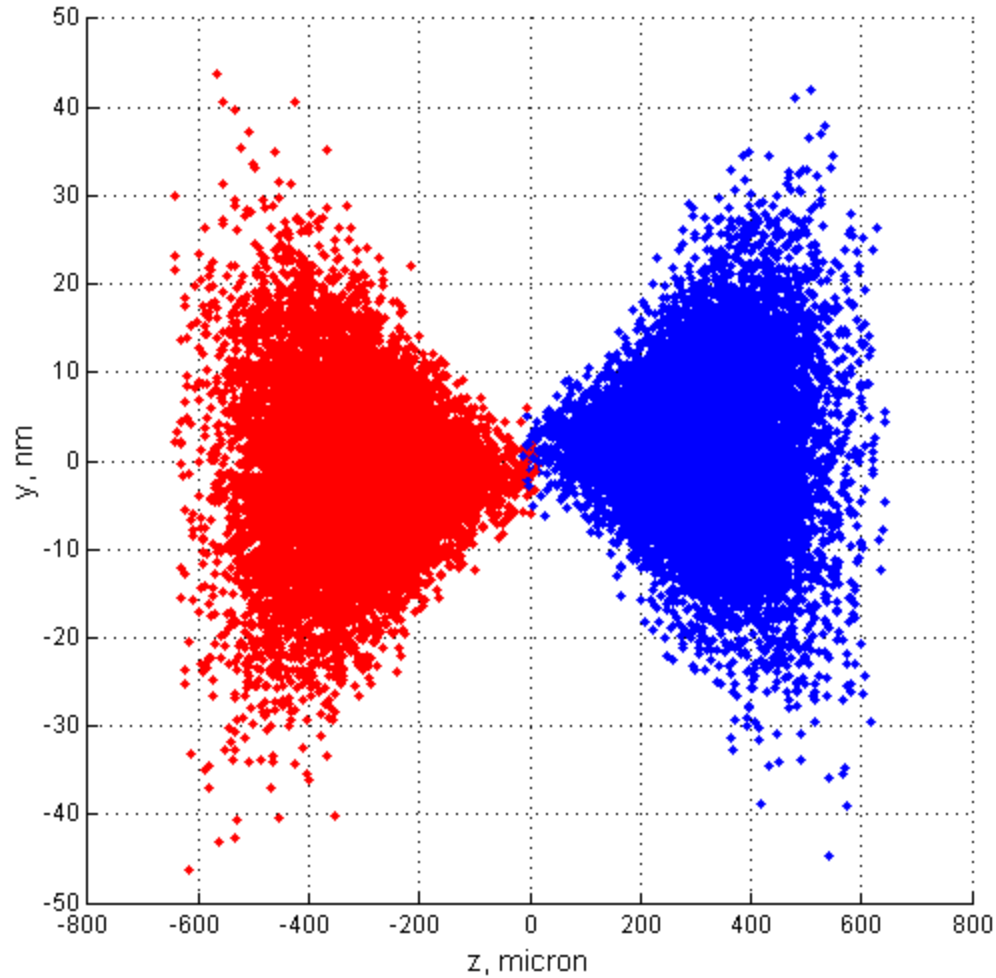
Beam-beam deflection

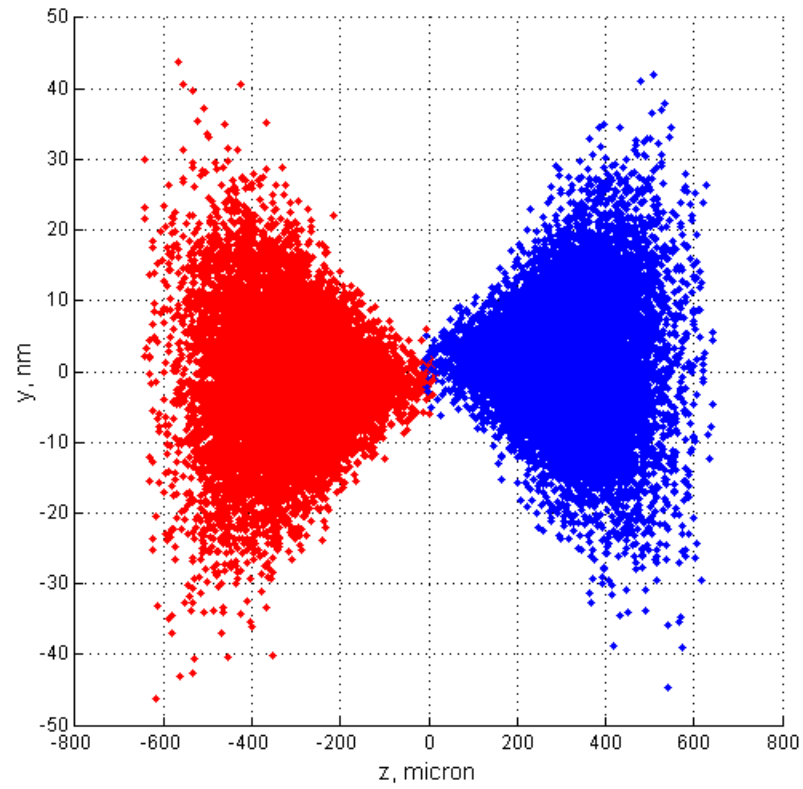


Sub nm offsets at IP cause large well detectable offsets (micron scale) of the beam a few meters downstream

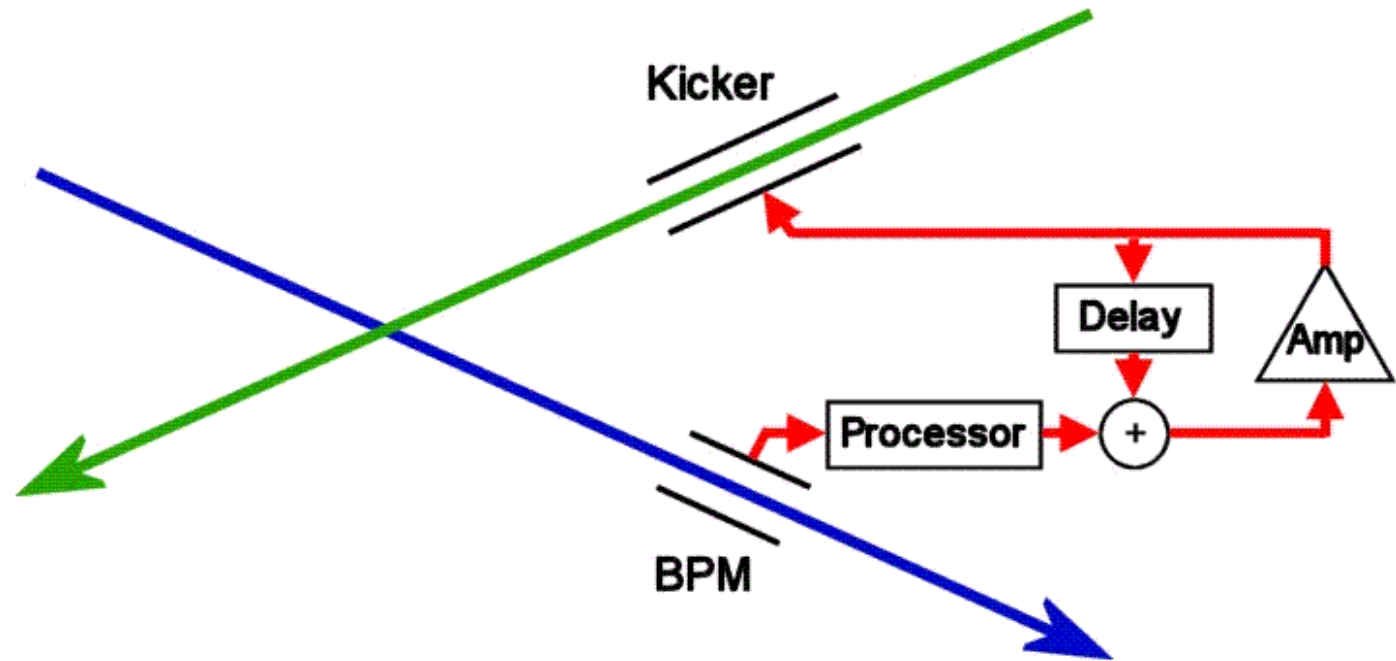


Beam-beam deflection allow to control collisions





Beam-Beam orbit feedback

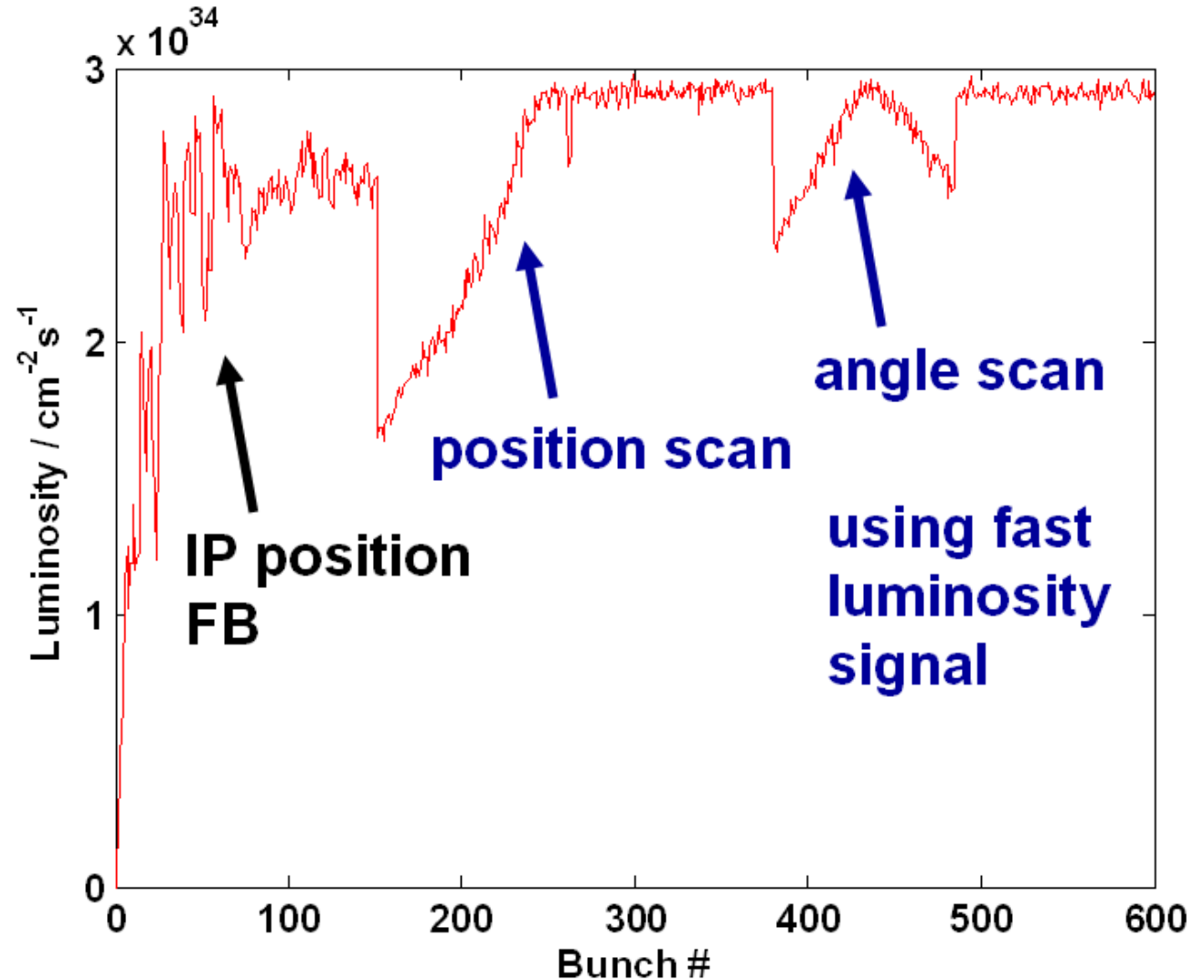


use strong beam-beam kick to keep beams colliding



ILC intratrain simulation

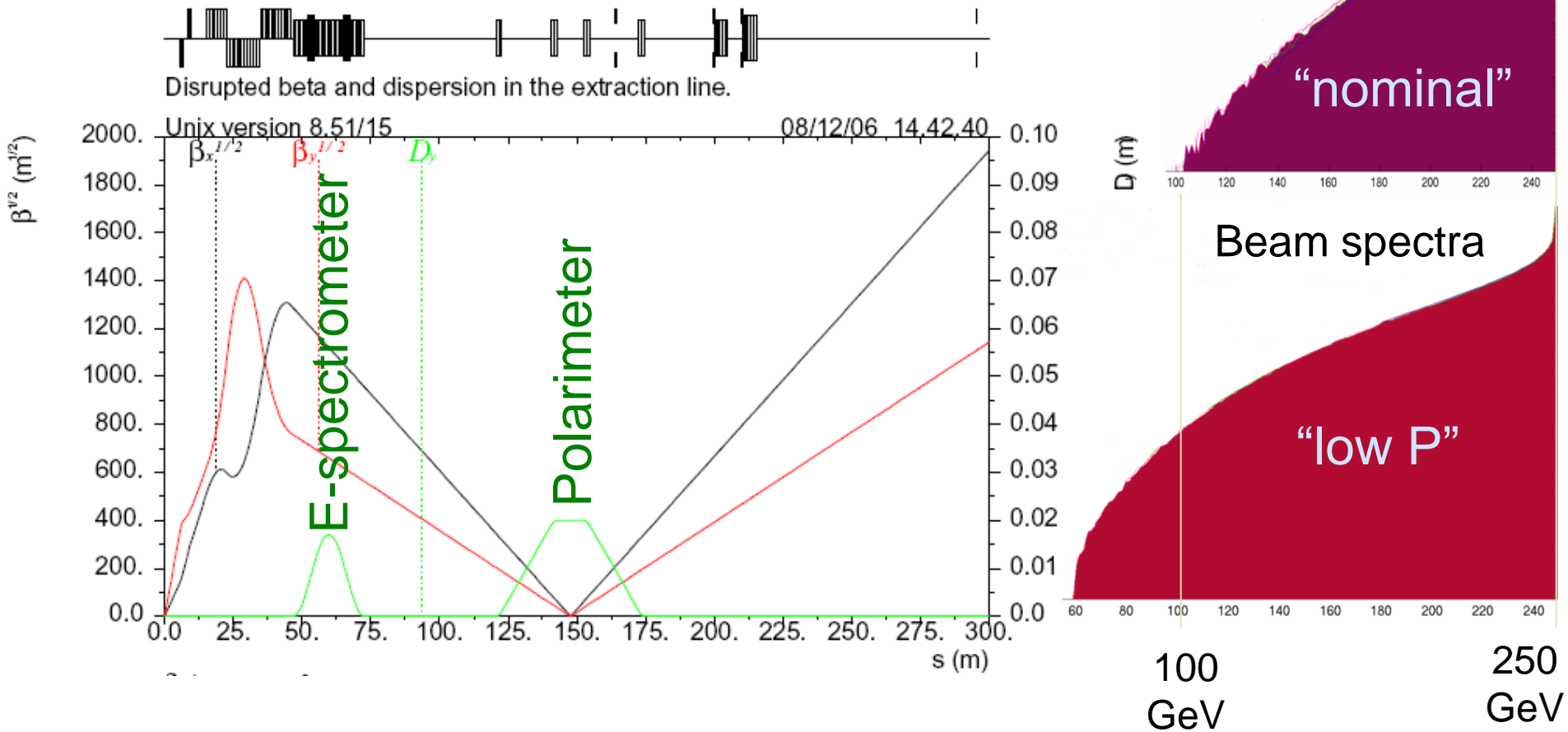
ILC intratrain feedback (IP position and angle optimization), simulated with realistic errors in the linac and “banana” bunches.



[Glen White]

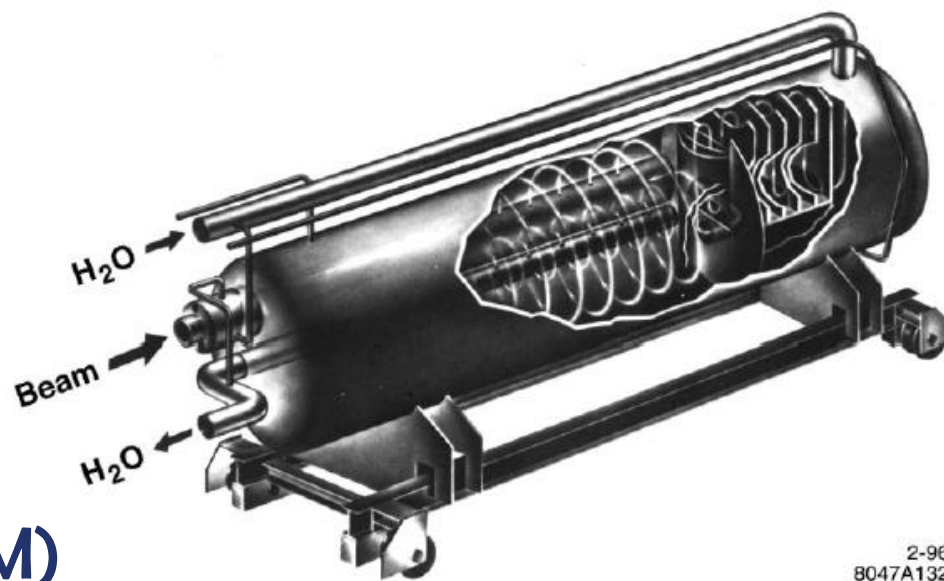


Optics for outgoing beam



Extraction optics need to handle the beam with ~60% energy spread, and provides energy and polarization diagnostics

Beam dump

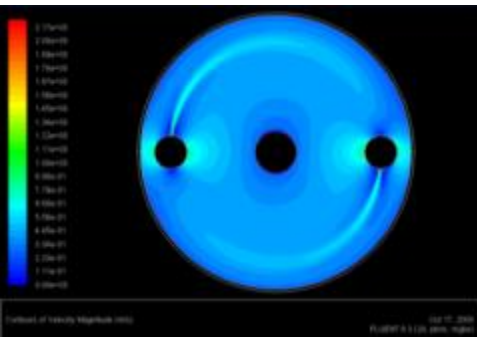


2-96
8047A132

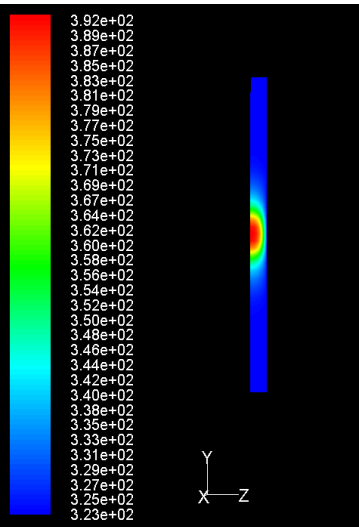
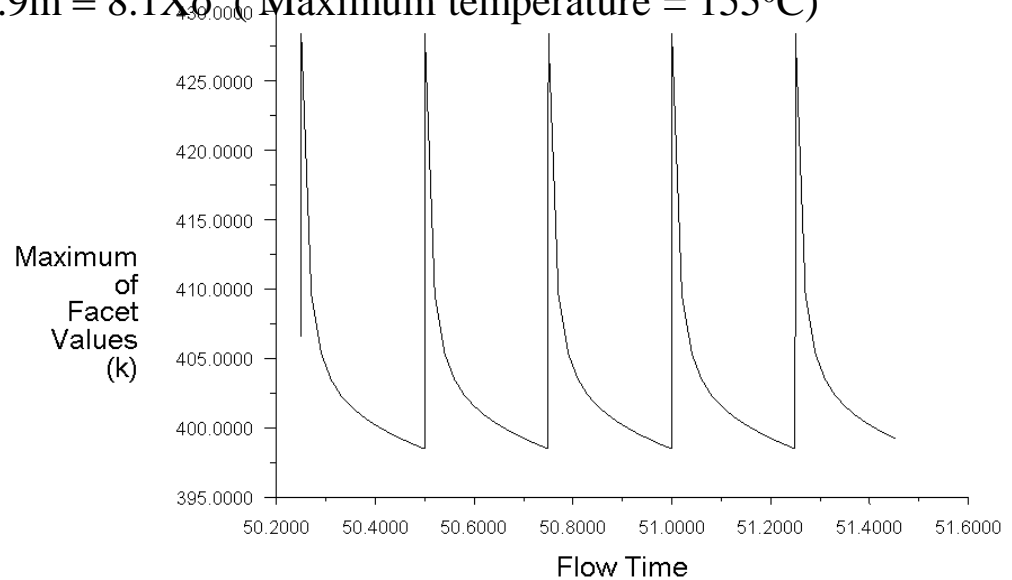
- 17MW power (for 1TeV CM)
- Rastering of the beam on 30cm double window
- 6.5m water vessel; ~1m/s flow
- 10atm pressure to prevent boiling
- Three loop water system
- Catalytic H_2-O_2 recombiner
- Filters for 7Be
- Shielding 0.5m Fe & 1.5m concrete

Beam dump design updates

Maximum temperature variation as a function of time at $z = 2.9\text{m} \equiv 8.1X_0$ (Maximum temperature = 155°C)

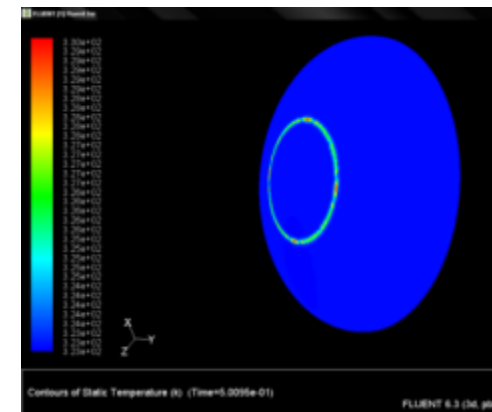


Velocity contours (inlet velocity: 2.17m/s , mass flux: $19\text{kg/m}^2\text{s}$)



Temperature distribution across the cross-section of the End plate

Window temperature distribution just when the beam train completes energy deposition. (Max temp : 57°C)



D. Walz , J. Amann, et al, SLAC
 P. Satyamurthy, P. Rai, V. Tiwari, K. Kulkarni,
 BARC, Mumbai, India

From IPAC10 paper



Beam Delivery & MDI elements

1TeV CM, single IR, two detectors, push-pull

grid: 100m*1m

Diagnostics

Beam Switch Yard

polarimeter

Sacrificial collimators

Collimation: β, E

Tune-up & emergency Extraction

Tune-up dump

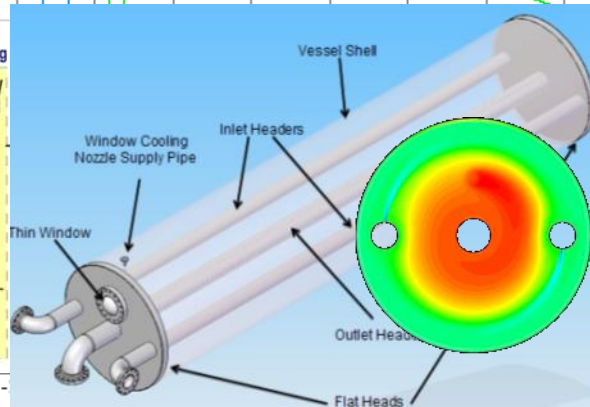
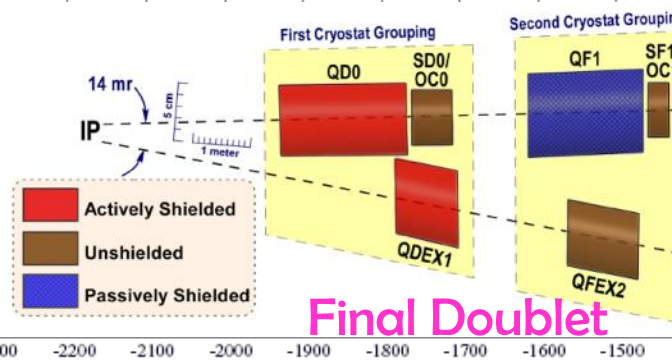
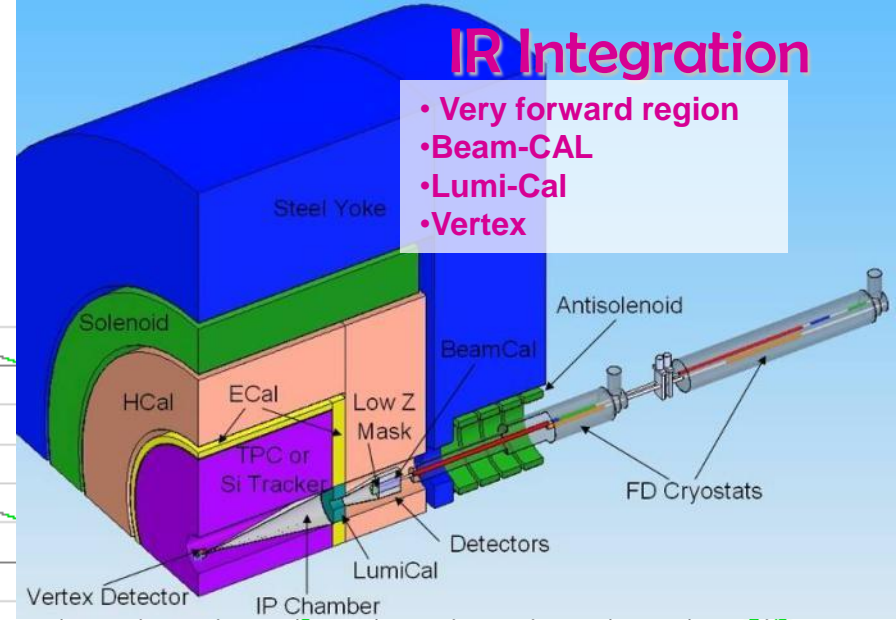
E-spectrometer

Final Focus

14mr IR

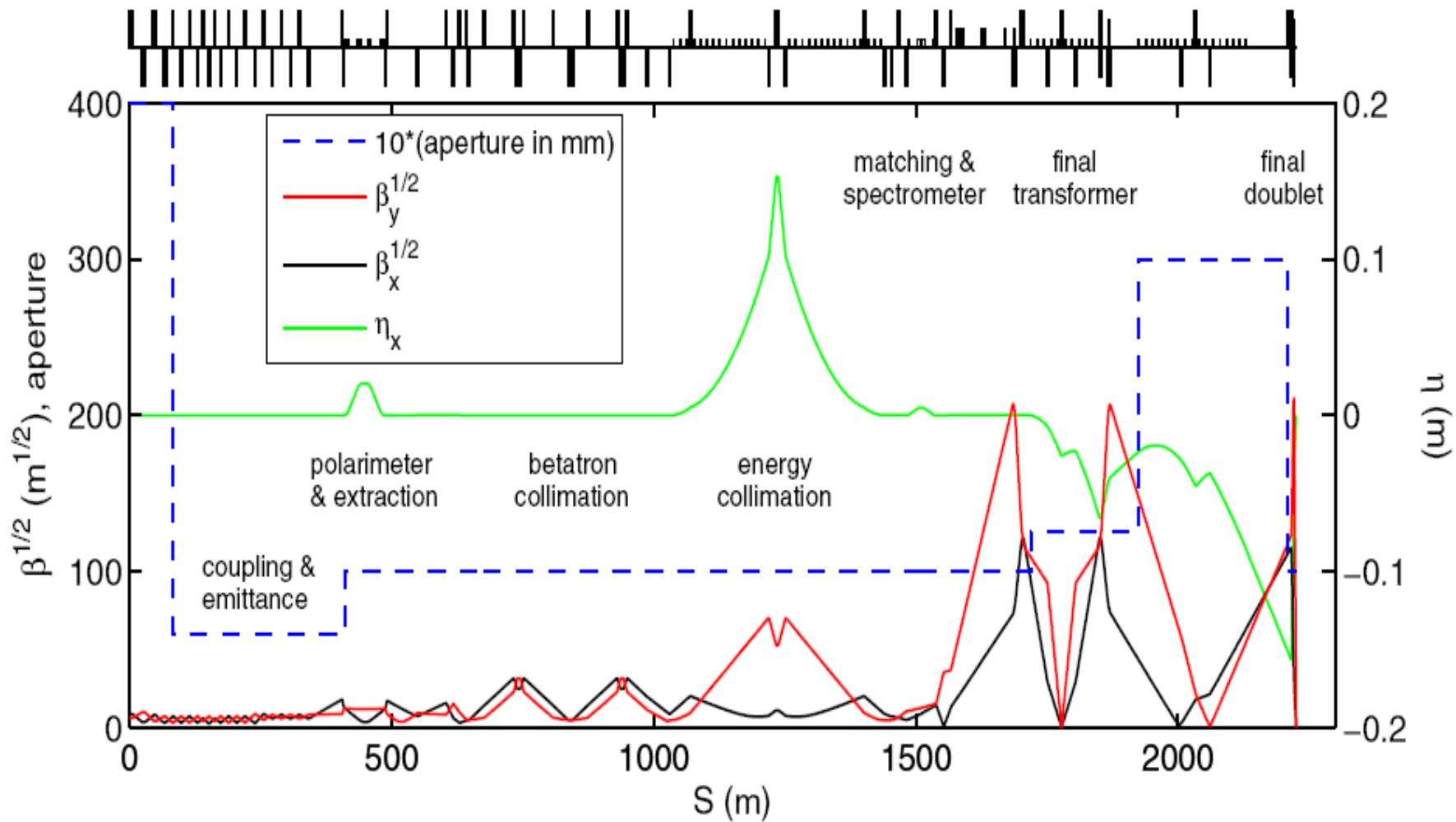
Muon wall
Main dump

Extraction with downstream diagnostics



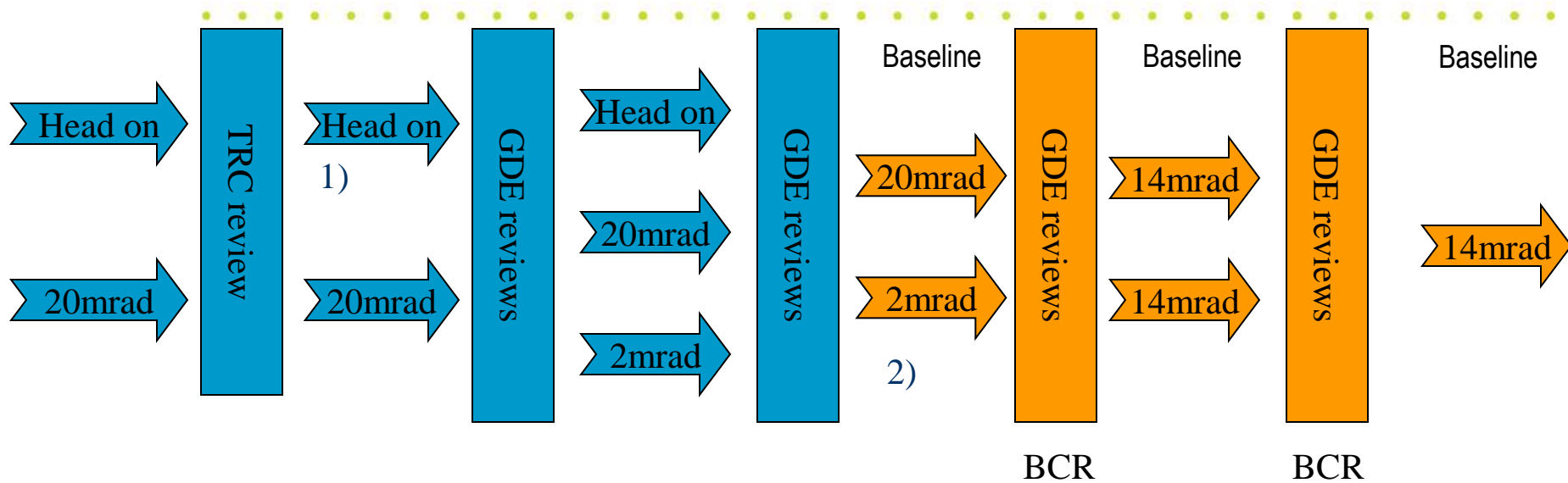


ILC BDS Optical Functions





BDS & MDI Configuration Evolution

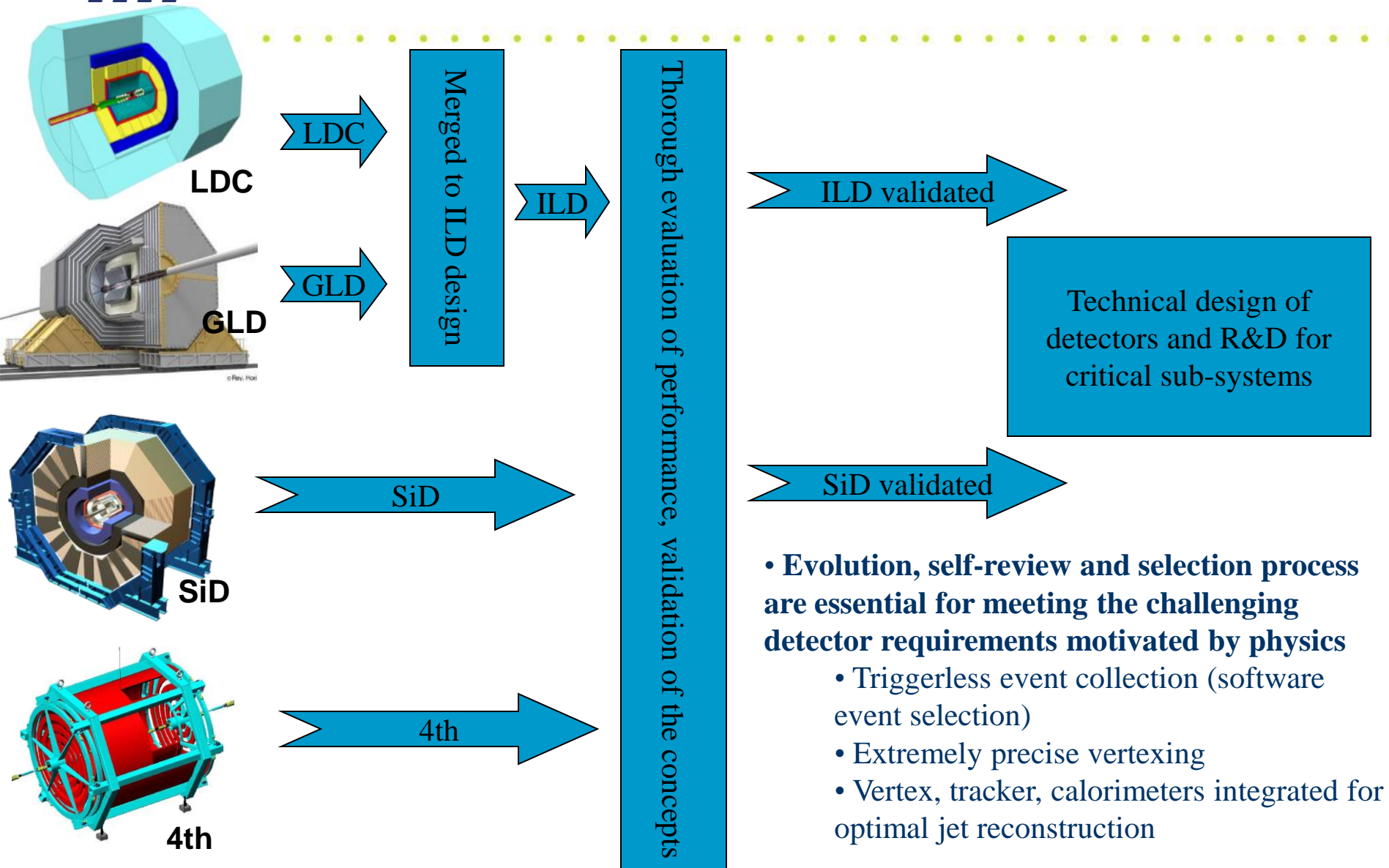


• Evolution of BDS MDI configuration

- Head on; small crossing angle; large crossing angle
 - MDI & Detector performance were the major criteria for selection of more optimal configuration at every review or decision point
- 1) Found unforeseen losses of beamstrahlung photons on extraction septum blade
 - 2) Identified issues with losses of extracted beam, and its SR; realized cost non-effectiveness of the design



Evolution of ILC Detectors





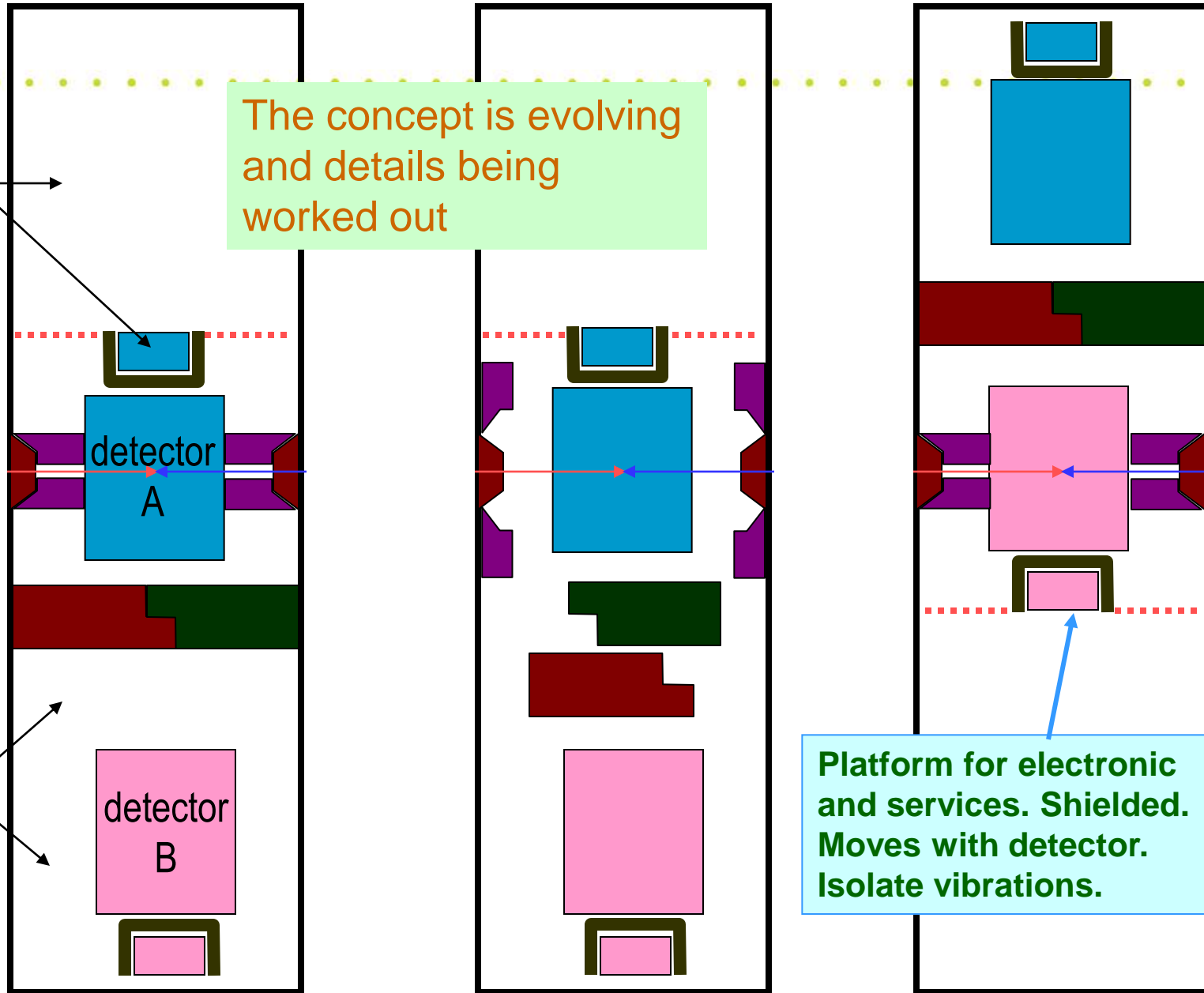
Concept of single IR with two detectors

may be accessible during run

The concept is evolving and details being worked out

accessible during run

Platform for electronic and services. Shielded. Moves with detector. Isolate vibrations.





Concept of detector systems connections

detector

detector service platform
or mounted on detector

sub-detectors
solenoid
antisolenoid
FD

low V DC for electronics
4K LHe for solenoids
2K LHe for FD
high I DC for solenoids
high I DC for FD
gas for TPC
electronics I/O

low V PS
high I PS
electronic racks
4K cryo-system
2K cryo-system
gas system

high V AC

high P room T He
supply & return

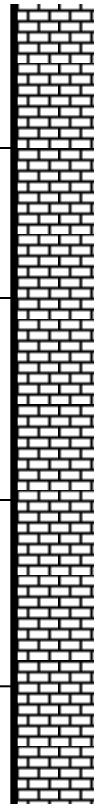
chilled water
for electronics

fiber data I/O

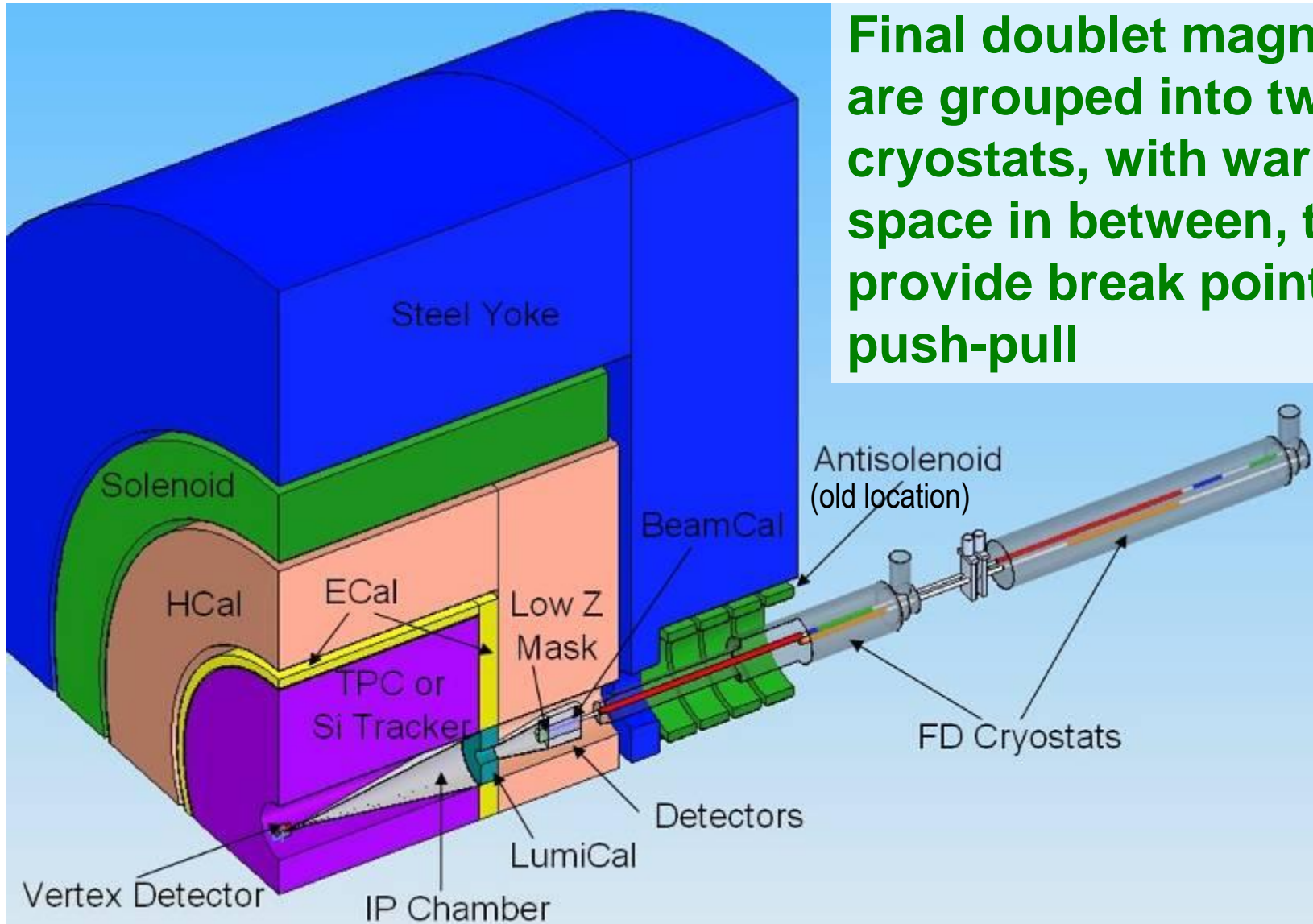
fixed
connections

long flexible
connections

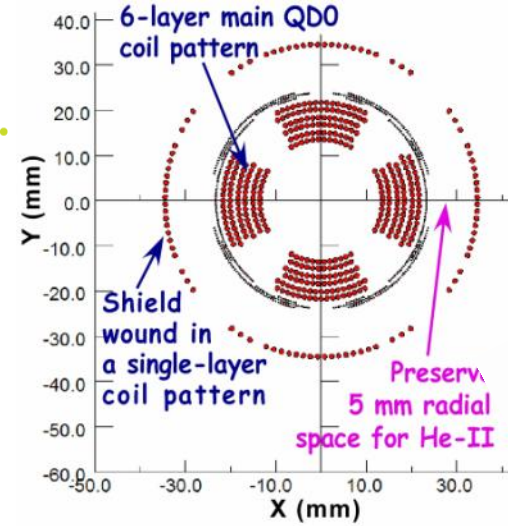
move together



IR integration



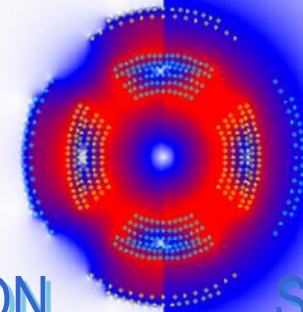
Final doublet magnets are grouped into two cryostats, with warm space in between, to provide break point for push-pull



Actively shielded QD0



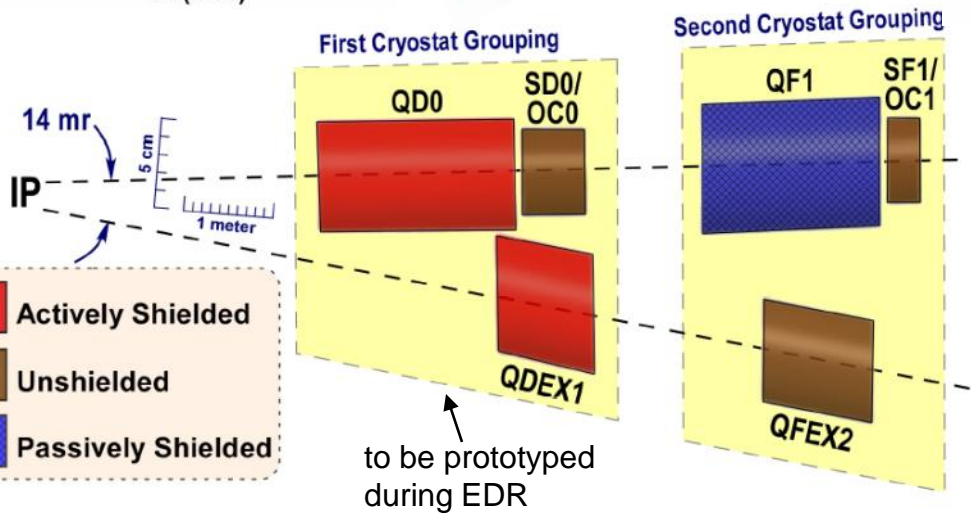
BNL



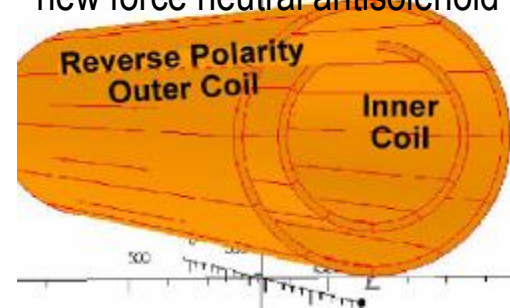
Shield ON

Shield OFF

Intensity of color represents value of magnetic field.



Two Coils; Different Radii
new force neutral antisolenoid



- Interaction region uses compact self-shielding SC magnets
- Independent adjustment of in- & out-going beamlines
- Force-neutral anti-solenoid for local coupling correction



IR magnets
prototypes at
BNL

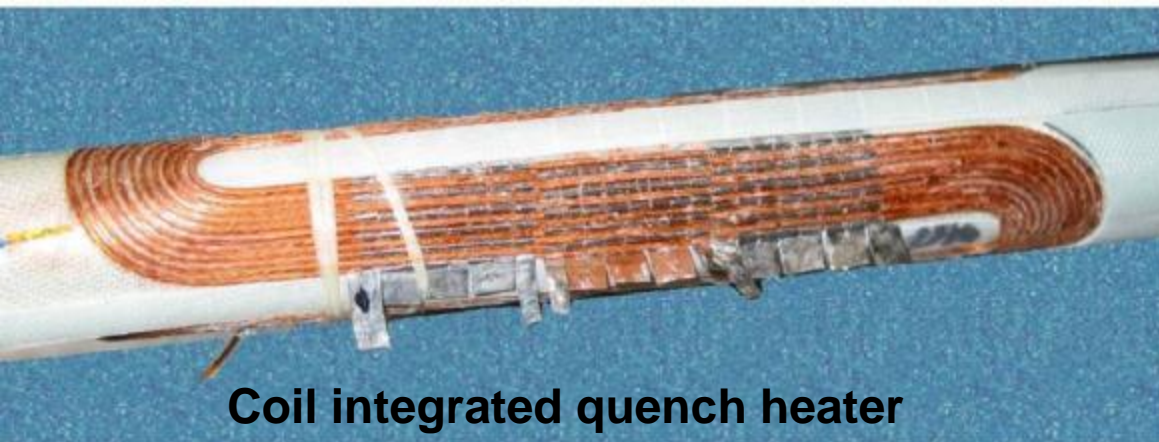
BNL prototype of self shielded quad



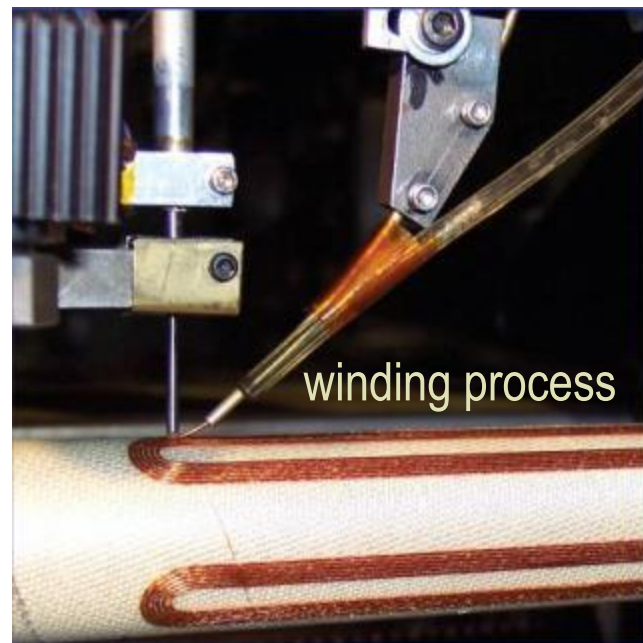
cancellation of the external field with a shield coil has been successfully demonstrated at BNL



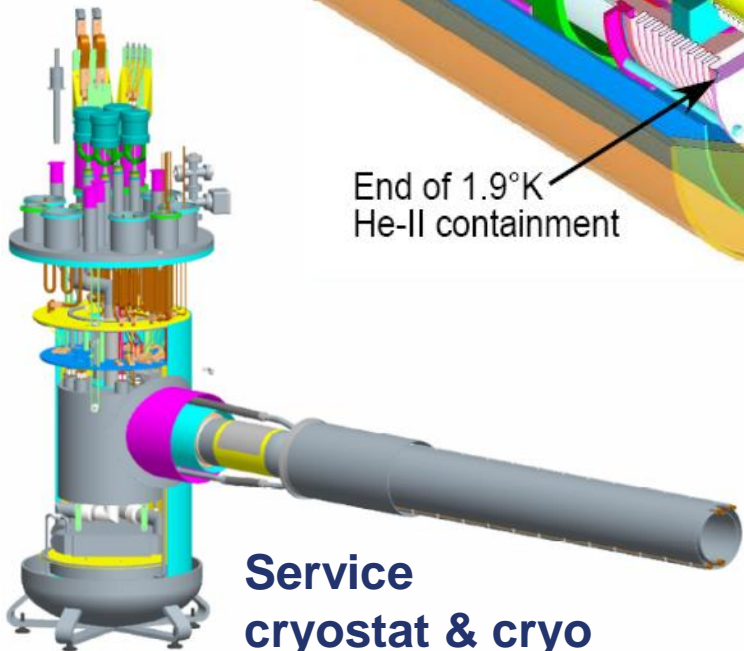
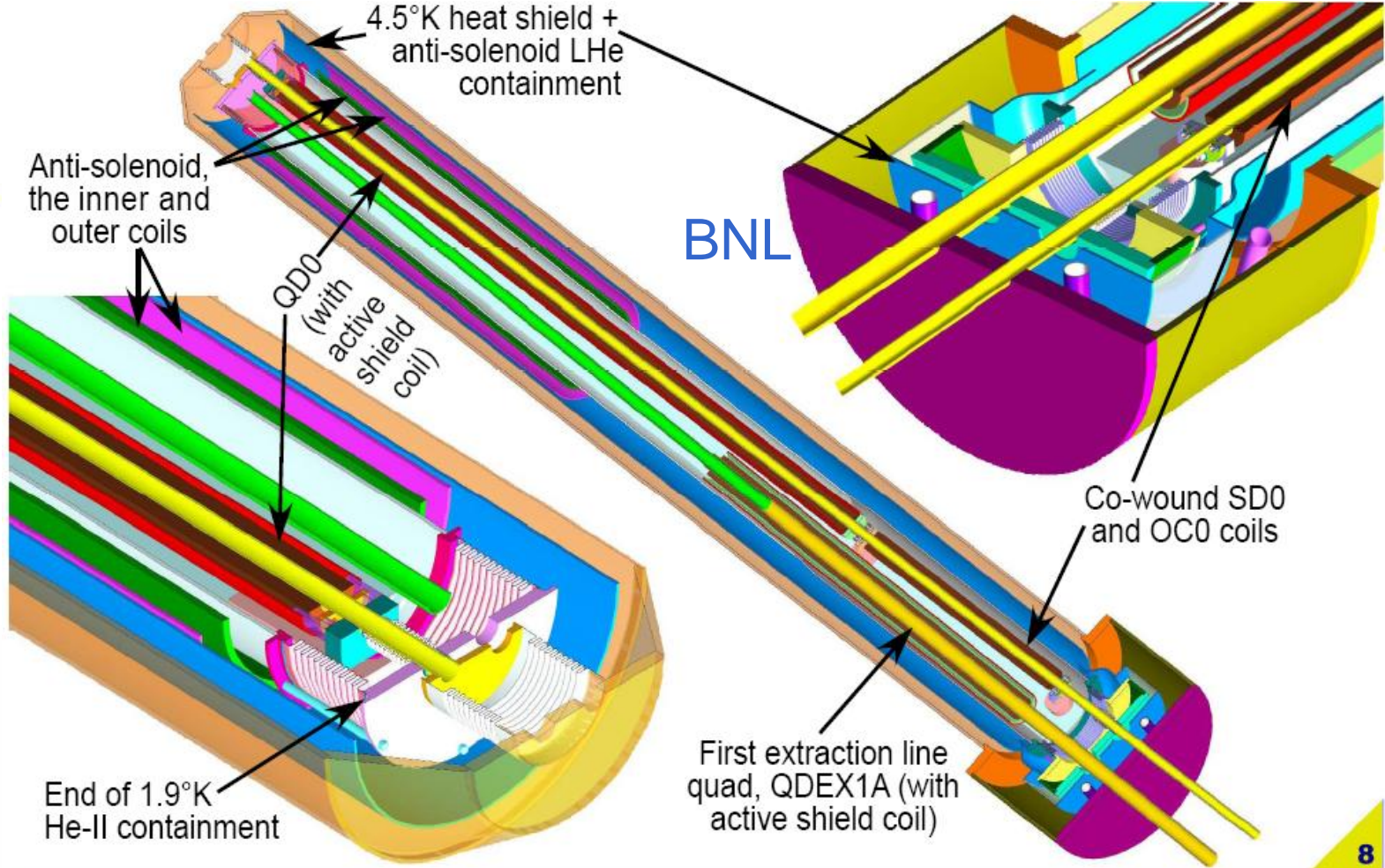
prototype of sextupole-octupole magnet



Coil integrated quench heater



winding process



- Detailed engineering design of IR magnets and their integration has started



Present concept of cryo connection



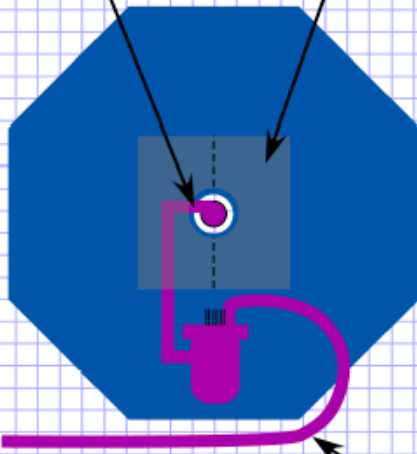
Vertical Layout for the Service Cryostat to QD0 Cryostat Transfer Line.

BROOKHAVEN
NATIONAL LABORATORY
Superconducting
Magnet Division

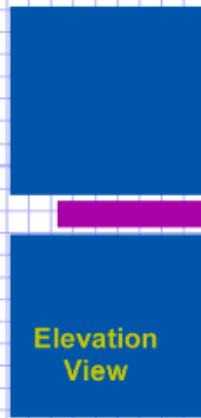
Line with 1 bar He-II and current leads to connect to QD0 cryostat.

Pacman shielding is thinner than full detector and separates horizontally.

Putting service cryostat above is also possible.

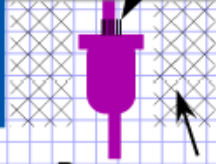


End View



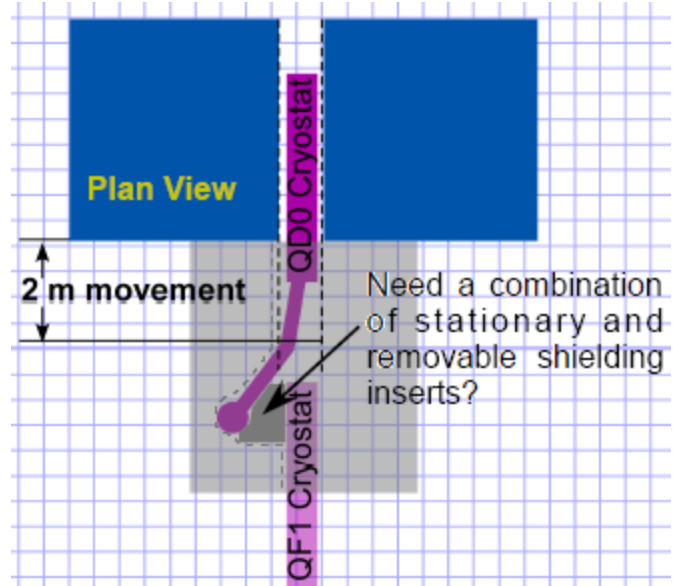
Elevation View

Single phase LHe supply and low pressure He return.



Pacman supported so that shielding can be moved out of the way when detector is opened.

Instrumentation and magnet current leads connection point.



Plan View

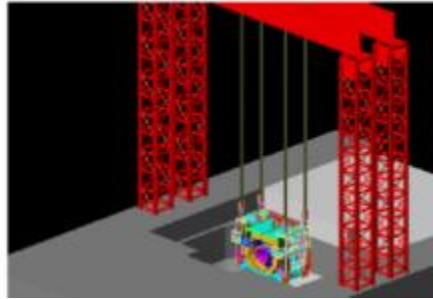
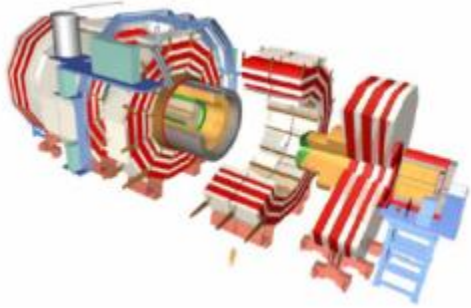
2 m movement

Need a combination of stationary and removable shielding inserts?

QD0-Service Cryostat connection line has to permit 2 m opening by door but vertical section must not point directly to incoming/outgoing beamlines.

B.Parker, et al

ILC Detector assembly

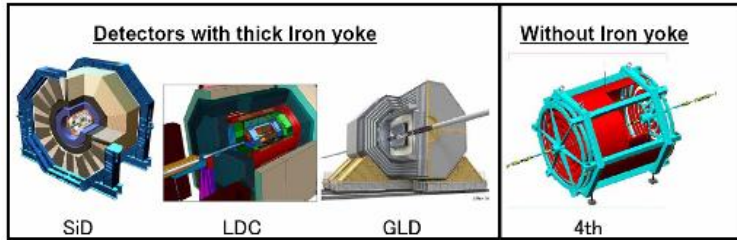


- CMS detector assembled on surface in parallel with underground work, lowered down with rented crane
- Adopted this method for ILC, to save 2-2.5 years that allows to fit into 7 years of construction

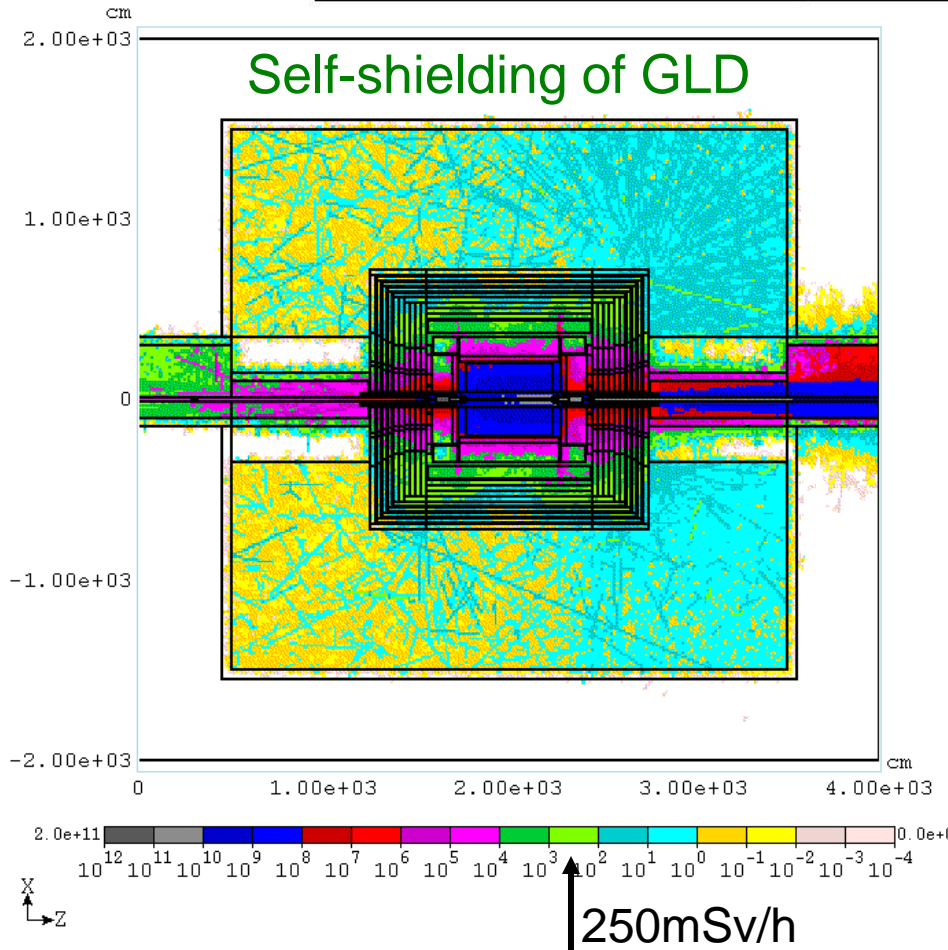




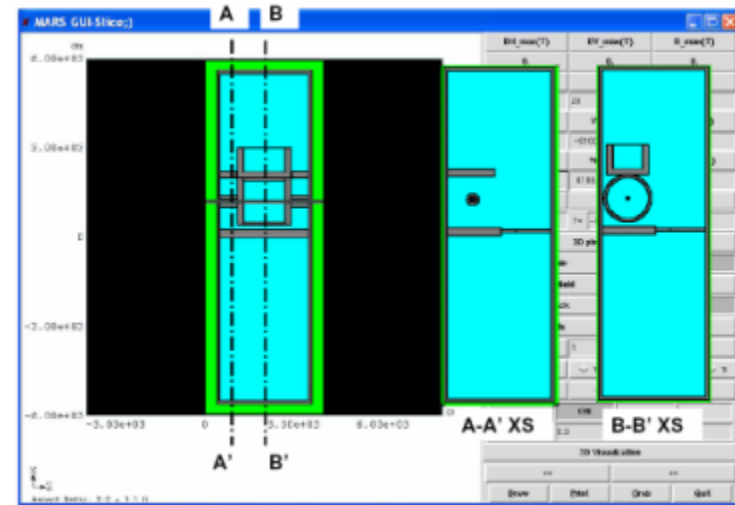
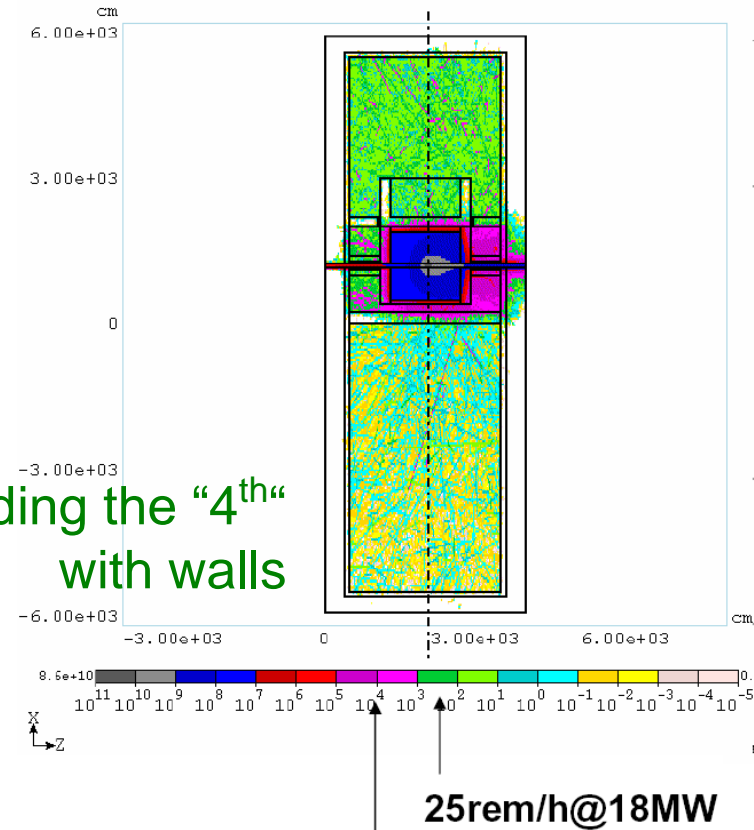
Shielding the IR hall



Self-shielding of GLD



Shielding the "4th" with walls

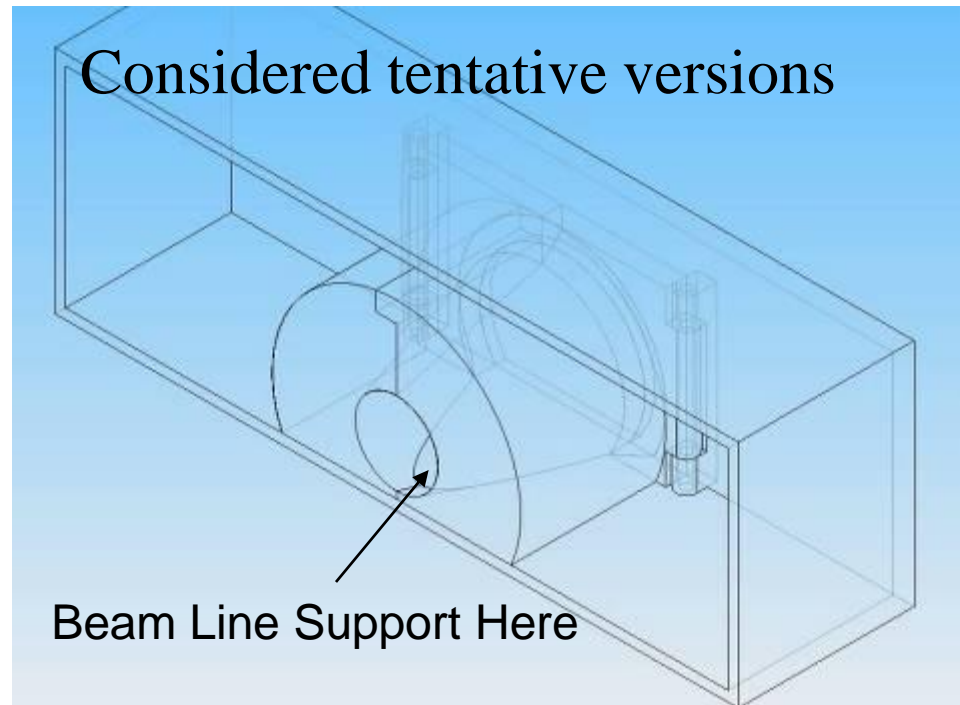
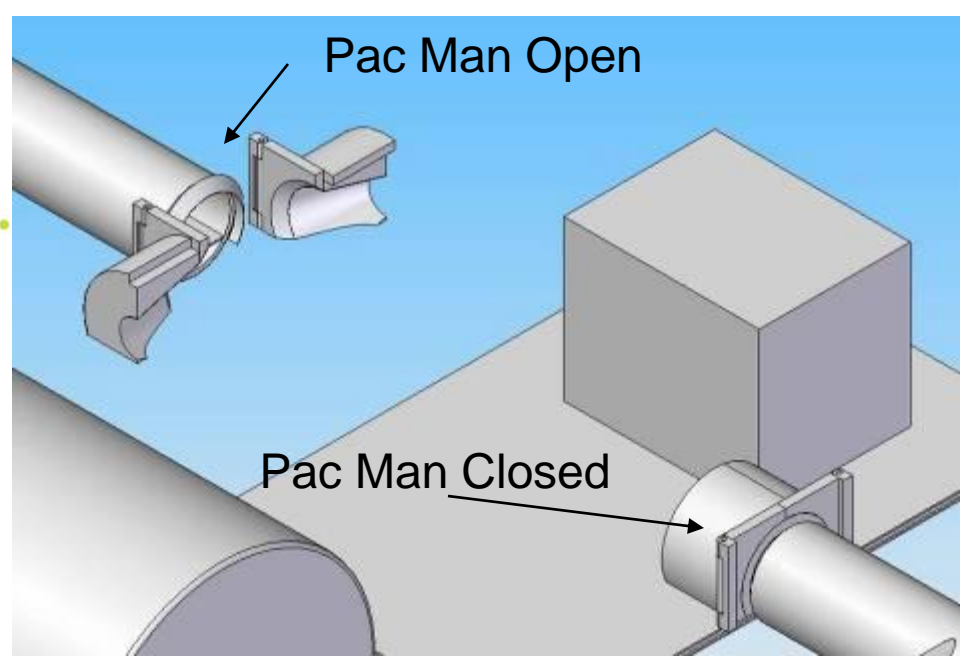


Pacman design

CMS shield opened

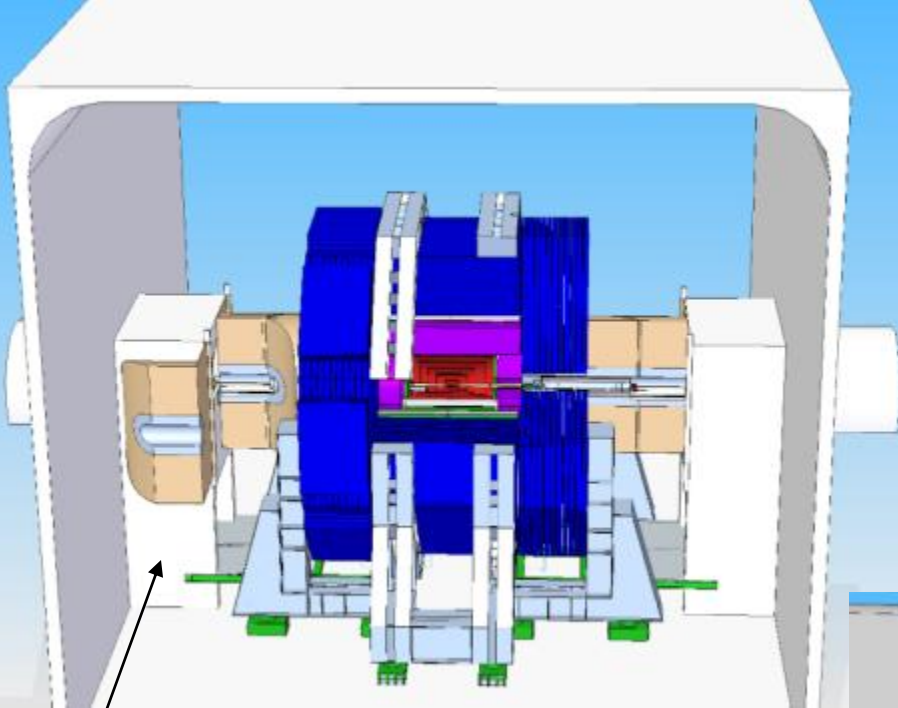


SLD pacman open



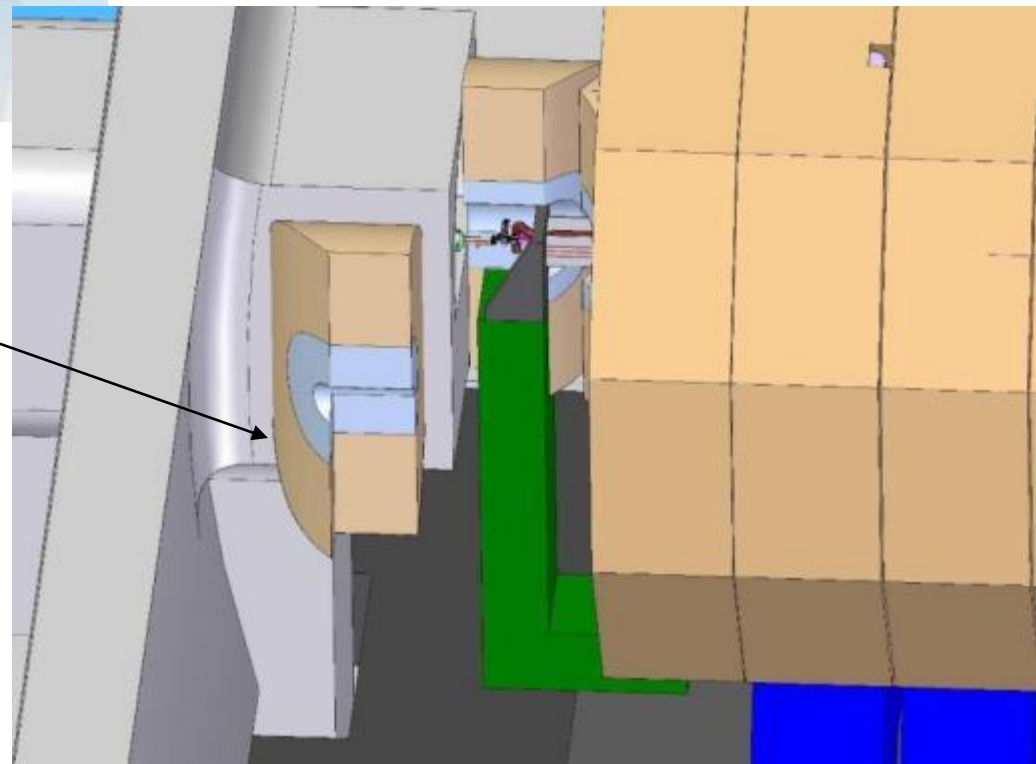
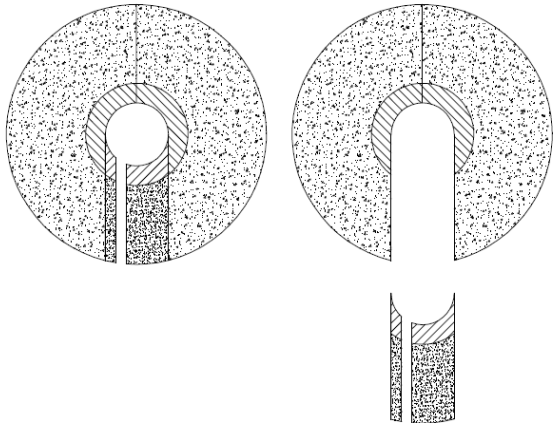
John Amann

Example of system where initially different designs converged on a single compatible solution:
CMS-Inspired Hinged PacMan w/ Cut-outs for ILD Pillar and Plugs



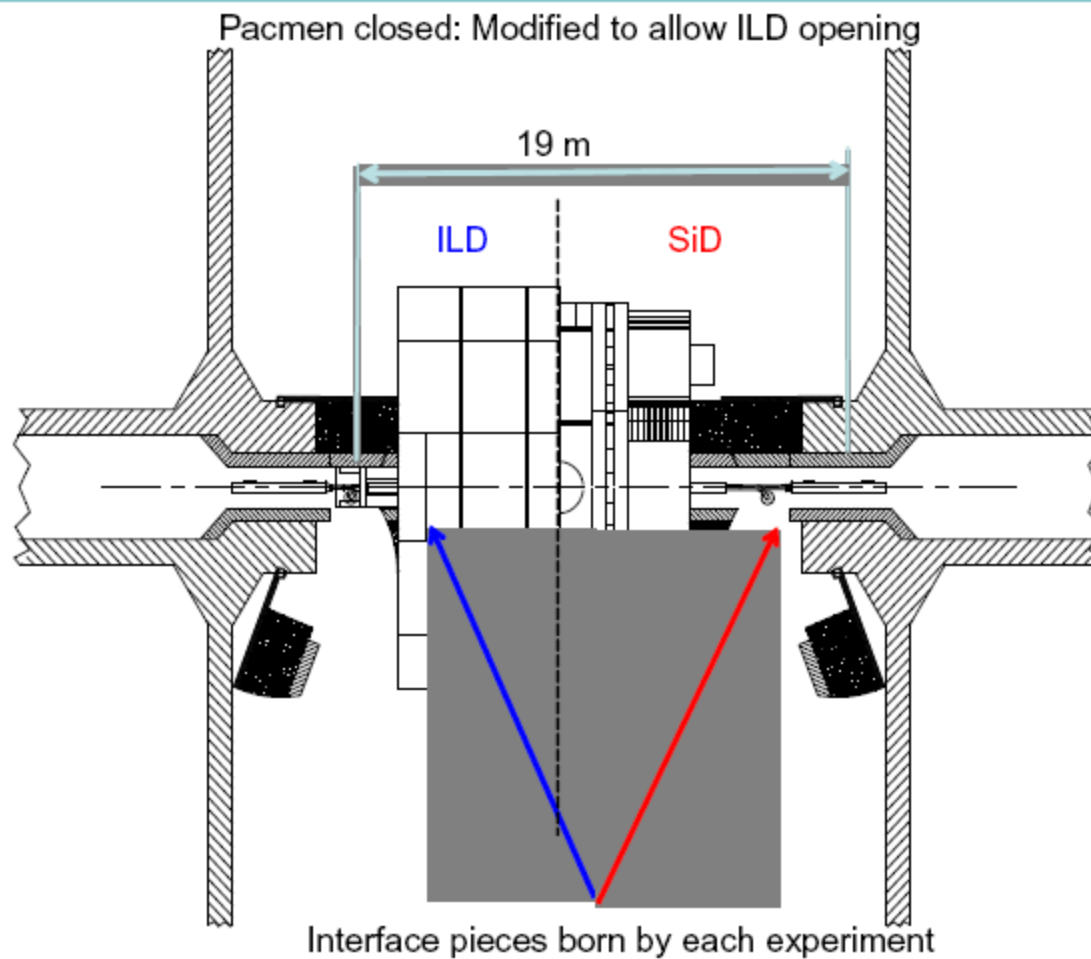
SiD

ILD



M.Oriunno, H.Yamaoka, A.Herve, et. al

Pacman compatible with SiD



From A. Hervé, K. Sinram, M. Oriunno



Moving the detector



XTWC

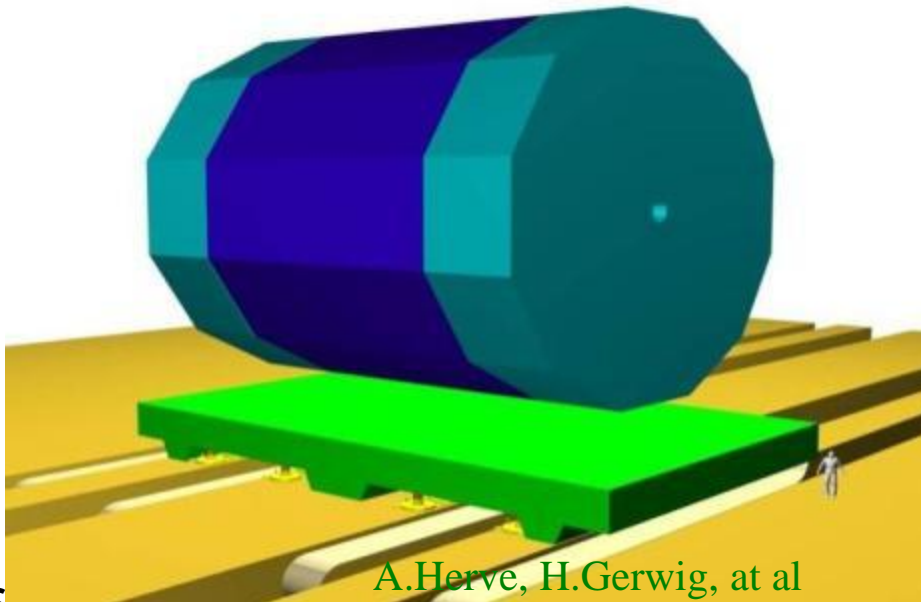
5000 ton Hilman roller module



Air-pads at CMS – move 2000k pieces

Is detector (compatible with on-surface assembly) rigid enough itself to avoid distortions during move?

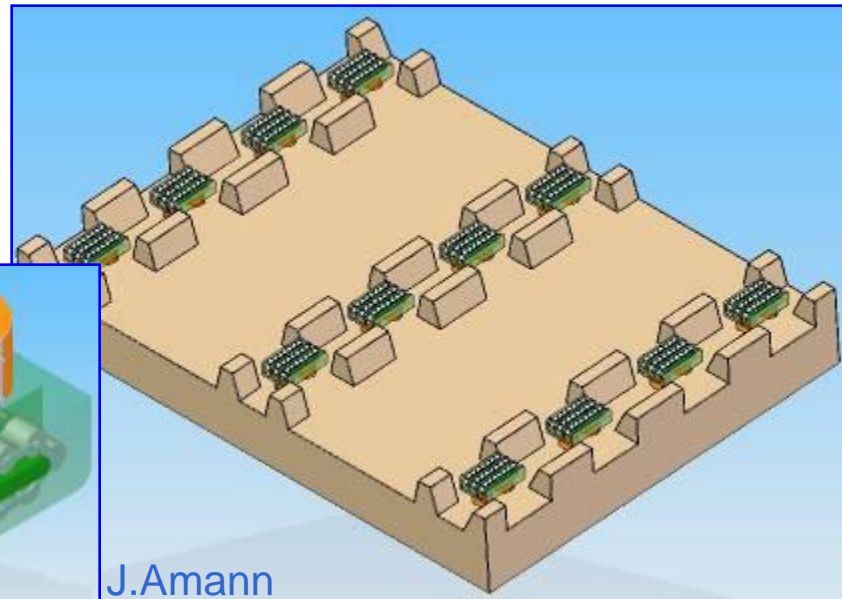
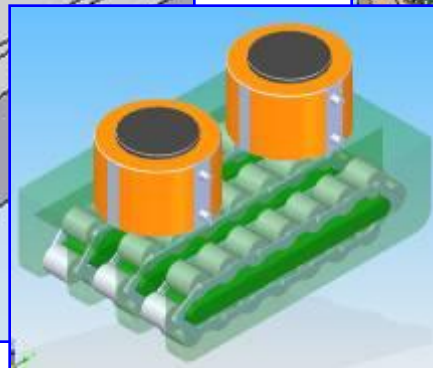
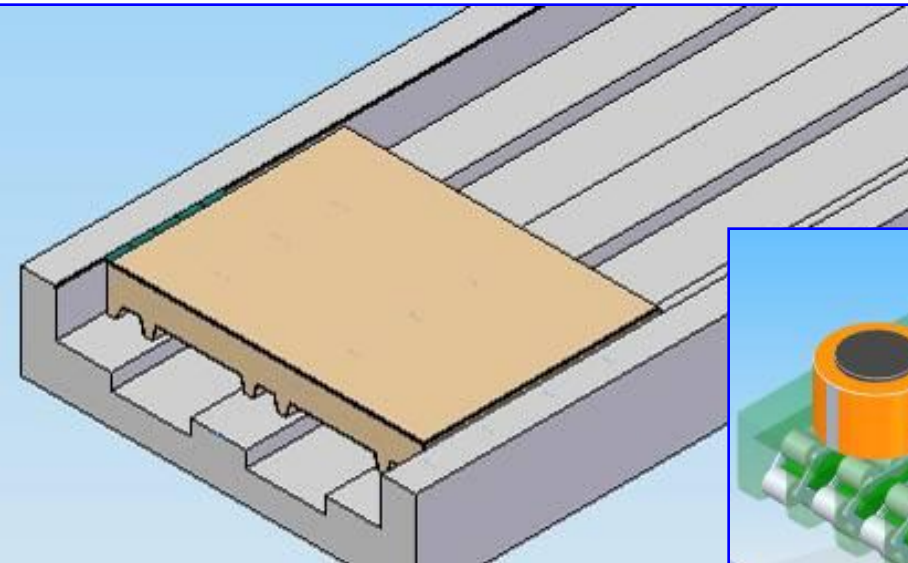
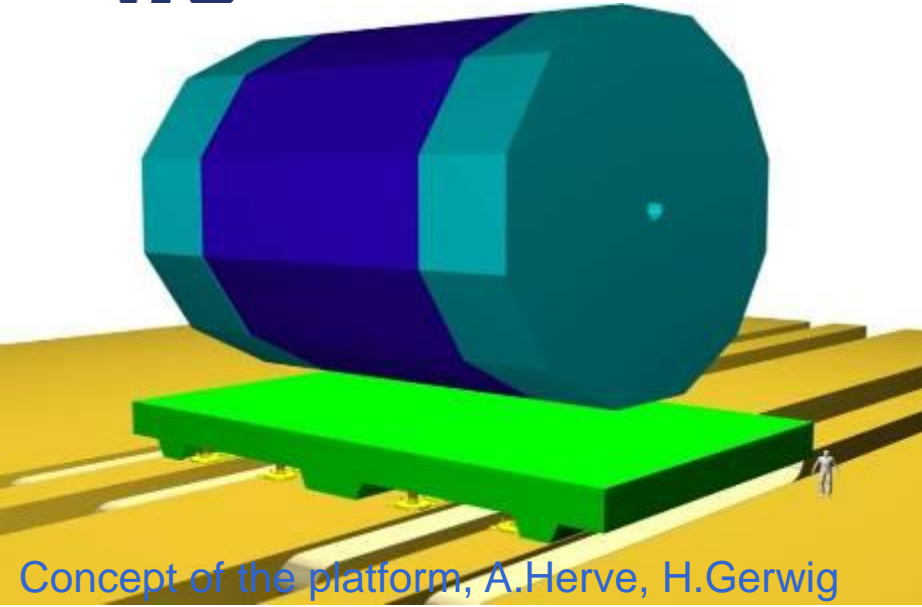
Concept of the platform to move ILC detector



A.Herve, H.Gerwig, et al



Moving the detector

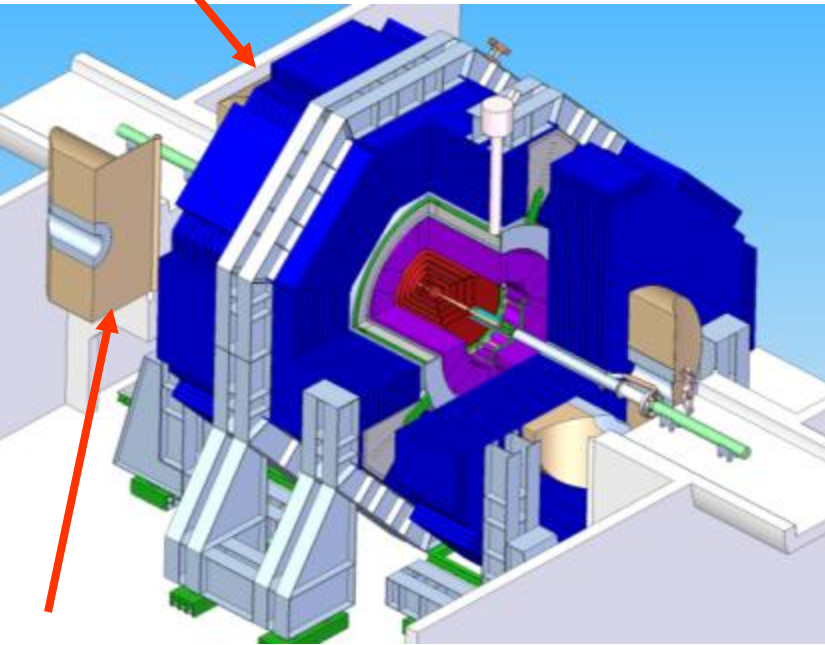


J.Amann

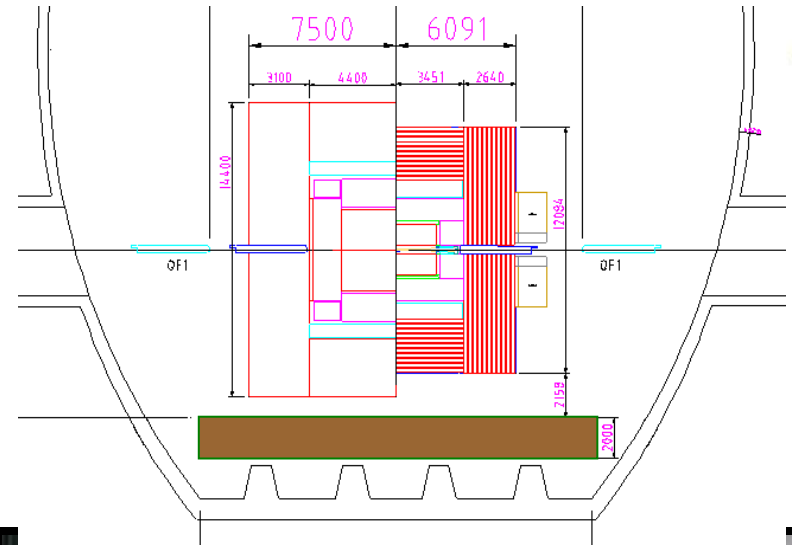


Example of MDI issues: moving detectors

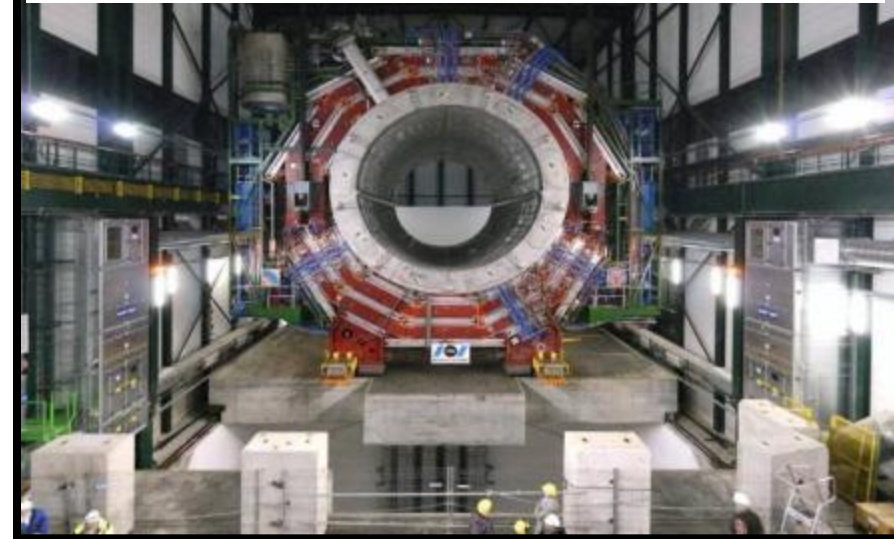
Detector motion system with or without an intermediate platform



Detector and beamline shielding elements

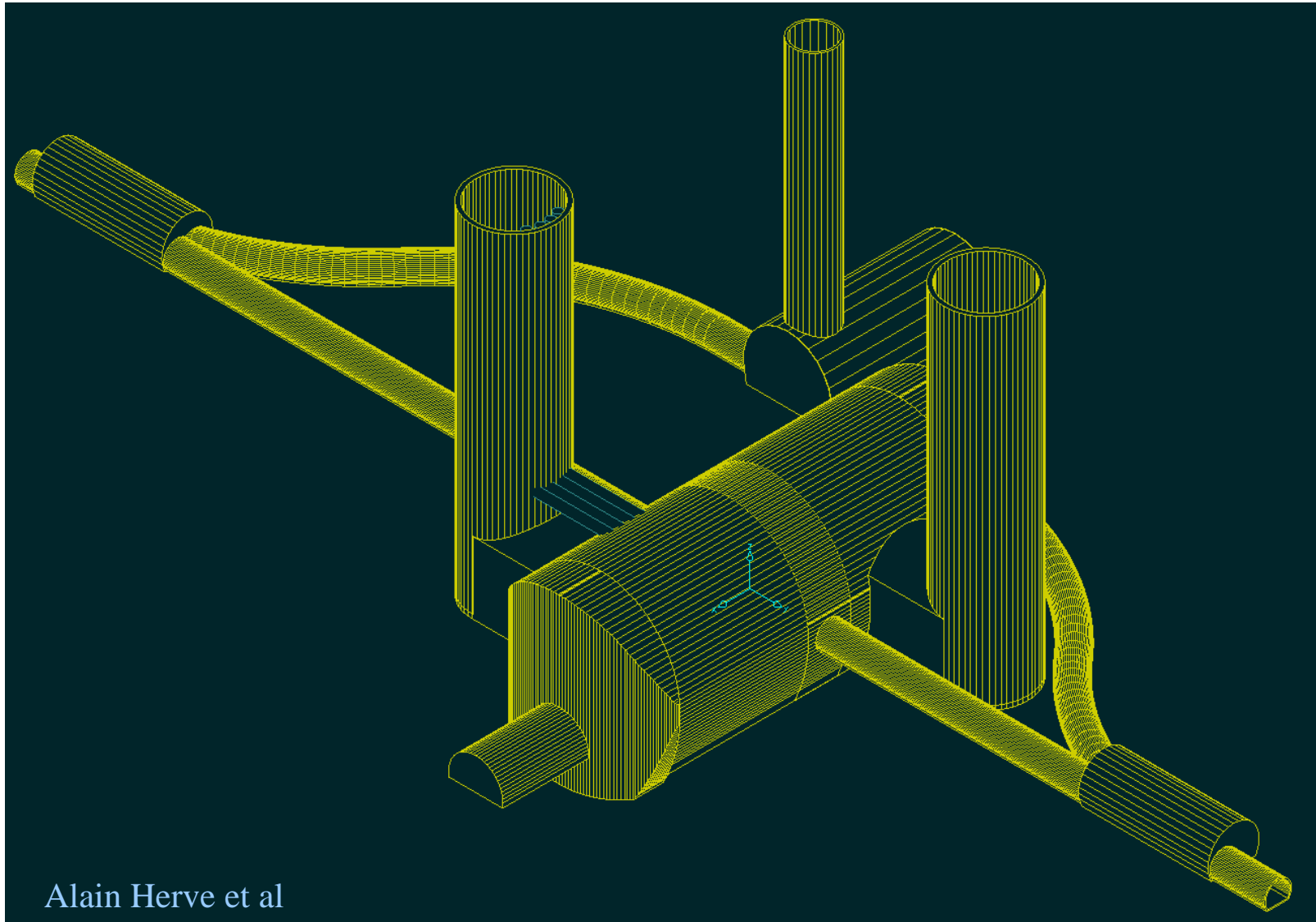


CMS platform – proof of principle for ILC





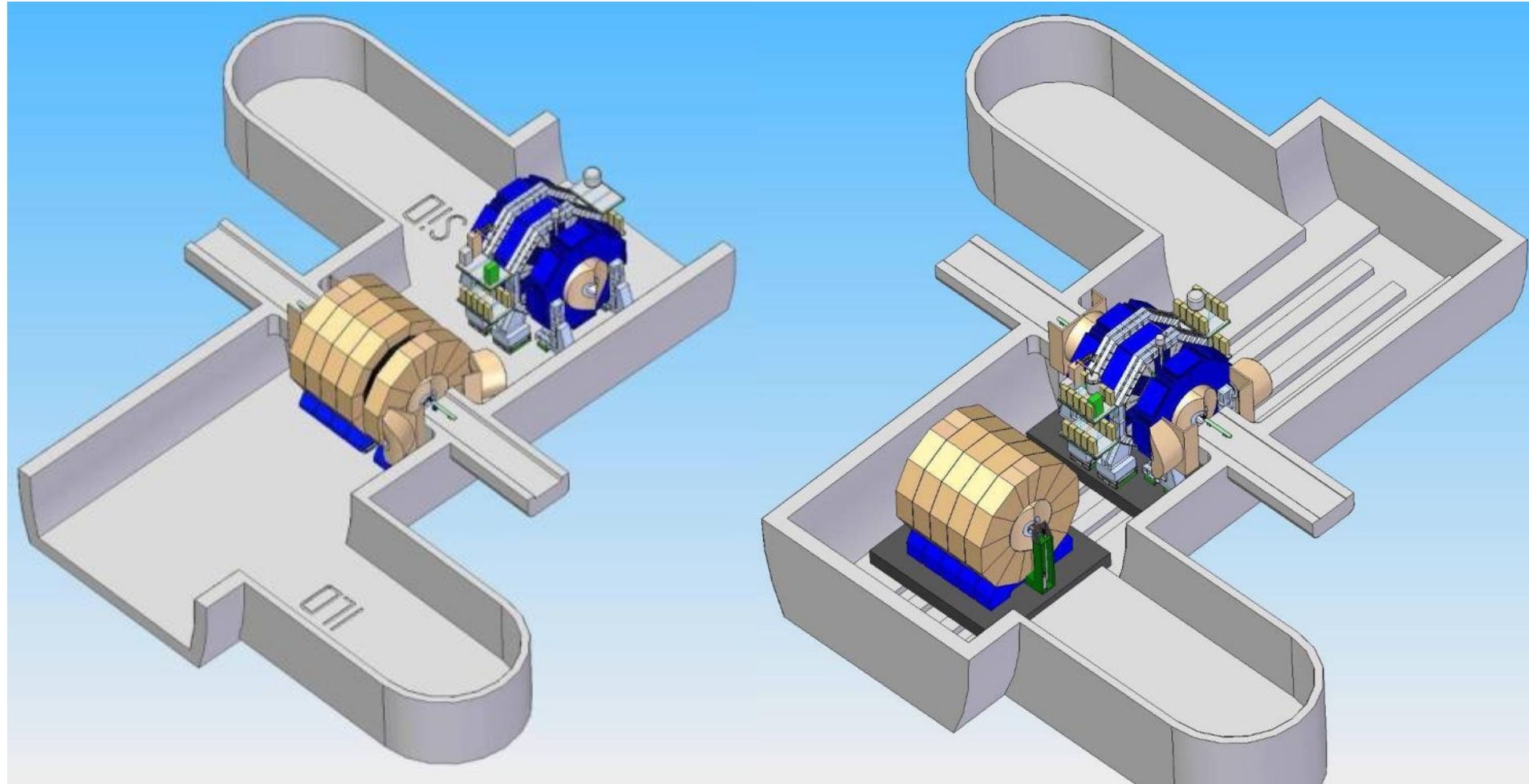
Configuration of IR tunnels and halls



Alain Herve et al

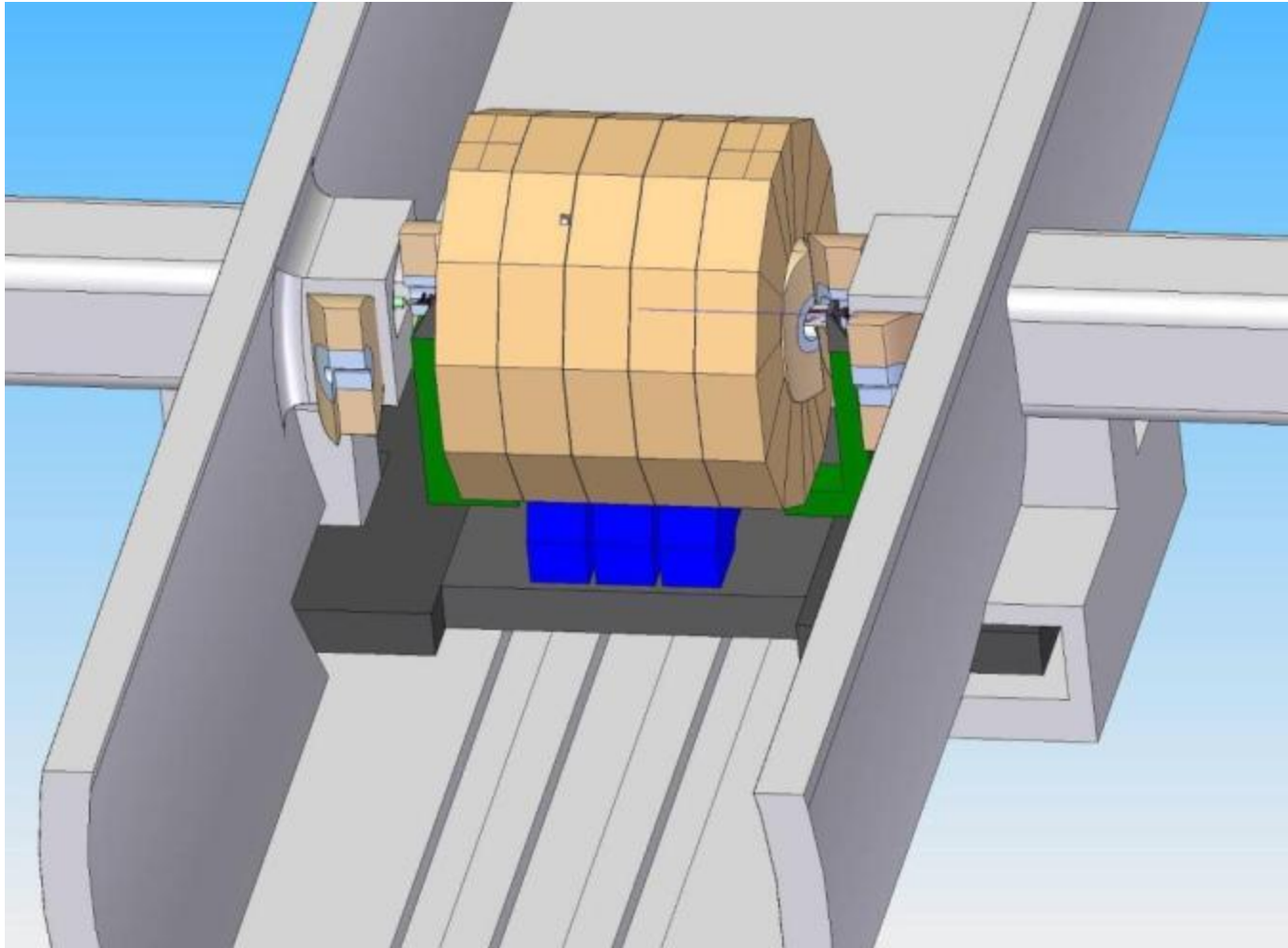


All detectors without / with platform



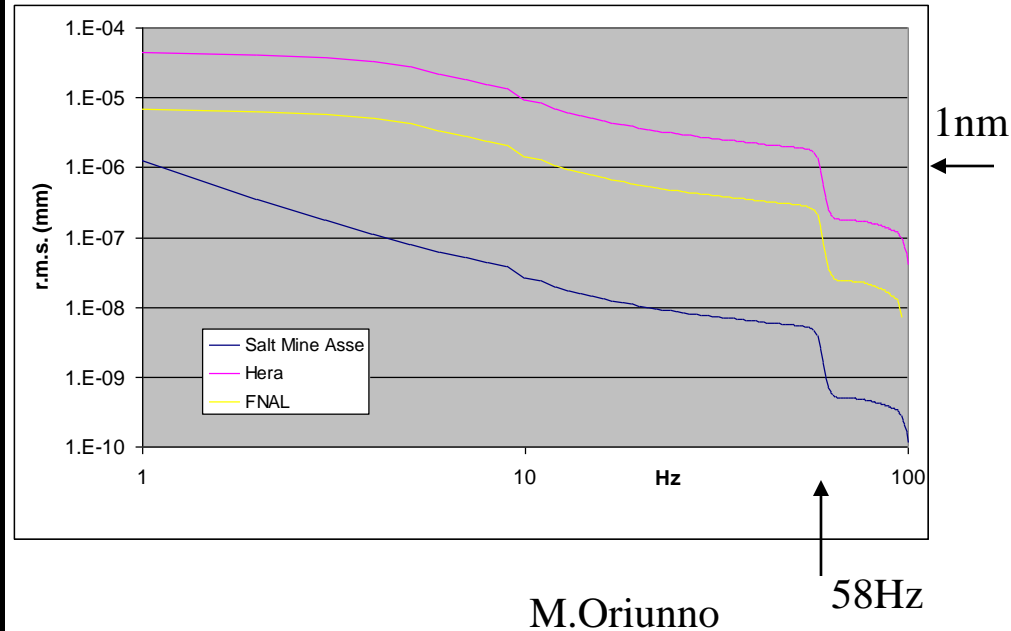
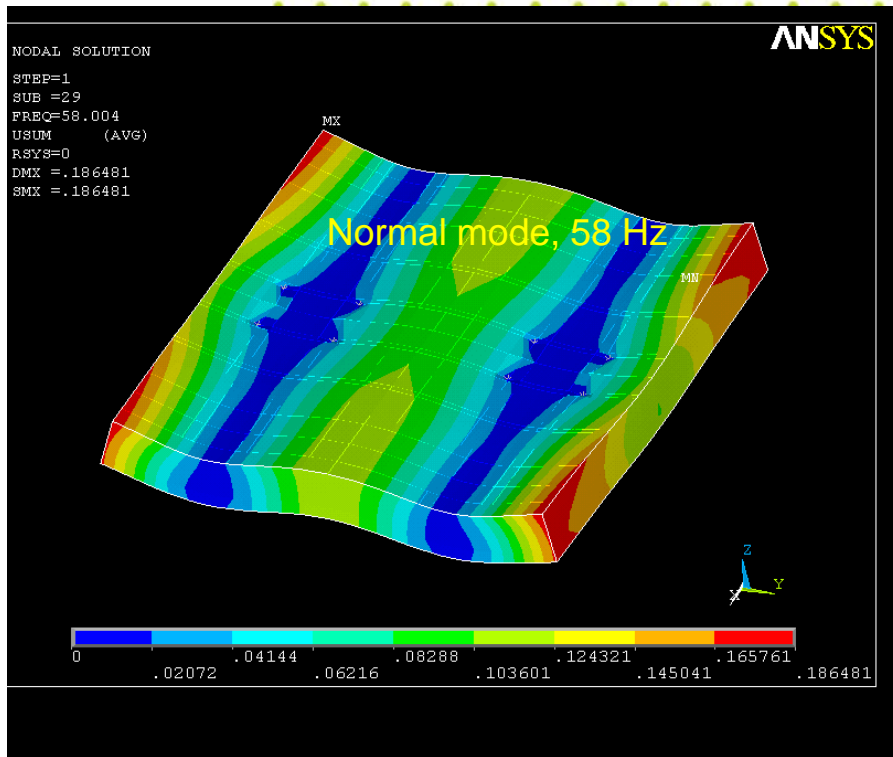


Half Platform w/ Pocket Storage

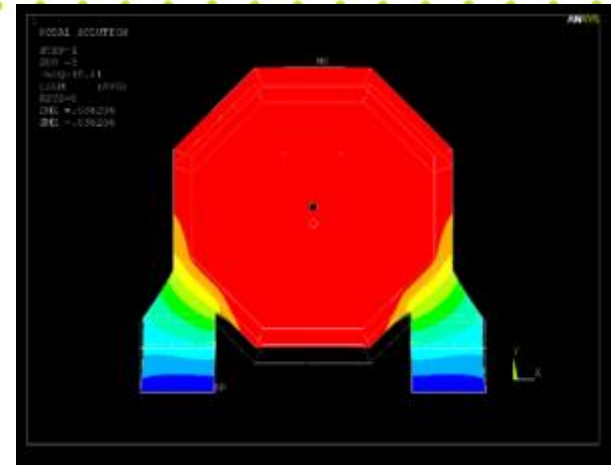
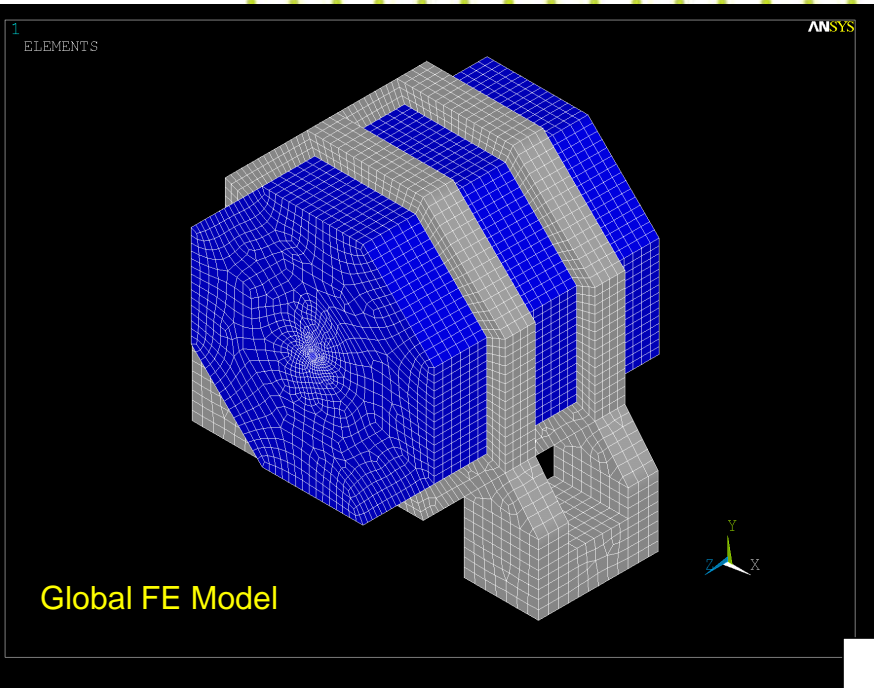


A.Herve, M.Oriunno, K.Sinram, T.Markiewicz, et al

Preliminary ANSYS analysis of Platform



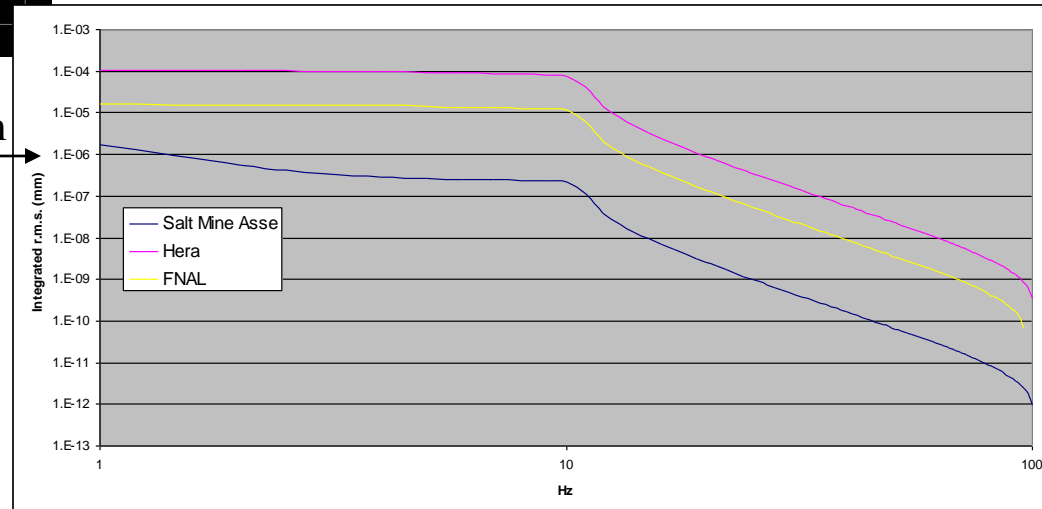
- First look of platform stability look rather promising: resonance frequencies are rather large (e.g. 58Hz) and additional vibration is only several nm



First vertical motion mode, 10.42 Hz

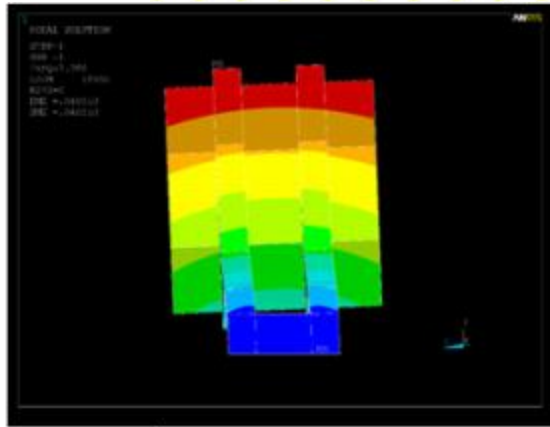
- First analysis shows possibilities for optimization
 - e.g. tolerance to fringe field => detector mass => resonance frequency

1 nm

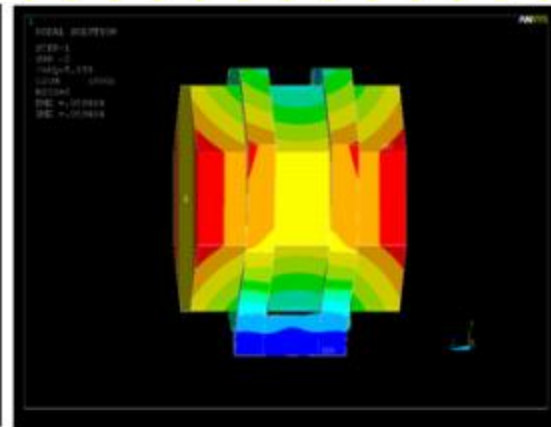




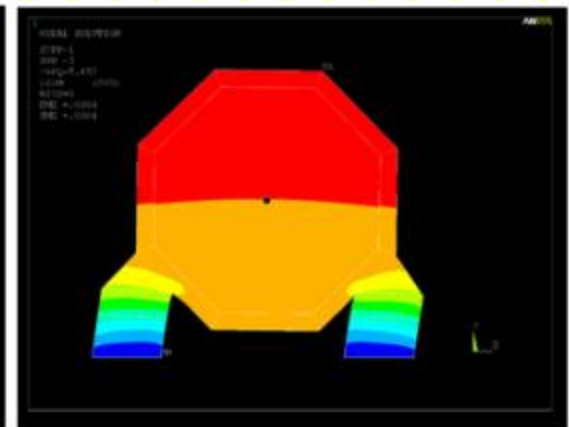
Free vibration modes of SiD



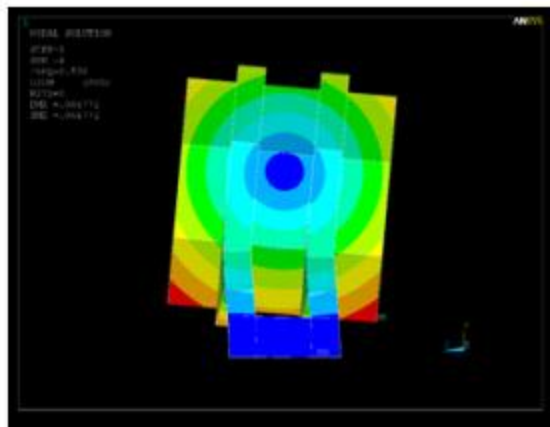
1st Mode, 2.38 Hz



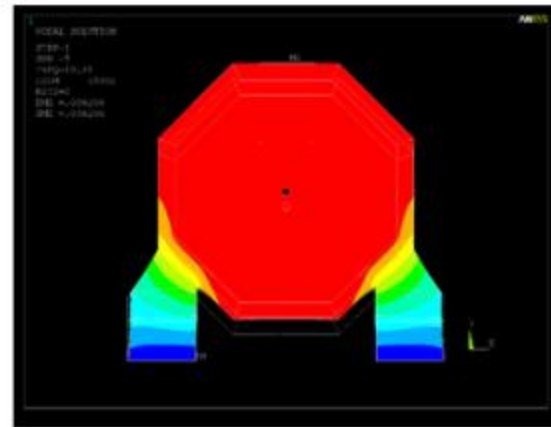
2nd Mode, 5.15 Hz



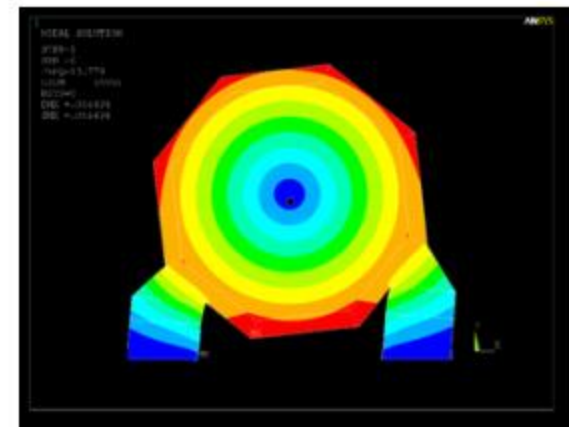
3rd Mode, 5.45 Hz



4th Mode, 6.53 Hz



5th Mode, 10.42 Hz



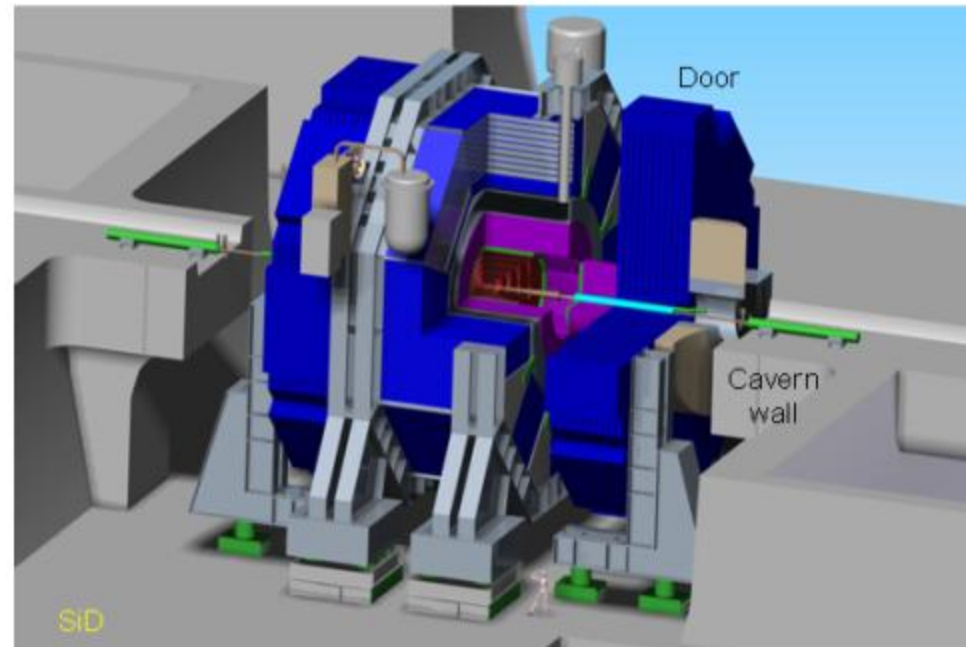
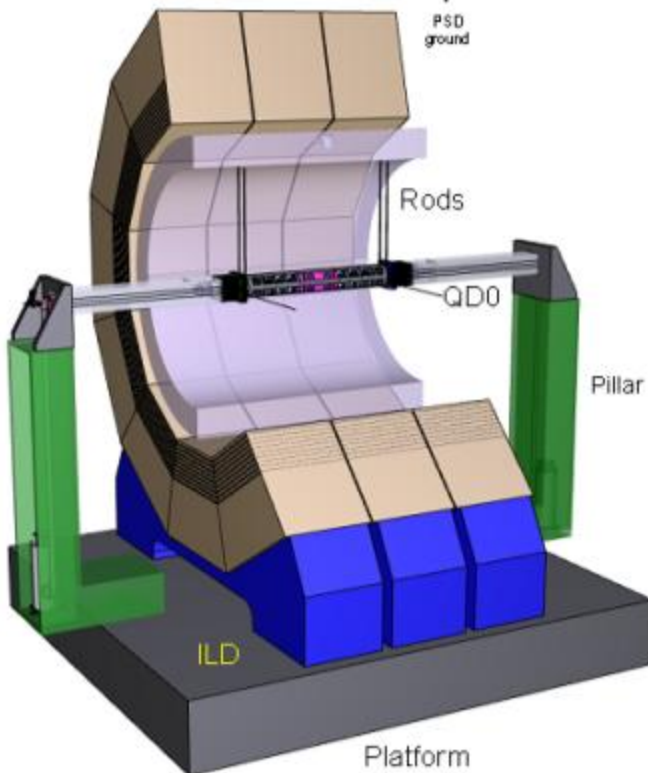
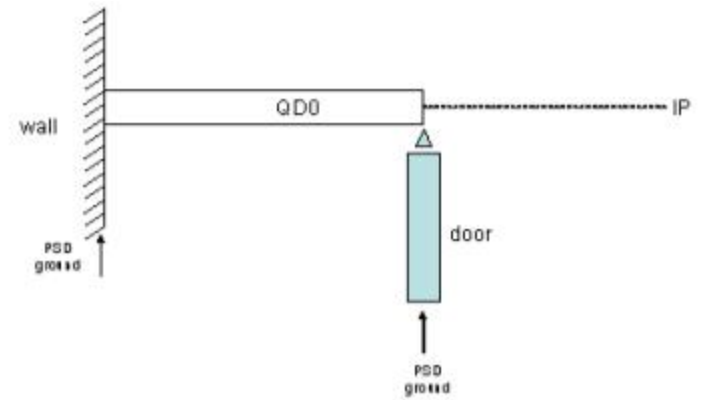
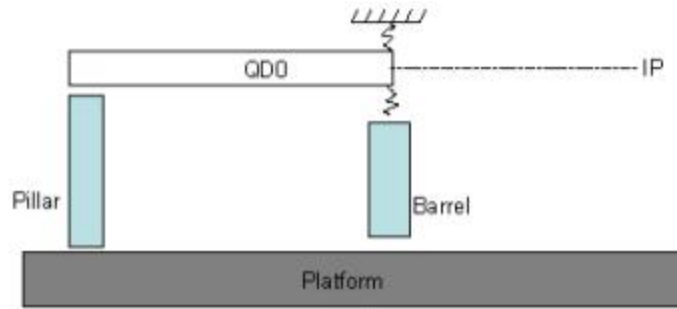
6th Mode, 13.7 Hz



Vertical motion

M.Oriunno

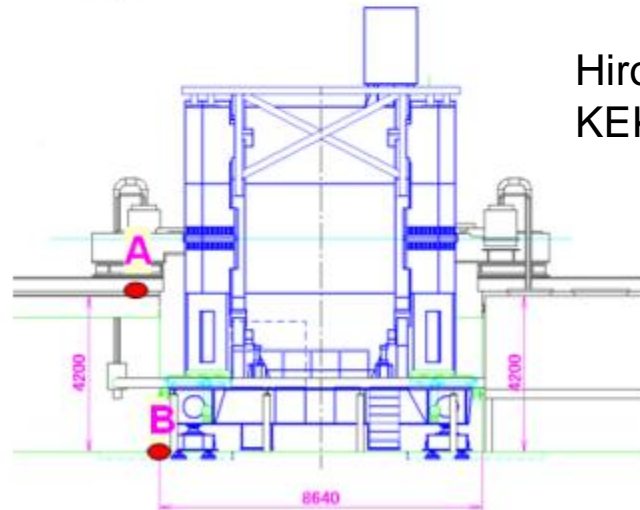
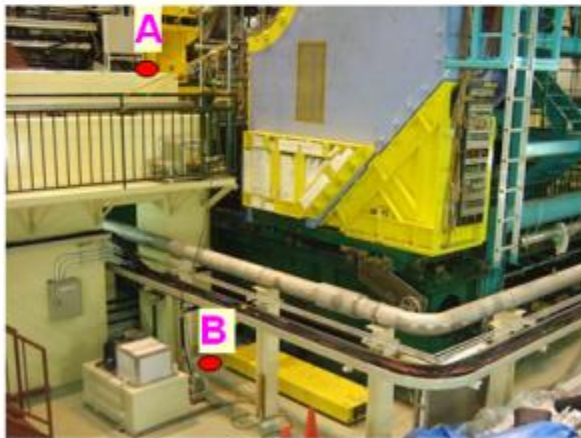
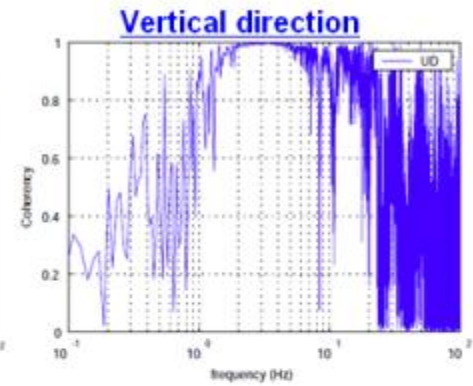
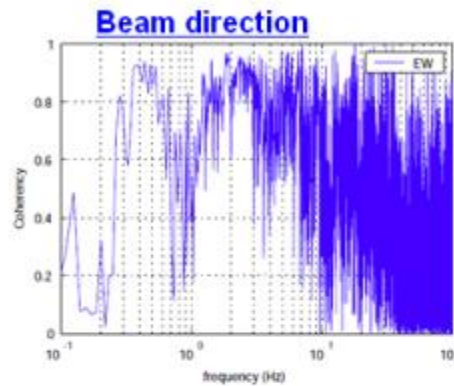
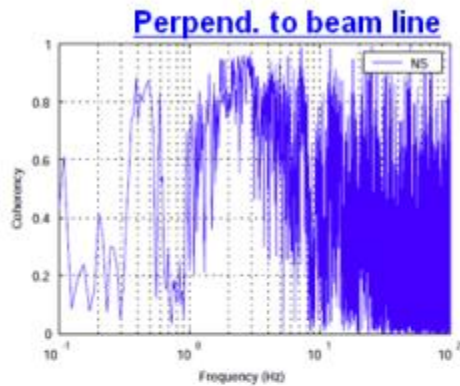
QDO supports in ILD and SiD



Stability studies at BELLE

Measurement: B

How is the coherency between the tunnel and floor?



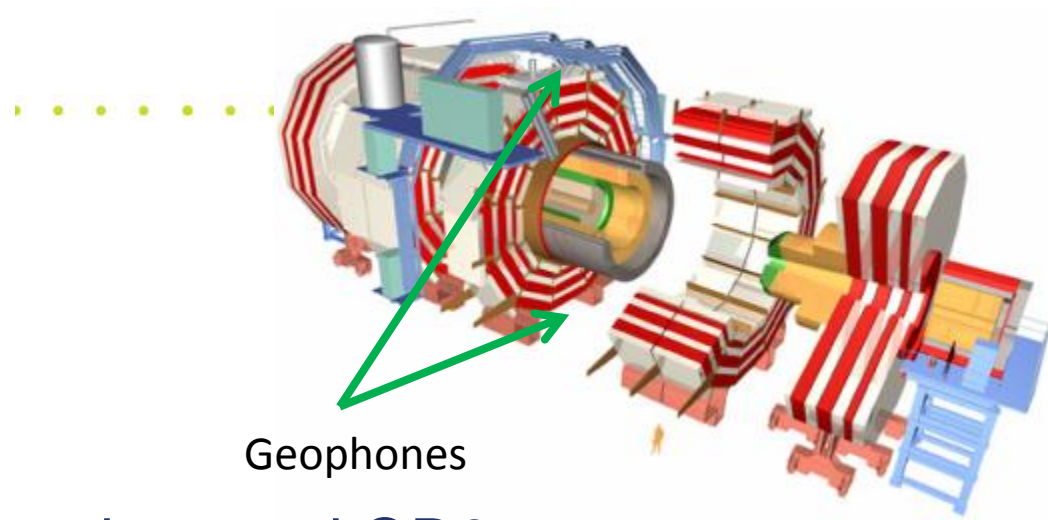
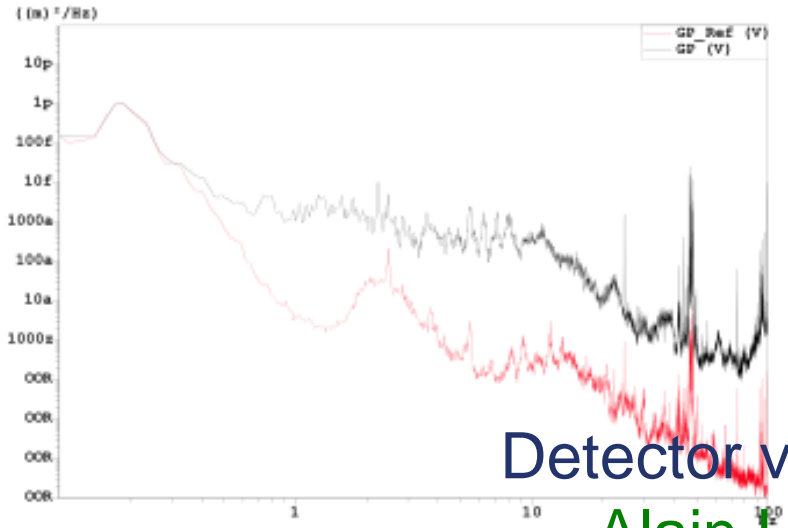
Hiroshi Yamaoka,
KEK

- Horizontal dir.: 0.~Hz, ~3Hz
- Vertical dir.: 1 ~ 20Hz



CMS top of Yoke measurement

PSD of the signals Vertical direction

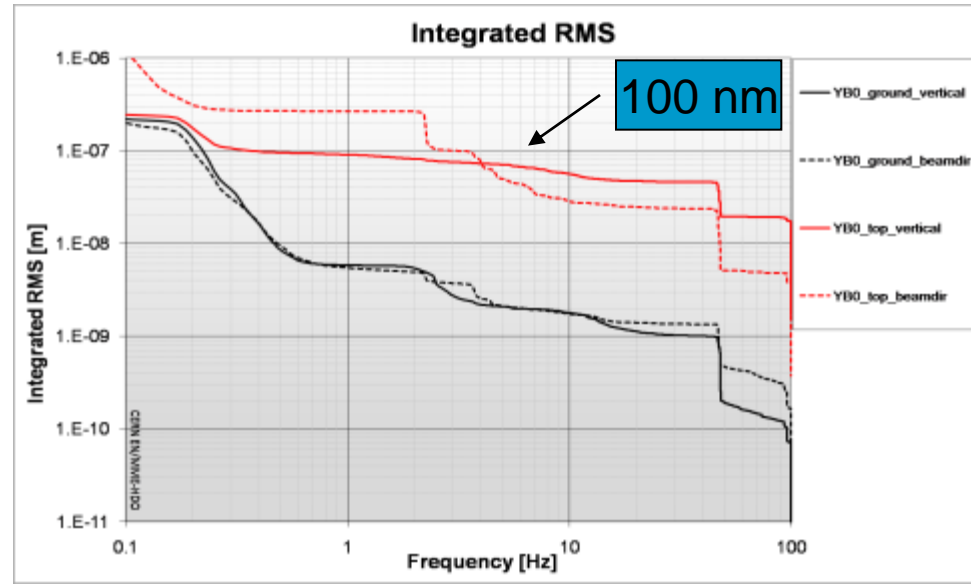
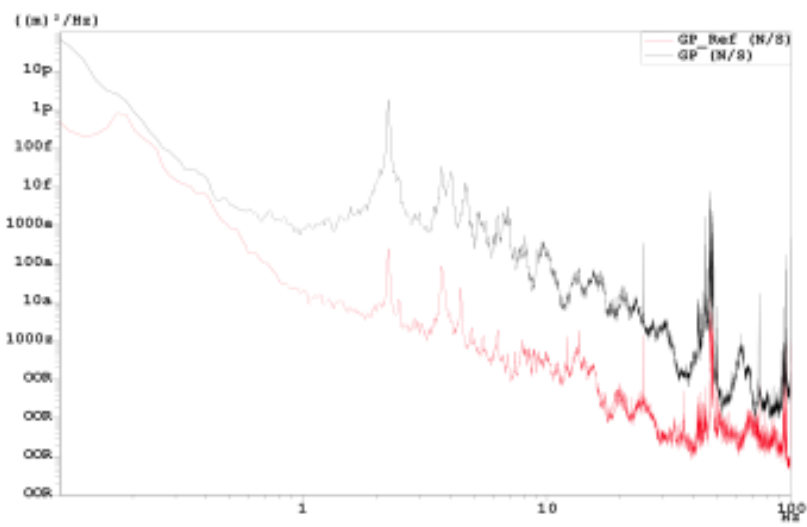


Detector vibrations and QD0 support

Cooling system OFF

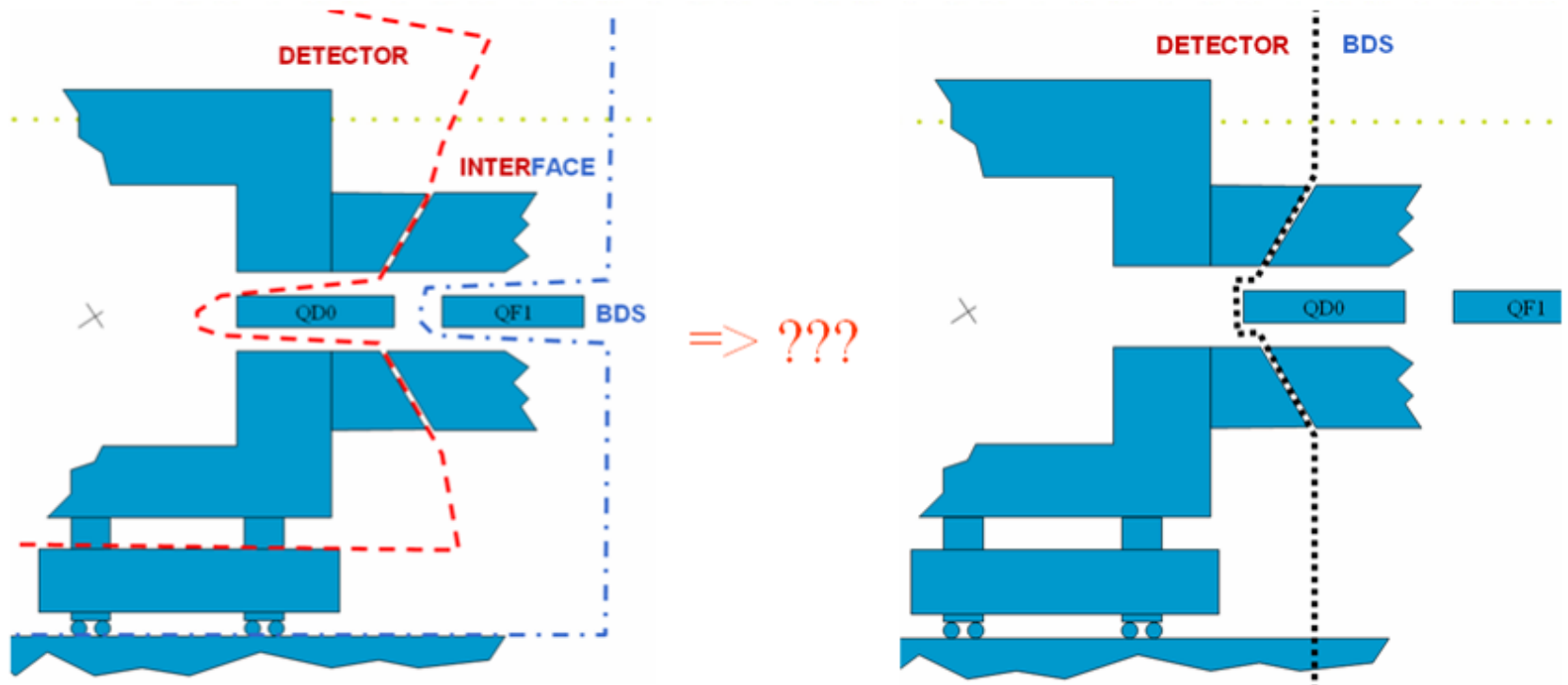
Alain Herve (ETH Zurich)

PSD of the signals Beam direction





Longer L^* \rightarrow Simplified MDI?



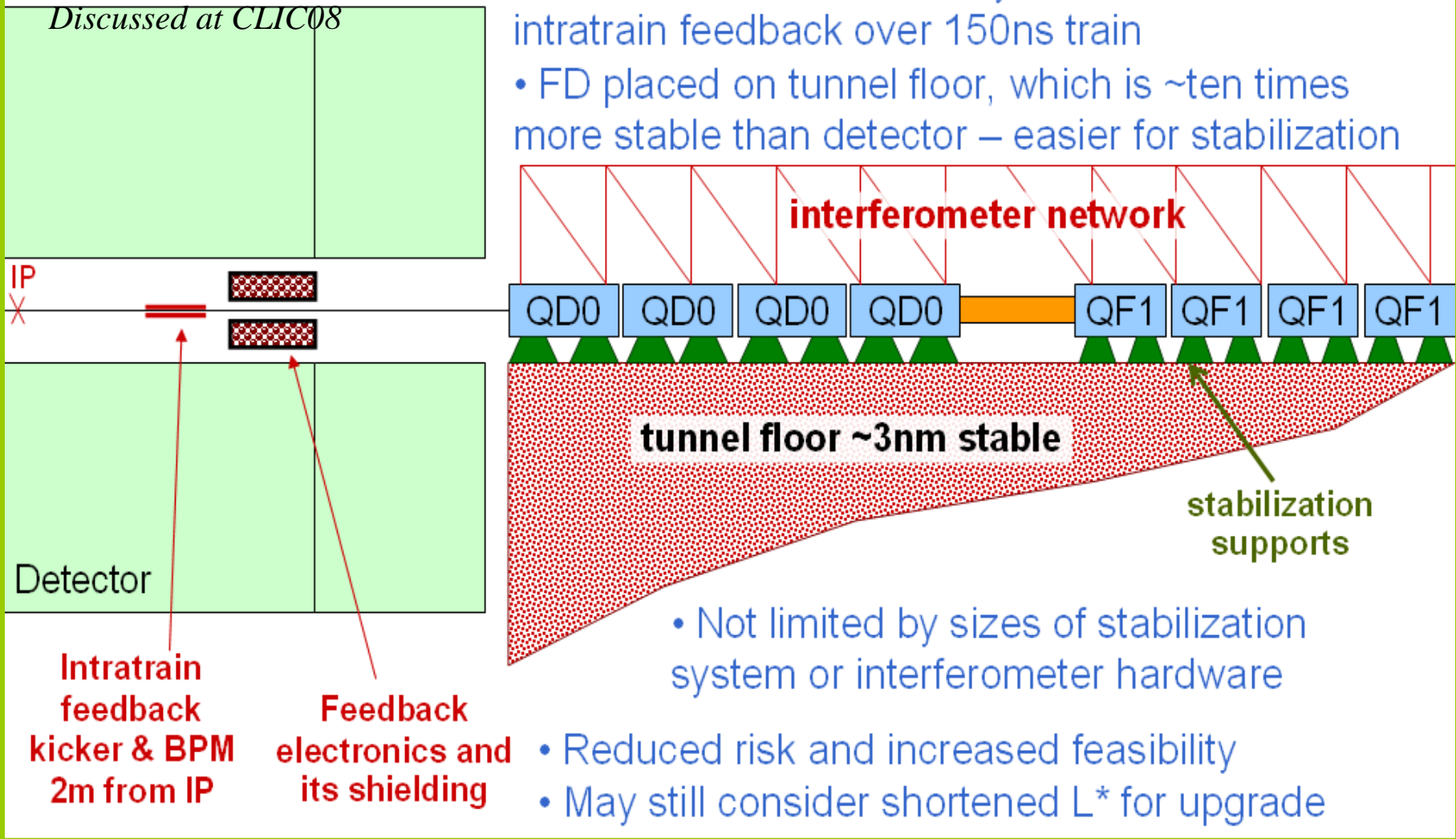
- If doubled L^* is feasible and acceptable then the MDI may be simplified tremendously
 - » and cost is reduced – do not need two extra sets of QDO
- An option of later upgrade for shorter L^* may always be considered
- Has to be studied further



Doubled L^* perhaps **necessary** for CLIC, where the FD stability requirement is ~ 0.1 nm

- Slower than $1/L^*$ dependence of $L_{um} \Rightarrow \uparrow L^*$
- Reduced feedback latency – several iteration of intratrain feedback over 150ns train
- FD placed on tunnel floor, which is \sim ten times more stable than detector – easier for stabilization

Discussed at CLIC08



- Not limited by sizes of stabilization system or interferometer hardware
- Reduced risk and increased feasibility
- May still consider shortened L^* for upgrade



FFS WITH L*=6M

In [12] it was proposed to use a longer L* to ease the QD0 stabilization challenge by supporting the FD on the tunnel. The initial lattice featured a L*=8m with about 30% lower luminosity than the current design and tighter pre-alignment tolerances to guarantee a successful tuning [2]. In the meantime the CLIC experiments have proposed to reduce the length of the detector to 6 m [13]. Consequently a new FFS has been designed with an L*=6m by scaling the old CLIC FFS with L*=4.3 m [14]. This lattice currently features IP spot sizes of $\sigma_x = 60.8$ nm and $\sigma_y = 1.9$ nm. Table 1 shows the total and energy peak luminosities for the different available FFS systems. Luminosity clearly decreases as L* increases. The L*=6 m case has a 16% lower peak luminosity than the nominal one (L*=3.5 m). Figure 5 displays the luminosity versus relative energy offset for all the FFS designs, showing a similar energy bandwidth in all cases.

L* [m]	Total luminosity [$10^{34} cm^{-2} s^{-1}$]	Peak luminosity [$10^{34} cm^{-2} s^{-1}$]
3.5	6.9	2.5
4.3	6.4	2.4
6	5.0	2.1
8	4.0	1.7

Table 1: Total and Peak luminosities for different L* lattices.

- [12] A. Seryi, "Near IR FF design including FD and longer L* issues", CLIC08.
- [13] CLIC09 Workshop, 12-16 October 2009, CERN ,
<http://indico.cern.ch/conferenceDisplay.py?confId=45580>
- [14] <http://clicr.web.cern.ch/CLICr/>

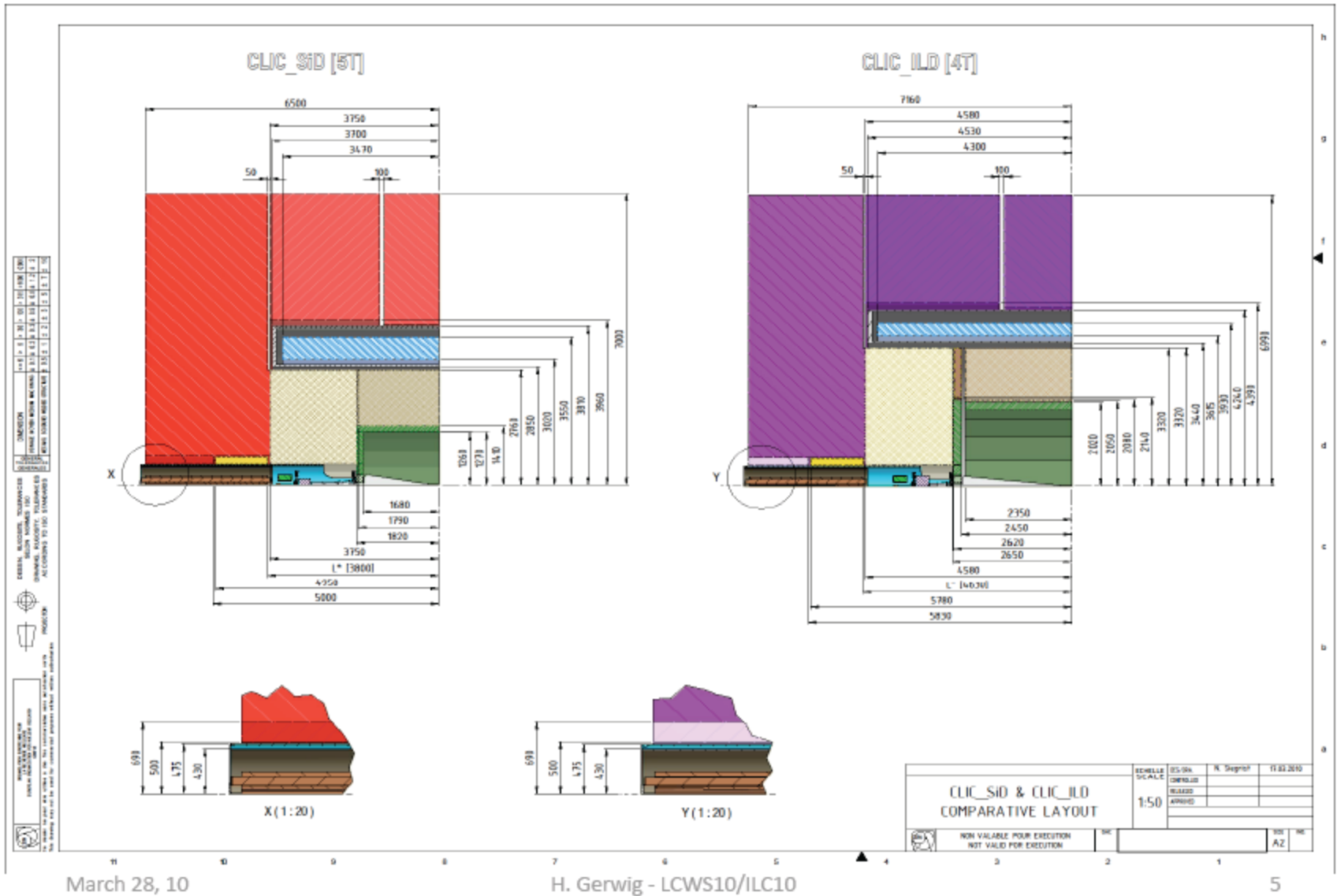
The CLIC Beam Delivery System towards the Conceptual Design Report

D. Angal-Kalinin, B. Bolzon, B. Dalena, L. Fernandez, F. Jackson, A. Jeremie, B. Parker
J. Resta López, G. Rumolo, D. Schulte, A. Seryi, J. Snuverink, R. Tomás and G. Zamudio

IPAC10



CLIC detector comparison



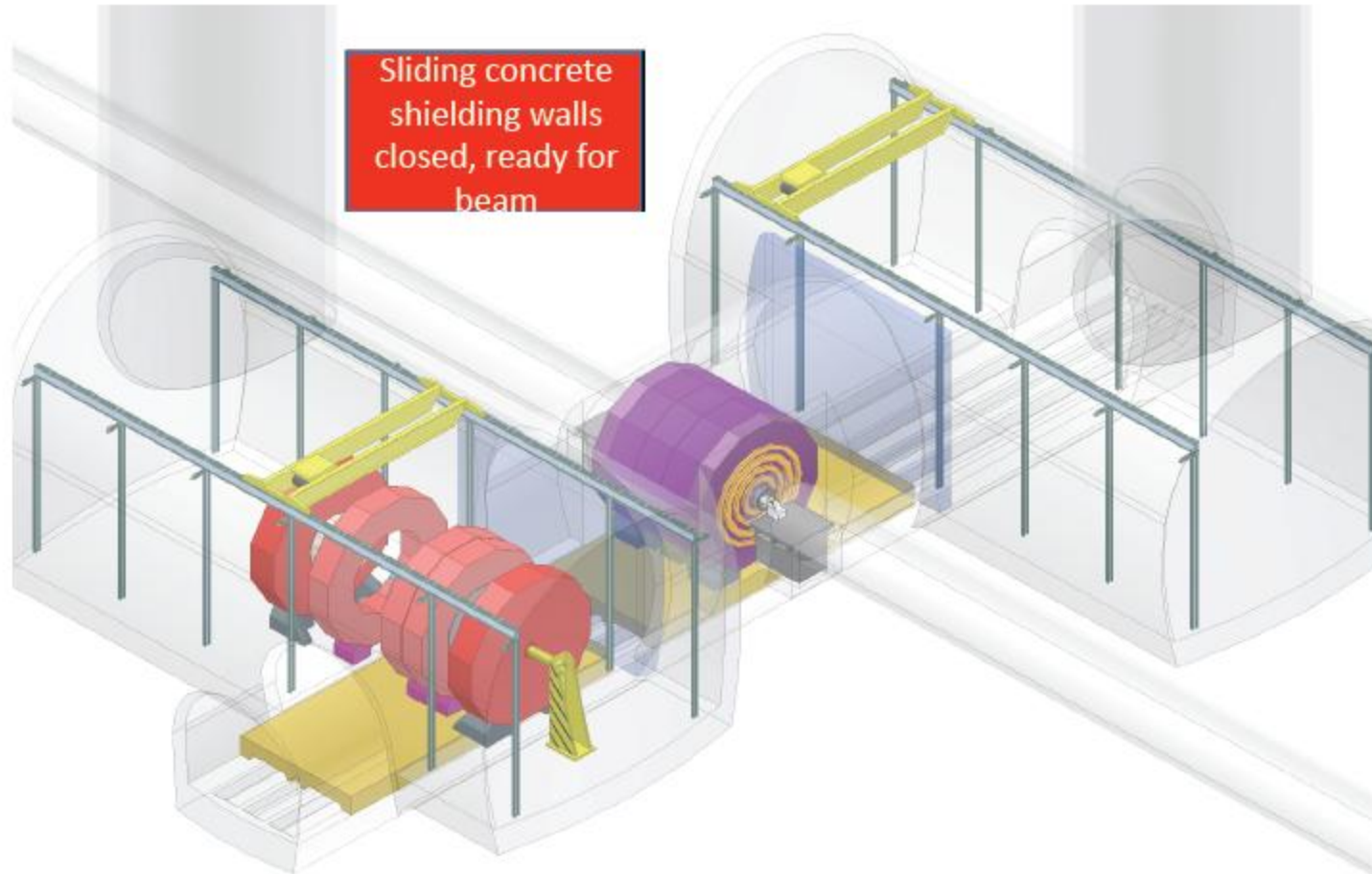
March 28, 10

H. Gerwig - LCWS10/ILC10

5

New concept of CLIC push-pull

Experiment 2 sliding on IP, shielding walls closed





New Low P parameter set

	Nom. RDR	Low P RDR	new Low P
Case ID	1	2	3
E CM (GeV)	500	500	500
N	2.0E+10	2.0E+10	2.0E+10
n_b	2625	1320	1320
F (Hz)	5	5	5
P_b (MW)	10.5	5.3	5.3
$\gamma\epsilon_x$ (m)	1.0E-05	1.0E-05	1.0E-05
$\gamma\epsilon_y$ (m)	4.0E-08	3.6E-08	3.6E-08
β_x (m)	2.0E-02	1.1E-02	1.1E-02
β_y (m)	4.0E-04	2.0E-04	2.0E-04
Travelling focus	No	No	Yes
Z-distribution *	Gauss	Gauss	Gauss
σ_x (m)	6.39E-07	4.74E-07	4.74E-07
σ_y (m)	5.7E-09	3.8E-09	3.8E-09
σ_z (m)	3.0E-04	2.0E-04	3.0E-04
Guinea-Pig $\delta E/E$	0.023	0.045	0.036
Guinea-Pig L (cm ⁻² s ⁻¹)	2.02E+34	1.86E+34	1.92E+34
Guinea-Pig Lumi in 1%	1.50E+34	1.09E+34	1.18E+34

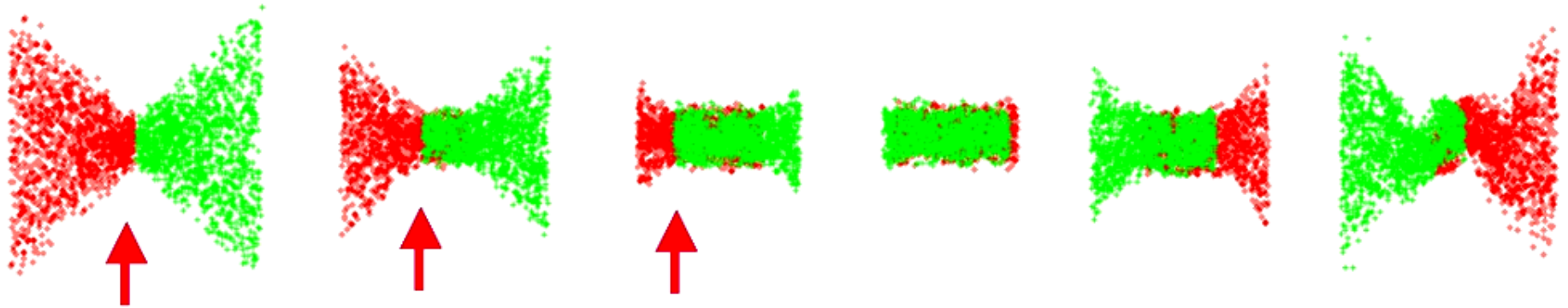
Travelling focus allows to lengthen the bunch

Thus, beamstrahlung energy spread is reduced

Focusing during collision is aided by focusing of the opposite bunch

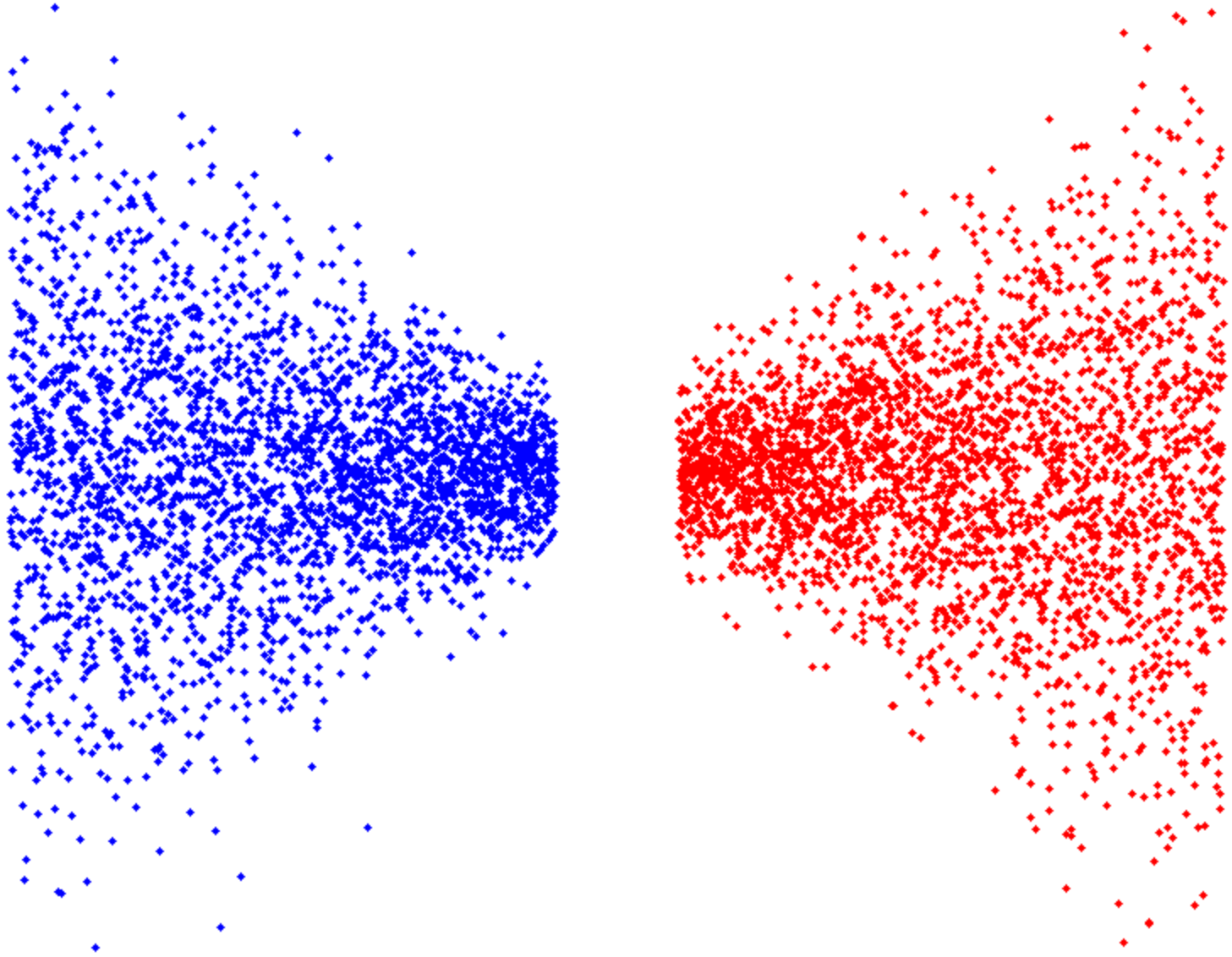
Focal point during collision moves to coincide with the head of the opposite bunch

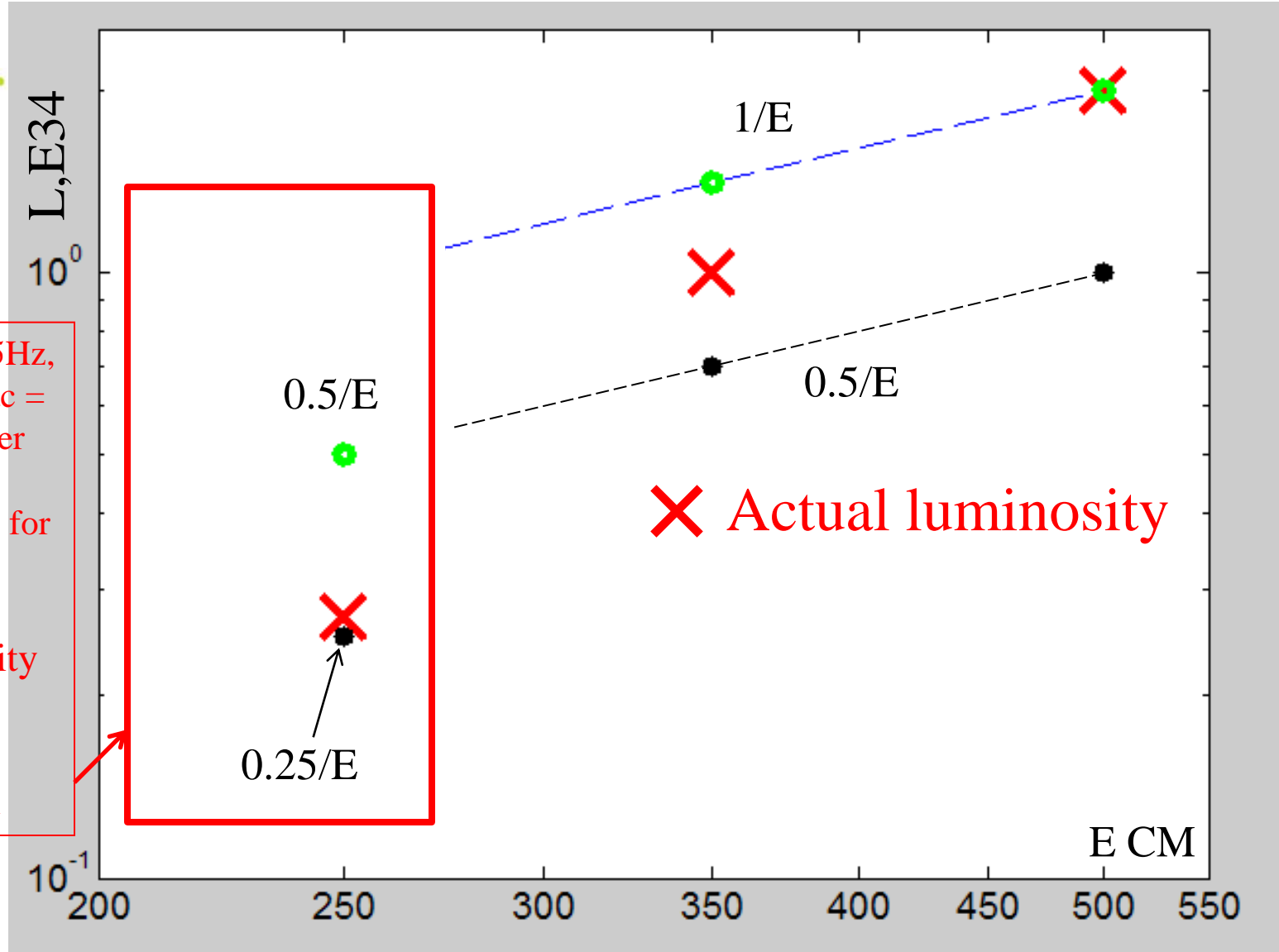
*for flat z distribution the full bunch length is $\sigma_z * 2 * 3^{1/2}$



- Suggested by V.Balakin in ~1991 – idea is to use beam-beam forces for additional focusing of the beam – allows some gain of luminosity or overcome somewhat the hour-glass effect
- Figure shows simulation of traveling focus. The arrows show the position of the focus point during collision
- So far not yet used experimentally

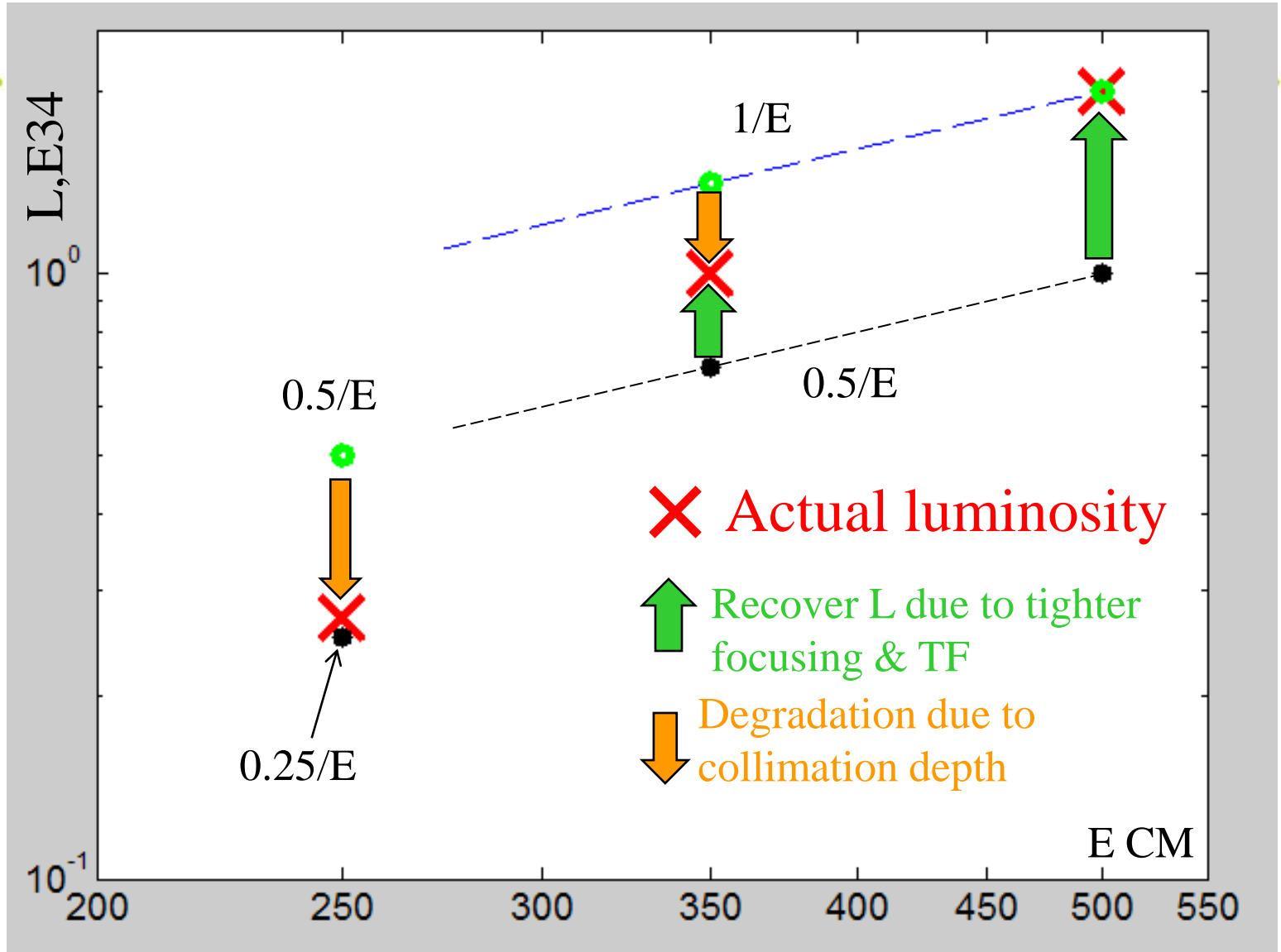
Collision with travelling focus





Rate at IP = 2.5Hz,
Rate in the linac =
5Hz (every other
pulse is at
150GeV/beam, for
e+ production)

Low luminosity
at this energy
reduces the
physics reach

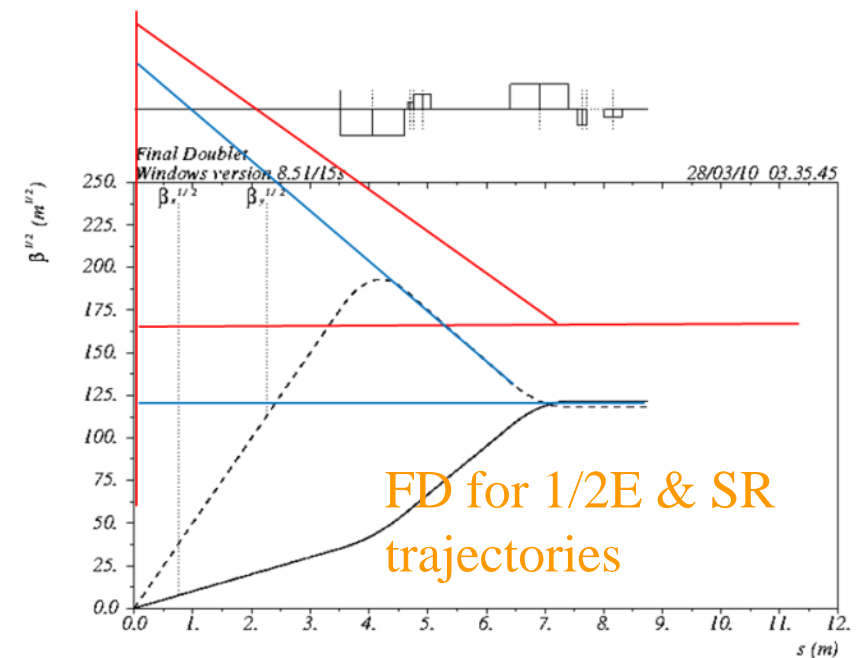
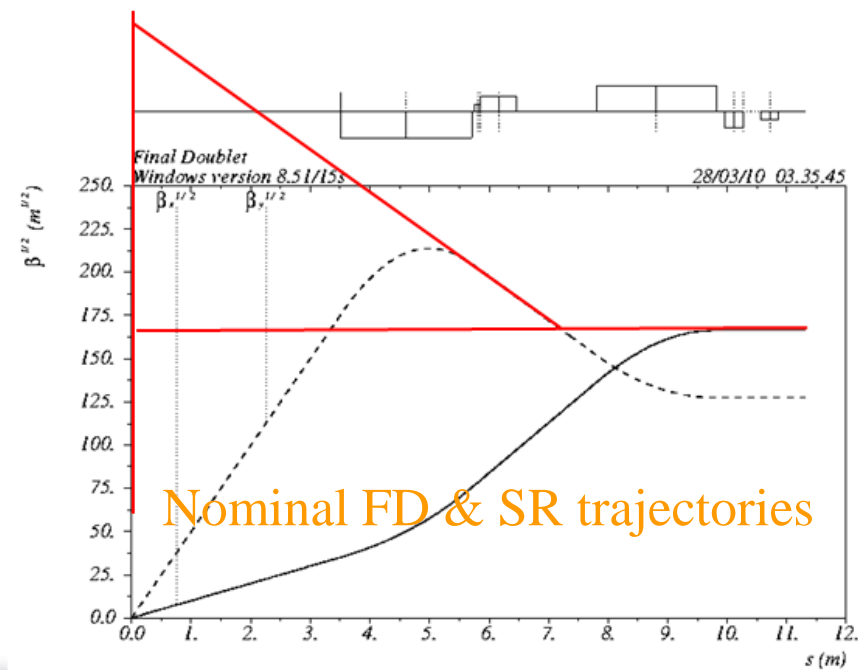
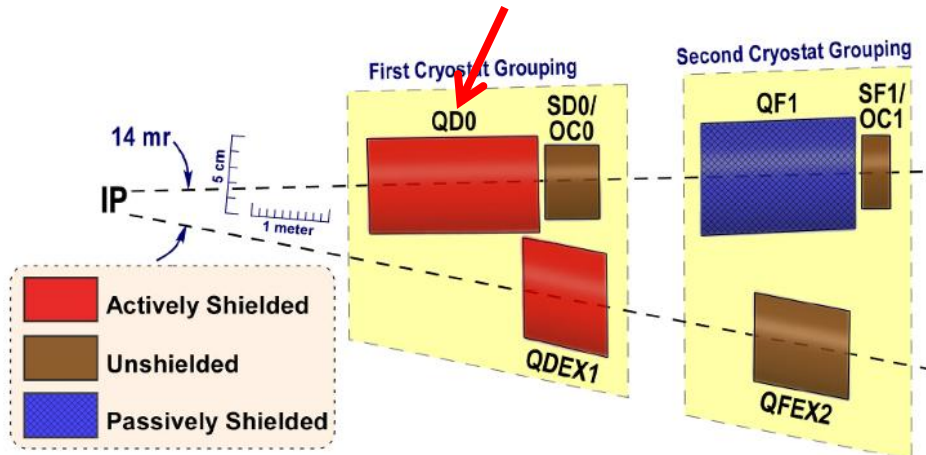


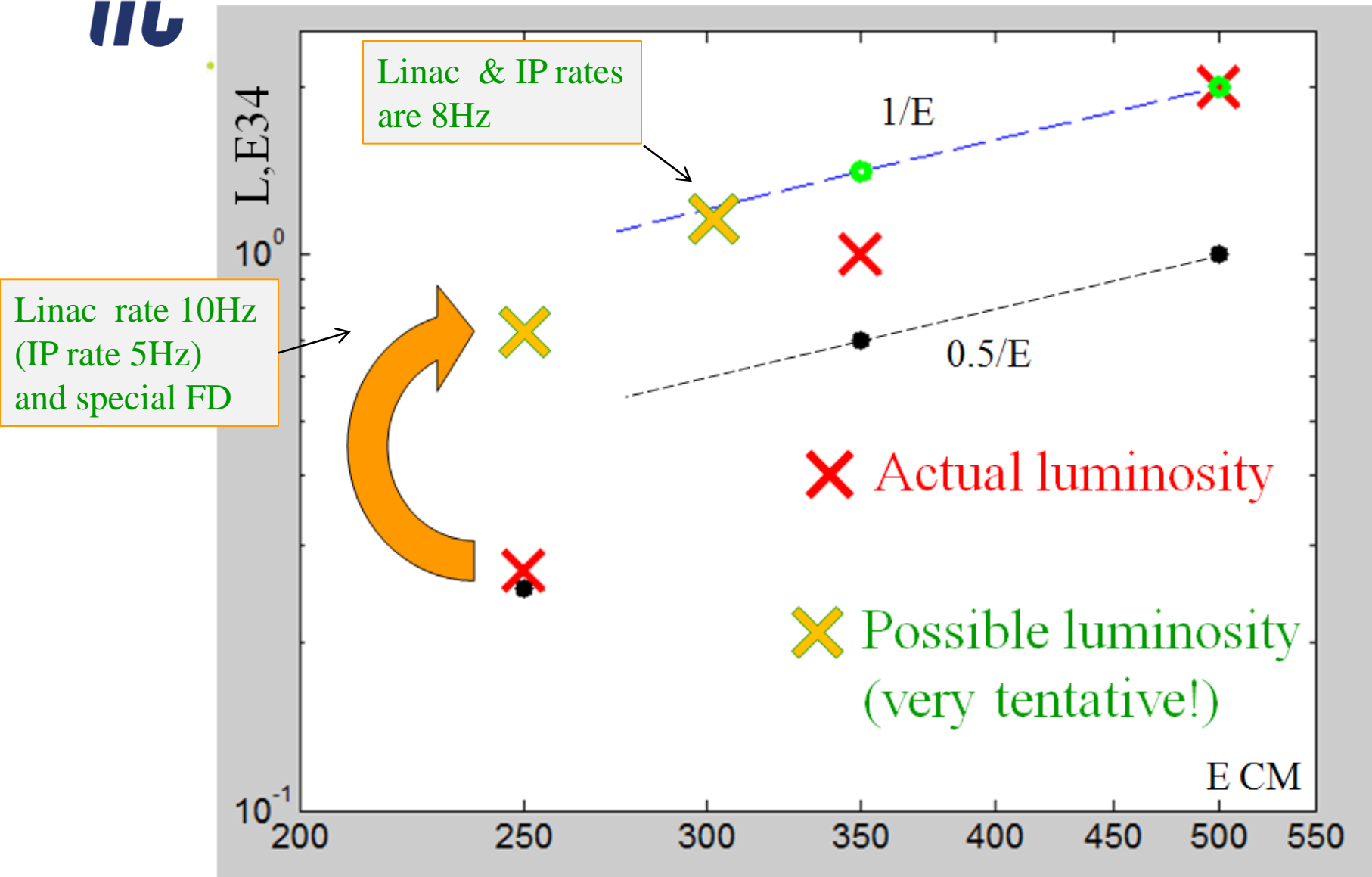


FD for low E

FD optimized for lower energy will allow increasing the collimation depth by ~10% in Y and by ~30% in X (Very tentative!)

- One option would be to have a separate FD optimized for lower E, and then exchange it before going to nominal E
- Other option to be studied is to build a universal FD, that can be reconfigured for lower E configuration (may require splitting QD0 coil and placing sextupoles in the middle)



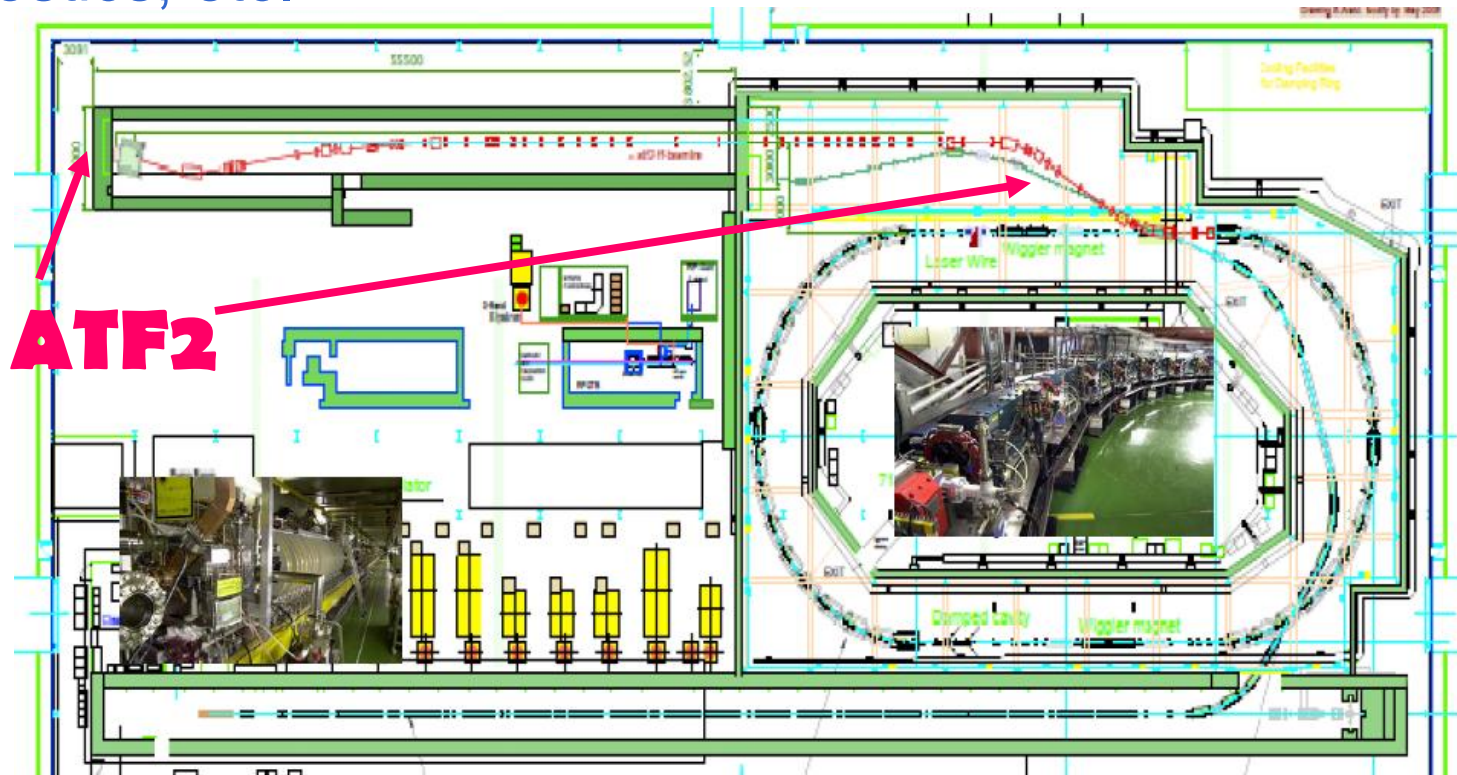
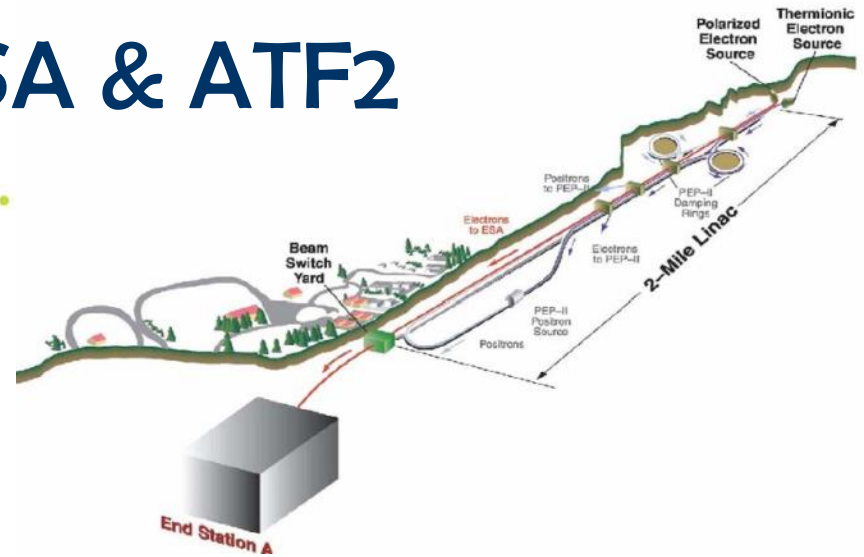




Test facilities: ESA & ATF2

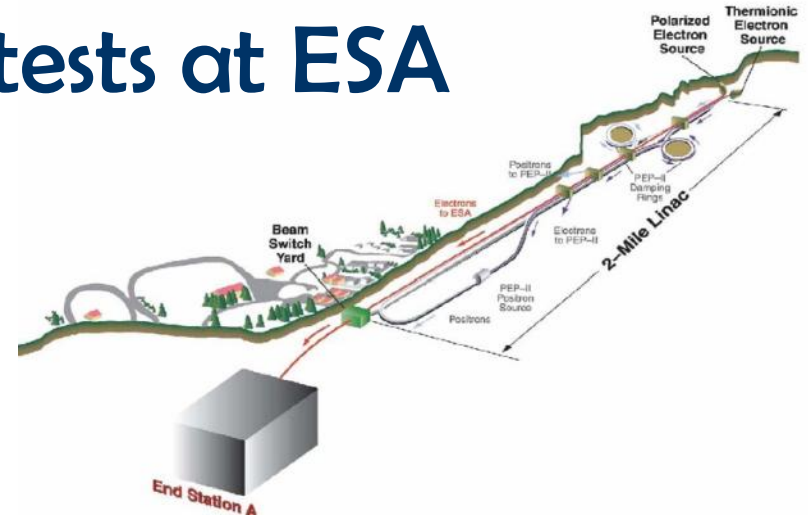
ESA: machine-detector tests; energy spectrometer; collimator wake-fields, etc.

ATF2: prototype FF, develop tuning, diagnostics, etc.

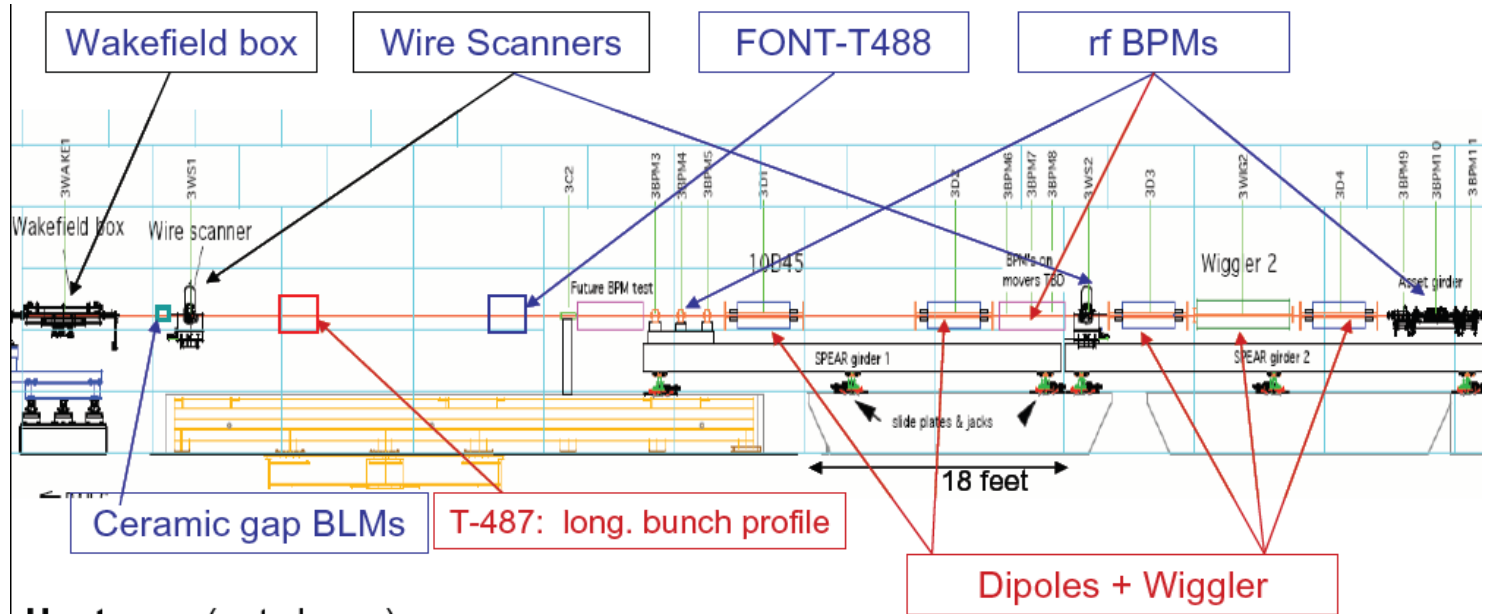




BDS beam tests at ESA



- Study:
- BPM energy spectrometer
- Synch Stripe energy spectrometer
- Collimator design, wakefields
- IP BPMs/kickers—background studies
- EMI (electro-magnetic interference)
- Bunch length diagnostics



Upstream (not shown)

4 rf BPMs for incoming trajectory
 Ceramic gap w/ rf diode detectors (16GHz, 23GHz, and 100GHz) and 2 EMI antennas

Downstream (not shown)

Ceramic gap for EMI studies
 T475 Detector for Wiggler SR stripe



Collimator Wakefield study at ESA

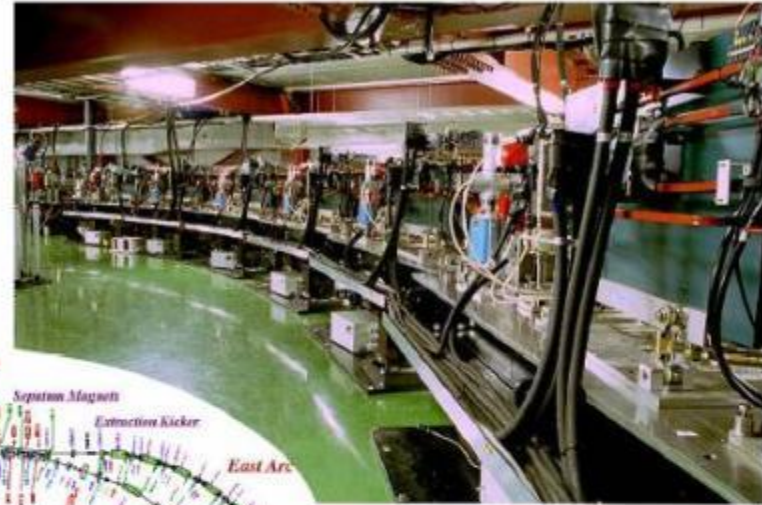


- Spoilers of different shape investigated at ESA (N.Watson et al)
- Theory, 3d modeling and measurements are so far within a factor of ~ 2 agreement

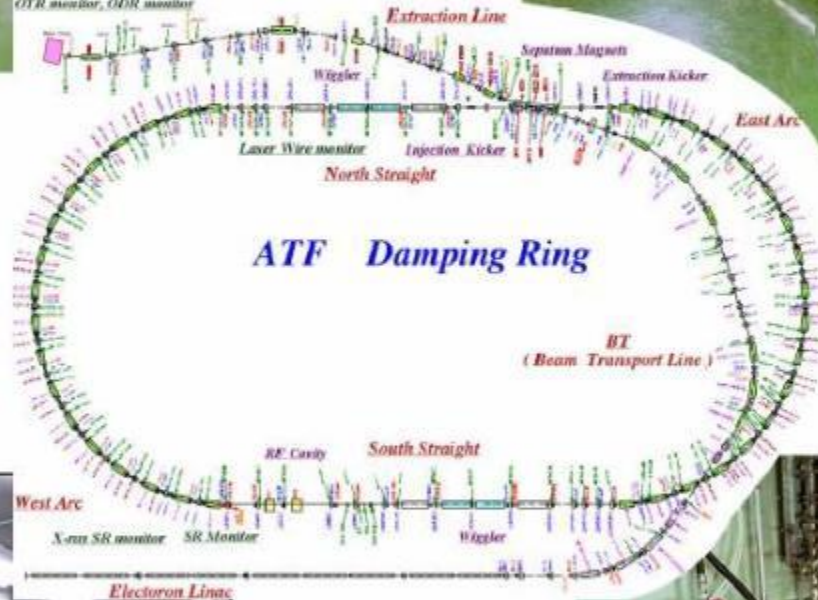




Extraction Line

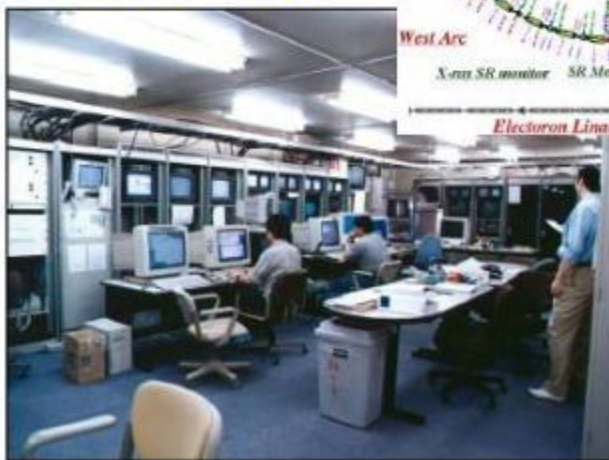


Damping Ring



ATF Damping Ring

Linac



Control Room



ATF and ATF2



Accelerator Test Facility, KEK

1997-2008

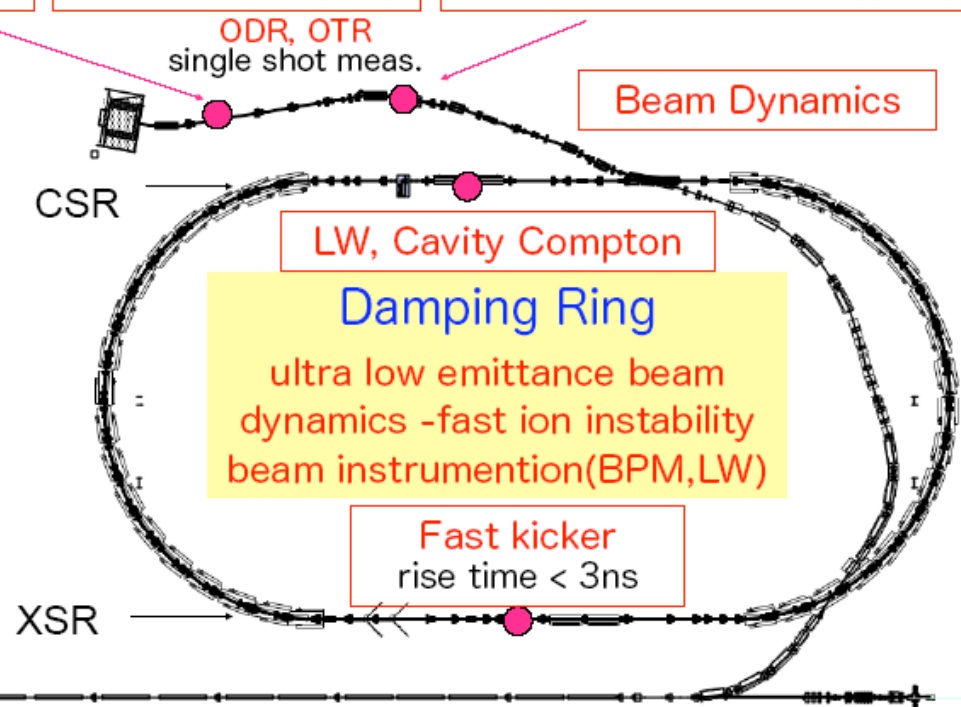
Extraction line :utilization of low emittance beam
beam instrumentation, collimator damage

Cavity BPM
nanometer res.

FONT
fast feedback (ns)

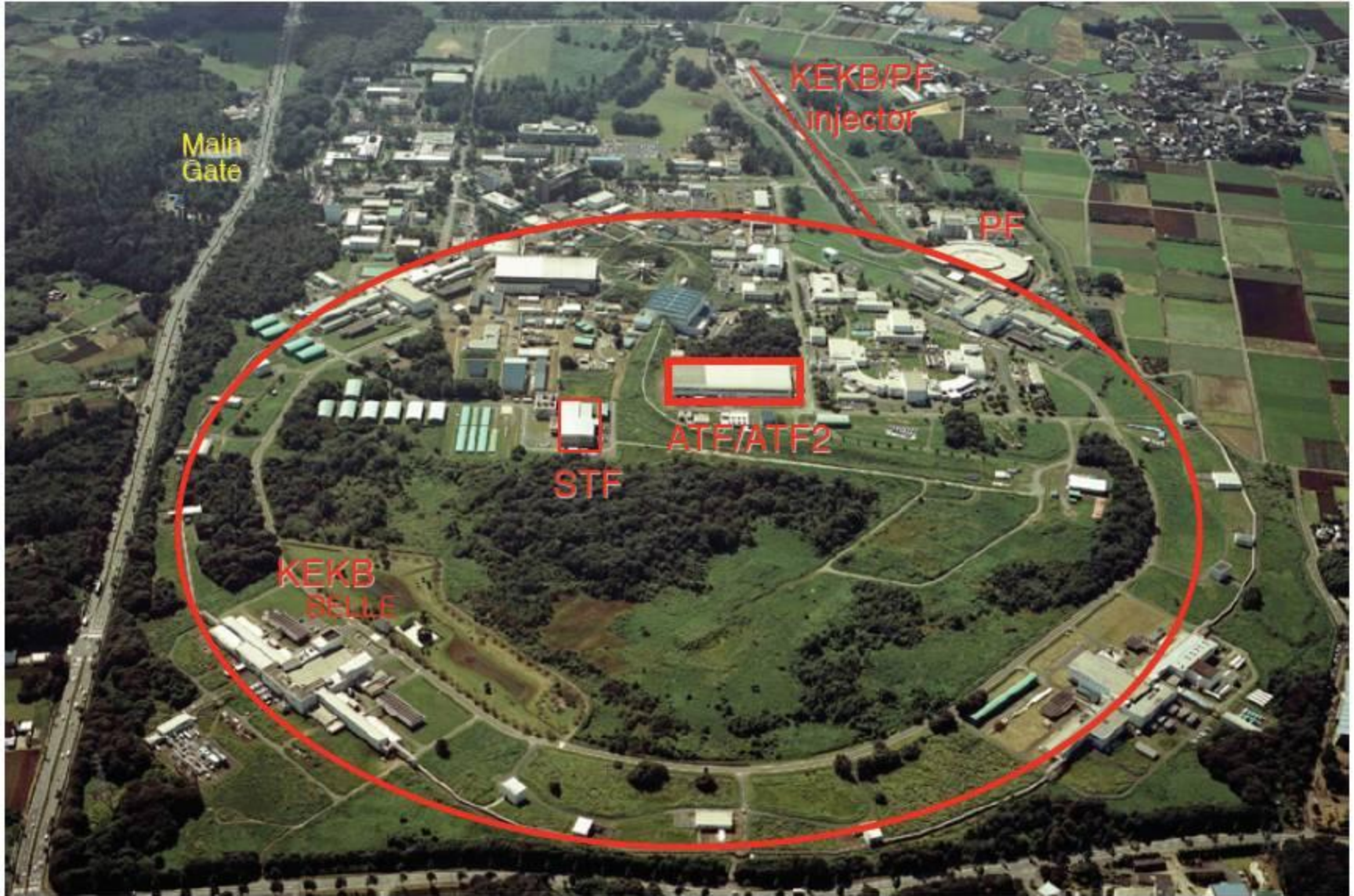
Pulsed Laser Wire Scanner
for beam size monitor (μm)

Energy: 1.28 GeV
Electron bunch:
 2×10^{10} e/bunch
1 ~ 20 bunches/train
3 trains/ring
1.56 Hz



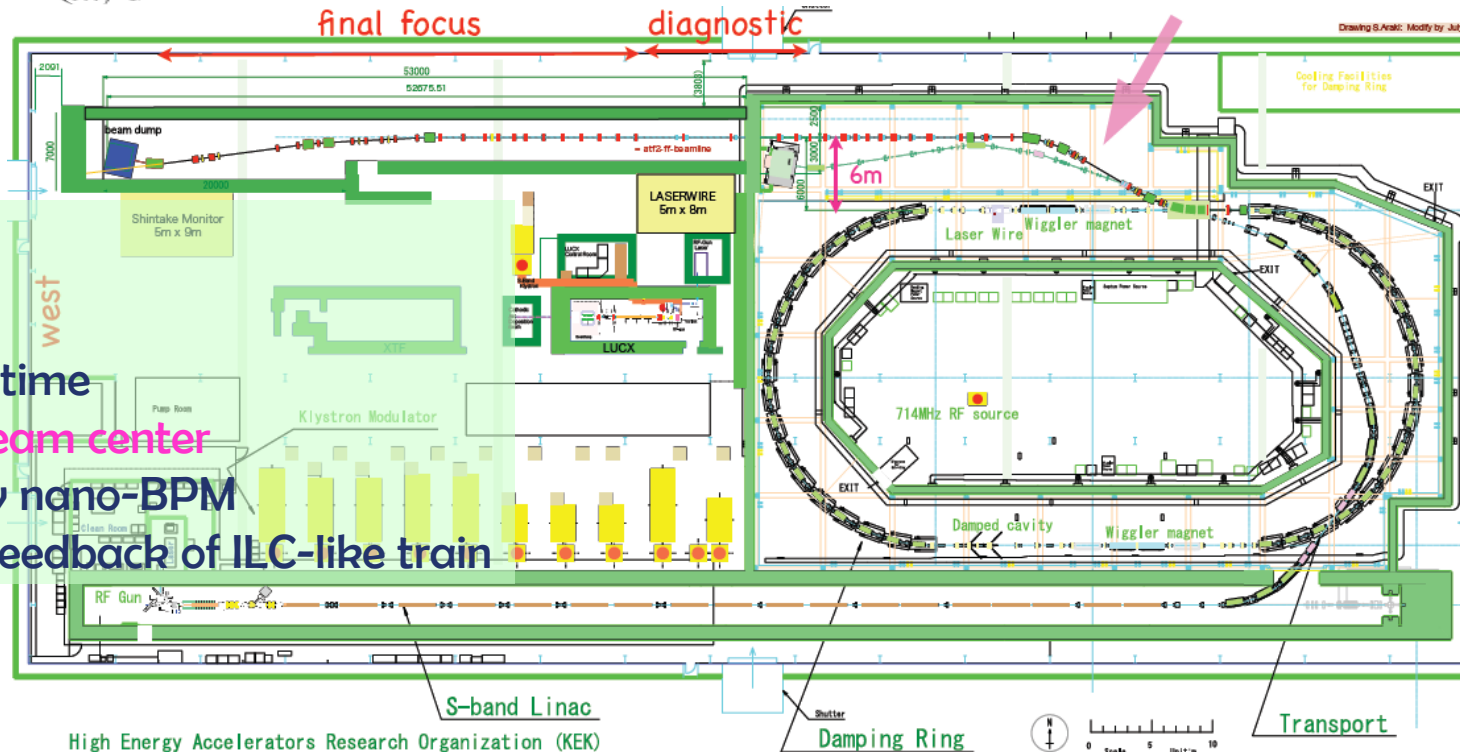
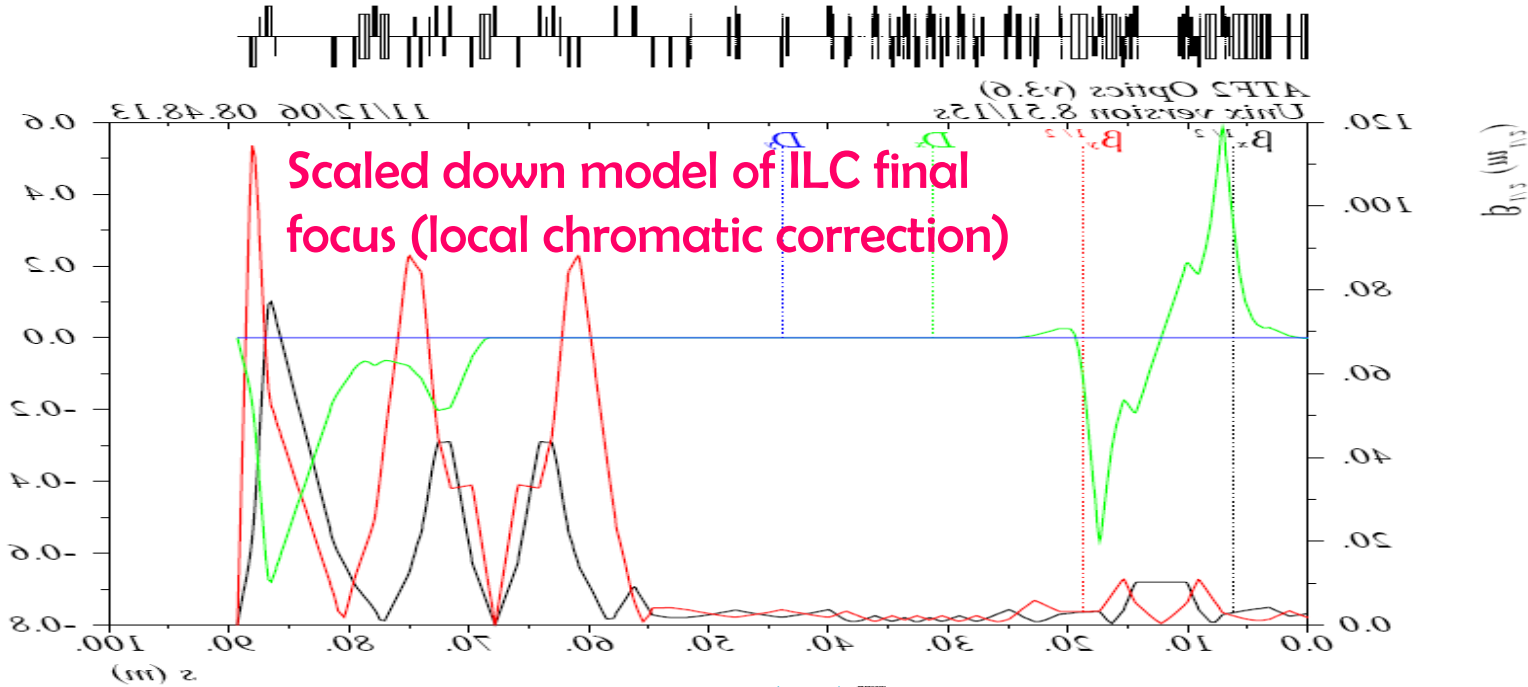
RF Gun
multi-bunch beam

S-band Linac (70m)
multi-bunch acceleration





ATF2 – model of ILC BDS



ATF2 goals

(A) **Small beam size**
 Obtain $\sigma_y \sim 35\text{nm}$
 Maintain for long time

(B) **Stabilization of beam center**
 Down to $< 2\text{nm}$ by nano-BPM
 Bunch-to-bunch feedback of ILC-like train

BDS: 120

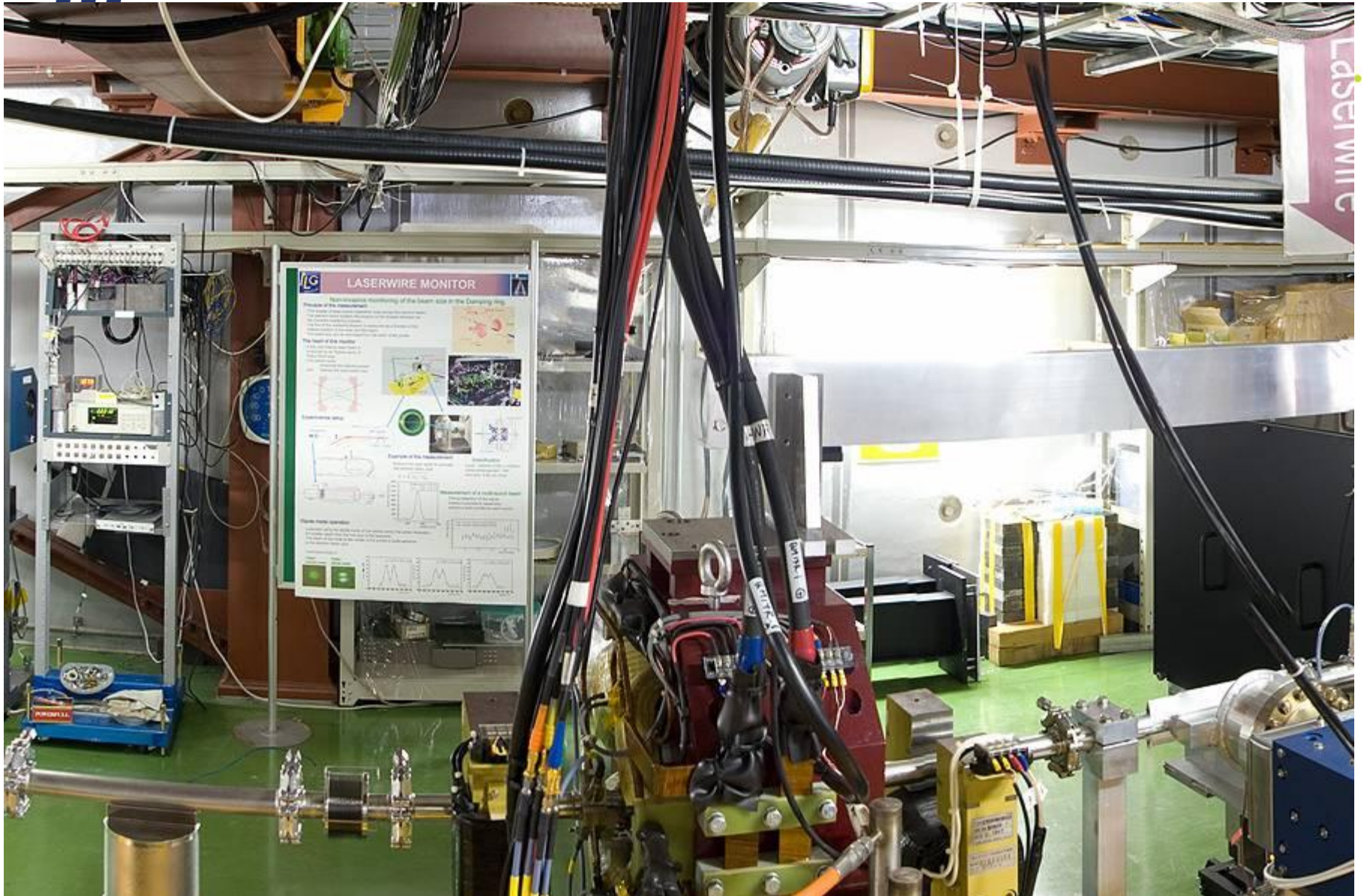


ATF collaboration & ATF2 facility

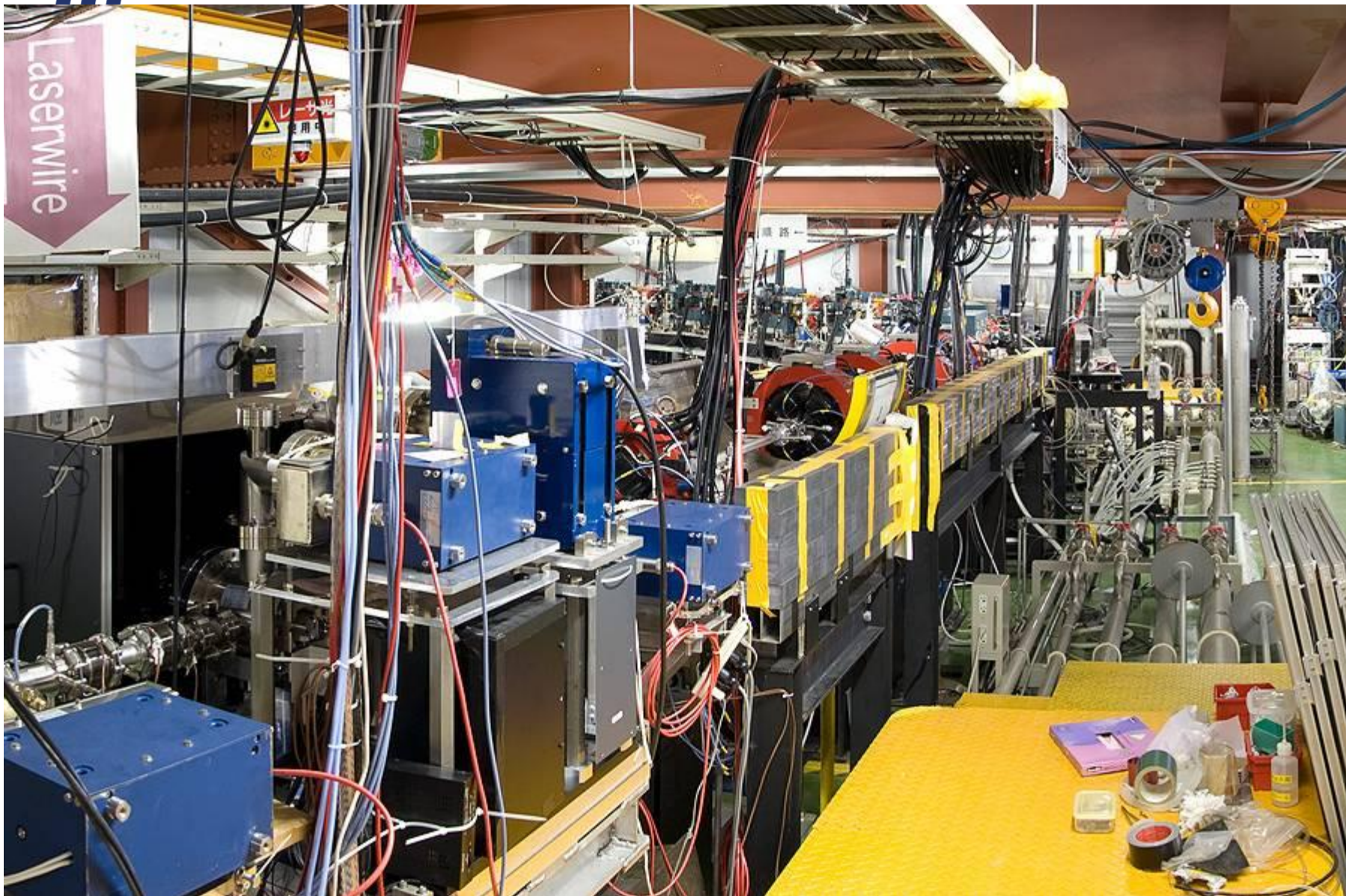
- ATF2 will prototype FF,
- help development tuning methods, instrumentation (laser wires, fast feedback, submicron resolution BPMs),
- help to learn achieving small size & stability reliably,
- potentially able to test stability of FD magnetic center.



- ATF2 is one of central elements of BDS EDR work, as it will address a large fraction of BDS technical cost risk.
- Constructed as ILC model, with in-kind contribution from partners and host country providing civil construction
- ATF2 commissioning will start in Autumn of 2008



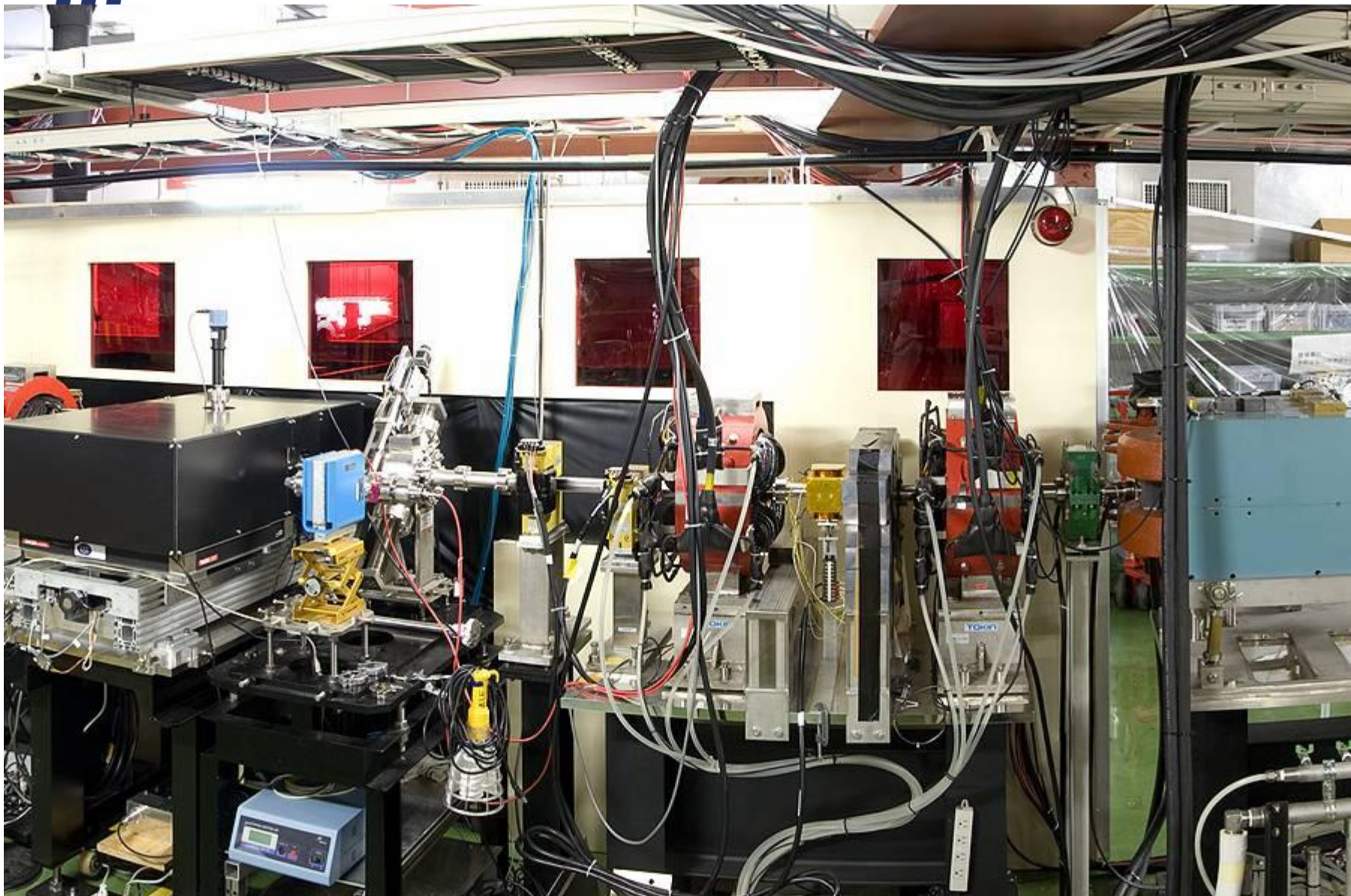
Panoramic photo of ATF beamlines, N.Toge



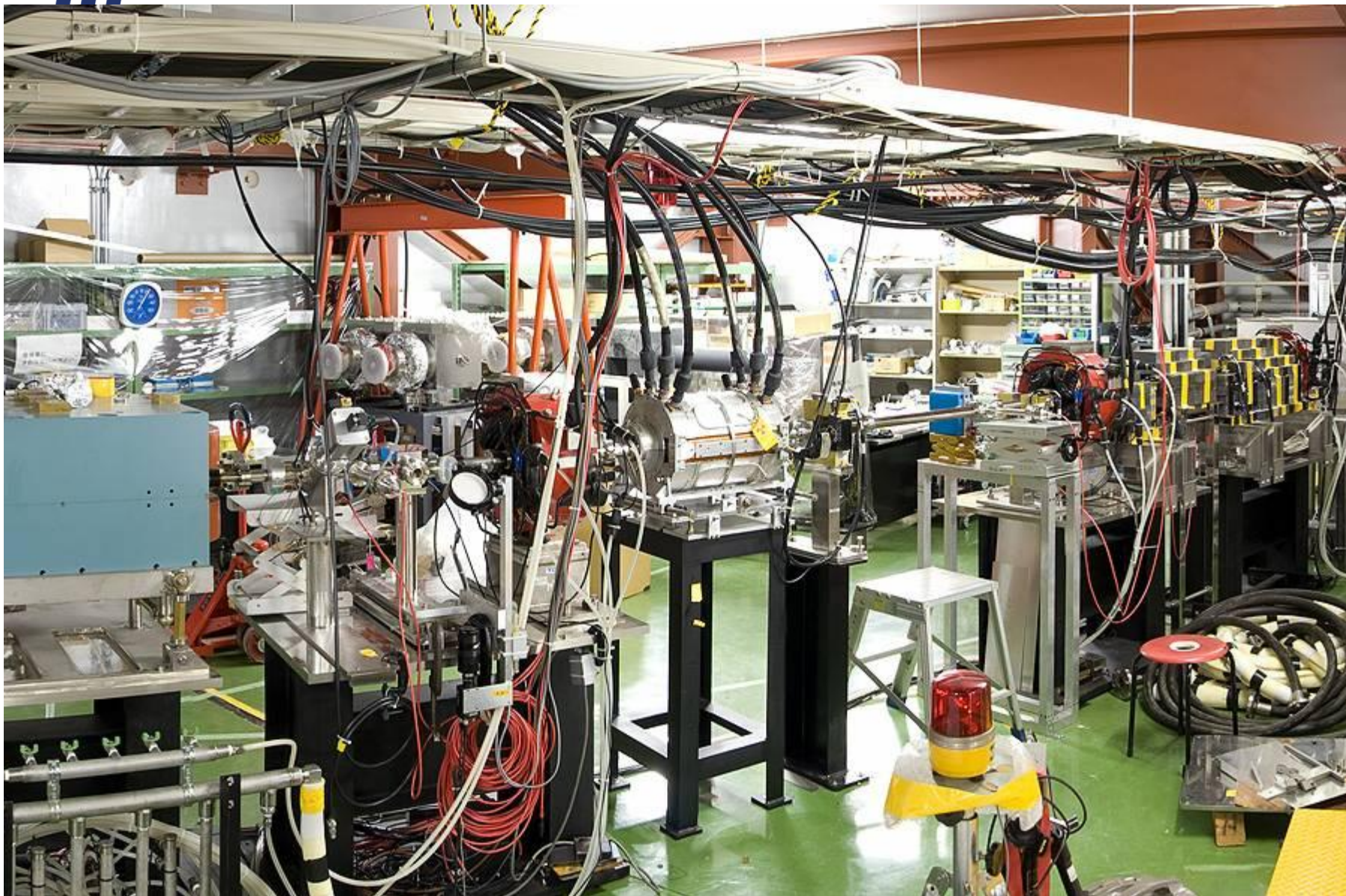
Panoramic photo of ATF beamlines, N.Toge



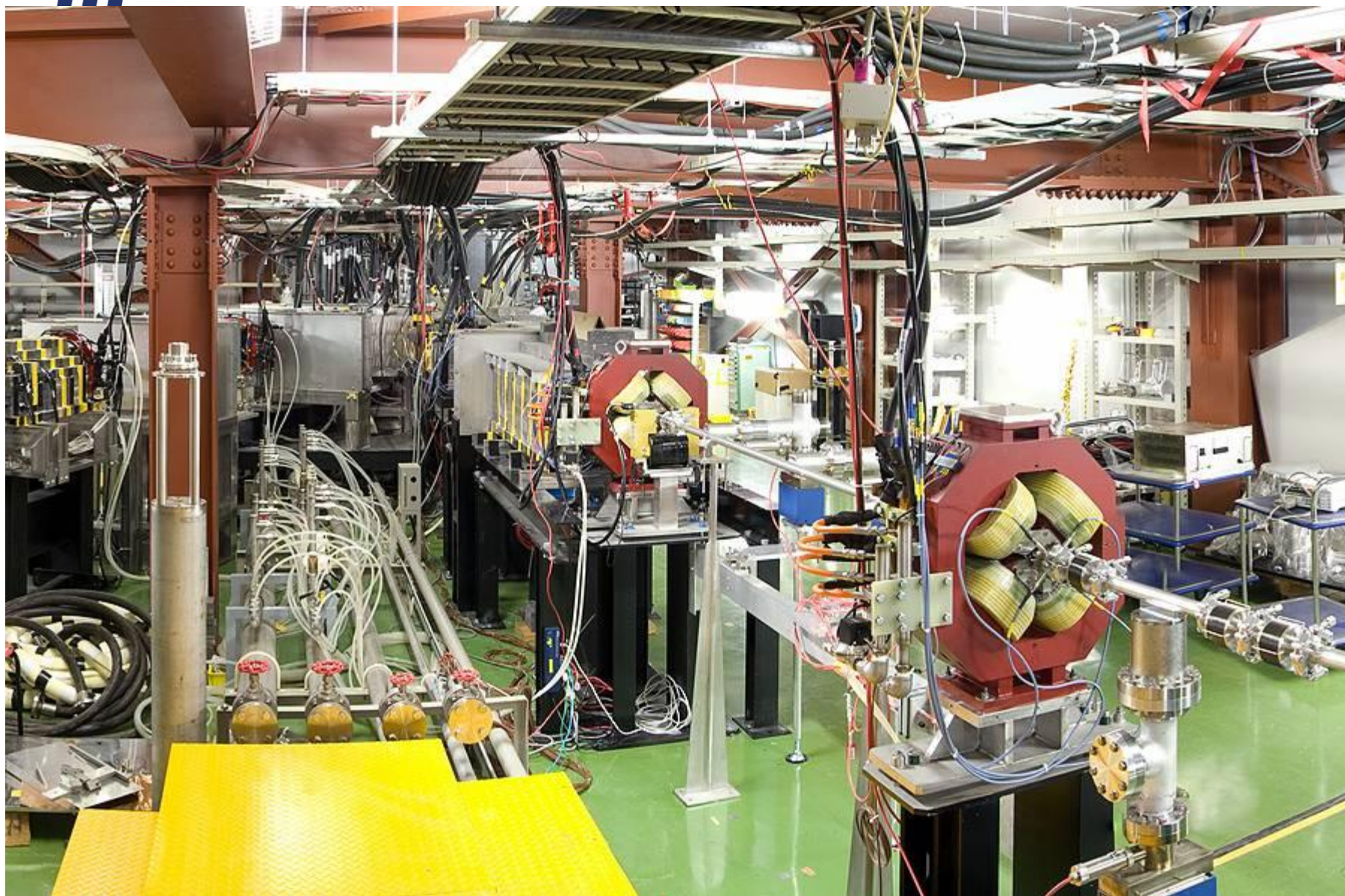
Panoramic photo of ATF beamlines, N.Toge



Panoramic photo of ATF beamlines, N.Toge



Panoramic photo of ATF beamlines, N.Toge



Panoramic photo of ATF beamlines, N.Toge



Panoramic photo of ATF beamlines, N.Toge

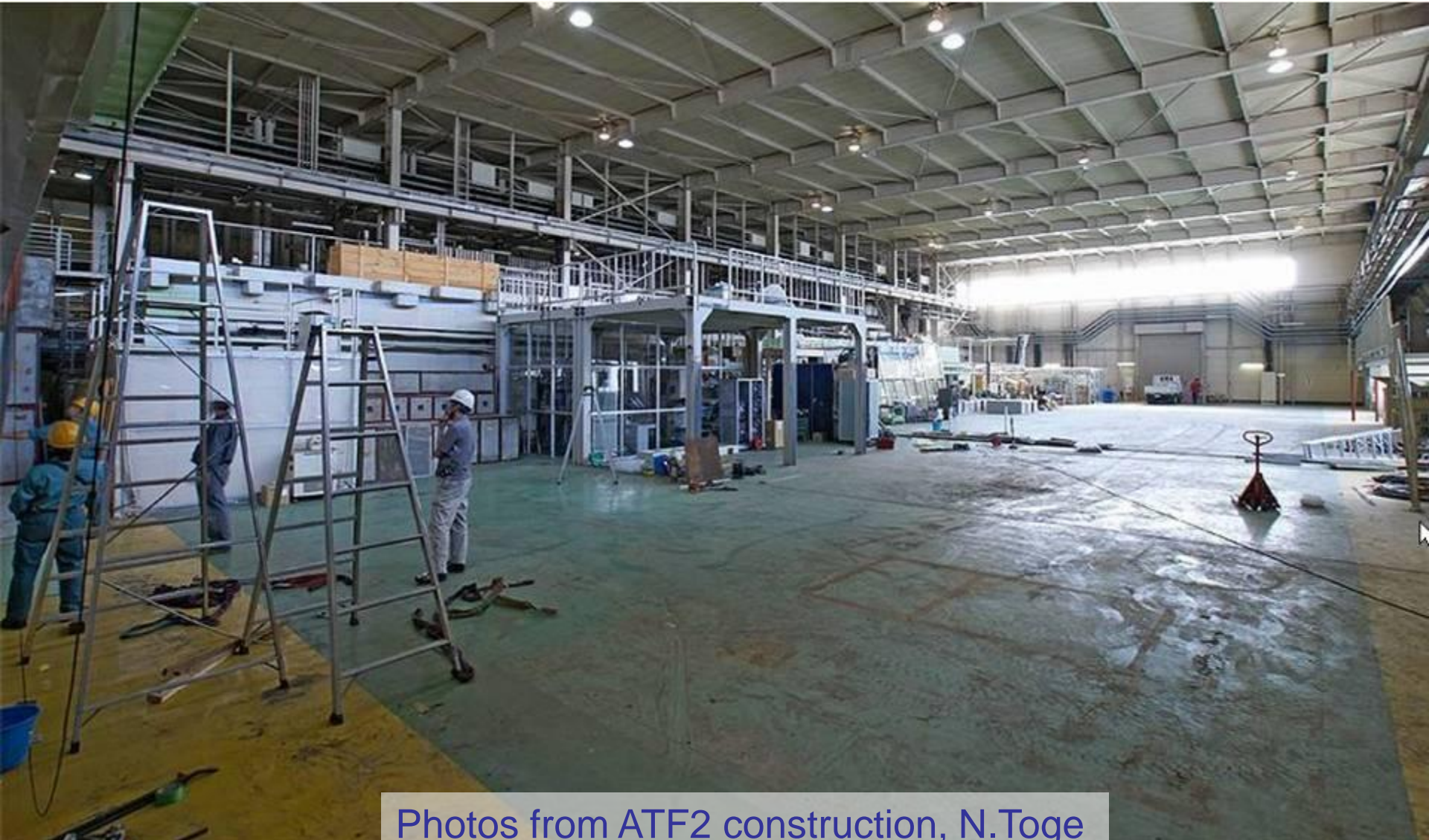


ATF hall before ATF2 construction



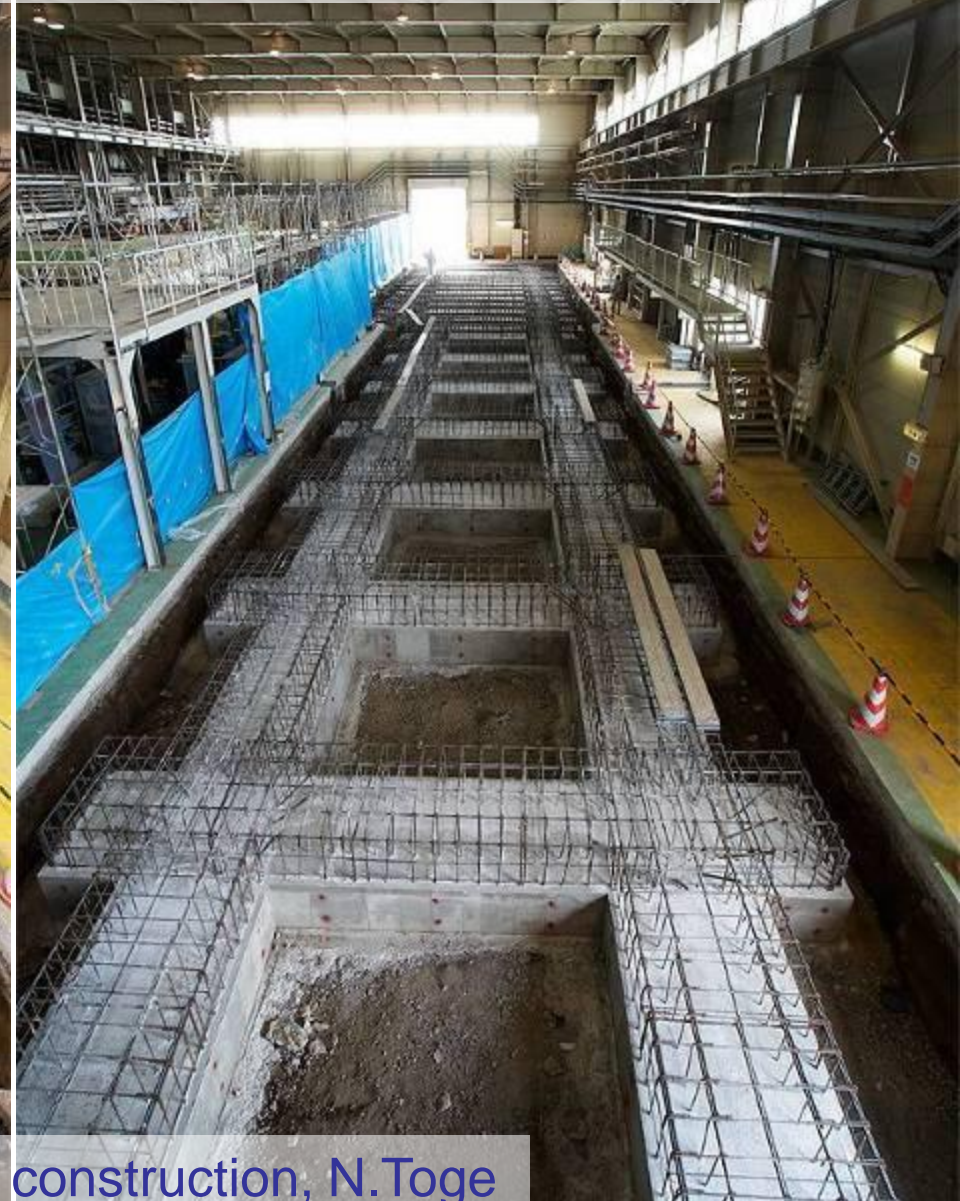
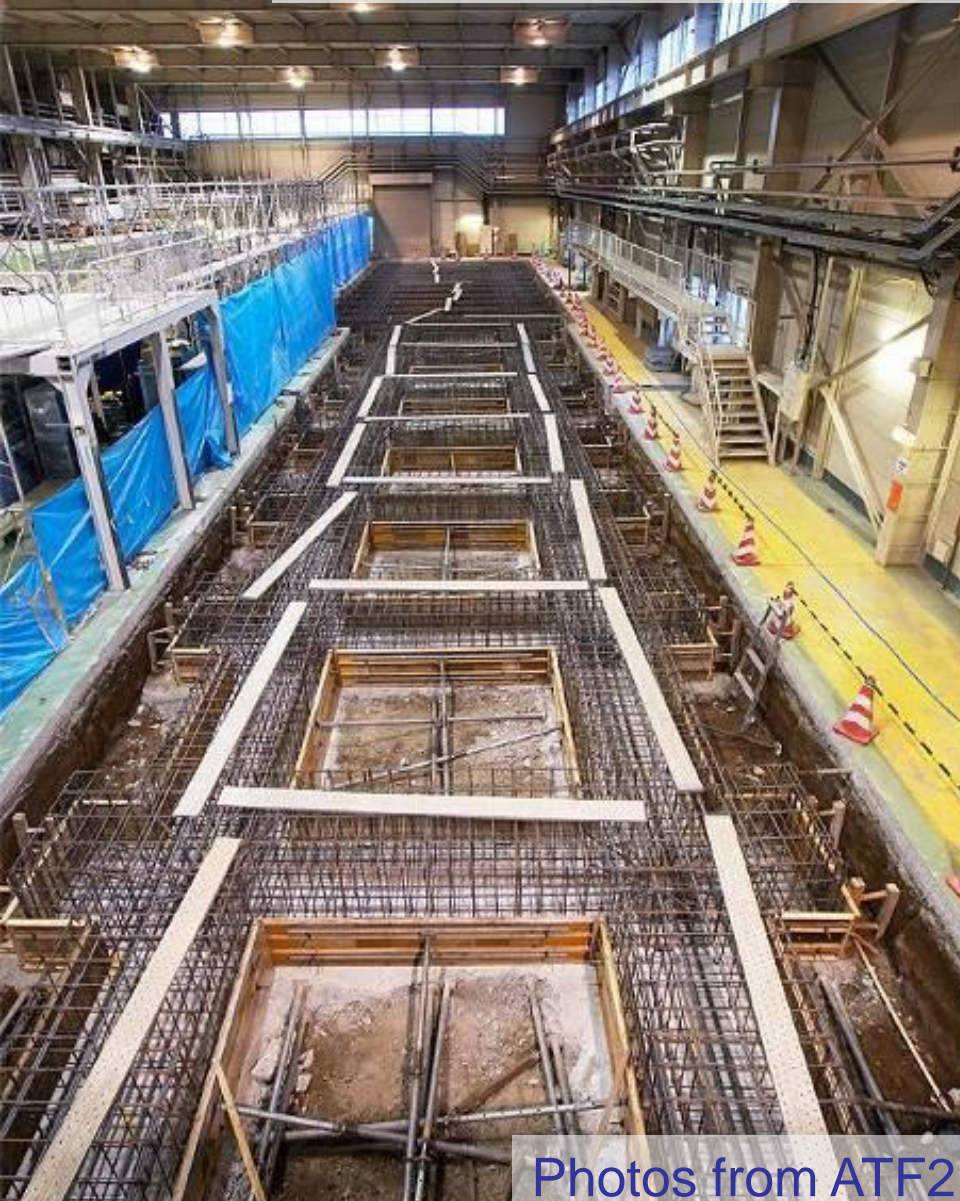


ATF hall emptied



Photos from ATF2 construction, N.Toge

Building the reinforced floor



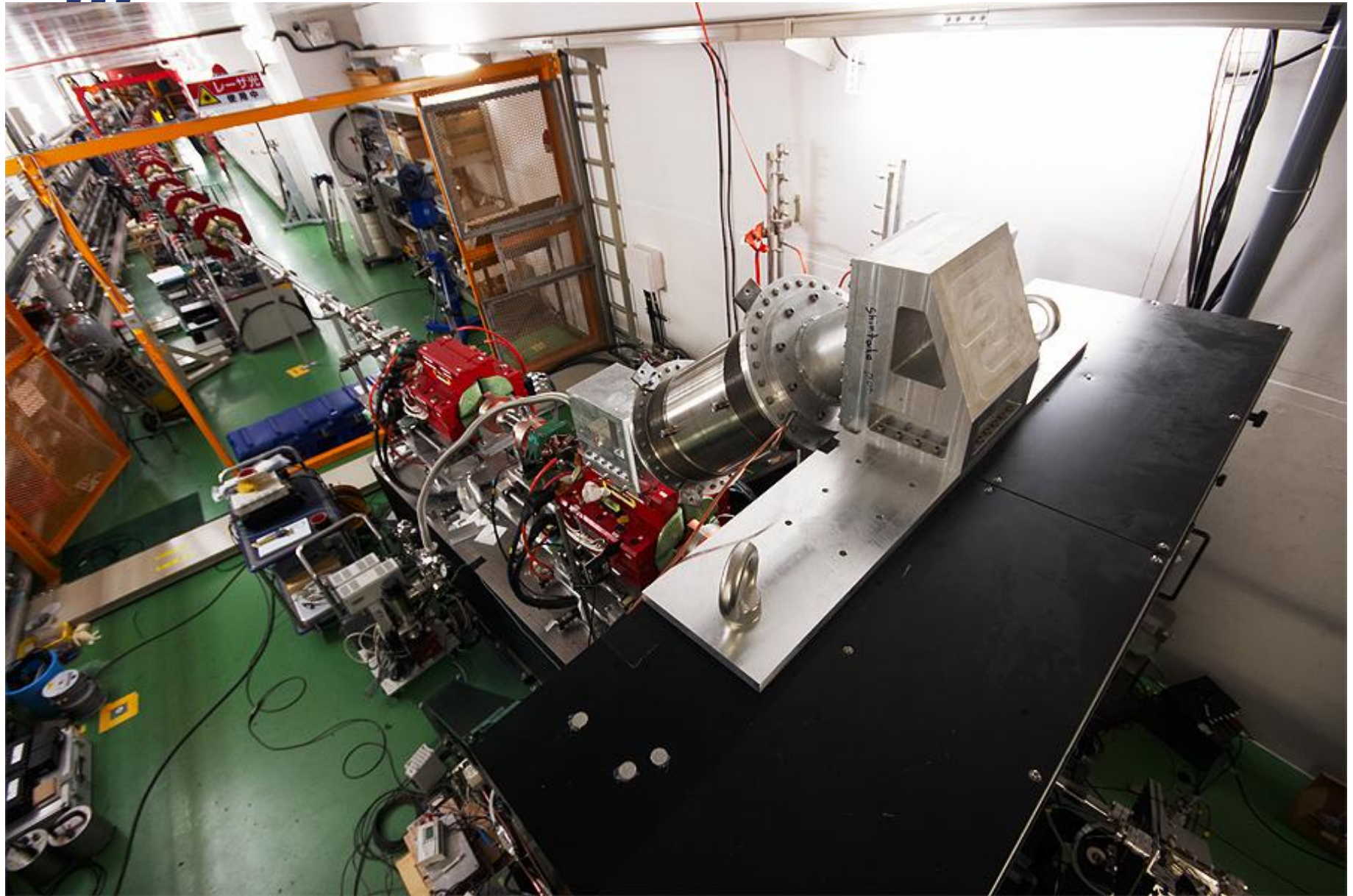
Photos from ATF2 construction, N.Toge

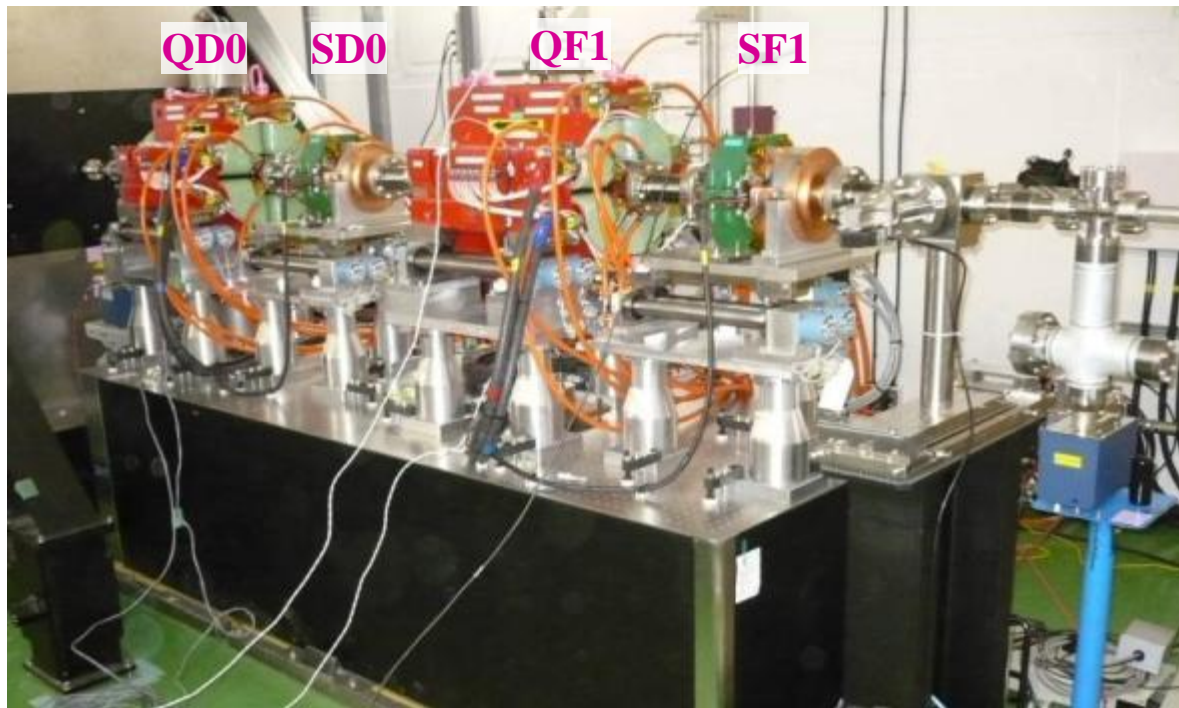


Finished reinforced floor for ATF2

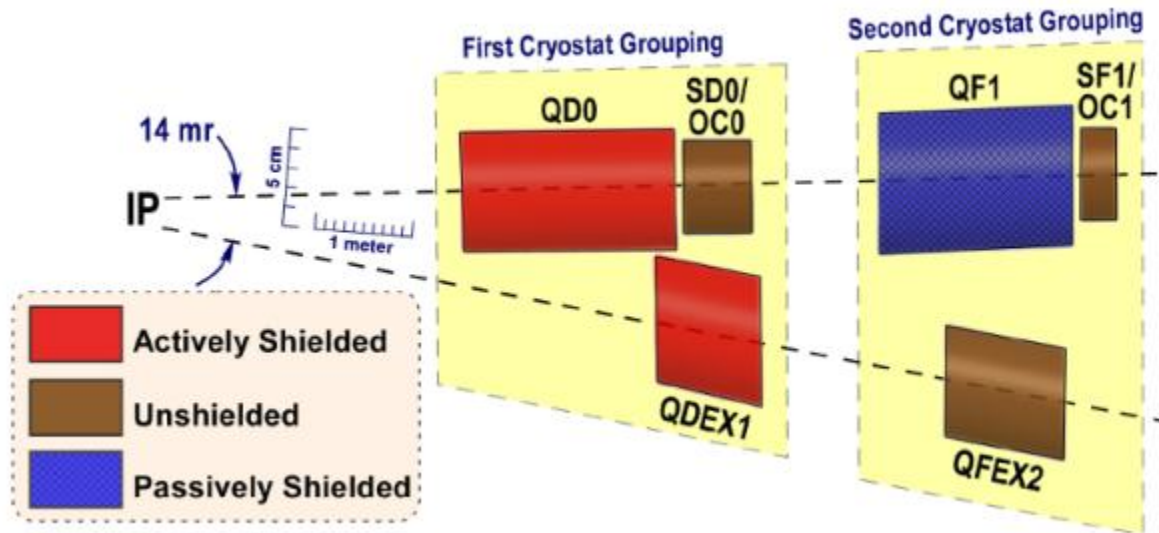


Photos from ATF2 construction, N.Toge





ATF2 final doublet

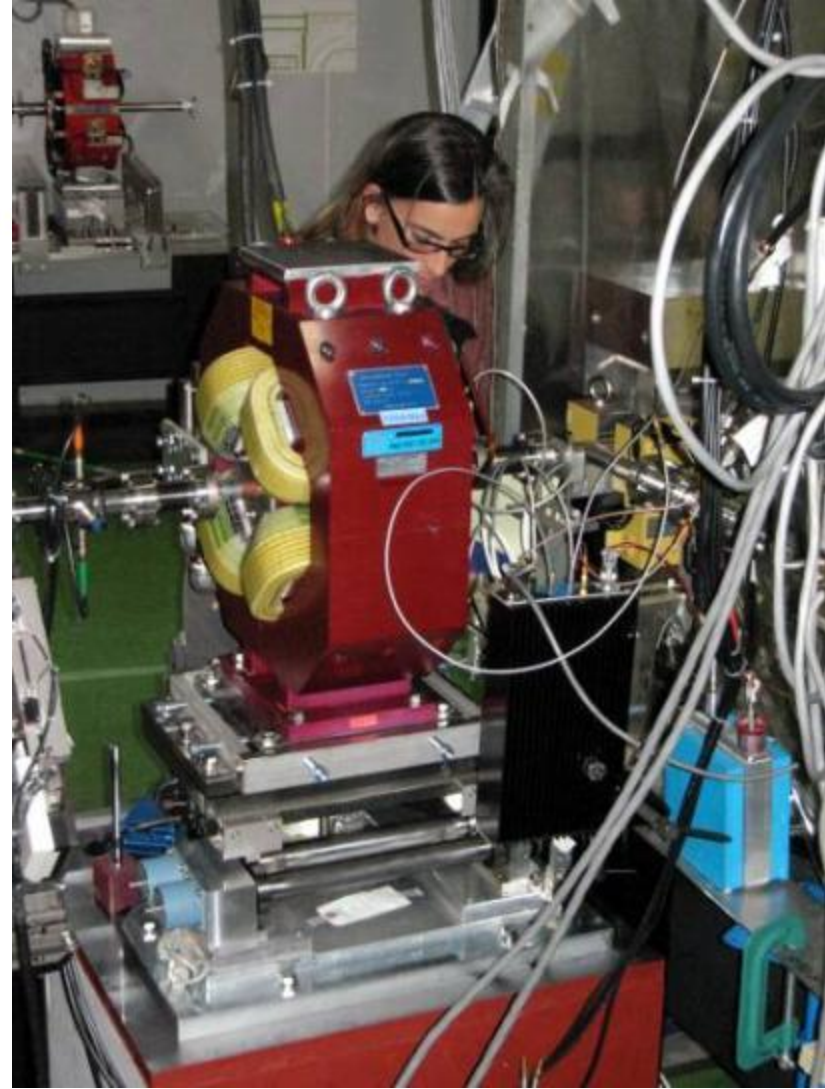


ILC Final Doublet layout

ilc ATF & ATF2



J.Nelson (at SLAC) and T.Smith (at KEK) during recent "remote participation" shift. Top monitors show ATF control system data. The shift focused on BBA, performed with new BPM electronics installed at ATF by Fermilab colleagues.

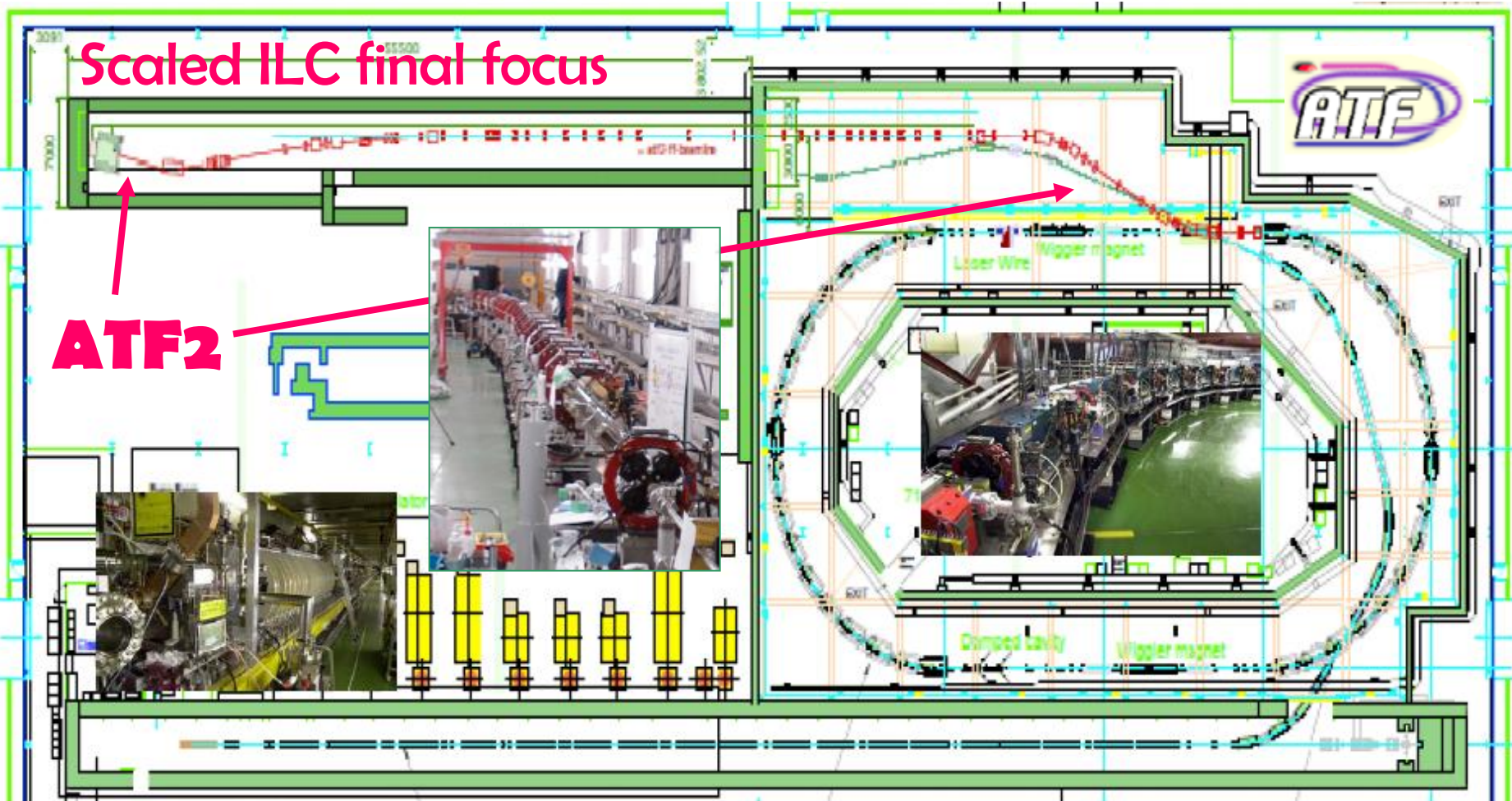


T.Smith is commissioning the cavity BPM electronics and the magnet mover system at ATF beamline

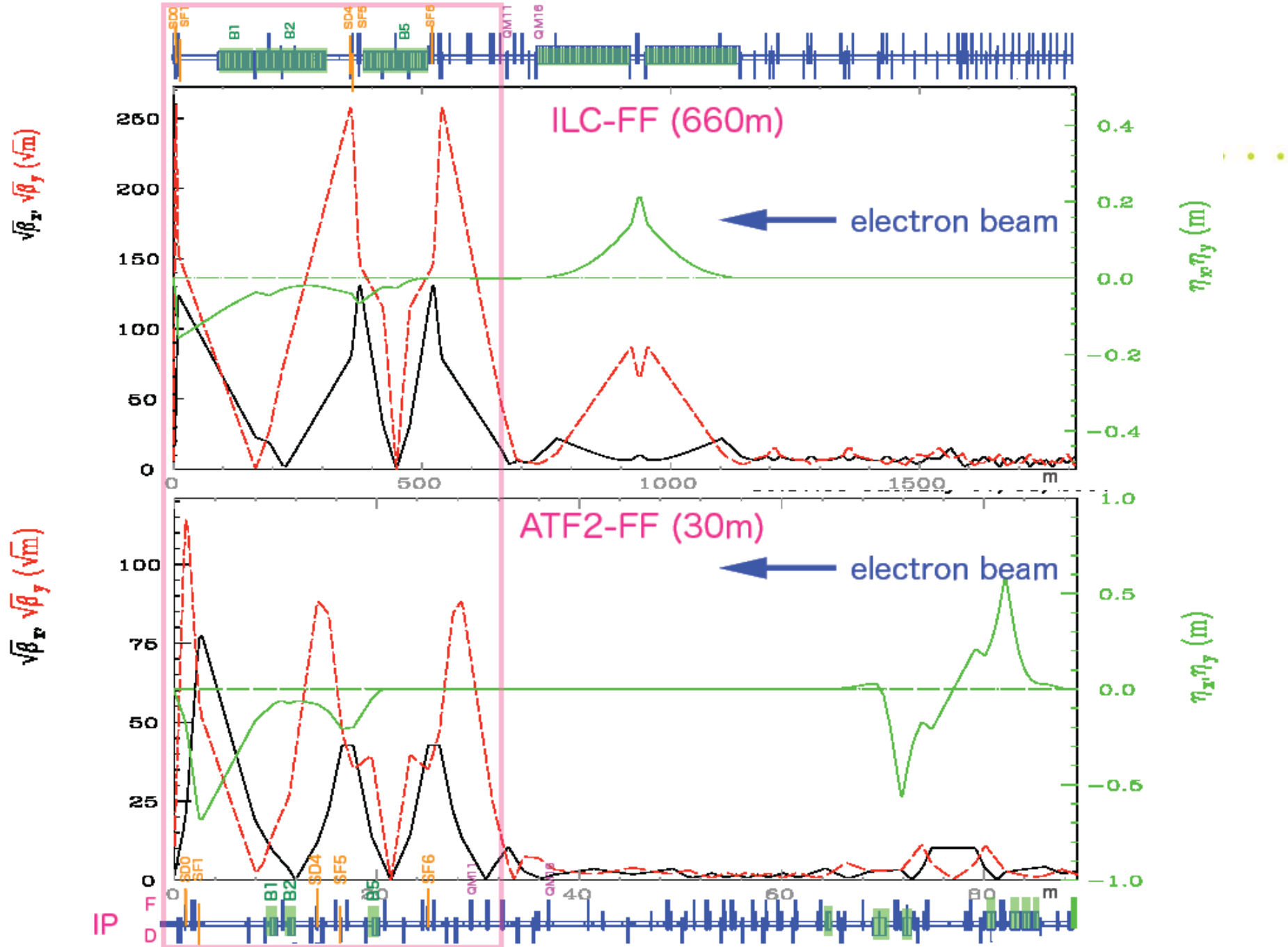


ATF2: model of ILC beam delivery

goals: ~37nm beam size; nm level beam stability



- Dec 2008: first pilot run; Jan 2009: hardware commissioning
- Feb-Apr 2009: large β ; BSM laser wire mode; tuning tools commissioning
- Oct-Dec 2009: commission interferometer mode of BSM & other hardware





ATF2 parameters & Goals A/B

Beam parameters achieved at ATF and planned for ATF2, goals A and B. The ring energy is $E_0 = 1.3$ GeV, the typical bunch length and energy spread are $\sigma_z = 8$ mm and $\Delta E/E = 0.08$ %.

ATF2 proposed IP parameters compared with ILC

	Measured	(A)	(B)
Single Bunch			
N_{bunch} [10^{10}]	0.2 – 1.0	0.5	0.5
DR $\gamma\epsilon_y$ [10^{-8} m]	1.5	3	3
Extr. $\gamma\epsilon_y$ [10^{-8} m]	3.0 – 6.5	3	3
Multi Bunch			
$n_{bunches}$	20	1 – 20	3 – 20
N_{bunch} [10^{10}]	0.3 – 0.5	0.5	0.5
DR $\gamma\epsilon_y$ [10^{-8} m]	3.0 – 4.5	3	3
Extr. $\gamma\epsilon_y$ [10^{-8} m]	~ 6	3	3
IP σ_y^* [nm]		37	37
IP $\Delta y/\sigma_y^*$ [%]		30	5

Parameters	ATF2	ILC
Beam Energy [GeV]	1.3	250
L^* [m]	1	3.5 – 4.2
$\gamma\epsilon_x$ [m-rad]	3×10^{-6}	1×10^{-5}
$\gamma\epsilon_y$ [m-rad]	3×10^{-8}	4×10^{-8}
β_x^* [mm]	4.0	21
β_y^* [mm]	0.1	0.4
η' (DDX) [rad]	0.14	0.094
σ_E [%]	~0.1	~0.1
Chromaticity W_y	~ 10^4	~ 10^4

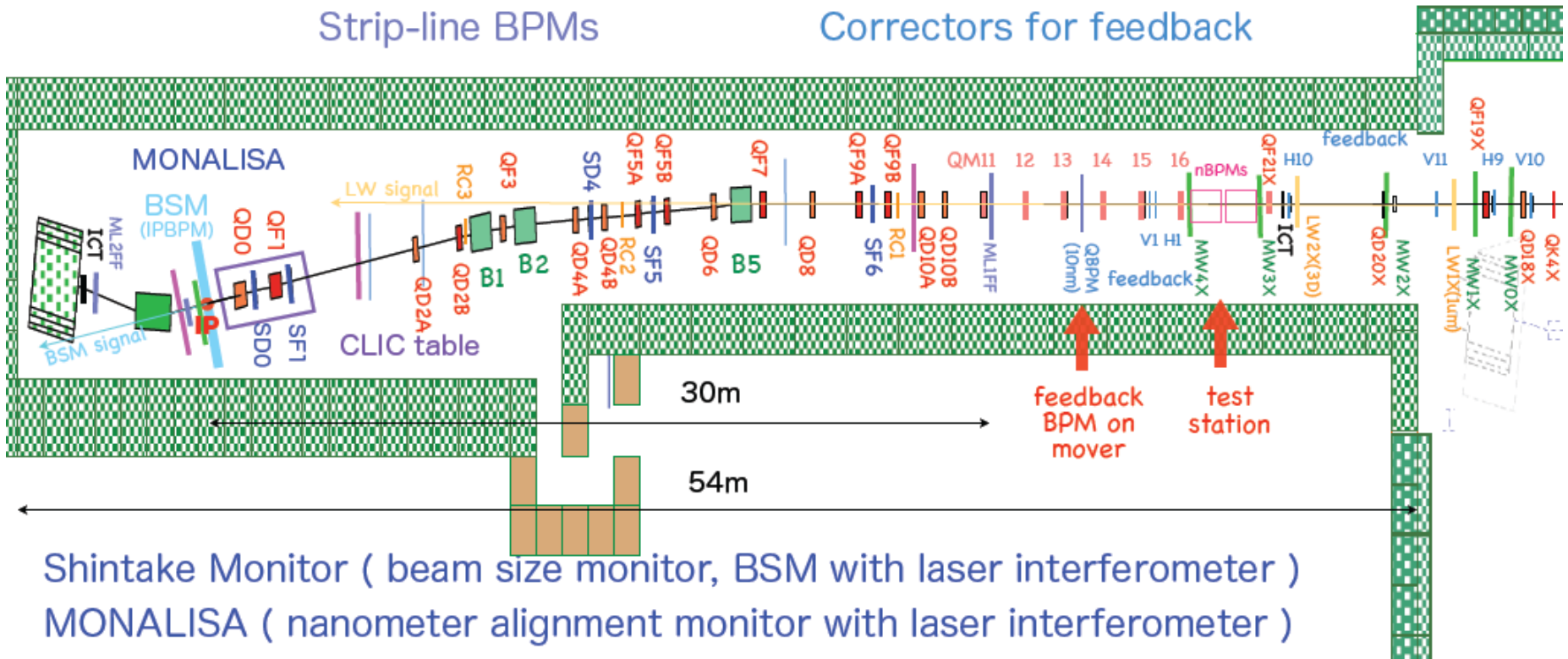
Magnets and Instrumentation at ATF2

22 Quadrupoles(Q), 5 Sextupoles(S), 3 Bends(B) in downstream of QM16

All Q- and S-magnets have cavity-type beam position monitors(QBPM, 100nm):

3 Screen Monitors
Strip-line BPMs

5 Wire Scanners, Laserwires
Correctors for feedback



Shintake Monitor (beam size monitor, BSM with laser interferometer)

MONALISA (nanometer alignment monitor with laser interferometer)

Laserwire (beam size monitor with laser beam for $1 \mu\text{m}$ beam size, 3 axes)

IP intra-train feedback system with latency of less than 150ns (FONT)

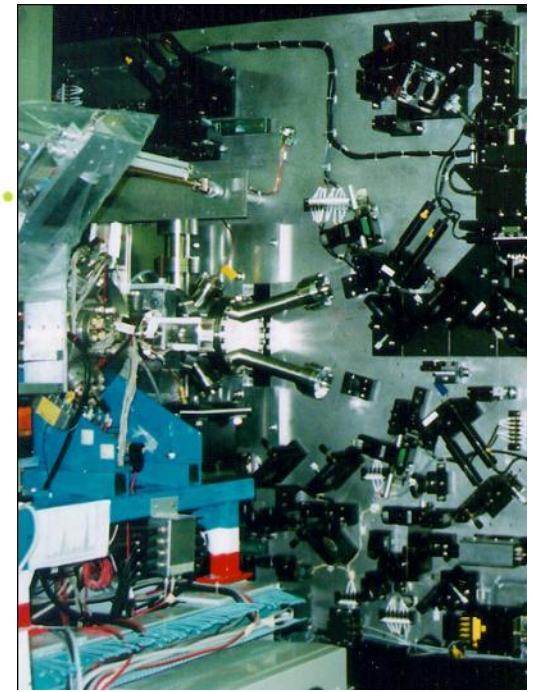
Magnet movers for Beam Based Alignment (BBA)

High Available Power Supply (HA-PS) system for magnets

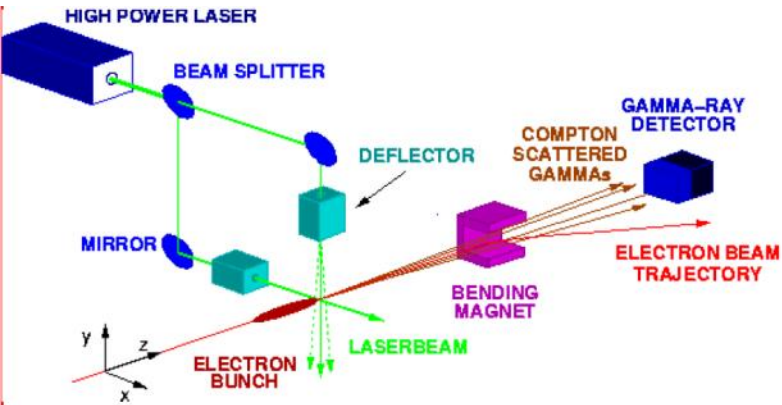


Advanced beam instrumentation at ATF2

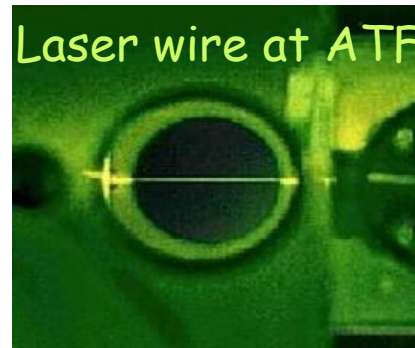
- BSM to confirm 35nm beam size
- nano-BPM at IP to see the nm stability
- Laser-wire to tune the beam
- Cavity BPMs to measure the orbit
- Movers, active stabilization, alignment system
- Intratrain feedback, Kickers to produce ILC-like train



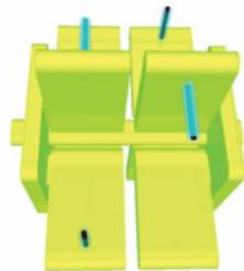
IP Beam-size monitor (BSM)
(Tokyo U./KEK, SLAC, UK)



Laser-wire beam-size Monitor (UK group)



Cavity BPMs with 2nm resolution, for use at the IP (KEK)



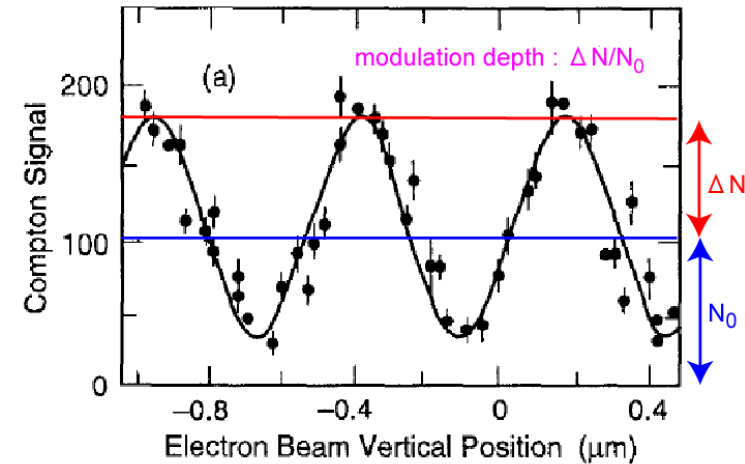
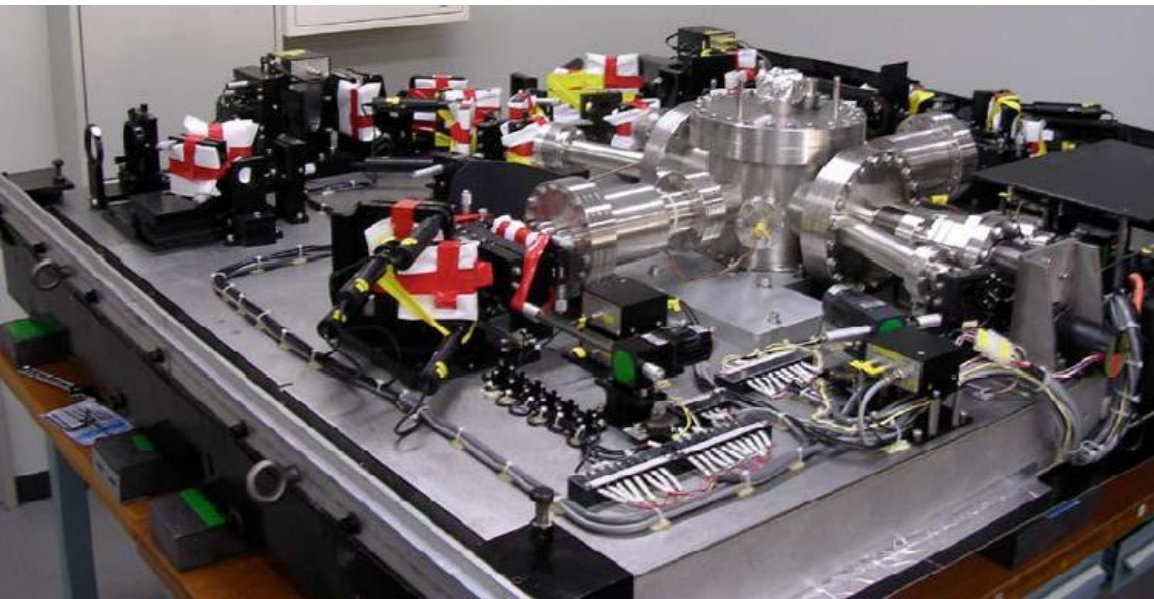
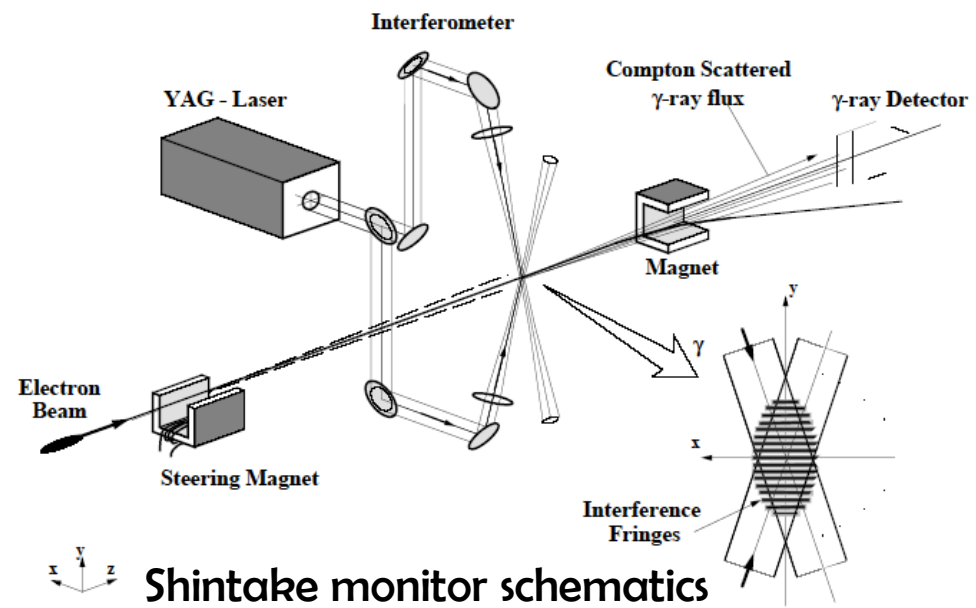
Cavity BPMs, for use with Q magnets with 100nm resolution (PAL, SLAC, KEK)



IP Beam Size monitor

- BSM:

- refurbished & much improved FFTB Shintake BSM
- 1064nm=>532nm



FFTB sample : $\sigma_y = 70 \text{ nm}$

Jul 2005: BSM after it arrived to Univ. of Tokyo

Ongoing R&Ds at ATF/ATF2

- **ATF**
- **low emittance beam**
 - Tuning, XSR, SR, Laser wire,...
- **1pm emittance** (DR BPM upgrade,)
- **Multi-bunch**
 - Instability (Fast Ion,...)
- **Extraction by Fast Kicker**

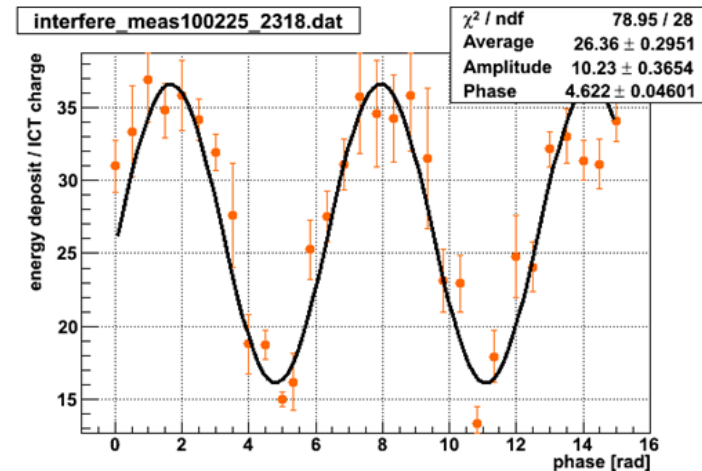
Others

- Cavity Compton
- SR monitor at EXT

ATF2

- **35 nm beam size**
 - Beam tuning (Optics modeling, Optics test, debugging soft&hard tools,...)
 - Cavity BPM (C&S-band, IP-BPM)
 - Beam-tilt monitor
 - IP-BSM (Shintake monitor)
- **Beam position stabilization (2nm)**
 - Intra-train feedback (FONT)
 - feed-forward DR->ATF2

Interfere mode scan



Beam size $\sim 2.4 \mu\text{m}$

Wire scanner measurement $\sim 3.1 \mu\text{m}$

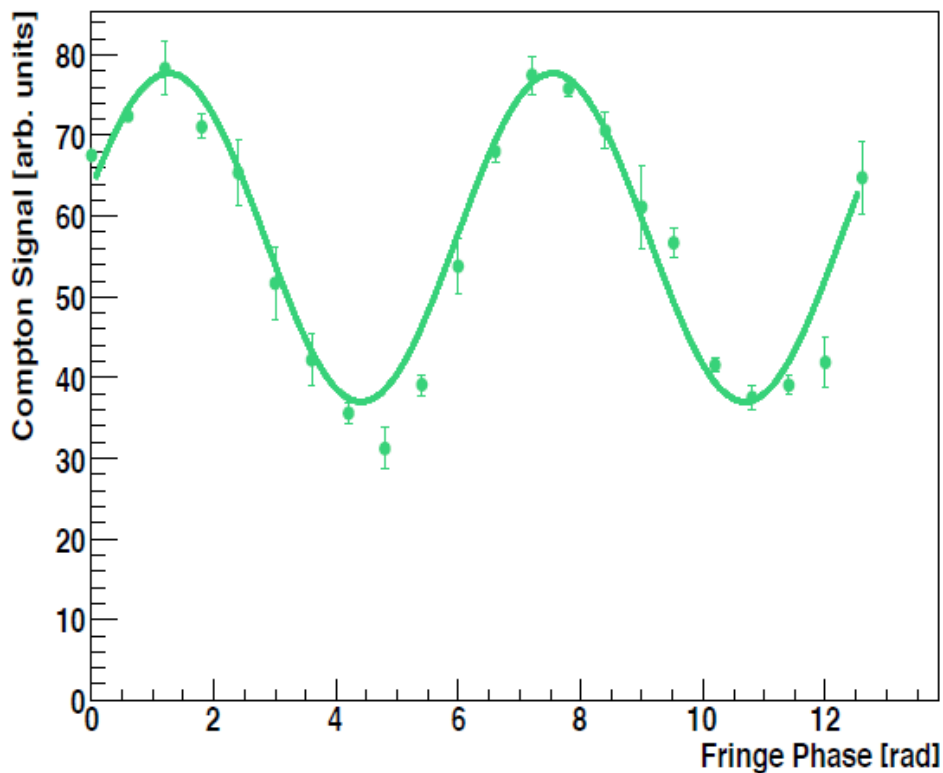
Others

- Pulsed 1um Laser Wire
- Cold BPM
- Liquid Pb target
- **Permanent FD Q**
- **SC Final doublet Q/Sx**

Fringe Scan Results (2 degree mode)

with coupling correction at PIP by QK1-4X (rough)

Fringe Scan



Crossing angle : 2.29 [deg]

Average of 4 bunches/point

Scan range 13.2[rad]

with a step of 600mrad

Fringe Pitch 13.3 μm

Modulation = 0.35 ± 0.01

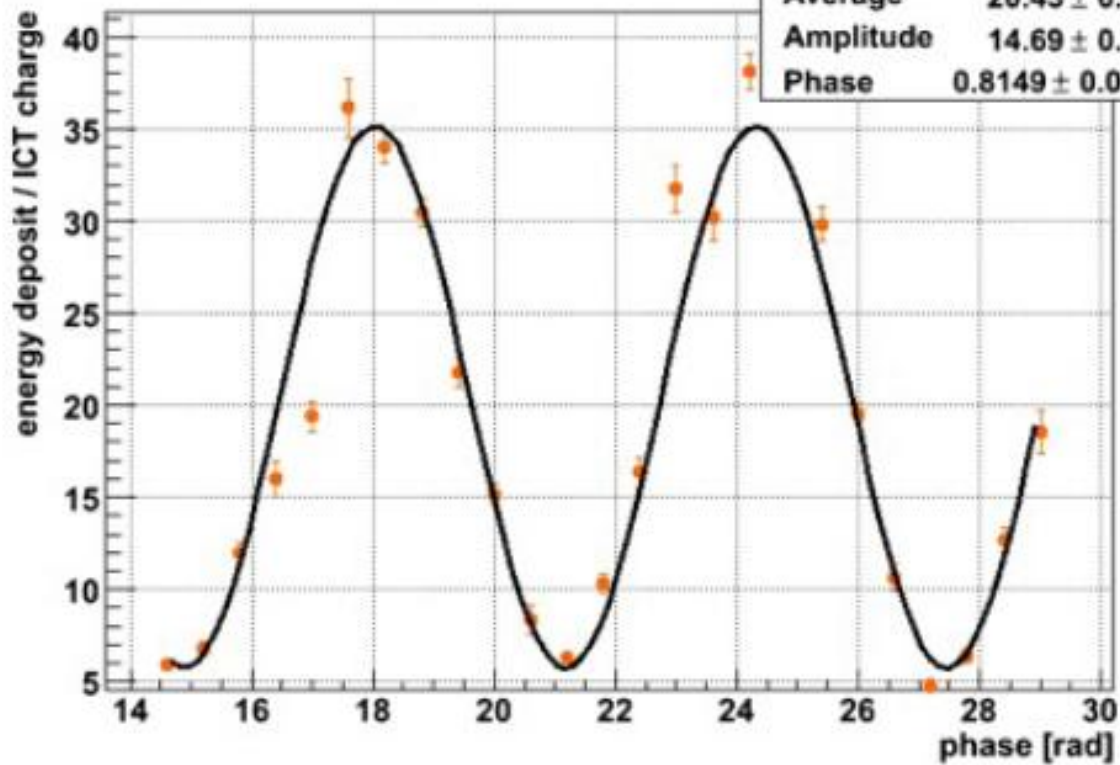
$\sigma_y = 3.1 \pm 0.03 \mu\text{m}$

QD0 current at 129 A

as expected from the PIP
beam size measurements !

interfere_meas100416_1017.dat

χ^2 / ndf	256.2 / 22
Average	20.43 ± 0.1687
Amplitude	14.69 ± 0.1983
Phase	0.8149 ± 0.01396

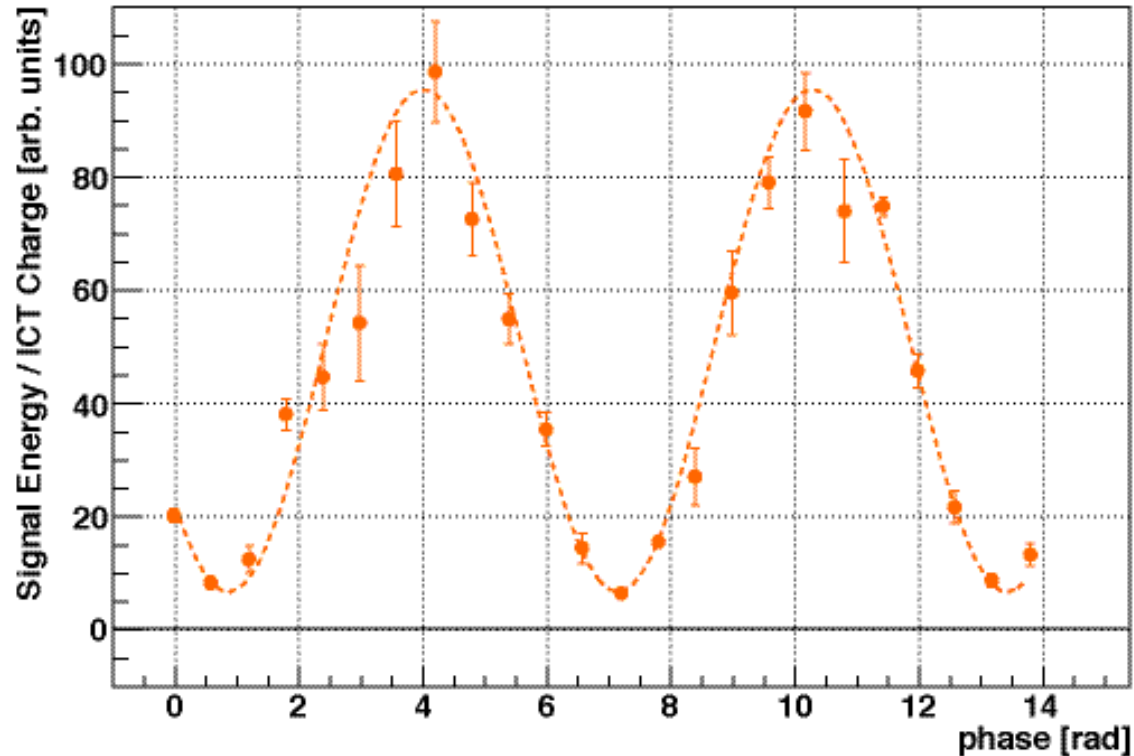


Crossing angle :4.12 [deg]
 20 average
 Fringe pitch 600 mrad
 Scan range 13.2[rad]

Modulation ~ 0.72
 $\sigma_y \sim 950[\text{nm}]$



Best result of continuous tune week: May 17-21, 2010



Yoshio Kamiya and Shintake monitor group.
Modulation Depth = 0.87 @ 8.0 deg. mode
Beam Size is 310 +- 30 (stat.) +0-40 (syst.) nm



[atf2-commissioning 380]

ATF2 continuous operations week

- We completed our first 1 week "continuous operations run" of ATF2 tuning, May 17 - May 21. During the run we reached a minimum IP vertical spot size of about 300nm. The run was a successful integration of tuning tasks tested in past shifts and has provided a lot of information on how to move forward from here. Below is a brief bullet-point summary of events during the week, more detail can be found on the wiki (<http://atf.kek.jp/collab/md/atfwiki/?Scheduling%2F2010May17May21>).
- DR tuning (ey ~10pm)
- 10* IP beta_x/beta_y optics loaded for EXT+FFS (4cm/1mm)
- Magnets standardised
- EXT dispersion correction
- EXT ey measured at ~11pm, no coupling correction required
- Cavity BPM systems calibrated
- Beam size brought to ~normal in x <2um in y at IP with W and C wire scanners (some wire scanners cut during scanning)
 - x and y waists brought to IP with alpha knobs
 - y beta function looks correct to within ~20% from PIP measurements with waist at IP
- vertical beam size acquired with IPBSM, starting size ~850nm
- Beam size reduced to 300nm with sextupole waist, coupling, dispersion multiknobs, qd0 current and roll scans.
- Beam size verified in 30-degree and 8-degree IPBSM modes.
- Could not scan with 30-degree mode as could not resolve larger size beam
- Attempted IP beta reduction to 0.5mm, but could not re-acquire beam
- Switch back to 8-degree mode, restore optics and tune back to ~350nm (reproducibility!)

Glen White (SLAC), on behalf ATF2 commissioning team.



ATF International organization is defined by MOU signed by 25 institutions:

CERN
DESY
IN2P3

LAL
LAPP

LLR

John Adams Inst.

Oxford Univ.

Royal Holloway Univ.

Cockcroft Inst.

STFC, Daresbury

Univ. of Manchester

Univ. of Liverpool

University College London

INFN, Frascati

IFIC-CSIC/UV

Tomsk Polytechnic Univ.

KEK

Waseda U.

Nagoya U.

Tokyo U.

Kyoto U.

Tohoku Univ.

Hiroshima U.

IHEP

PAL

KNU

RRCAT

SLAC

LBL

FNAL

Cornell Univ.

LLNL

BNL

Notre Dame Univ.

<http://atf.kek.jp/>

MOU: Mission of ATF/ATF2 is three-fold:

- ATF, to establish the technologies associated with producing the electron beams with the quality required for ILC and provide such beams to ATF2 in a stable and reliable manner.
- ATF2, to use the beams extracted from ATF at a test final focus beamline which is similar to what is envisaged at ILC. The goal is to demonstrate the beam focusing technologies that are consistent with ILC requirements. For this purpose, ATF2 aims to focus the beam down to a few tens of nm (rms) with a beam centroid stability within a few nm for a prolonged period of time.
- Both the ATF and ATF2, to serve the mission of providing the young scientists and engineers with training opportunities of participating in R&D programs for advanced accelerator technologies.



Ph.D. thesis at ATF2 (as of May 2010)

Year	university	country	Name	title
2007.11.12	Université de Savoie	France	Benoit Bolson	Etude des vibrations et de la stabilisation a l'echelle sous-nanometrique des doublets finaux d'un collisionneur lineaire
2007.12.21	University of Tokyo	Japan	Taikan Suehara	Development of a Nanometer Beam Size Monitor for ILC/ATF2
2009.4.14	Royal Holloway, University of London	UK	Lawrence Deacon	A Micron-Scale Laser-Based Beam Profile Monitor for the International Linear Collider
2010.6.8	UNIVERSITAT DE VALÈNCIA	Spain	María del Carmen Alabau Pons	Optics Studies and Performance Optimization for a Future Linear Collider: Final Focus System for the e-e- Option (ILC) and Damping Ring Extraction Line (ATF)
2010.5.8	IHEP CAS	China	Sha Bai	ATF2 Optics System Optimization and Experiment Study
2010.6.11	Université Paris-Sud 11	France	Yves Renier	Implementation and Validation of the Linear Collider Final Focus Prototype ATF2 at KEK (Japan)
	Oxford university	UK		FONT studies
2011.12.1	University of Tokyo	Japan	Masahiro Oroku	Beam Tuning with the Nanometer Beam Size Monitor at ATF2
2011.12.1	Kyungpook National University	Korea	Youngim Kim	IPBPM and BBA
2011.12.1	University of Manchester	UK	Anthony Scarfe	Tuning and alignment of ATF2 and ILC
2012.2.xx	University of Tohoku	Japan	Taisuke Okamoto	cavity-type tilt monitor of beam orbit for ILC
2012.12.1	Kyungpook National University	Korea	Siwon Jang	IPBPM and BBA
2012.12.1	CERN	Spain	Eduardo Marin Lacoma	Ultra Low Beta Optics
	Oxford university	UK		FONT studies
	ICIF, Valencia university	Spain	Javier Alabau- Gonzalvo	emittance, coupling measurements with multiple OTR system



BEAM DELIVERY



Thanks to Bill Barletta for the picture



- Many thanks to colleagues whose slides, results or photos were used in this lecture, namely Tom Markiewicz, Nikolai Mokhov, Daniel Schulte, Mauro Pivi, Nobu Toge, Brett Parker, Nick Walker, Timergali Khabibouline, Kwok Ko, Cherrill Spencer, Lew Keller, Sayed Rokni, Alberto Fasso, Joe Frisch, Yuri Nosochkov, Mark Woodley, Takashi Maruyama, Eric Torrence, Karsten Busser, Graeme Burt, Glen White, Phil Burrows, Tochiaki Tauchi, Junji Urakawa, and many other

Thanks to you for attention!